RESEARCH TOWARDS NOVEL IMMUNOTHERAPEUTIC VECTORS: CALIXARENE SCAFFOLDS

Muriel Funck

A thesis submitted in partial fulfilment of
the requirements of Nottingham Trent University
for the degree of Doctor of Philosophy

June 2011

ACKNOWLEDGEMENTS

ABSTRACT

The aim of this project was to generate a new type of therapeutic delivery system and immunogenic vector, based on calixarenes, that is able to not only deliver immunogenic peptide but also act as a potential cancer vaccine. The introduction presents calixarenes derivatives in the context of supramolecular chemistry. Their properties on the nanoscale allow them to be potential adjuvants for cancer immunotherapeutics.

The synthetic study of these materials presented in Chapter II compares traditional synthetic protocols and a new greener approach utilising microwave irradiation. Initial studies in this area concentrate on alkyl-footed derivatives of both the resorcin[4]arene and pyrogallol[4]arene macrocycles but have also been expanded to the previously problematic aromatic derivatives. This microwave method has been optimised to produce the *rccc* diastereoisomer for both the alkyl and aromatic derivatives, showing that the nature of the substituent on the pendant chains does not have a great effect on the conformation using this green protocol. The solution and solid state studies of these new aromatic pyrogallol[4]arene macrocycles, in the *rccc* cone conformation, have been investigated and demonstrate their future potential application in hydrogen storage.

The synthesis of polar analogues, described in Chapter III, was achieved by functionalising the pendant chains with polar groups, including amines, alcohols and carboxylic acids. The importance of the solvent in the crystallisation process is highlighted by single crystal X-ray diffraction study, showing that it can act as templating agent or guest.

Access to polar footed calixarenes has enabled the project to investigate their potential to link bioactive therapeutics including amino acids and peptides, towards nano-vectors exposed in Chapter IV. The traditional synthesis in solution was challenging due to purification issues, and only succeeded in the attachment of three trialanines. The method was therefore tuned towards solid phase synthesis, which opened up to the new development of Merrifield resin functionalised with calixarenes.

As the macrocycle will be considered for immunisation in the future, the lead macrocycle from this study have been screened for potential downstream biological applications. Preliminary studies, including haemolytic properties and cytotoxicity studies did not show any toxicity at the workable concentrations.

CONTENTS

LIST OF FIGURES AND SCHEMES

A. LIST OF FIGURES

B. LIST OF TABLES

C. LIST OF SCHEMES

ACCRONYMS AND ABBREVIATIONS

ADMA	1-(9-anthryl)-3-(4-dimethylaniline) propane
ADP	adenosine diphosphate
AFM	atomic force microscopy
AK	adenylate kinase
APC	antigen presenting cell
Ar	Aromatic
ATP	adenosine triphosphate
ATR	attenuated total reflectance
$BF_3.OEt_2$	ethereal boron trifluoride
Boc	di-*tert*-butyl dicarbonate
BSA	bovine serum albumin
CTL	cytotoxic T lymphocytes
CTV	cyclotriveratrylene
d	Doublet
DC	dendritic cells
DCC	*N,N'*-dicyclohexylcarbodiimide
DCM	dichloromethane
Df	distortion factor
DIC	*N,N'*-diisopropylcarbodiimide
DICU	*N,N'*-diisopropylcarbodiimide urea
DIEA	*N,N'*-diisopropylethylamine, Hunig'sbase
DMAP	4-dimethylaminopyridine
DMF	dimethyl formamide
DMSO	dimethyl sulfoxide
DNA	deoxyribonucleic acid
EDC	1-ethyl-3-(3-dimethylaminopropyl) carbodiimide
eq.	equivalent
FDA	food and drug administration
FITC	fluorescein isothiocyanate
Fmoc	fluorenylmethyloxycarbonyl
GM-CSF	granulocyte macrophage colony-stimulating factor

HBTU	O-benzotriazole-*N,N,N',N'*-tetramethyl-uronium-hexafluoro-phosphate
HLA	human leucocyte antigen
HOBt	hydroxybenzotriazole
HPLC	high performance
IFN	interferon
IR	infrared
LPS	lipopolysaccharide
m	*meta*
m	multiplet
MALDI	matrix-assisted laser desorption/ionization mass spectrometry
MHC	major histocompatibility complex
MHRA	medicines and healthcare products regulatory agency
MPS	mononuclear phagocyte system
MRI	magnetic resonance imaging
mRNA	messenger ribonucleic acid
MTT	3-(4,5-dimethylthiazol-2-yl)-diphenyl tetrazolium bromide bromide
NHS	*N*-hydroxysuccinimide
NMP	*N*-methyl pyrrolidone
NMR	Nuclear magnetic resonance
o	*ortho*
p	*para*
PBA	pyrene butyric acid
PEG	polyethylene glycol
PI	propidium iodide
Poly I. C.	polyinosinic-polycytidylic-acid
PS	polystyrene
*p*TSA	*p*-toluenesulfonic acid
RNA	ribonucleic acid
RP-HPLC	reverse phase high performance liquid chromatography
s	singlet
SAM	self-assembled monolayer
SEM	scanning electron microscopy

SPPS	solid phase peptide synthesis
SPR	surface plasmon resonance
t	triplet
TEM	transmission electron microscopy
TEMPO	(2,2,6,6,tetramethylpiperidine-1-yl)oxyl
TFA	trifluoroacetic acid
TIS	triisopropylsilane
TOF	time-of-flight
UV	Ultra violet
VEGF	vascular endothelial growth factor
W	Watt
WHO	world health organisation

CHAPTER I: INTRODUCTION

A.SUPRAMOLECULAR CHEMISTRY

Since the early age of scientific discovery, scientists have tried to understand the bigger picture behind a given phenomena. The role of chemists is not only focussed on the understanding of the formation of chemical bonds but also on the interactions of those molecules with their surroundings. This could be considered as the foundations of supramolecular chemistry, also known as the chemistry beyond the molecule. The field of supramolecular chemistry, was further refined when molecules were designed to achieved the highest interactions or recognition with other entities.subodh[1] Originating from the study of host-guest recognition, it has now opened up into self-assembly and self-organisation of macrocycles; moving from the molecular scale to the nanometre scale.[2]

As described by one of the pioneer of supramolecular chemistry, Nobel Prize winner Jean-Marie Lehn:

"Beyond molecular chemistry, supramolecular chemistry aims at constructing highly complex, functional chemical systems from components held together by intermolecular forces".[3]

Research is moving one step closer towards constitutional dynamic chemistry and adaptive chemistry. The supramolecular chemistry field is now interdisciplinary and so wide that it cannot be restricted to one specific area;[4-5] however, the essence of the subject still relies on the various interactions occurring at the molecular level.

1. SUPRAMOLECULAR INTERACTIONS

Although of different natures and different strengths, supramolecular interactions always comprise one important feature, they are non-covalent and are based on dipole interactions.

Ion-ion interactions, Figure 1, are a result of the attraction of a cation towards an anion. The strength of this ionic bond is comparable to that of a covalent bond, but without the overlapping molecular orbitals.
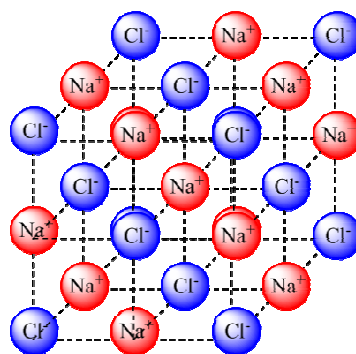
Figure 1: Crystal lattice based on ion-ion interactions in sodium chloride.

In heteroatomic covalent bonds, the electronegativity of an atom may differ from the one it is bound to, resulting in a partial displacement of the electron density from one atom to another, creating polarity between the atoms that in turn forms a dipole. In the presence of ions, dipoles can form coordinate bonds (Figure 2a) which are the basis of many inorganic complexes, *e.g.* in *cis*-platin. Dipoles can also interact with other dipoles, by aligning with one another in different manners, either perpendicularly or in parallel, as shown in Figure 2b and 2c respectively.
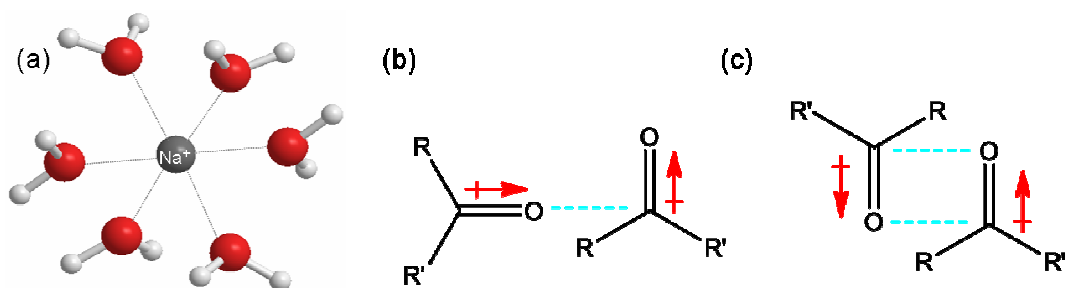
Figure 2: (a) Ion-dipole coordinate bond between sodium and water (b) perpendicular dipole-dipole interaction and (c) parallel dipole-dipole interaction between two carbonyls.

Hydrogen bonding is one of the most significant non-covalent interactions, mainly due to its involvement in the recognition and the stability of DNA, wherein two complimentary oligonucleotides come together to form a double helix held together by hydrogen bonding. One hydrogen attached to a strong electronegative atom (usually oxygen or nitrogen) called the donor (D) binds to another electronegative atom that generally has a lone pair called the acceptor (A) and is often referred to as D-H··A (Figure 3).
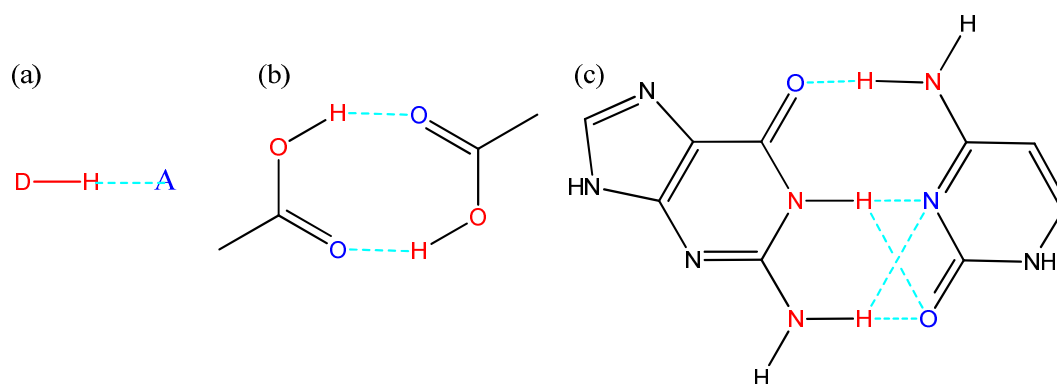
Figure 3: Hydrogen bonding between (a) a donor and an acceptor, (b) two carboxylic groups, (c) and two complementary DNA bases (guanine and cytosine) (Hydrogen bonding interactions are represented by dashed lines)

As seen in Figure 3, hydrogen bonds can have different geometries, *i.e.* linear (Figure 3a), bent (Figure 3b) or bifurcated (c). Depending on the electronegativity of the donor and acceptor, hydrogen bonds can vary in length and strength, as shown in Table 1.

	Strong	Medium	Weak
Bond energy (kJ.mol^{-1})	60-120	16-60	<12
H$\cdots$A Bond length (Å)	1.2-1.5	1.5-2.2	2.2-3.2
D$\cdots$A Bond length (Å)	2.2-2.5	2.5-3.2	3.2-4.0
Bond Angle (°)	175-180	130-180	90-150
NMR shift downfield (ppm)	14-22	<14	
Example	Proton sponge HF-complex Strong acid/base	Acids Alcohols Biological molecules	D-H$\cdots$ π bond C-H$\cdots$H bond

Table 1: Hydrogen bond characteristics [6]

Solvents, especially polar ones, also interact with molecules *via* electrostatic interactions. This process is known as the solvation effect and can interfere with other chemical binding and recognition. If carefully considered, solvents can also play an integral role in self-assembly by becoming incorporated into the supramolecular structure. When water is involved into this process, it is known as the hydrophobic effect. As shown in Figure 4, the hydrated guest is included into the solvated host resulting in a hydrated host-guest complex. This effect can lead to the exclusion of non-polar entities from aqueous solution.[7]
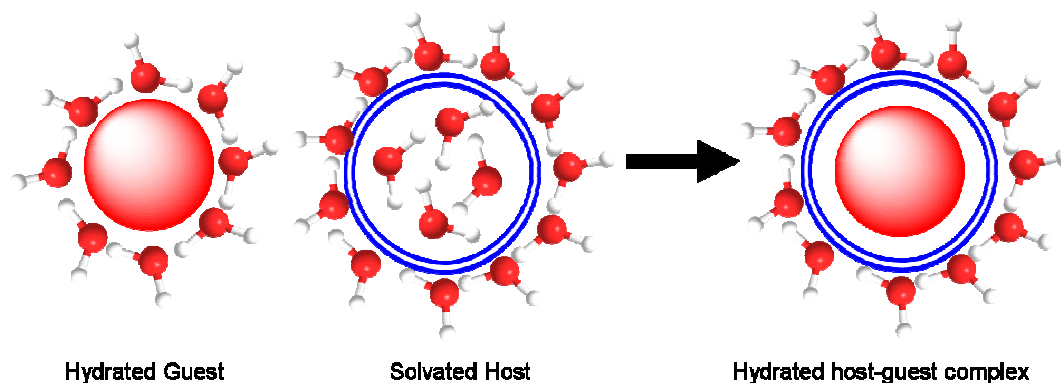
Figure 4: Hydrophobic effect on host -guest complexation

In aromatic compounds, the electron rich π system has no permanent dipole moment itself, but a partial negative charge is hosted above and below the plane of the aromatic ring (Figure 5a). This enables the system to interact with ions and most interestingly with itself. This π -π interaction can take two forms, face-to-face (Figure 5b) or edge-to-face (Figure 5c). This is also seen in nature for example in DNA stacking.
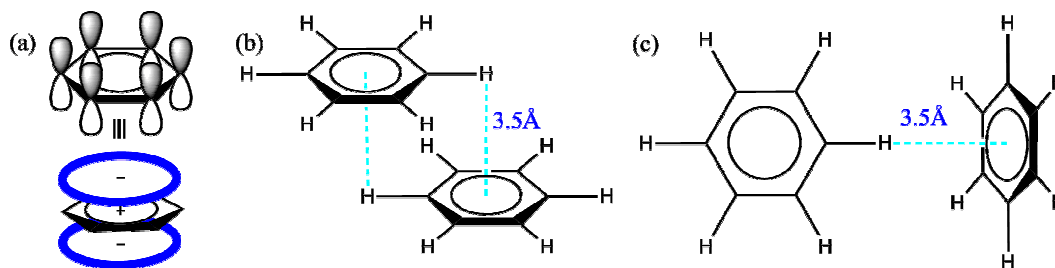
Figure 5: (a) π-system in benzene; π-π interactions (b) face-to-face (c) edge-to-face

2. MACROMOLECULES

A macrocycle is a cyclic molecule, usually constituted of a minimum of nine atoms arranged in a ring with several binding sites.[8] The most commonly used classes of macromolecules are crown and lariat ethers, cryptands and heterocryptans, hemi-, crypta- and full spherands, heterocrowns, curcubiturils, catenanes, rotaxanes, cyclotriveratrylenes (CTV) and calixarenes.[9] These macrocyclic compounds are inherent players in supramolecular chemistry; they are built to offer the optimal design for many guests, by exploiting intra- and intermolecular interactions.

a) Calixarenes

Calixarenes are a three dimensional class of macrocycles which are known to adopt cup-like motifs. They are known to bind to cations as well as other molecular guests in solution.[10] They can also undergo self-assembly with themselves to form inclusion capsules and cages on the nanometre scale and therefore contribute to a wide array of supramolecular chemistry research.

In 1872, Adolph von Bayer was in search of a new type of dyes. He mixed formaldehyde and phenol together and heated them up into a new material, which had exceptional properties, but was not fully characterised. A few years later, using a similar method, Leo Baekeland developed a polyphenolic resin called Bakelite. These new applications drove scientists to probe the synthesis of this new material in more detail.[11] This first synthetic plastic became the material of choice for building heat resistant appliances such as radios or kitchenware.

Although the first calixarene structure was characterised by Cornforth in 1955,[12] research into their potential properties and applications only kick-started twenty years later, when Gutsche turned his attention to this class of molecules and formally named them calixarenes. This name originates from their shape representing a Greek bowl, named a calyce (Figure 6b).[13]

Made from the controlled condensation of *tert*-butylphenol and formaldehyde under basic conditions, their synthesis has not changed much since their first discovery. Greener approaches such as the use of microwave induced condensation is one of the rare modifications to the procedure.[14] The cyclic oligomers formed during the condensation can be seen to have an increasing number of monomer units (n), varying from four to ten as shown in Figure 6. The size of the ring can be controlled by the temperature of reaction used in the cyclisation. The nature and size of the cation of the base used also play a pivotal role in ring size formation.[15]
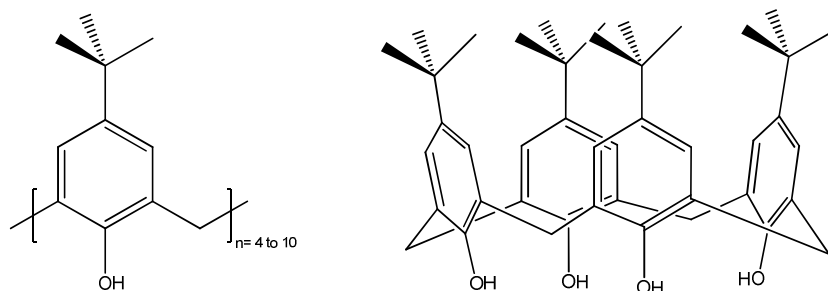
Figure 6: (a) tert-Butylcalix[n]arene (n= 4 to 10) and (b) tert-butylcalix[4]arene cyclic oligomer in cone conformation

Many calixarene derivatives are available today; the tetramers being the most commonly studied are used in a wide range of applications such as electrochemical and optical sensors, as well as chiral recognition devices and have been established as scaffolds for protein surface recognition.[10, 16-18] In this work, only calixarenes relevant to biological systems or with demonstrated potential for biopharmaceutical applications will be further considered.[19]

The nature and therefore the properties of the calixarenes are dependent on their pendant chains, as well as their aromatic starting material. Generally made from phenols; they can be composed of aromatic heterocycles or phenol derivatives such as resorcinol and pyrogallol (Figure 7).[20]

b) Resorcinarenes and pyrogallolarenes

Calixarenes containing hydroxyl groups, derived from the 1,3-*di*-hydroxybenzene and 1,2,3-*tri*-hydroxybenzene are commonly referred to as resorcinarene and pyrogallolarene respectively (Figure 7). It should be noted that pyrogallolarenes taxonomy varies and other terms such as pyrogallol[4]arene, pyrogallolcalix[4]arene, calix[4]pyrogallolarene, 5,11,17,23-tetrahydroxyresorc[4]arene, often replace the IUPAC name: 2,8,14,20-tetraalkylpentacyclo[19.3.1.1^{3,7}.1^{9,13}.1^{15,19}]octacosa-1(28),3,-5,7(25),9,11,13(26),15,17,19(27),21,23-dodecaene-4,5,6,10,11,12,16,17,18,22,23,24-dodecol.
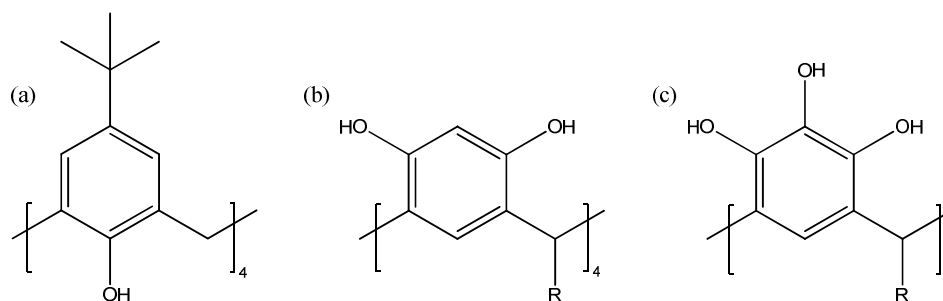
Figure 7: Calixarenes: (a) tert-butylcalix[4]arene (b) resorcin[4]arene (c) pyrogallol[4]arene

The addition of extra hydroxyl groups to the calixarenes macrocyclic ring enables more intermolecular interactions due to their greater accessibility to hydrogen bonding. This subsequently plays an essential role in the self-assembly of these monomers to form carcerants,[21-22] cavitands[23-24] and capsules.[25] It also improves their host-guest complexes wherein the hydrophobic pocket, formed by the benzene rings of the macrocycle, also contains a hydrophilic rim made up of the hydroxyl groups (Figure 8).
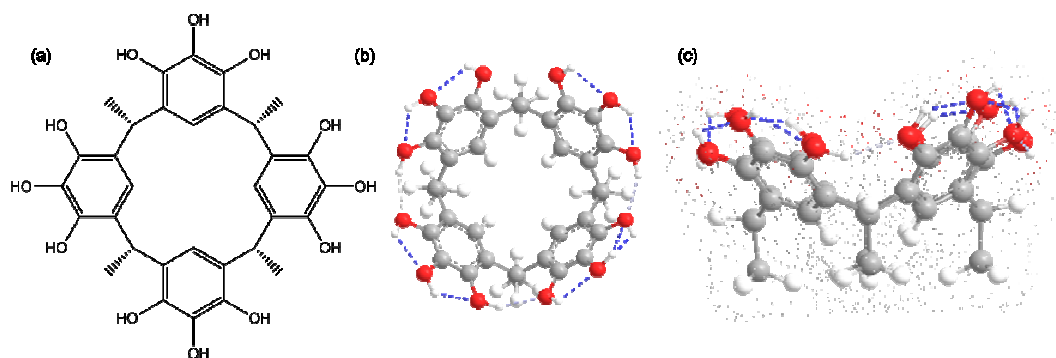
Figure 8: (a) Pyrogallol[4]arene structure (b) View of the upper rim of the monomers, doted lines represent the intramolecular hydrogen-bonding (c) side view of the hydrophobic pocket

Several interesting properties of resorcin[4]arene and pyrogallol[4]arene have been exploited in various applications such as metal complexing agents,[26-28] sensors,[29-30] water soluble traps,[31-33] phase transfer extraction of heavy metals[34] or hydrocarbon gas[35] and novel stationary phases for chromatography.[36-38]

(1)   Stereoisomers

The thermodynamic tetramer products exist as a number of different stereoisomers, depending on the orientation of the pendant chains on the methine bridge, in either axial of equatorial position and the overall shape of the macrocycle (Figure 9).[39]
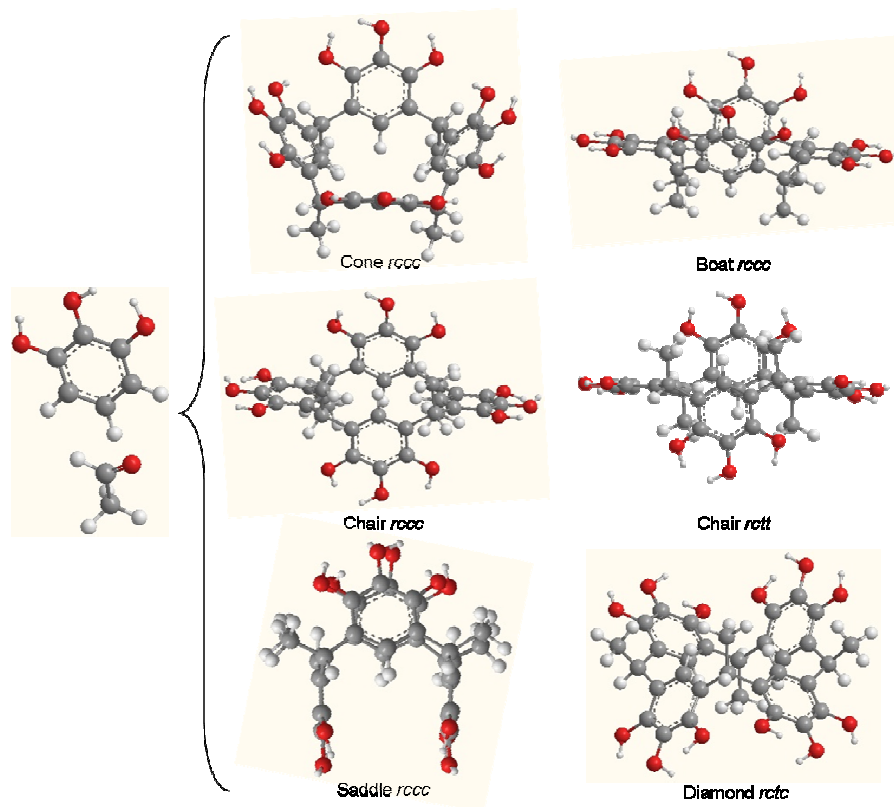
Figure 9: Main isomers of the pyrogallol[4]arene tetramer

Generally, the all *cis* (*i.e.* all side chains are *cis* to one another) conformer *rccc*; the cone (or crown) shaped tetramer, precipitates during the course of the reaction because of its low solubility in acidic aqueous media and drives the reaction thermodynamically. The other most common form is the kinetic diastereoisomer *rctt* chair conformation. The polarity and solubility of the compound in the reaction solvent is one of the driving forces towards the formation of the calixarenes. By precipitating out of solution, the equilibrium is thermodynamically displaced towards the formation of the desired product. The cone *rccc* conformation is highly stable due to four intramolecular hydrogen bonds, which are not accessible in the other all *cis* chair, saddle and boat conformations.

The formation of other isomers is driven by the choice of pendant chain, largely due to steric hindrance, but can also be altered by the presence of an electron-withdrawing group in the α-position of the phenolic residue of resorcinol. This has previously been demonstrated to interfere with the cyclisation process.[21]

Reaction time is also reported to play an important role in both conformation and configuration, wherein the ratio of C_{4v} (cone) to C_{2v} (boat) isomeric products are time dependent; longer reaction time favours the C_{4v} product.[40] In a similar manner, the *rctt* isomer forms faster than the *rccc*, but it is isomerised back to the more stable *rccc* through reversible protoalkylation/protodealkylation under the synthetic conditions. Barriers of ring inversion are low enough to allow conformational equilibrations to occur rapidly at ordinary working temperature. Thus in configurational assignments, conformations can formally be ignored.[21] The ratio of C_{4v} to C_{2v} is dependant on the electronic character of the pendant chain, as for example with electron withdrawing groups like nitrile only *rctt* is detected. Only one rare example of 2,8,14,20-*tert*-butyl-pyrogallol[4]arene exhibits a unusual *rcct* conformation, whereby three chains are down and only one is up.[41]

The host-guest chemistry that drives the vast majority of research and applications of these materials relies on the formation of the *rccc* cone conformer that is also preferred in the design of larger assemblies. This cone, crown or cup can be functionalised on the upper rim *i.e.* the wider top of the cup or the lower rim *i.e.* the narrow bottom part of the cup. Examples of their possible applications as host include a variety of macrocycles. Phosphorylated resorcinarenes, undecylcalix[4]resorcinarene and other calixarenes were used as neutral ionophores to compose the liquid membrane electrodes in cation exchange HPLC, for the screening of β-adrenergic and β-blocking chiral drugs.[42] Stationary phase based on calixarenes and resorcinarenes have been prepared for reverse phase HPLC (RP-HPLC), their selectivity seems to be higher towards steroids than their C18 equivalents, showing the application of host guest chemistry.[43] Pyrogallol[4]arene can be used to complex as dopamine sensors at the air-water interface of phospholipids monolayers.[30]

(2) Synthesis

Despite the rapid emergence and utilisation of these materials, the original synthesis remained relatively unchanged for over a hundred and thirty years.[44]

It is based on the cyclocondensation of resorcinol or pyrogallol with an aldehyde under acidic conditions for up to seven days at reflux (Scheme 1).[40] The first synthesis based on the condensation of pyrogallol and aldehyde as a modification of the Hoegberg synthesis, was reported in 1990.[45]
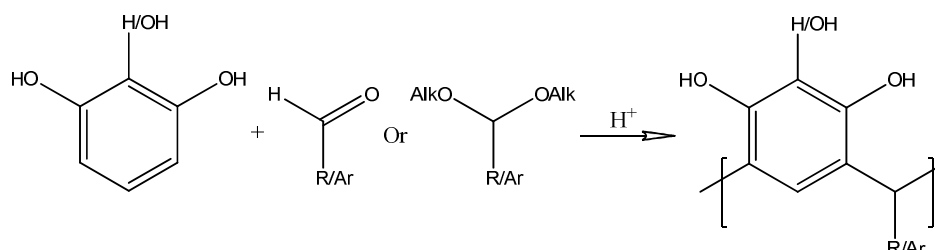
Scheme 1: Synthesis of resorcinarene (H) or pyrogallolarene (OH) with alkyl (R) or aryl (Ar) chains

The studies of resorcin[4]arene formation and conformation were followed by Weinelt who suggested a potential mechanism *via* the formation of an acetal, [46] the latter can be used as a starting material as well.[47]

NMR and HPLC studies have been used to show that during the polymerisation process (Figure 10), larger oligomers with n=5 and n=6 *i.e.* a pentamer and a hexamer, are produced in the first two hours of reaction but are isomerised at different rates to completely obtain the tetramer after six hours.[47]
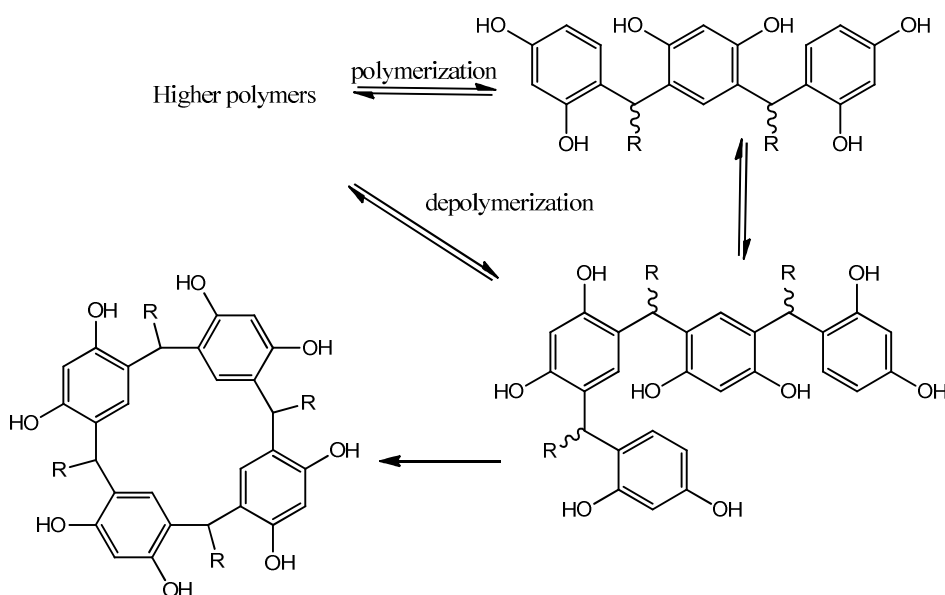
Figure 10: Polymerization leading to the resorcin[4]arene

The tetramer can also be obtained by fragment condensation of aldehydes with two dimers (obtained by changing the molecular ratio of resorcinol and aldehyde from 4:4 to 2:1). This approach facilitates the introduction of diverse pendant chains onto the same monomer in an alternate manner.[48]

More recently a novel approach led to the formation of resorcin[4]arene octaisopropyl ether, also referred as "resorcin[4]arene parent", by treatment of 2,4-diisopropoxybenzyl alcohol with chlorotrimethylsilane (Scheme 2). Although these compounds have a main aromatic core they have no pendant chain and require a deprotection step to reach the hydroxyl derivative.[49]
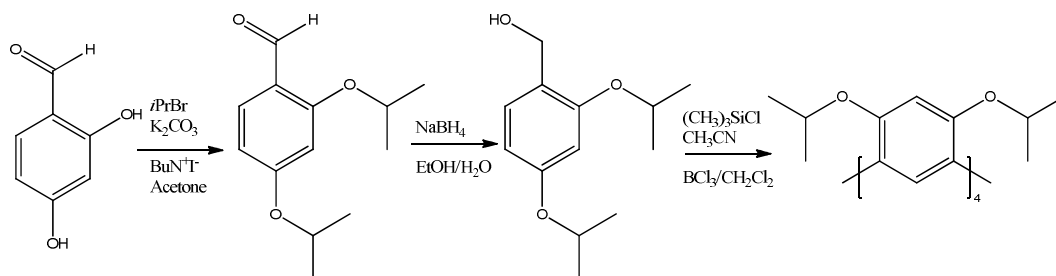
Scheme 2: Synthesis of resorcin[4]arene parent

Resorcin[4]arene octamethyl ether tetraesters can also be obtained by the reaction of 2,4-dimethoxycinnamates with etheral boron trifluoride (BF$_3$.OEt$_2$) as a Lewis acid catalyst (Scheme 3).[50] This synthetic apparaoch results in three conformational states, the 1,2-alternate (*rccc*), the 1,3-alternate (*rccc*) and flattened cone (*rccc*). Their ratio depends on the nature of the ester as well as the reaction conditions.
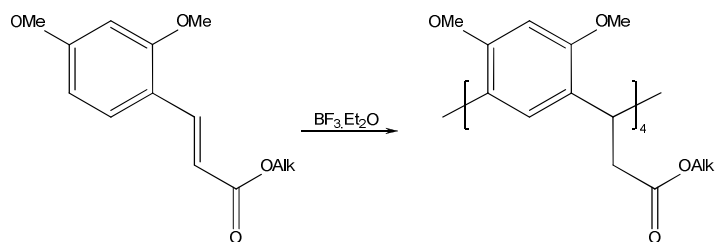
Scheme 3: Synthesis of resorcin[4]arenes octamethyl ether tetraester

Octamethoxyresorcin[4]arene derivatives, in the crown conformation, can be synthesised by a Friedel-Crafts type condensation, with a dimethoxybenzene and a variety of Lewis acid. [51] The catalyst leading to the highest yields and the conformation selectivity using this strategy is tin (IV) chloride in chloroform.

Methoxypyrogallol[4]arene can also be formed in the presence of tin(IV) chloride with trimethoxybenzene and trioxane.[52] Brönsted acid catalysis also plays an essential role in the selective formation of the *rctt* chair stereoisomer of *octa*-O-alkyl-resorcin[4]arenes.[39]

Although calix[4]arenes require a base catalysed condensation, resorcin[4]arenes and pyrogallol[4]arenes are commonly synthesised *via* acid catalysis; however, the exception to the rule is for nitroresorcin[4]arene, that can not be obtained by the usual acidic cyclocondensation. Instead, it is synthesised by using sodium hydroxide as a basic catalyst.[53]

Research towards greener synthetic approaches has resulted in novel methods emerging over the last ten years. The first to be reported was the solvent-free method, wherein equimolar amount of dihydroxybenzene and an aldehyde are ground together with a catalytic amount of *p*-toluenesulfonic acid (*p*TSA) resulting in aryl-resorcin[4]arenes and alkyl-pyrogallol[4]arenes. [54-55] Interestingly, the calixarenes self-assemble into a capsule.

Advances in microwave-assisted technologies allowed other green methods to yield to calixarenes. Brönsted acid catalyst, the Keggin-type tungstophosphoric acid (TPA) combined with microwave irradiation have been shown to synthesise resorcin[4]arenes.[56] This work was later developed to include the pyrogallol[4]arene macrocycles by Yan *et al*.[57] Microwave-assisted synthesis can also be employed to further functionalise the upper rim of the calixarenes as shown by the alkylation of tetra-*p*-hydroxyphenyl-pyrogallol[4]arene.[58]

(3)   Self-assembly

Calixarenes are able to form capsule and cage like architectures. This can be achieved *via* covalent linking as Cram and Warmuth have demonstrated,[59] or introducing more versatility by utilising non-covalent interactions. Examples include dimeric capsules also known as "tennis balls" or "soft balls".[60]

The unique combination of pyrogallol[4]arene's shape and hydrogen bonding potential leads to multitudes of possible hydrogen bonding networks creating capsules and layers that can expand into three dimensional frameworks (Figure 11).[61] The hydrogen bonds can be replaced by partial or complete inclusion of metal coordination bonds. Their self-assembly in both solid state and liquid state has been extensively studied by the use of X-ray crystallography and diffusion NMR techniques. [62-63]
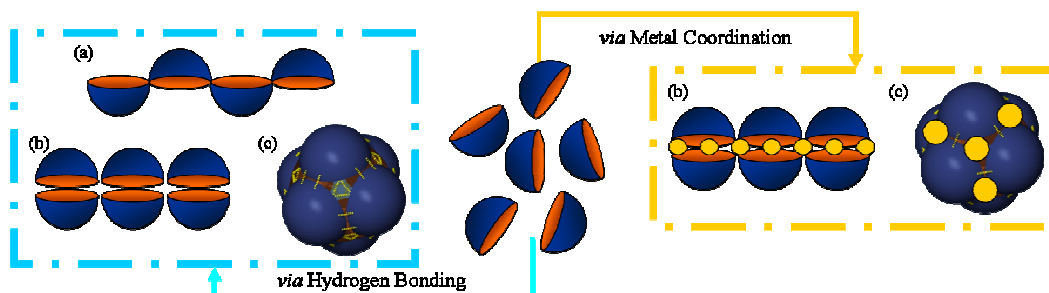
Figure 11: Self-assembly into (a) layer (b) dimeric capsule (c) hexameric capsule

(a) In layer-like Assemblies

Packing control is achieved by tuning the environement, usually *via* the solvent selection, the nature of the pendant chain or a relevant guest that can act as a templating agent.[64] Polar protic solvents such as alcohol or DMSO, take part in the hydrogen bonding network and often lead to the formation of layer-like assemblies.[65] The addition of 4,4-bipyridine molecules to the pyrogallol[4]arene leads to an hydrogen bonded extended cavity (Figure 12).[66]
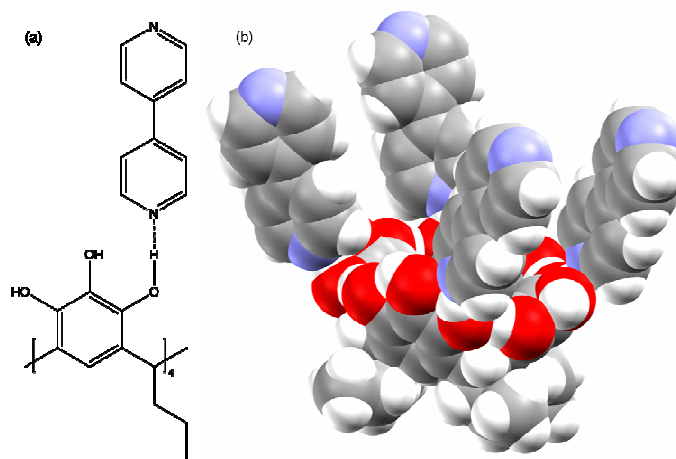
Figure 12: Extended cavity (a) Hydrogen-bonding interaction, (b) space filling view [66]

The nature of the pendant chain also plays a role in the self-assembly of the calixarene. When long alkyl chains are present ($C_{15} H_{31}$), the amphiphilic properties take precedence over the hydrogen bonding capacity of the macrocycles, leading to the formation of vesicles in solution.[67] Additionally, at the air-water interface, pyrogallol[4]arenes with alkylated branched side chains have the ability to self-assemble into cogged hydrogen bonded nanotubes (Figure 13).[68] The presence of other

organic compounds such as pyrene, can lead to the formation of organic nanotubes in the solid state. Their stability in solution remains to be fully understood.[69]
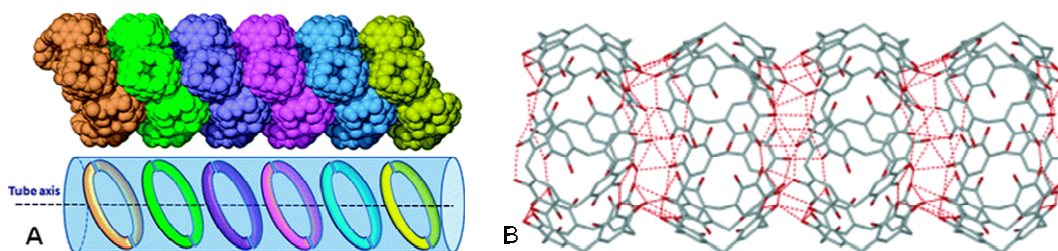
Figure 13:Nanotubes (a) Cogged hydrogen bonded and (b) pyrene mediated

Water soluble aminoamide substituted lipophilic resorcinarene are also seen to form micro-tubes, that can be observed by electron microscopy.[70] These tubular properties have been further exploited by capping gold nanoparticles with the calixarene to form bifunctional microtubes (Figure 14).[71]
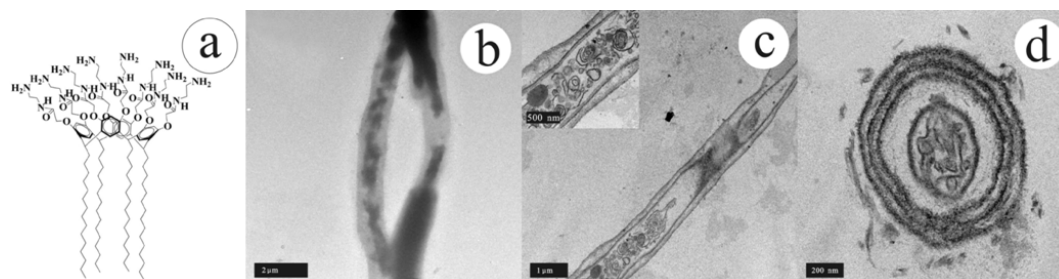
Figure 14: Resorcinarene hydrazine: (a) molecular structure, (b-d) TEM images of microtubes cross sections [71]

(b) In capsules

The formation of a large hexameric capsule, was first observed with six *C*-methyl-resorcinarenes and eight water molecules, self-assembling through sixty hydrogen bonds into a sphere with an interior volume of *ca* 1375 $\mathring{A}^3$, when grown from a water/nitrobenzene mixture.[72] *C*-tetra-isobutyl-resorcin[4]arene has also been observed to form analogous capsules when crystallised from acetonitrile.[73]

The addition of extra hydroxyl groups at the upper rim, achieved by substituting resorcinol for pyrogallol leads to the formation of the hexamer with a reinforced hydrogen bonding network. Pyrogallol[4]arenes are able to form supramolecular nanometre-sized host capsules (Figure 15). Constructed from six pyrogallol[4]arene macrocyclic cavitands, these self-assemble *via* seventy-two hydrogen bonding

interactions into globular capsules, with an internal volume of *ca.* 1300 Å^3.[74] The first example of this capsule was isolated from methanol and acetonitrile.[75]
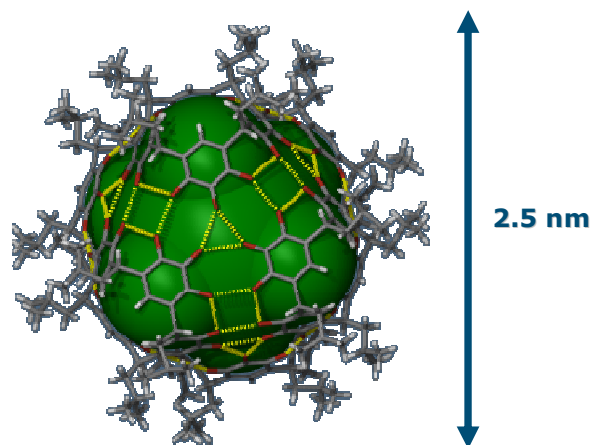
Figure 15: Pyrogallol[4]arene hexamer, hydrogen bond (yellow) and internal volume (green)

C-Alkylhydroxycalixarenes tend to form hexameric capsules in the solid state when grown from acetonitrile, aqueous acetonitrile, ethyl acetate, chloroform and rarely benzene and methanol. The formation of the hexameric capsule is now well understood and has been reported using various techniques such as NMR[76] and mass spectrometry[77] moreover the controlled assembly-disassembly was investigated using spinning disk processing.[78] Consequently, scientists started the extensive study of the self-assembly properties of the pyrogallol[4]arene and compared them to the resorcin[4]arene.

The ability of the macrocycles to form hexameric capsules in solution has been extensively studied using diffusion NMR.[79] As the diffusion coefficients for both undecyl-pyrogallol[4]arene and undecyl-resorcin[4]arene are similar, it is assumed that both capsule are analogous in solution. It was also showed that the pyrogallol[4]arene capsules are more stable than the resorcinarene ones in solution, as they required more polar molecules such as DMSO or methanol to break the hydrogen network, therefore demonstrating that four extra hydroxyl groups per macrocycle make a significant difference.[80] As resorcin[4]arene requires the presence of water or alcohol to complete the hydrogen bonding network they are much less stable than the pyrogallol[4]arene capsules.

The influence of water in the crystallisation of *C*-alkyl-pyrogallol[4]arenes (propyl to octyl) in acetonitrile was explored in the absence of any guests. It was confirmed that water can interfere with the formation of the hexamer and that the chain length play an important role as longer chains favour the self-assembly at the upper rim.[81]

Following this work, other capsules from longer alkyl chains have also been obtained for butyl to octyl, the chain length control (C_nH_{2n+1}, n = 3 to 11) over the nano-capsule packing has been shown to have a dramatic effect on the extended packing (Figure 16). The inter-capsule separations decrease from n = 4 (*ca*. 22.5 Å) to the lowest when n = 6 (19.1 Å) and increase nearly linearly to 23 Å when n = 11.[82] The most favourable inter-capsule hydrogen bonding is observed in the solid state when n = 6.[83]
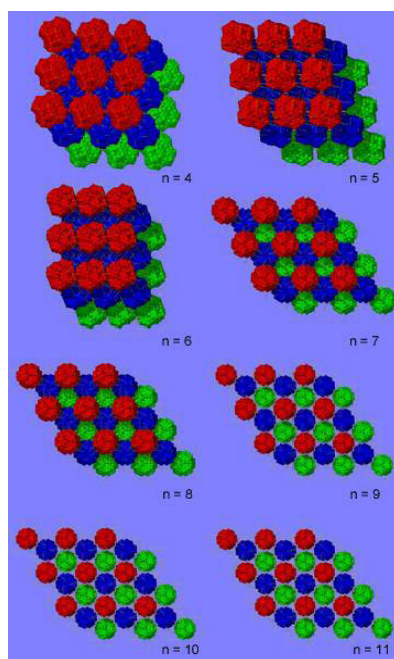
Figure 16: Effect of the chain length on the packing[82]

The interactions of the side chains of the hexamers lead to different packing in the solid state, the lipophilic chains partially interpenetrate (C_5H_{11} and C_7H_{15}) or can assemble into nano-rods (C_6H_{13}).[83] The effect within the chain can be reflected on the organisation of the structure in the solid state: as the number of carbon atoms in the side chain increases, the intermolecular interactions become more sizable, as viewed by Transmission Electron Microscopy (TEM).[84] It results in larger spherical aggregates (Figure 17) with a diameter of *ca* 80 nm, made of hexameric pyrogallol[4]arene capsule with cross-section of about 4 nm.[85]
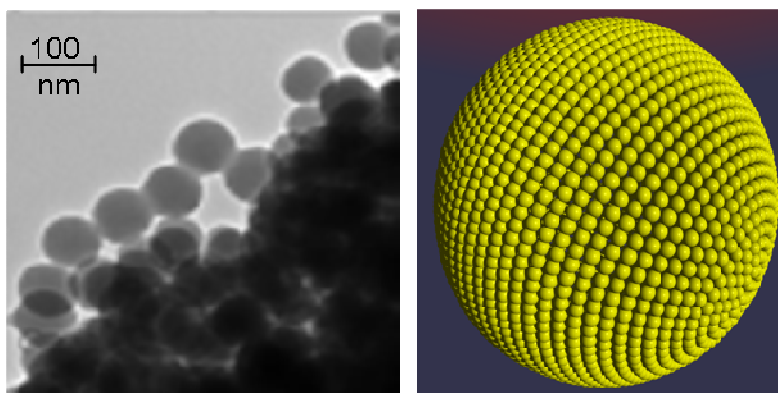
Figure 17: TEM image of the spherical aggregates and its theoretical representation [85]

The encapsulation properties of the resorcinarenes alone and in the presence of various guests have been reviewed in some detail.[86-89] The hexameric containers have different encapsulation properties, whilst pyrogallol[4]arene has only been demonstrated to encapsulate neutral tertiary alkylamines, resorcinarene can accommodate both the amines and the respective ammonium salts, showing that such a system could be used as a potential molecular pH switch.[90] Even in really apolar solvent such as alkanes, pyrogallol[4]arenes retain the ability to not only self-assemble into hexamers but also to encapsulate the hydrocarbons. In this case, 40 to 50% of the capule internal volume is occupied by the guest, which is within the limit of the 55% rule.[91] The encapsulation properties extend to the encapsulation of the solvent such as chloroform and benzene.[92]

The hexameric capsule can also be composed of mixed macrocycles containing both resorcinol and pyrogallol, showing a molecular "self-sorting".[93] The self-assembly was then shown to proceed by self-recognition as the mixture of two macrocycles of different type resulted in no instantaneous formation of heterohexamers but an equilibrium towards heterohexamers is attained after a week.[94]

(c) Metallo-capsules

Inspired by the coordination properties of phenols and catechols, the ability of the hydroxyl groups to coordinate to metal and metal hydrides was exploited to form metallo-hydroxycalixarenes complexes. Advancement into supramolecular design was achieved when the hydrogen network was substituted by metals, forming metallo-supramolecular capsules either dimeric (zinc) or hexameric capsules (copper and gallium), [95-96] Even though the loss of four intramolecular hydrogen bonds can increase the flexibility of the cone monomer,[97] the complexes keep similar size and volume to

their hydrogen-bonded homologues. Comprehensive reviews on metallo-supramolecular capsules and mixed metal-organic nanocapsules demonstrate the advances in this field.[26, 98] These capsules are readily prepared by dissolving hydroxycalixarenes in a methanolic solution of the metal nitrate, and crystallising the resulting solid from an appropriate solvent.

The rapid self-assembly of a copper nanocapsule was described as a possible cause for the formation of discrete metal-organic assemblies (Figure 18).[99] Six *C*-propan-3-ol-pyrogallol[4]arenes coordinate to twenty-four Cu(II) to form an hexameric capsule with an internal volume of *ca* 1200 Å^3.[100] The synthetic ion channel based on copper sealed *C*-undecyl-pyrogallol[4]arene capsule keeps its shape, even in phospholipids bi-layers.[101]
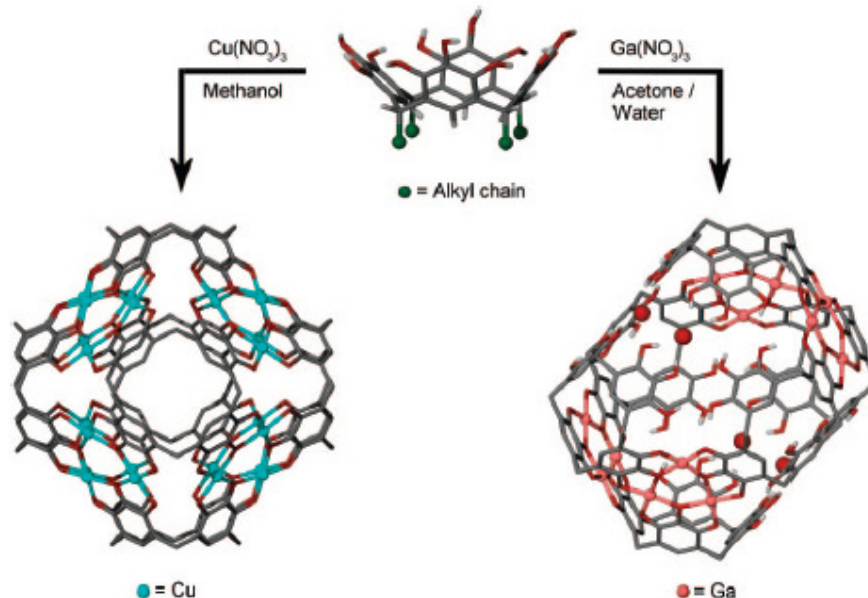
Figure 18: Example of metal-organic capsules.[96]

The substitution of copper by gallium leads to the formation of a "rugby ball" with an estimated internal volume of 1150 Å^3. These hexamers encapsulate six to seven acetonitrile molecules or twelve metal ions (Ga^{3+}) and four coordinated water molecules.[62] The characterisation of the latter was obtained by X-ray crystallography and matrix-assisted laser desorption/ionization mass spectrometry (MALDI-TOF MS).[95, 100] Other pyrogallol[4]arenes were considered as potential ion transporters when caesium and silver were found to move to the interior of metal (Ga (III)) organic capsules.[96] Capsules containing multiple metals, *i.e.* gallium (III) and copper (II), are

obtained by exploiting the capacity of a metal (gallium) to replace other metal sites (copper) trapped in the preformed capsule.[102]

The metal coordination seems to have an important effect as it can generate a conformational change with the calixarenes.[103] The deformation of the capsule shape is explained by the incorporation of structural water molecules in gates to the interior of the assembly with gallium whereas for copper insertion, water is not involved and afford a near spherical nanocapsule.[96, 100]

C-Chlorobutanyl- and *C*-hexyl-pyrogallol[4]arene form ionic dimeric capsules when mixed with caesium chloride in head-to-head and one offset manner respectively.[104] Dimeric zinc capsule entrapping methyl-pyridine was obtained from *C*-propyl-pyrogallol[4]arene and [$Zn(NO_3)_2$(3-methylpyridine)$_3$] in methanol and DMSO, which was coordinated to the zinc centres (Figure 19a).[105] Pyridine can easily replace the DMSO molecules, forming a Pelton wheel (Figure 19b). [95-96]
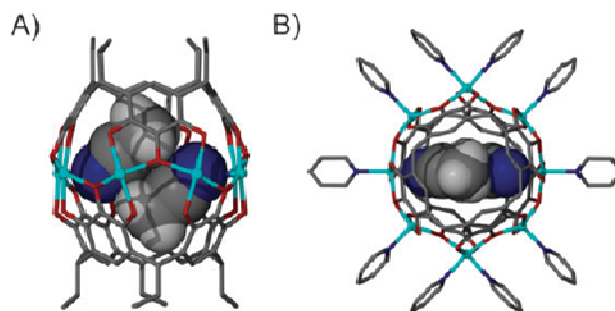
Figure 19: Examples of dimeric metal-organic capsule[106]

When zinc is replaced by paramagnetic metals like nickel and cobalt, the complex retained their magnetic properties.[106] Metallopyrogallol[4]arenes' potential as an ion carrier, by forming large stable conductance pores, has been investigated using conductance studies, when in the bi-layer form or metal (Cu) capsule. The metal-calixarenes capsules are able to reversibly switch over a wide range of potentials.[107]

(d) Traceable capsules

Pyrogallol is known to have chemiluminescence properties, when cyclised into a water soluble tetramer, with sulphonated pendant chains. The chemiluminescence intensity is 1.3 times greater than the pyrogallol monomers.[108] The colorimetric values of resorcinarenes and some boronic derivatives have been considered for the visual investigation of saccharides binding.[109-111]

Following this work, fluorescent chiral resorcinarenes, with tetraarylboronate feet have been used for the chiral recognition of amino acids, especially for lysine.[112] Exploiting the advantages of both self-assembly and encapsulation, fluorescent capsules have been described, using two approaches either the encapsulation of a fluorophore or the covalent attachment of fluorescent entities. Functionalised pyrogallol[4]arene with fluorophores (one donor and one acceptor) on their pendant chains have been assessed for their ability to self-assemble into a hexameric capsule (Figure 20) by fluorescence resonance energy transfer (FRET).[113-114] This work not only proved that pyrogallol[4]arene capsules have a slower monomer exchange than resorcinarenes one, it also confirmed water was not required for the self-assembly to occur. This demonstrated that pyrogallol[4]arenes which are less sensitive to concentration of mixing, are much more stable than the resorcinarene in polar media and the macrocycles have the ability of self-sorting.[115]
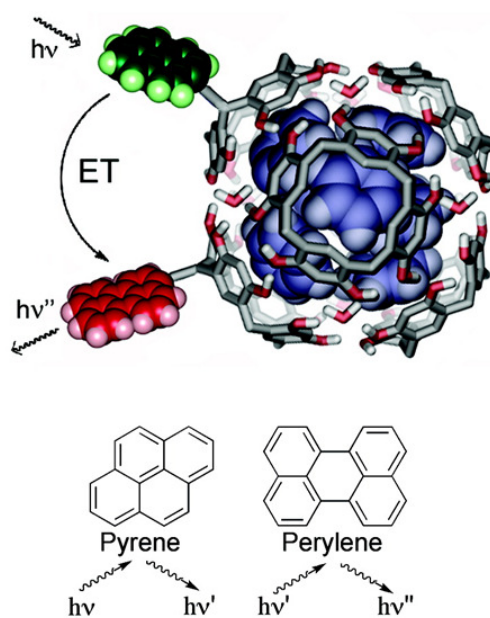
Figure 20: Hexameric capsule containing pyrene and perylene [116]

The encapsulation of pyrene butyric acid (PBA) by *C*-hexyl-pyrogallol[4]arene was used to investigate the internal chemical environment of the capsule. Absorption and fluorescence emission results showed that the two encapsulated PBA are kept apart by more than 7 Å (Figure 21)[116]. Similar results were obtained for the hydroxyl derivative pyrene butanol.[117]

When large fluorescent molecules such as benzo[α]pyrene (B[α]P) and pentacene were trapped by the assembly, it was assumed that only one of those large molecules can occupy the capsule at a time due to size restriction.[118]
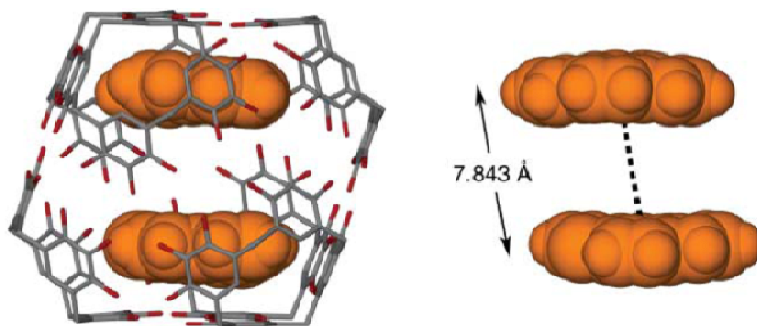
Figure 21: Encapsulated PBA molecules (orange and space filled) in the hexamer[119]

A fluorescent molecule with an in-built quencher, 1-(9-anthryl)-3-(4-dimethylaniline) propane (ADMA) has been encapsulated within the hexamer. The X-ray structure of the *exo*-capsule was presented showing the intercalation of the fluorophore within the pendant chains.[119] When ADMA is encapsulated in both hexyl-pyrogallol[4]arene (acetonitrile and ethyl acetate) and decyl-pyrogallol[4]arene (ethyl acetate) hexamers, it resides in both the *exo*-capsule within the pendant chain (Figure 22) and the *endo*-capsule (inside the hexamer), it had an enhanced fluorescence emission intensity compared to the free ADMA.[120]
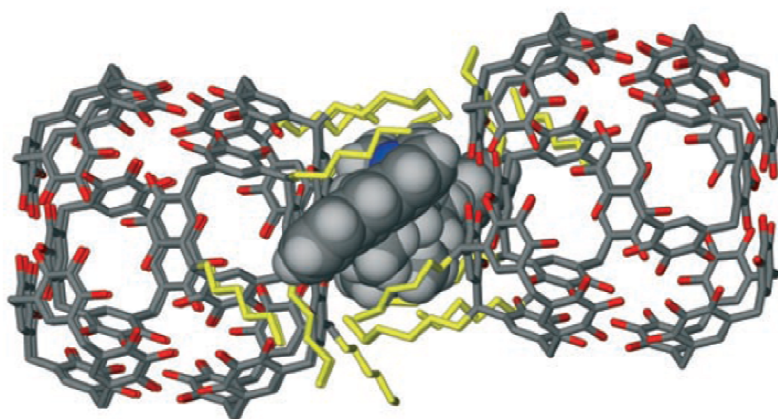
Figure 22: ADMA (spacefilled) intercalated into the pendant chains (yellow)[119]

36

Although much research has been performed on the resorcinarene derivatives and their extended cavitands, less has been achieved on the pyrogallol[4]arene. Although they have similar structures and only differ by the number of hydroxyl groups available for hydrogen bonding. By reviewing the latest research on the resorcinarenes, it is possible to understand their behaviour and properties which could be extrapolated to pyrogallol[4]arenes.

a) Modification of the upper rim

Resorcinarenes are a well-studied class of molecules that have received much interest in recent years, mainly as carcerants or cavitands. Cram and co-workers have made an enormous contribution to this class of macrocycles, by developing novel synthesis to extend their cavity that can accommodate bigger guests.[21, 121] Gibb has also created a new range of "deep-cavity" cavitands, by extending the upper rim of resorcinarenes.[122]

The resorcin[4]arene upper rim is modified by bridging the phenol hydroxyl groups at position 1 and 3, leading to cavitands that can be easily functionalised at the lower rim. This enforced cavity induces a synthetic viability with rigidity, but removes the ability to self-assemble *via* hydrogen bonding. The basic cavitand is made from a simple methylene bridge, (R_1=H in Figure 23) or extended with other aromatic rings, such as resorcinol (R_1=$C_6H_3(OH)_2$) which is available for further substitution.[123]
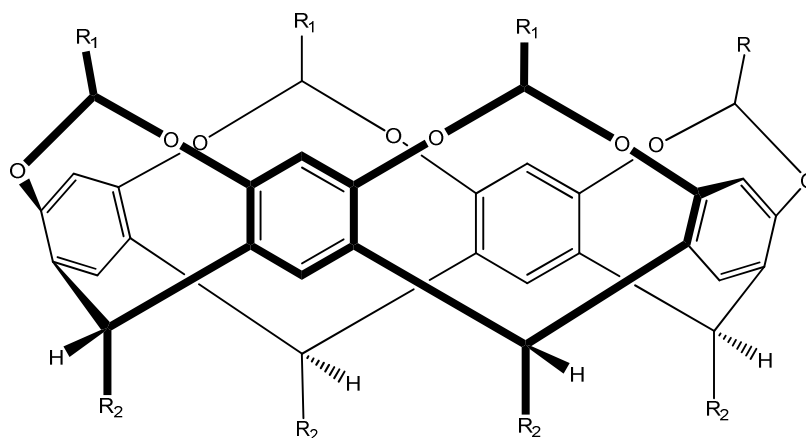
Figure 23: Ethylene bridged cavitand

Other aromatics such as pyrazine, quinoxaline (Figure 24) and benzimidazole can be directly bound to resorcinol to form switchable cavitands whereby the upper rim can be transformed from a deep cavity to a flat extended surface.[24, 124]
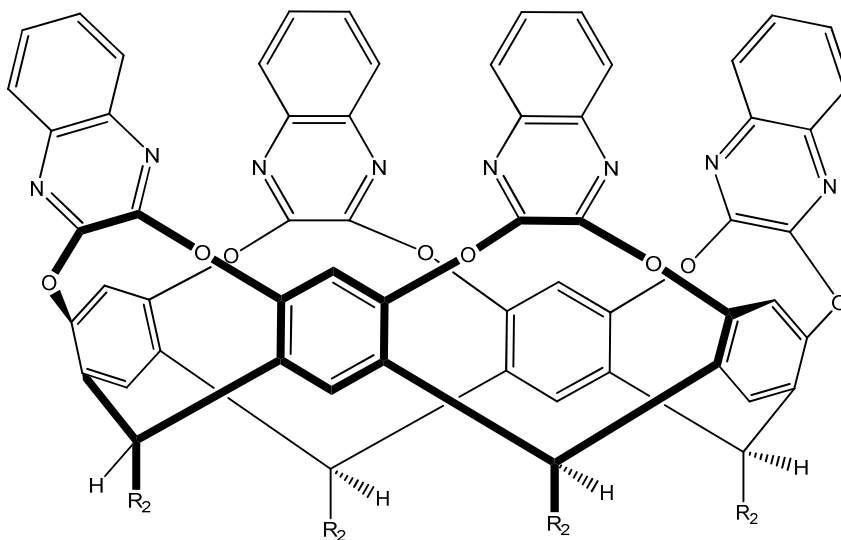
Figure 24: Quinoxaline bridged cavitand

The first readily accessible preparation of the bridged cavitands containing pendant chains with sensitive functionality such as alcohols was achieved using ethylene ditosylate, as well as bromochloromethane, and silicon bridging using trimethylsilyl chloride. The resulting cavitands were typically synthesised over one to two days under mild temperatures (40 - 60 °C) in a 10 to 80% yield. [125]

Amino acid derivatives, as well as small peptides, were attached on the upper rim of the cavitands in order to obtain a model synthesis for de novo proteins, using the rigid macrocycle as a scaffold. This was achieved by transformation of phenols and thiophenols on the 2-position of the upper rim of the cavitands with halo-acetylated peptides (Figure 25). This methodology was also applied to the cyclotriveratrylene (CTV) macrocycle and their ability to hydrogen bond was measured by IR and NMR spectroscopy.[126]

A series of *di-* and *tri-*peptides have been attached onto the upper rim of the cavitands *via* a 1-ethyl-3-(3-dimethylaminopropyl) carbodiimide and hydroxybenzotriazole (EDC/HOBt) coupling, affording a stable inclusion complex with acetonitrile in chloroform solution. To date, it is one of the rare peptide-cavitand based on resorcinarenes.[127]

(a)

(b)

R=OCH₂CO-Phe-OEt
R=OCH₂CO-GlyGly-OEt
R=SH(CH₂)nCO-Phe-OEt
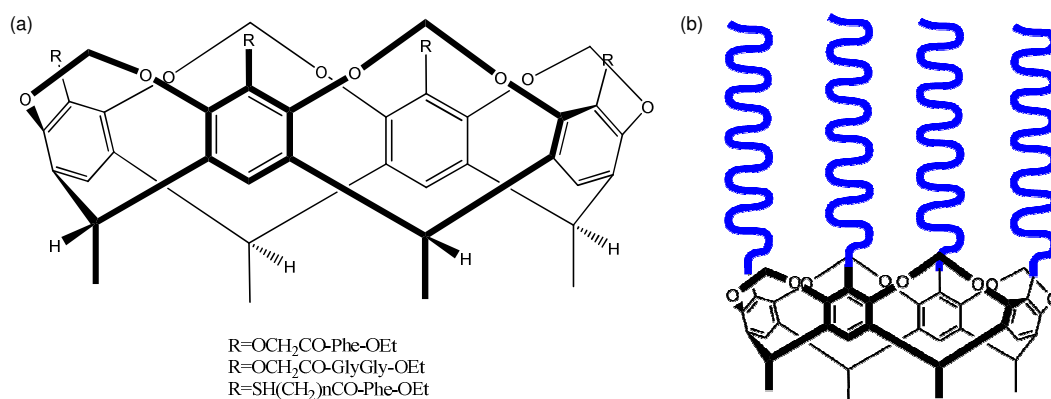
Figure 25: Peptido-cavitands (a) precursors, (b) its schematic view

In the study towards water soluble cavitands, a series of methylene bridged resorcin[4]arenes containing hydroxyls and phosphates at their lower rims with bromoethyl and thiomethyl on their upper rim have been investigated.

The introduction of a bromine at the phenolic 2-position was achieved by bromination of resorcin[4]arenes using *N*-bromosuccinimide, and subsequent transformation led to a thiol using thiourea.[125] These new materials can be further functionalised and used as building blocks for aqueous supramolecular chemistry.[128]
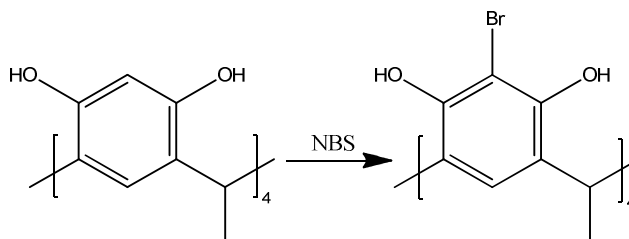
Scheme 4: Bromination of resorcin[4]arene[129]

Commonly, methyl-resorcinol derivatives are obtained from the commercially available 2-methyl-1,3-*di*-hydroxybenzene. Cram *et al.* speculated that cyclic tetramers could not be obtained from any aldehyde with either 2-nitroresorcinol, 2-bromoresorcinol or 2-carboxyresorcinol, due to the deactivation of the resorcinol nucleus towards electrophilic substitution; both with respect to forming cyclic oligomers and equilibrating them once formed. Instead, the cyclic macrocycle must be preformed and then functionalised.[21] A number of resorcinarenes have been transformed in this respect by replacement of the hydrogen in the 2-position of resorcinol by different functional groups, examples include the aminoethyl, sulfomethyl, alkoxy, acyloxy and bromethyl. The attachment of an oxidising agent such as

(2,2,6,6,tetramethylpiperidine-1-yl)oxyl (TEMPO), or a more biologically relevant group such as L-proline have been utilised in this manner.[130-138] These last transformations were either achieved on the unprotected resorcinarene or on the protected macrocycle, *i.e.* the transformation of octa-O-methyl resorc[4]arene.[139] Other derivatives such as hydrazinocarbonyl-methyl-resorcinarenes and pyrogallolarenes were synthesised for their unique inclusion properties with promising binding ability for metal extraction.[140]

b) Modification of the pendant chains

The nature of the calixarenes is highly dependent on their pendant chains. These chains have been reported to play an essential role in the structural conformation, solubility and self-assembly of the macrocycle.

(1) Apolar derivatives

Alkyl derivatives are by far the most studied due to their ease of formation and their high solubilities in organic solvents. In early work, Cram synthesised a library of aliphatic and aromatic resorcinarenes as building blocks for cavitands in order to understand the limitation of the condensation to the tetramers and the investigation into the various symmetries.[21] Most of the aromatic pyrogallol[4]arene reported in the literature are in the *rctt* chair conformation (Figure 26), which although it is the kinetic product, is found to be the predominant isomer observed with aromatic pendant chains.[141-142] Various substituted phenyl-pyrogallol[4]arene macrocycles (cyano, bromo, chloro, fluoro) have been synthesised in the *rctt* conformation *via* the acidic condensation of the respective aldehyde with pyrogallol under reflux for one day. Many of these have been crystallised in DMSO and studied in the solid state. [143] The effect of the aromatic substituent at the four position has been assessed in some details.

The steric and electronic properties of the aromatic substituent on the pendant chains are reported to play a role in the host ability to bind the guest. The strength of the hydrogen bonding can also be increased *via* the fluorine substituent.[144]
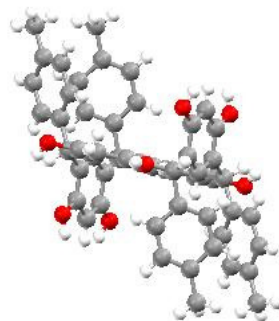
Figure 26: Example of the rctt chair diastereoisomer

A series of aromatic pyrogallol[4]arenes (C_6H_5, *p*-$C_6H_4CH_3$, *p*-$C_6H_4OCH_3$, *p*-C_6H_4Cl, *o*-$C_6H_4OCOCH_3$ and *p*-$C_6H_4OCOCH_3$) were synthesised as the *rctt* isomers by microwave irradiation in 2-ethoxy-ethanol. These were further acetylated or alkylated at the upper rim *via* the use of acetic anhydride or benzyl bromide.[57] Microwave-assisted synthesis was employed to alkylate tetra-*p*-hydroxyphenyl-pyrogallol[4]arene in the *rctt* chair conformation with comparable results compared to the conventional heating methods.[58] A series of acylated phenyl and ferrocenyl pyrogallol[4]arenes were synthesised using a microwave protocol showing the *rctt* and the *rccc* conformations respectively.[145]

(2) Polar derivatives

In order to develop calixarenes that can be further functionalised at the lower rim, functional groups such as amino, carboxylic acid and thiols have been attached at the pendant chains. However, their synthetic precursors must be first prepared. The table below represents all the documented derivatives of this class of functionalised macrocycles (Table 2), as seen in Scheme 5, R is the function on the 2-position of the dihydroxybenzene and R' the pendant chain.
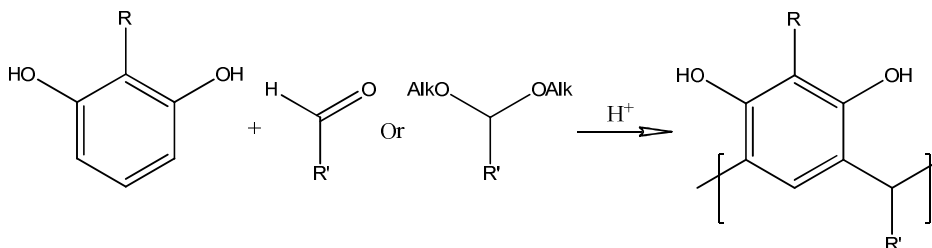
Scheme 5: Synthesis of resorcin[4]arene (H) or pyrogallol[4]arene (OH) with alkyl (R) or aryl (Ar) chains

Cycle (R)	Chain (R')	Synthesis via		Ref.
		Ald	Other	
H	$(CH_2)_2SO_3^-$		✓	146
OH	$(CH_2)_4Cl$	✓		147
OH	$(CH_2)_8Br$	✓		147
H	$(CH_2)_4OH$	✓		21, 125
H	$(CH_2)_3OH$	✓		125
Br	$(CH_2)_4OH$	✓		125
Br	$(CH_2)_3OH$	✓		125
H	$p\text{-}C_6H_5Br$	✓		21
H	$p\text{-}C_6H_5NO_2$	✓		21
H	$(CH_2)_5Cl$	✓		21
H, CH_3	$MeC(O)N(CH_3)CH_2, CH_2NH_2, CH_2N(CH_3)PO(EtO)_2,$ $CH_2NHCH_3, CH_2NHC(O)NHPh$	✓		148
H	$(CH_2)_3NHBoc$		✓	149
H, OMe	$CN, CH_2OH, CH_2Br, CH_2N_3, CH_2NHAc, CH_2NH_2$ CH_2COOH and dipeptides		✓	150-153
H	$(CH_2)_{10}SH$		✓	154

Table 2: Documented polar footed derivatives aldehyde (ald.) is ticked when the derivatives are synthesised from the aldehyde or its acetal.

Highly water soluble tetraethylsulfonate derivatives of 2-methyl-resorcinarenes have been used as an additives in capillary electrophoresis.[146] The resorcinarene derivatives were bound to hydroxyproline groups *via* a Mannich condensation and evaluated as a chiral NMR solvating agent.[138] Chiral phase-transfer catalysts derived from cinchona alkaloids were prepared for the enantioselective synthesis of α-amino acids with good results.[155]

The first tetrasulfonate derivative (R=$(CH_2)_2SO_3Na$) of resorcin[4]arene provide the host with the ability in water to interact with guests such as hydrophobic monosaccharides and nucleosides.[156] Sulfonato-footed resorcin[4]arene containing *L*-proline moieties have found application as chiral NMR shift reagent for aromatic guest in water.[157]

Gibb synthesised hydroxyl derivatives of resorcin[4]arene as precursors to hydroxyl cavitands, using dihydropyran and dihydrofuran as masked aldehydes.[125] The monofunctionalised alcohol resorcinarene was synthesised by monoepoxidation of an alkene and then attached to a polymer in an eleven steps synthesis.[158] Monofunctionalised resorcinarenes can also be synthesised in low yield, in a single step, by reacting three equivalents of one alkylaldehyde, with one equivalent of the functionalised aldehyde, such as 3,4-dihydro-2*H*-pyran, with four equivalents of resorcinol.[159]

Phosphate derivatives of methylene-bridged resorcin[4]arenes are accessed by phosphorylation of the hydroxyl feet with *di-tert*-butyl-*N,N*-diethylphosphoramidite (DDP) followed by oxidation with hydrogen peroxide and subsequent removal of the *tert*-butyl group with trifluoroacetic acid (TFA).[128] These phosphorylated resorcin[4]arenes synthesis can be simplified by reacting resorcinol with phosphorylated acetals.[148]

Four cavitands modified at the lower rim with cyano and pyridyl functional groups (Figure 27), have been coordinated to transition metals such as Ni(II), Ag(II) and Pd(II). They have been obtained by acetylation of hydroxyl-footed cavitands with isonicotinoyl chloride hydrochloride; this can only be done on the cavitands as the presence of the free phenols will interfere with the reaction. [160] Halogenated derivatives have been obtained and crystallised both in a bi-layer structure and hexamer analogous to those reported for the alkyl pyrogallol[4]arenes.[147] However, this study is limited to solid state studies.
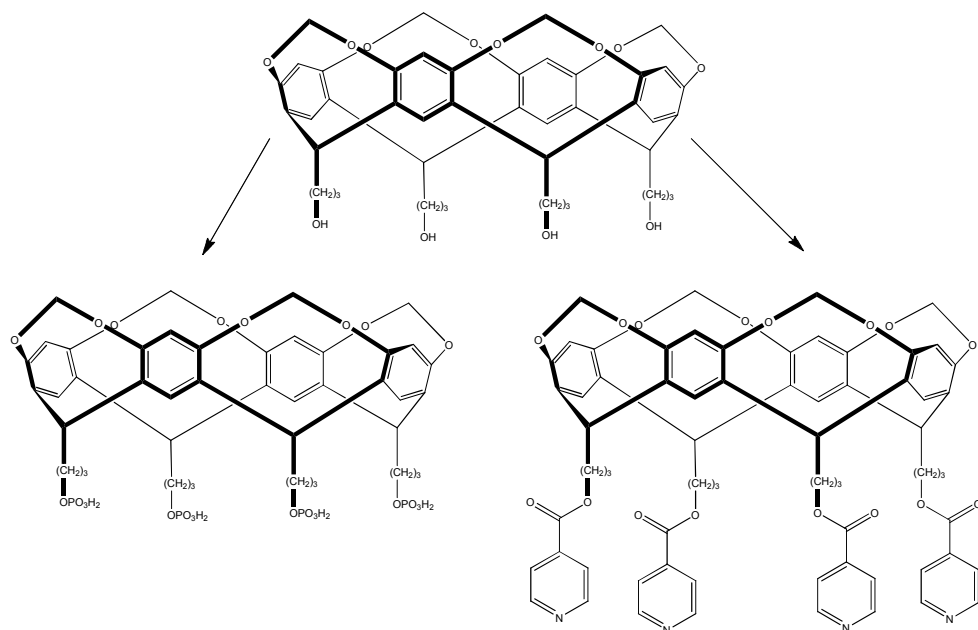
Figure 27: Modified cavitands

Boc protected amine footed extended cavitands were developed, in order to engineer water soluble cavitands that can mimic receptors by modification of *C*-hydroxybutyl resorcin[4]arene.[149] It was a lengthy process of six steps, (Scheme 6) which involved several protection and deprotection steps with an overall yield of 31%.

The cavitands were then used as hosts in NMR spectroscopy binding studies with many water-soluble amines as guests.[161-162]

a) BnBr, NaI, K$_2$CO$_3$, acetone, 58%
b) MsCl, Et$_3$N, CH$_2$Cl$_2$, 91%
c) NaN$_3$, DMF, 80°C, 76%
d) Boc$_2$O, Raney/Ni, H$_2$, EtOH/EtOAc, 90%
e) Raney/Ni, EtOH, 95%
f) 1,2-Di-fluoro-4,5-dinitrobenzene, Et$_3$N, DMF, 70°C, 91%
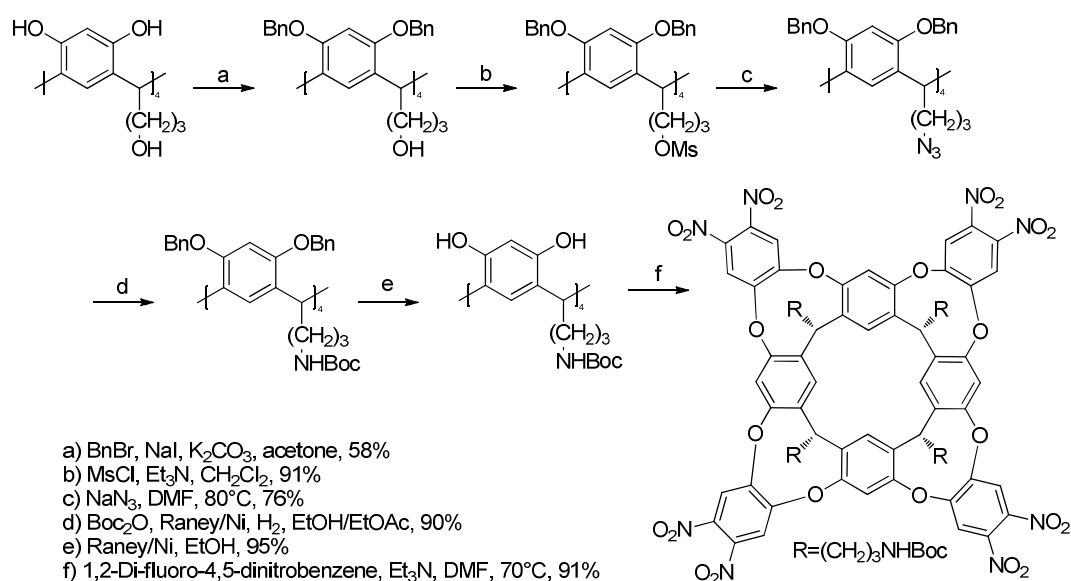
Scheme 6 : Synthesis of the amino footed cavitand

The same cavitands were immobilised, by their pendant chains, onto a polymer base *via* isocyanate linkage to understand the ability of self-recognition and the formation of inclusion complexes on supports. The hydroxyl footed derivative was attached *via* formation of tetrahydropyranyl ethers.[163] Amino and nitrile calixarenes were immobilised on a polymeric backbone to evaluate the ability of chromium extraction with promising results.[164] The reaction of *N*-functionalised acetals, such as phthalimidoacetal derivatives with resorcinol and methyl-resorcinol, lead to resorcin[4]arenes which can be hydrolysed with hydrazine hydrate in a basic solution to the corresponding amine (Figure 28).[148]

R= H, CH$_3$
R'=MeC(O)N(CH$_3$)CH$_2$, CH$_2$NH$_2$,
CH$_2$N(CH$_3$)P(O)(EtO)$_2$,
CH$_2$NHCH$_3$, CH$_2$NHC(O)NHPh
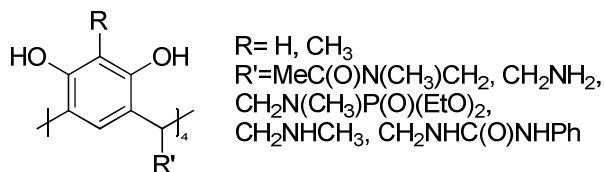
Figure 28 N-Functionalised resorcin[4]arene

Only the halogenated salt dimers are obtained by mixing equimolar quantities of resorcinol and methyl resorcinol with *N*-methylaminoacetaldehyde. The free amine

44

could not be isolated due to the ionisation of the hydroxyl groups in alkaline media and the formation of soluble phenolates. The dimer was then reacted with formaldehyde using the acidic aqueous mixture to form a tetramer (Scheme 7). Linear oligomers linking two pendant chains were also obtained by addition of diisocyanate.[165] This approach demonstates potential to control the formation of difunctionalised calixarenes.
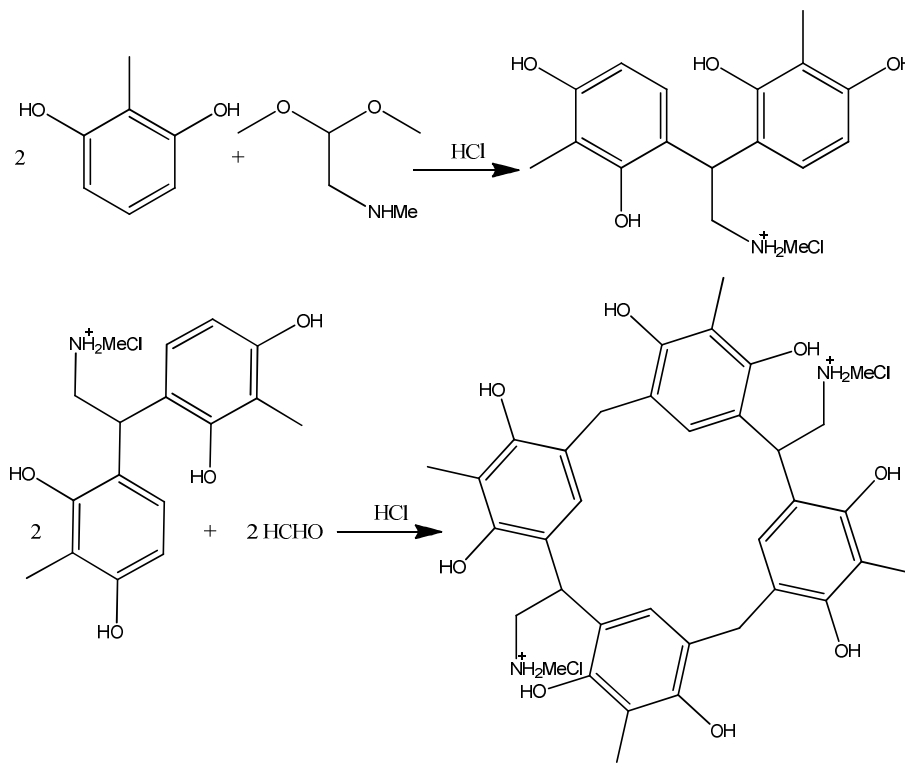
Scheme 7: Synthesis of methylresorcin[4]arene with two N-methylaminomethyl pendant chains

Using a different approach, a resorcin[4]arene octamethyl ether tetrabromide was obtained from a tetraalkyl derivative and transformed to a tetraamine *via* the tetraazide as the reduction from the tetracyanide was not a viable route.[152]

Tetrathiol footed resorcinarene derivatives with various functionalities on the upper rim, obtained by anti-Markovnikov addition of a thiol to the terminal double bond of an alkenyl pendant chain,[166] were investigated as a self-assembled monolayer absorbed on gold.[167] Their selective guest-host associations with lactones were investigated.[154] In similar work the interaction of self-assembled monolayers (SAMs) of thiocalixarenes on gold films with bovine serum albumin (BSA) was investigated by surface plasmon resonance (SPR).[168] A series of mono functionalised thio-derivatives at the lower rim were prepared by convenient differential protection or derivatisation of the upper and lower rims.[169] Thiol footed resorcinarene derivatives have also been

employed as a building block for a novel stationary phase bearing polar head groups in reversed phase HPLC.[36]

(3)   Biologically relevant derivatives

(a) Calixarenes

Peptidocalixarenes have received little attention compared to other substituted calixarenes, although they have interesting molecular recognition properties.[170] *N*-linked dipeptides have been attached onto protected calixarenes (Figure 29a) *via* the acid chloride derivatives,[171] and used to assess their ability to bind various amino acids.[172] *C*-linked dipeptides were described later and were found to have better interactions with anion interactions than their *N*-linked derivatives. Alanine was attached on the upper rim of calix[4]arenes and their ability to self-associate into a dimer was assessed.[173]

A class of calixarene based hydrogen bonding receptors was obtained by linking amino acids, peptides and sugar moieties to calixarenes.[174-175] Ungaro's group have concentrated on the synthesis of *N,C*-linked peptide-calix[4]arenes as "pseudo-peptides" and the study of their conformational self-assembly and molecular inclusion properties.[176] New linear and cyclic *N,C*-linked peptido-calix[4]arenes were produced by condensing calix[4]arene based amino acids during the step-wise elongation sequence of a peptide using solid phase microwave synthesis based on fluorenylmethyloxycarbonyl (Fmoc) chemistry (Figure 29).[177]
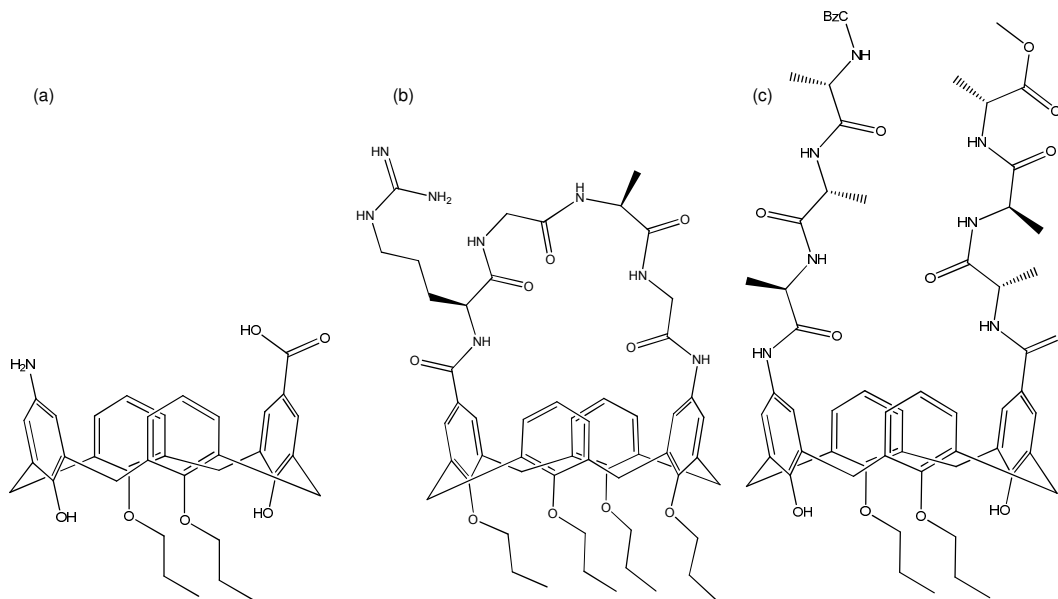
Figure 29: (a) Amino-carboxylic acid calix[4]arene, (b) cyclic peptide calix[4]arene (c) protected di-C,N-trialanyl calix[4]arene

Using the upper rim to add functionality impedes the cavitands' ability to self-assemble into globular structures and therefore only their inclusion properties can be exploited. Interestingly, only two of the four hydroxyls on the bottom rim were protected in order to functionalise the upper rim. As they disclosed in the study, the two hydroxyl groups played an important role to reduce the conformational flexibility through hydrogen bonding. By comparing the role of the phenols for calix[4]arene and pyrogallol[4]arene, it be can assumed that the 2-position of the pyrogallol, that is not involved in the intramolecular hydrogen bonding, may still interfere with the functionalisation.

(b) Resorcin[4]arenes

In the nineties, Botta *et al.* discovered a novel route to protected resorcinarenes with ester functionalised pendant chains. The tetramerization of 2,4-dimethoxycinnamates with a Lewis acid, $BF_3.OEt_2$, resulted in the 1,2-alternate, the 1,3-alternate and the flattened- cone conformers.[178] The reaction was then optimised for an increased selectively to the flattened cone (60%) and an 1,2-alternate chair (40%) conformations.[50] Studies were extended to the formation of a resorcinarene lower rim "basket" (Figure 30).[150, 179]
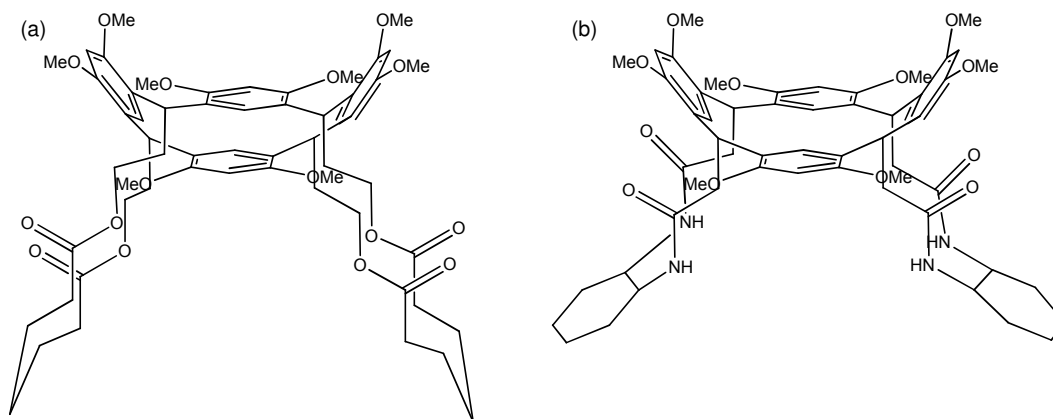
Figure 30: Lower rim basket (a) with polymethylene bridge, [179] (b) diaminocyclohexane chiral bridge.[150]

Chirality was introduced by functionalisation of the pendant chain with *D*- and *L*-valine.[180] The enantioselectivity of binding of the amido[4]resorcorcinarene cavity was assessed with a range of amino acids.[181-182] The host-guest binding is highly dependent on the conformation of the macrocycle.[183] The flattened cone favours the

enantioselective allosteric effect.[184] The selectivity in the gas phase allows the separation of three classes of amino acids.[185] Their complexes with aromatic amino esters are stable in both gas phase and solution and have the potential to show a receptor ability for amphetamine[186,187] The side chains can interact with various metals including iron and copper.[151-152] They also complex with nitrosium and vinca alkaloids. [153, 188]

In 2007, the formation of peptidoresorcinarenes (Figure 31), by conjugation of the acid chloride derivatives with peptides, showed that recognition also occurs on a larger scale.[189] The macrocycles are capable of recognising the homologous dipeptides (valine-leucine) as guests both in solution and in the gas phase. They are also reported to be resistant to chromatographic purification but not to heating.[190]

The gas phase enantioselective reactions in non-covalent ion-molecule complexation have recently been investigated.[191] Their potential to form adducts with ethanolamine neurotransmitters showed potential.[192]
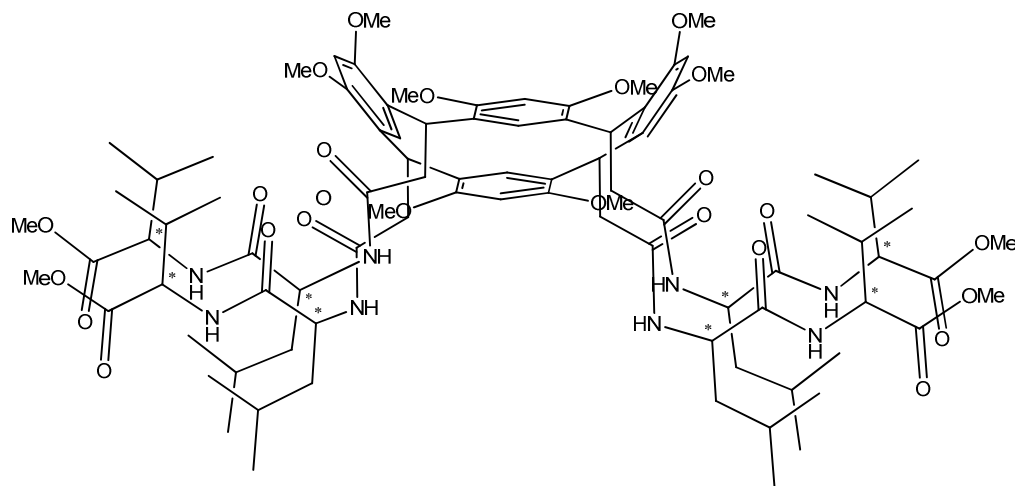
Figure 31: Peptide footed methoxyresorcinarene[190]

In all reported cases of lower rim amino functionalised resorcinarenes, the upper rim is protected *via* an ether. However, there has been no reported attempt to deprotect the upper rim to free the phenolic hydroxyls. If this was achieved the macrocycle could act as a host by exploiting its hydrogen bonding potential for amino acid. It is also noticeable that the lower rim can be functionalised on each of its four feet, which means that the steric hindrance should not play an important role in the attachment of peptides, although a protection step may be required.

In the only example of a peptide attached on one foot of the unprotected resorcinarene, an small anti-inflammatory peptide was attached onto a pegylated chain of a resorcinarene and immobilised on glass in attempt to generate an bioactive anti-inflammatory model.[193] The monofunctionalised precursor of this macrocycles was obtained after protection of the upper rim by hydroboration/oxidation of the monoalkene, or radical addition of a mercapto derivative (Figure 32).[169]

It would be interesting to see how the presence of extra hydroxyl on the upper rim would interfere with the recognition and therefore similar work should be considered, applied to the synthesis of new class of molecules: the peptide footed pyrogallol[4]arenes.
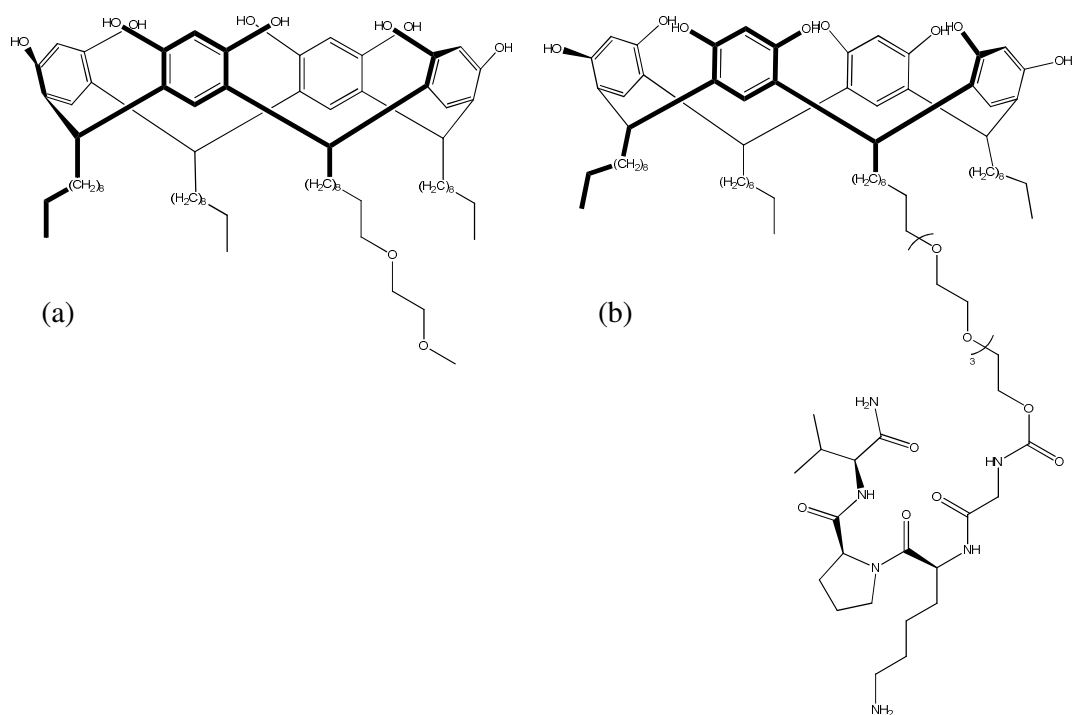
Figure 32: Pegylated (a) precursor (b) peptido-resorcin[4]arene.[193]

49

B. FROM SUPRAMOLECULAR TO NANOMEDICINE

Exploiting the ability of pyrogallol[4]arene to self-assemble into nanocapsules, with twenty-four pendant chains assuring multi-functionality, they will be considered as nanovectors for cancer immunotherapy.

1. NANOTECHNOLOGY AND NANOMEDICINE

a) Nanotechnology

Nanotechnology, which has bloomed in the last twenty years, is defined as the knowledge of technical operation (technology) in the nanometre-scale (10^{-9} m) and encompasses anything from 0.1 to 100 nanometres.

Although often represented as reduced sized apparatus or robot able to solve problems, this theoretical view needs to be demonstrated. Nanotechnology now has many definitions and may be the seed of some scientific arguments,[194] but the appeal towards nanotechnology remains thanks to its interdisciplinary nature and its purposes. Realising their potential, European governments and funding bodies are looking to invest more in nanotechnology related projects in the future years.[195]

The range of applications is wide and nanomaterials are already components of some everyday products. Nanomaterials are used in energy production as fuel catalysts and photochemical devices for solar thin-films. Titanium dioxide and zinc oxide nanoparticles are used in sunscreen and anti-wrinkle cosmetics. Nanopore properties are exploited by fabric manufacturers to render the materials stain or perspiration resistant. Nanocomposites are introduced into car parts to make them lighter, cheaper and with higher resistivity, in the same way that carbon nanotubes are used in tennis rackets.[196-198]

Nanomaterials can be designed by the top-down approach, whereby nanometre scale components are obtained by reduction of larger materials, using micro- or nano-fabrication methods. While the bottom-up approach is the synthesis of nanostructures and nanomaterials by means of nanochemistry, using supramolecular and biomimetic systems.[8]

Scientists are now able to engineer molecules to achieve their goals by controlling matter on the molecular or atomic scale. Thanks to the development of different analytical technologies including X-ray crystallography, TEM, SEM, atomic force microscopy (AFM) and two-photons to microscopy techniques, it is now possible

to visualise and analyze matter on the nano-meter scale, which was not possible a few years ago mainly due to the lack of computing tools.

b) Nanomedicine

Most biological pathways, such as DNA pairing and antibody or receptor recognition also occur at the nanoscale, (Figure 33) and therefore nanomaterials have the ability to interact on the cellular level, highlighting the possibility of a new type of treatment based on nanomedicine.
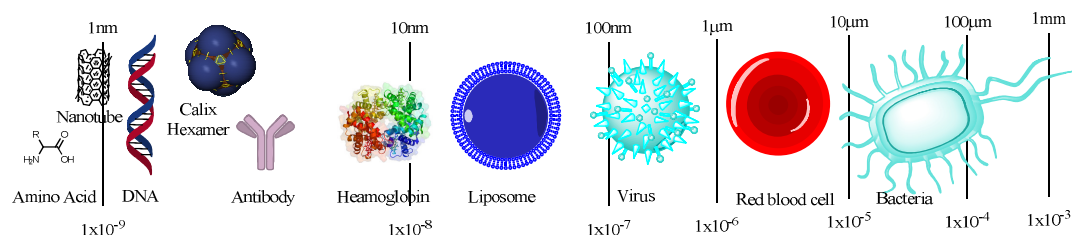
Figure 33: Nanoscale and biological systems

Richard P. Feynman, Nobel physicist in 1965, was one of the visionaries of nanomedicine. He described his view on the future of medicine in a lecture in 1959.[199] Over fifty years later, nanomedicine is an innovative science that uses new technology and engineered nanomaterials to selectively treat diseases. The latest researches in nanomedicine focus on imaging, diagnosis and treatments of disease including cancer, infections, inflammations, metabolic and autoimmune disease but also tissue engineering and regeneration.[200-201]

In this field, the nanomaterials taxonomy is broad "nanopharmaceuticals", "nanoparticles", "nanocapsules", "nanospheres", "nanovector", "microcapsules", "microspheres", "colloidal carriers" and "lattices". Nevertheless, they all describe any materials in the nanometre scale with biological purposes.

A review on recent progress for the rational design of therapeutically active polymer based nanoparticles retraced the latest development in nanomedicine. The main events in the advancement of nanomedicine are summarised in the following timeline (Figure 34).[202-203]
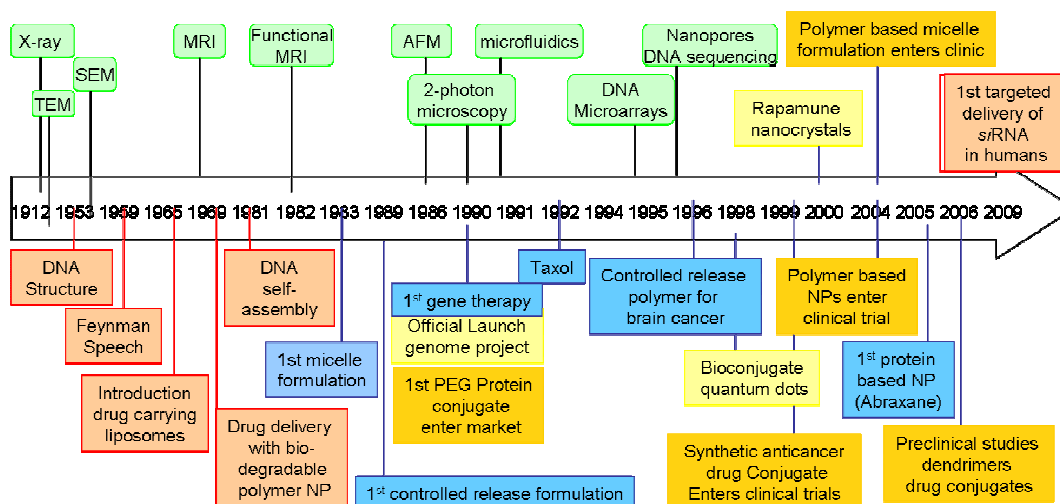
Figure 34: Timeline of the main discoveries in nanomedicine, (adapted from[214-215])

Although great breakthroughs have been achieved in nanomedicine, their applications in diagnosis seems to surpass those in therapeutics, maybe due to the safety concerns that still remain to be addressed.[204]

Sanhai summarised them into seven challenges to overcome:[205]

- determination of the distribution of the nanoparticulate carriers in the body following systemic administration through any route
- understanding of mass transport across compartmental boundaries in the body;
- development of radiolabelled nanoparticles;
- prediction of risk and benefits;
- establishment of standards or reference materials;
- development of new mathematical and computer models;
- realisation of an analytical toolkit for nanopharmaceutical manufacturing.

As a result, approval by the food and drug administration (FDA) and its British equivalent, the medicines and healthcare products regulatory agency (MHRA) can be challenging. Generally due to the novelty of those nanopharmaceuticals that can play an important role in the drug formulation. So far, the FDA approved nanomaterials that dominate the research of drug delivery are based on liposomes and a polyether, polyethyleneglycol (PEG).[215]

The multiple pathways involved in the processing of the nanoparticles are still insufficiently understood, due to the novelty and the multifunctionality of those materials. Some work still remains to be completed to obtain homogeneous distribution of the drug, with a high drug loading that must retain in the carrier until destination, and

the release of the drugs must be controlled.[204] Their routes of excretion certainly differ from the free drugs and are still not fully defined. In addition, more *in vivo* studies are needed to reinforce the studies performed in *in vitro* cell lines.

An appreciation of the behaviour of the biomaterials within the body is essential; it depends on the size, shape, surface and the cytotoxicity of the nanoparticles. The biological barriers encountered by any pharmaceutical exist at different levels. Some organs act as a natural filter and only let through particles under a certain size. The spleen only tolerates particles from 200-250 nm, whilst the liver excludes particles over 150 nm and particles under 5 nm are removed by extravasation or renal clearance.
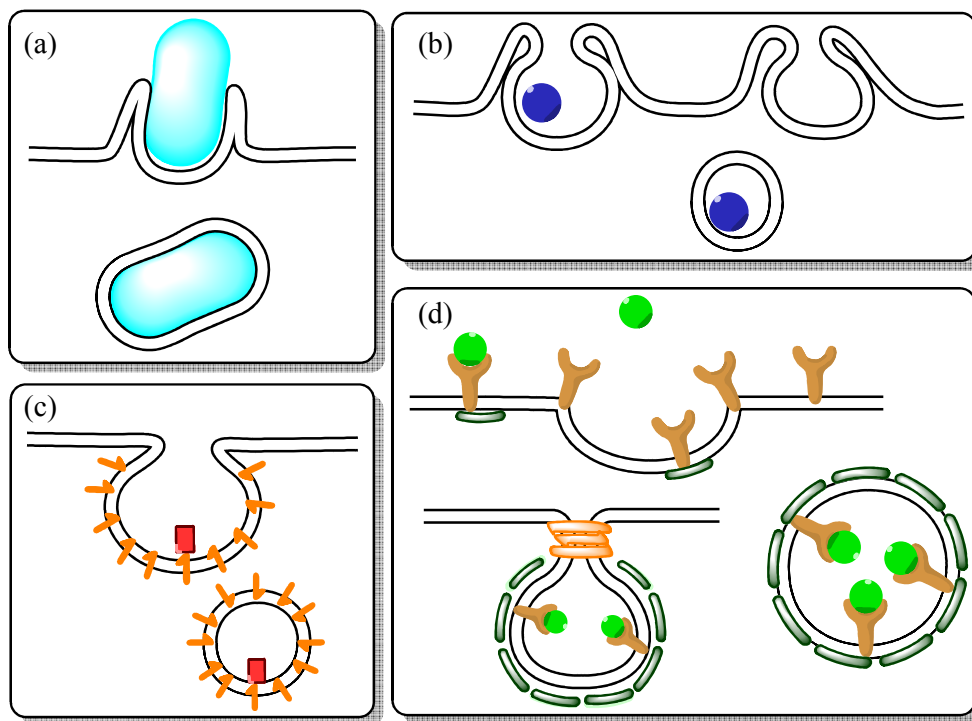
Figure 35: Endocytosic pathways: (a) Phagocytocis (b) macropinocytosis (c) caveolar endocytosis (d) chlatrin mediated endocytosis [202]

At the cellular level, the first barrier is the mononuclear phagocyte system (MPS) or reticuloendothelial system, which eliminates particles from 100-200 nm. Endocytosis is one of the key process for the nanoparticles internalization at the cellular level.[206] It can be sub-divided into four main categories: phagocytosis, clathrin-mediated endocytosis, caveolar-mediated endocytosis and pinocytosis (Figure 35). Phagocytosis generally happens first, in phagocytes, and it is size-independent. Clathrin-mediated endocytosis, which is the main route of cellular entry is usually involved in the uptake of essential nutrients in mammalian cells and is receptor

53

dependent. Caveolae are a membrane type of lipid raft that can induce endocytosis. Pinocytosis is the only non-specific internalization that is used for the transport of extracellular fluids to the cell. By understanding the endocytosis pathways receptor mediated targeting can be considered, being either passive for particle under 100 nm by the size dependent take-up by the MPS, or active by using specific ligands.

c) Nanomedicine and cancer

Nanotechnology is involved with both cancer detection in a search for high throughput devices and cancer therapy with the aim to find suitable vectors. It could potentially overcome the problems of drug resistance at the tumour and cellular level by improving the cell penetration, as well as reducing its toxicity and increasing the biodistribution, biotransformation and the clearance of anticancer drugs.[200, 207] Tumour capillaries rarely exceed 300 nm, meaning that the nanoparticles can accumulated in tumours, which can be enhanced by the permeation and retention effect (EPR) found in the tumour environment.[208]

The applications of nanoparticles in cancer therapy started to emerge from 1979 and has expanded since.[209] To date, from the eighty-eight clinical trials that are assessing nanoparticles, seventy-one are involved with cancer treatments.[210] From the various types of nanotechnologies involved in cancer therapeutics, the most prominent and most widely studied are nanoshells, carbon nanotubes, dendrimers, quantum dots, superparamagnetic nanoparticles and liposomes as summarised in Table 3.[211-213]

Independently of their nature, they all utilise encapsulation, conjugation (either covalent or non-covalent) and adsorption of modalities such as drugs, peptide, protein, DNA, RNA, antibodies, ligands and stealth molecules (Figure 36). Their main asset is their multifunctionality, which enables them to achieve the recognition and location of the tumour, as well as visualisation and imaging. Release of the therapeutic can be triggered by the use of external factor (*e.g.* hyperthermia, MRI or light), enzymes or a change in the microenvironment, like the acidity around the tumour, or reductive environment in the cytosol (using disulfide bridges).

Nanoparticle drug delivery is thought to improve the therapeutic response to anticancer drugs.[214-215] An interesting example is Doxorubicin, which is a chemotherapeutic agent with many side effects. These adverse effects were reduced by a change in the formulation, by incorporating the drugs into pegylated liposomes and non-pegylated liposomes.

Nanoparticles' class	Size (nm)	Material	Used with	Detection	Therapies
Quantum dots	1-10	CdSe, CdTe, InP, InA	Ab, siRNA Peptides, PEG	Tumour cell labelling	
Superpara-magnetic nanoparticles SPIOs	10 <50	Fe_3O_4	Dextran PEG peptides	Contrast Agent for MRI	Thermal ablation therapy
Dendrimers	<5 <1000	Polymer (C/N) or sugar	Fluorescein Gd	Tracer	Drug delivery
Carbon nanotubes	1-2	Carbon	DNA siRNA		Transport DNA thermal
Nanobeads Polymeric nanosphere	40-50	Polymer	Antigen coated, Enzyme, drugs		Delivery system
Liposomes	90-150	Lipid bi-layer	Drug, RNA, DNA, PEG		Delivery system
Nanoshells	120	SiO_2 core coated with Au shell	Ab-PEG complex		Thermal ablation therapy

Table 3 Nanoparticles involved in cancer therapies and detection
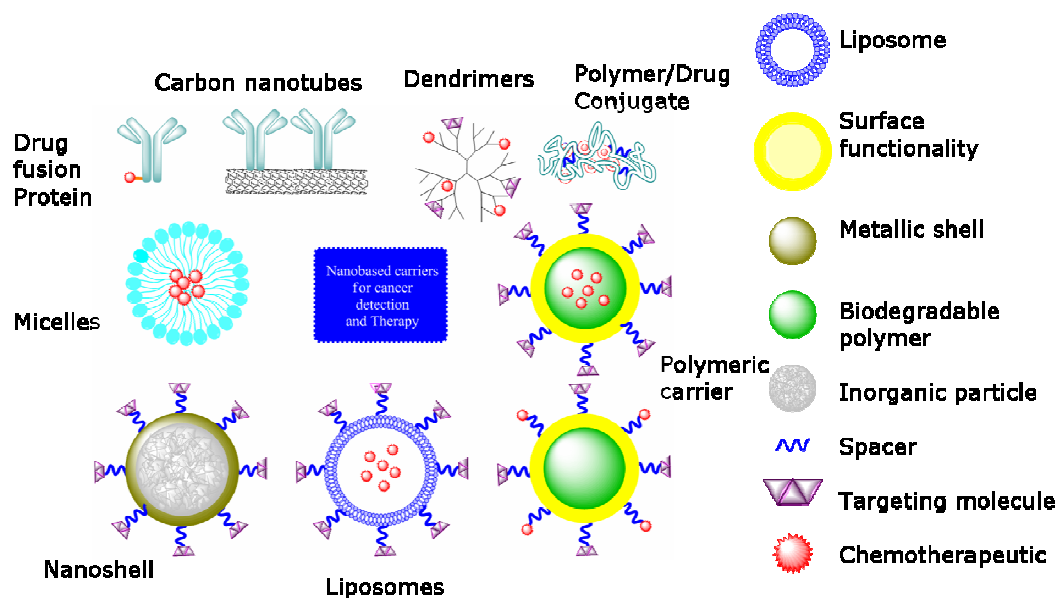
Figure 36: Nanocarriers for cancer detection and therapy[216]

Stealth nanoparticles are made to be unperceivable by the macrophages and are less likely to be excreted. They almost always contain PEG that reduces the uptake by the RES and the MPS and is known to accumulate into tumours.[208] The efficacy of the treatment can be improved by the use of a nanoparticle, by reducing the toxicity using liposomes and micelles, controlling biodistribution (PEGylated nanoparticles) and improving intracellular penetration (PEGylated liposome and micelle). Pegylated entities are covalently bound to polyethylene glycol, which has excellent water-soluble properties and low toxicity. The presence of PEG prevents the absorption by opsonin (binding molecule in phagocytosis) by repulsion of plasma protein due to its hydrophilic properties and results in the non-clearance by the macrophages.

Increase in selective delivery of the drugs to cancerous cells can be achieved by using active targeting molecules for instance *via* the use of folate-binding protein or RDG. The αvβ3-integrin receptors are over expressed on the tumour surface for this cell penetrating peptide.

2. TOWARDS CANCER DETECTION AND THERAPY

a) Cancer Overview

According to the World Health Organisation (WHO), cancer is a leading cause of mortality (13%) in the world. In most of the developed countries, it is the 2nd cause of mortality after heart disease. According to Cancer Research UK, a third of the population will develop some form of cancer during their lifetime. Due to its high incidence, one of the main priorities in pharmaceutical research is the quest for the ultimate cure for cancer. Unfortunately, as cancer can spread in every organ, so far there is no universal therapy.

Over two hundred distinct cancer types exist as tumours can be found within various organs. The most frequent tumour sites are the lung and bronchus (*ca* 30%), prostate (10%) and breast (15%), followed by colon and rectum (10%) and skin (4%).[217]

Cancer is a very complex disease caused by the dysfunction of ones' own cells and is connected with modification of many biological pathways such as gene regulation, signalling and cell metabolism. Although it is recognised to be induced by various external factors such as carcinogenic substances, inflammations or viruses, it is still not fully explained by the somatic mutation theory (SMT) or the tissue organisation field theory (TOFT).[218]

Cancer is defined as an abnormal growth of cells caused by multiple changes in gene expression.[219] The accumulation of new cells results in a new solid growth: a tumour that can be benign or malignant. Benign tumours usually stay encapsulated and remain localised; as they grow by extension, they alter normal tissue functions by pushing them aside. On the other hand, malignant tumours invade and destroy surrounding tissues by metastases. As metastatic cells lose the ability to adhere. They gain invasive properties and an increased capacity to migrate from the primary tumour site to other organs, to grow new mass or tumours through the lymphatic and blood vessels, hence they are also called haematological malignancies.[201, 220] If those cells reach organs that are highly regenerative such as the liver, spreading of the disease can be aggravated.

The alterations in the cell physiology and morphology involved in the malignant growths were classified by Weinberg[221] as the tumour cell's ability to:

- have self-sufficiency in growth signals;
- be insensitive to growth inhibitory (antigrowth) signals;
- evade programmed cell death (apoptosis);
- have limitless replicative potential;
- sustain angiogenesis (growth of new blood vessels);
- invade tissues and metastasise.

All the above pathways are tuned to avoid the tumour cell death and the ability of tumour cells to evade the immunosurveillance, they also contribute to their survival in the body.[222] Although, the immune system is able to detect some tumours, they develop the aptitude to escape the immune surveillance through the production of soluble immunosuppressive factors and the recruitment of immune cells.[223]

b) Detection

Cancer symptoms are cancer type specific and therefore not always obvious enough to detect. The best chances for cancer remission are usually favoured by its early detection, even before the symptoms have started and most importantly before cells start to metastasise. Frequent check ups and routine tests are usually the first stages of detection, especially for prostate and breast cancer.

The most appropriate non-invasive technique to assess the presence of tumour are imaging techniques that give morphological, structural metabolic and functional information. The most commonly used is X-ray based in the form of computed

tomography (CT). In addition techniques such as ultrasonography, scintigraphy (radiodiagnosis) and magnetic resonance imaging (MRI) are also widely used.[224] Imaging is not only used for detection but also for screening, biopsy guidance for detection, staging, prognosis, therapy planning, guidance and response, recurrence and palliation.[225]

If a tumour is found, a biopsy is performed by fine needle aspiration (FNA) or core needle biopsy (BPA) to take a sample of the lesion. It is then analysed by biochemical tests to assess the stage and the aggressiveness of the tumour. The main techniques used are immunohistochemistry to measure the protein expression using labelled antibodies and fluorescence *in situ* hybridisation (FISH) to measure the genetic changes.

c) Therapies

Even though many treatments, either curative or palliative, are available for cancer patients, they are often associated with considerable side effects, mainly due to their non-specificity caused by the challenge of differentiating cancerous cells from normal cells. The choice of treatment depends on the location of the tumour, its stage and aggressiveness; and is generally used post-surgery when the bulk tumours is accessible for removal. Targeted therapies such as immunotherapy, hormone therapy and angiogenesis inhibitors are treatments that are used alone or in combination with the most widely used chemo- and radio-therapy.

Radiotherapy: is used in 50% of the cancer treatments, it employs radiation (usually from X-ray) targeting DNA inside cancerous cells, thus reducing their replicating power. There are two types of internal radiotherapy; brachytherapy (solid source close to tumour) and radioisotope therapy (radioactive substances are injected). Due to its harshness, it comes with both immediate and long-lasting side effects.

Chemotherapy: is the use of drug molecules that affect cell division, in the form of alkylating agents similar to mustard gas and can act as inhibitors, anti-metabolite treatments or topoisomerase inhibitors that inhibit the enzyme that unwinds DNA. [226-227] Chemotherapy usually target fast replicating cells, but unfortunately hair follicle, skin and the cells lining the gastrointestinal tract are the fastest growing cells of the body and are often damaged. The research in chemotherapy is mainly focussing now on improving the treatment by using alternative administration routes and pharmaceutical formulations adjusting both the pharmacokinetics and the pharmacodynamics by using

liposomal and polymeric drug carrier systems.[228]

Anti-angiogenic therapeutics are designed to inhibit the growth of new blood vessels (angiogenesis) around the tumour. These are usually highly vascularised with blood vessels creating a nutrient supplying networks, in an organ-like manner. Commonly they target the inhibition of the vascular endothelial growth factor (VEGF) by the means of human antibodies or drugs and have mild side-effects.

Immunotherapy: exploits the ability of the body's own immune system to fight against various pathogens, especially to respond to tumour specific antigens in order to reduce the growth and produce a long-term immune memory, which may reduce relapse. Its basis will be outlined in more details below.

3. CANCER IMMUNOTHERAPY

a) Cancer vaccine

Cancer immunotherapy can have different aspects; immunoprotective or preventive in the case of cancers that are known to express viral-antigens. One of the most common examples is the cervical cancer vaccine that has been used in the prevention of infection by the human papilloma virus (HPV) in teenage girls. Immunotherapy can also be active, whereby the immune system could potentially be trained to recognise cancerous cell markers, therefore making it able to unlock the cascade of event to attack them. The concept of cancer immunotherapy stems from the proposed function of the immune system, called immuno-surveillance, to protect growing tumours. It appears that the immune system is able to control the tumour development until it undergoes enough mutations to be able to escape the immune system check points.[229]

Research is now concentrating on finding new biomarkers that could not only be used in cancer diagnosis, but will help to target the therapy towards the most suitable treatment and assess the outcome of the therapy. One of the difficulties in oncology research is to find specific markers, which have altered expression in tumours compared to healthy cells. Fortunately, novel techniques such as proteomics and micro arrays have shown promise for their identifications. Cancer biomarkers include mutant genes, RNA, proteins, lipids carbohydrates and small metabolites. The mutant genes are separated into two categories, oncogenes which are responsible for mutations leading to cell proliferation and tumour suppressor genes that are inhibit cell proliferation.[230]

When over expressed they encode for products called tumour associated antigens or tumour specific antigens, that can be both used as targets in cancer immunotherapy.[231]

The recent emergence of many newly discovered tumour associated antigens, thanks to new techniques such as proteomics, is reflected in the number of late stage clinical trials.[232] Cell-based and protein based vaccines are the most commonly used, followed by DNA, virus, antibodies, carbohydrate and mRNA.[233] Each of the vaccine types has its advantages and drawbacks, but in the research of cancer therapeutics field, drug candidates have offered more candidates than cancer vaccines in the last twenty years.[234] Unfortunately many only show weak immune response thought to be caused by the low expression of those over-expressed antigens and the close similarities between cancer and normal cells. The weak or moderate immune response is also due to the inhibition of the high avidity T cells that are suppressed in the thymus. The T cells remaining are only the T reg that do not have the same efficacy in the long term.

b) Immune system

Immunity is separated into two components that are linked; innate immunity and adaptive immunity. Innate immunity is a non specific response that constitutes the first line of defence against pathogens whereas adaptive immunity is specific and varies depending on the pathogen.

Dendritic cells (DCs) are a key player in the immune system as they are at the interface of the innate and the adaptive immunity (Figure 37). Naïve, immature dendritic cells engulf and process antigens leading to their maturation, recognised by the presence of cell surface markers (*e.g.* CD40, CD80 and CD86) and an increased production of IL-12, an interleukin that recruits and stimulates other lymphocytes. Also referred to as professional antigen presenting cells (APCs), once matured, they are able to transport, process and present antigen fragments to specific lymphocytes (B and T) that mediate adaptive immunity.

Major histocompatibility complex (MHC), also known as the human leucocytes antigen system (HLA) in humans, genetically encodes for the MHC molecules that are responsible for the presentation of the antigenic peptides. The MHC molecules are separated in two classes, depending on their structure and their resulting peptide binding clefts.[235] Dendritic cells present endogenously processed antigens, as eight to ten amino acid long peptides, *via* MHC class I to the $CD8^+$ cytotoxic T lymphocytes (CTL) which are then able to recognise and lyse tumour cells. Exogenous antigens, as 13 to 18 amino

acids long peptides, are presented on MHC class II molecules to the CD4$^+$ T helper cells.[236] In humans, DCs are the only cells in the body that constitutively express HLA Class II,[237] which is an important target for tumour immunology.[238]
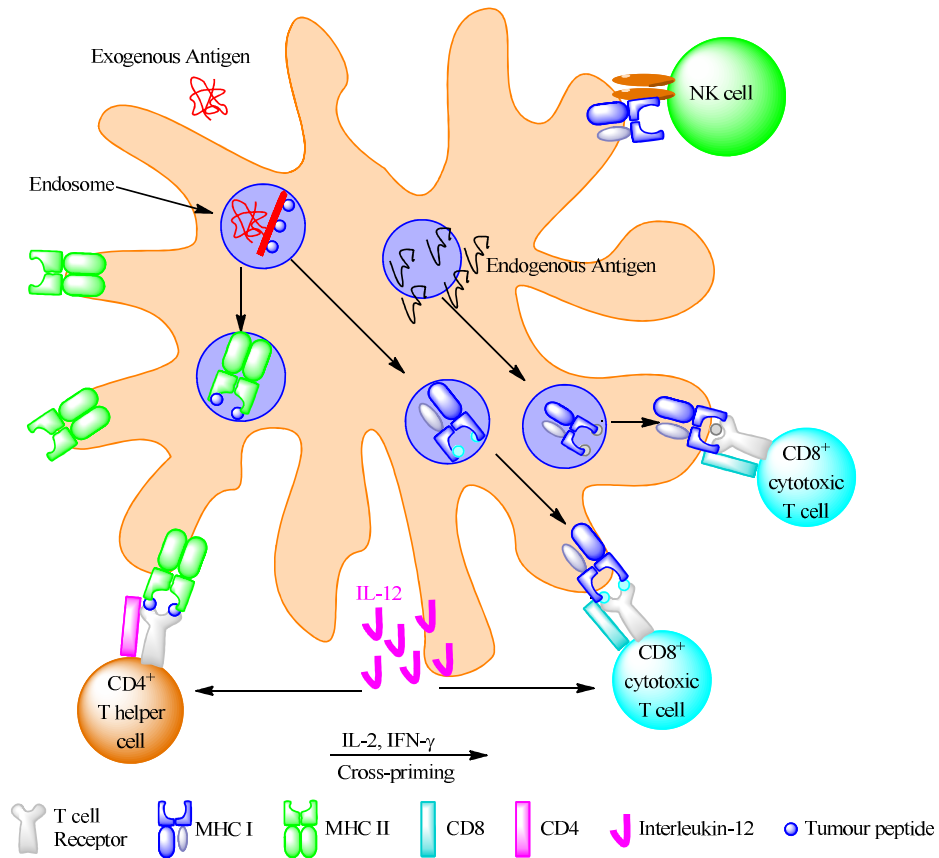
Figure 37: Interaction between DCs and lymphocytes[236]

By involving DCs in the vaccine design, the active therapy can rapidly generate an effective response against a tumour antigen, by activating CTLs and simultaneously generating an immune memory through the B lymphocytes activated by T helper cells.[239] The immune system would therefore be able to recognise recurrent tumours and prevent relapses. Many studies have used different vaccination modalities to generate an immune response in dendritic cells, using different pathogens such as peptides, viruses, bacteria, DNA and proteins, that can be part of the vaccine formulation administrated *in vivo*. Dendritic cells can also be stimulated *ex vivo* when harvested, matured with specific antigens and then reintroduced to the body.[240] More than 150 clinical trials in phase I/II for cancer treatment, mainly melanoma, using or targeting DCs have been reported so far. Although showing some results, they are not clinically consistent enough to be used in a later phase trial.[241]

c) Peptide vaccine

Oncogenes or products they encode for, such as proteins and their truncated versions, peptides, such as previously identified in-house novel immunogenic HLA-DR1 and HLA-DR4 restricted class I/II peptides derived from tyrosinase and p53, are usually over expressed by tumour cells and could be targeted.[242] Compared with cellular vaccines, peptide vaccines have the advantage of being similar to existing vaccine approaches used for decades in immunization programs against infectious agents.[233] The use of peptides as a vaccine modality is increasing due to their availability and the ease with which they can be manufactured at low cost, but it also introduces some challenges.

Synthetic peptide based vaccines can exhibit low immunogenicity, thought to be caused by their rapid biodegradation, the presence of cryptic T cells epitope, the low stability of the MHC-peptide complex or simply their overly high purity (aseptic and endotoxin-free).[243] In addition, APC's preferentially present endogenously synthesised tumour peptides rather than exogenously (or synthetic) derived peptides.[244] This can be overcome by using recombinant viruses that encode for the epitope. The peptide can be released within the cell by introducing a multi-epitope spacer, such as small peptides AAA and NKLR, which contain three trypsin-like cleavage site associated with the proteosome.[245] The choice of the spacer may have its importance as for example using arginine rich peptides can help to cross the cell membrane barrier or aid the endocytosis.[246] The low immunogenicity of highly purified or synthetic antigens, can also be increased by the choice of an appropriate adjuvant in the vaccine formulation.[243]

d) Vaccine adjuvant

A vaccine adjuvant is defined as any component co-administered with vaccines antigens or strategy that improves the adaptive immune response or that stimulates the innate immune system to induce desired effectors or mediators. *In vivo*, adjuvant effects can be divided into delivery and immune potentiation based on their mechanism of action.[247] Individual adjuvants have often more than one mechanism or more than one characteristic. Adjuvant or delivery systems have the ability to stimulate humoral, cellular and mucosal immune responses and induce not only innate but also memory immune responses. This was illustrated by Glaxo Smith and Kline's research for the melanoma vaccine MAGE-3, that has seen significant improvement by transforming their adjuvant mix.[233] Many treatments have been improved by adding some immune

stimulatory molecules and nine successful formulations with varied approaches (*e.g.* Oncophage, BiovaxID, Melacrine, CreaVaxRCC, Hypercell, OncoVax, dSlim/Midge, CimaVax EGF, Provenge) are now on the market. Vaccines based on mixtures of tumour peptides with strong adjuvants like Toll-Like Receptor (TLR) agonists can be potent inducers of the immune response.[229]

Today the most common licensed vaccine adjuvants for humans, throughout the world are salt based, *i.e.* aluminium hydroxide, aluminium phosphate and calcium phosphate. Oil-in-water emulsion like the incomplete freund adjuvant (IFA) are only used in animal models but MF59, a similar nano-sized adjuvant composed of nanodroplets (< 250 nm) with strong immunogenicity, was approved for human use outside the USA. Other potential adjuvants are products of bacteria like lipopolysaccharides (LPS) and their synthetic derivatives (liposomes), which are also widely used.

e) Nanomaterials as cancer vaccines adjuvants
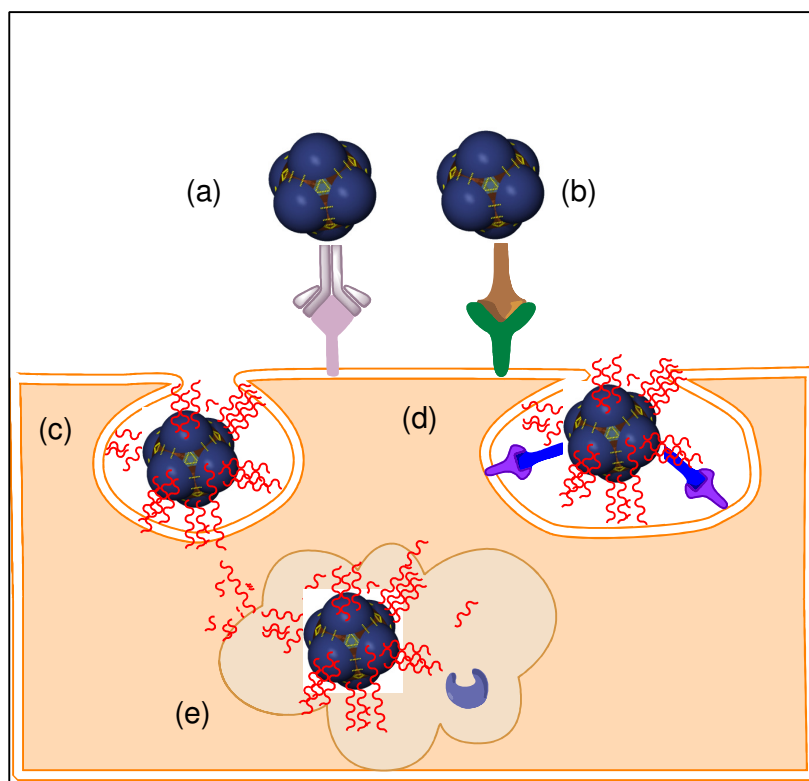
Figure 38: DC interactions with nano-sized materials. Targeting receptors with (a) Antibodies (i.e anti-CD11c) or (b) danger signal, internalization through (c) phagocytosis or (d) receptor mediated endocytosis. (e) Release of the internalised antigen in the cell. [248]

Novel nanoparticle based delivery systems or vaccine adjuvants considered for cancer immunotherapy usually target dendritic cells to deliver the antigen,[249] as they have the ability to interact with biomaterials (Figure 38).[248] Their interaction on the especially on the nano-meter scale is achieved; either by binding them to receptors that then trigger internalization through endocytosis (*e.g.* mannose-grafted particles) or by controlling their size. They can also simply be internalised by macropinocytosis (using nanoparticles in the size range of macromolecules) or phagocytosis (using microparticles) without specific recognition.

A number of nanoparticle based vaccine adjuvants and delivery systems are still under investigations but are not yet approved by the FDA or MHRA as seen in Table 4. Although many are showing good promise, they have not always reached the market as their toxicity is still not well understood.[250]

Adjuvant type	Application
Viral vectored vaccines	Non replicating virus containing genetic material
Virus-like particles and virosomes	Like viral vector without genetic material
Immunostimulating complexes (ISCOM)	*ca* 40 nm cage-like particles composed of protein antigen, cholesterol, phospholipids and saponin adjuvant Quil A
Monophosphyryl lipid A	MPL®an immunostimulating TLR-4 receptor antagonist composed of detoxified LPS
Calcium phosphates nanoparticles	made of a mixture of calcium chloride, sodium phosphate and sodium citrate
Polymeric nanoparticles	biocompatible and biodegradable approved for use in human use in vaccine
Non-degradable nanoparticles	from gold, latex, silica or polystyrene
Liposome	phospholipids bi-layer shell with aqueous core, encapsulation in the core or buried in the non-viral lipid bi-layer or absorbed on the surface

Table 4: Example of nano-based adjuvant

C. AIMS AND OBJECTIVES

Immunotherapy is an appealing treatment for cancer as it can induce a long lasting protection against the reoccurrence of tumour cells. Unfortunately, it has many drawbacks including targeted delivery. When using immunogenic peptides, derived from oncogenic proteins, such as p53, it often requires the need of an adjuvant that can be engineered to increase its potency and selectivity. This can be achieved by the attachment of target molecules for specific receptors or by size modification, as dendritic cells, professional antigen have shown to favour the processing of nanoparticles. This programme of work aims to investigate the potential of nano-scaffolds, based on multi-functional calixarene macrocycles, as vectors systems for immunogenic peptides towards the formulation of a peptide based cancer vaccine using the p53 model, as represented in Figure 39.

The first objective investigates the synthesis and full characterisation of a library of molecular building blocks that demonstrate potential to self-assemble into nanometre scale scaffolds to anchor immunogenic peptides. The molecular building blocks are to be based upon resorcin[4]arene and pyrogallol[4]arene macrocycles with accessible terminal groups, including primary alcohols, amines and carboxylic acids to covalently attached peptides. The self-assembly of these molecular building blocks into supramolecular nanometre scale scaffolds will be investigated in both the solid-state and solution, using X-ray crystallography, electron microscopy, dynamic light scattering and multinuclear one and two dimensional NMR techniques including pulse filled diffusion.

To demonstrate the potential of downstream implementation of this technology and to investigate high throughput screening of these molecular building blocks, the rapid synthesis of these materials, *via* microwave irradiation and polymer bound supports, will be investigated towards the high throughput synthesis of novel materials in high yield with minimal purification requirements. Lead molecular building blocks will be investigated for toxicity and inertness *in vitro*. This work involves heamolytic properties on red blood cells and their effect on dendritic cells. The latter will be assessed by studying the effect of varying concentration of the lead macrocycle on the viability and proliferation of the cells.

Known immunogenic peptides based on the p53 model will be synthesised alone, with bio-cleavable linkers, such as tri-alanine linker, and fluorescently labelled. Synthetic methods to attach these peptides to the bioavailable molecular scaffolds

will be investigated; these methods include traditional peptide coupling reactions and combined polymer support microwave irradiation techniques. The potential of nano-scaffolds as peptide pro-drug systems for model peptides will be investigated both *in vitro* and *in vivo*, using a p53 mouse model, and compared to the model peptides on their own and combined with a traditional adjuvant IFA.
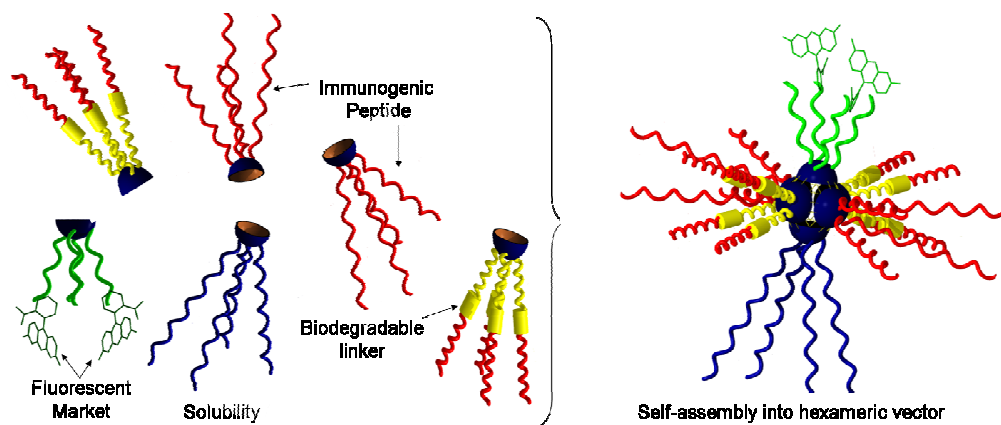
Figure 39: Representation of the optimal calixarene based nanovector.

CHAPTER II: APOLAR FOOTED CALIXARENES

Although pyrogallol[4]arenes are well studied, their synthesis has remained unchanged for the last hundred and thirty years. The use of greener techniques, such as a solvent-free method[54-55] and the new microwave-assisted synthesis described herein,[251] allow not only the rapid synthesis of this class of macrocycle but also ensure the formation of the *rccc* cone conformation that is needed to form higher self-assemblies such as hexameric capsules.[74] The aliphatic derivatives being the most studied of all, their investigation provides a good basis for the optimisation of the greener synthesis.[252] In order to demonstrate that this selective control over the stereoisomer formation of both the resorcin[4]arene and pyrogallol[4]arene conformation have been maintained, aromatic as well as heterocyclic compounds, inherently known to form the *rctt* chair conformation, were also investigated.

A. MICROWAVE SYNTHESIS

From the modified conventional domestic microwave oven to specific microwave reactors, microwave energy is now widely used as a greener tool for organic synthesis.[253] Exploiting the electromagnetic irradiation between IR and radiofrequency, within a frequency range of 0.3 to 300 GHz,[254] microwave-assisted organic synthesis (MAOS), adapted from conventional microwave has been used since the 1970s.[253] Based on the same principle, domestic microwaves are multi-modal which means that the waves are produced in multiple directions whereas chemistry specific microwaves are mono-modal. The wave is directed onto the reaction vessel, creating a constant wave independent of the stirring, which may interfere. Any material with a dielectric constant is able to absorb the energy and convert it to heat. It is controversially thought that the microwave also has its own effect, mainly due to the fast heating profile that cannot be reproduced by using conventional heating.[254] The monitoring of the temperature inside the reaction mixture can be done using infrared sensors (external, -40 to 400 °C) or a fibre optic probe (internal, 0 to 330 °C). The reactions can also be done under controlled pressure in a sealed vessel or at atmospheric pressure (open-vessel).

Two synthetic chemistry microwaves are dominating the market, the Biotage Initiator™ 60 and CEM Discover-SP™ instruments, their main differences rely on their waveguides, which are rectangular and circular respectively, and the CEM also allows open vessel reactions whereas controlled pressure is necessary in the Biotage system. Microwave irradiation has emerged as a versatile tool for organic synthesis using its

ability to reach high temperatures rapidly *via* electromagnetic waves and has found applications in a wide range of reactions.[255] The synthesis of calixarene macrocycles is no exception and is a considerable improvement from the traditional synthesis that can take up to five days.[256] Calixarene derivatives have only been reported to be synthesised in microwaves in the last four years, Brönsted acid[39] and tungstophosphoric acid, Keggin type can be combined with microwave irradiation to synthesise resorcin[4]arenes.[56] This work was later developed to include the pyrogallol[4]arene macrocycles.[57] However, in all cases when highly hindered substituted aldehydes such as aryl or tolyl are used, like in the conventional heating method, the favoured diastereoisomer is *rctt* chair conformation.

B. ALIPHATIC

In order to ensure the conformation of the macrocycles, the following method has been tuned to produce the *rccc* stereoisomer, as the major product, independently of the pendant chain length or steric hindrance; thereby, substantially increasing the accessibility to a wider range of diverse macrocycles *via* greener technologies. Additionally, by controlling the reaction conditions, the work-up procedure was reduced to a simple filtration.[251] The general procedure consisted of premixing equimolar quantities of resorcinol or pyrogallol with an aldehyde in an acidic reaction medium. The reaction vessel was sealed and subjected to microwave irradiation for five minutes at a constant temperature of 100 °C using a CEM Discover-SP™. Upon cooling, the *rccc* product crystallised from solution, whereupon it can be collected by filtration as the pure product.
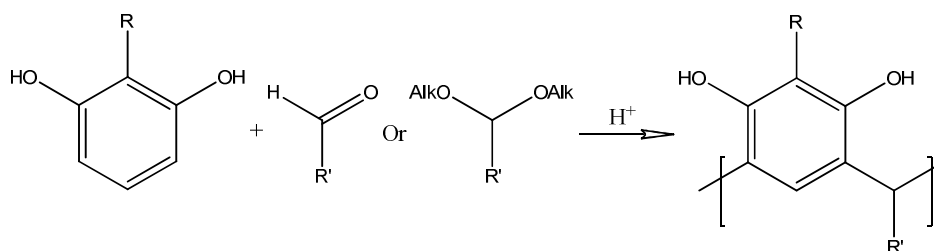
*Scheme 8: Synthesis of resorcin[4]arene (R = H) or pyrogallol[4]arene (R = OH) with alkyl (R')
or aryl (Ar) chains*

1. Conformational studies

The rapid synthesis of the macrocycles using this microwave technique has enabled the exploration and the study of the effects of the varying reaction conditions on the formation of the different stereoisomers. These studies were conducted, on the well-studied, *C*-butyl-pyrogallol[4]arene as a model synthesis.[17-18] The effects of changing reaction conditions including time, temperature, solvent and acid catalyst were assessed and are summarised in Table 5.

Time (min)	T (°C)	Solvent	Yield (%)	*rccc* [a] (%)	Time (min)	T (°C)	Solvent	Yield (%)	*rccc* [a] (%)
1	100	EtOH	Oligomer [b]		5	40	EtOH	Oligomer [b]	
2			57	77		60		Oligomer [b]	
3			65	79		80		77	85
4			60	80		120		Decomposed [b]	
5			73	83		140		Decomposed [b]	
6			76	86	5	100	MeOH	56	66
7			79	86			*n*PrOH	40	88
8			66	83			*n*BuOH	76	96
9			72	86			EtOAc	25	96
10			70	86			H_2O	56	4

Table 5: Conformational study of the microwave-assisted synthesis of C-butyl-pyrogallol[4]arene
[a] Stereoisomer yields based on ^{1}H NMR integration. [b] Product was not isolated.

To assess the stereoisomeric control caused by the varying synthetic parameters, the crude product of the reaction was isolated *via* precipitation with water. The ^{1}H NMR spectrum of the precipitate, in d_6-DMSO, displayed one triplet with a chemical shift around 4.10 ppm, as highlighted in Figure 40. The satellite triplets around 4.10 ppm can be attributed to the unreacted aldehyde or the oligomer. The main difference in the aromatic region (6.5 – 7.5 ppm) is indicative of the presence of both stereoisomers. When in the *rccc* cone isomer; only one singlet is present at 6.85 ppm, whereas when in the *rctt* chair isomer, two singlets are present in the aromatic region at 6.85 ppm and 6.77 ppm (2 ArH$_{horizontal}$ and 2 ArH$_{planar}$). The relative percentages of both stereoisomers present in the crude product were assessed by ^{1}H NMR integration techniques. Integration of the characteristic singlet for the pyrogallol aromatic proton at 6.85 ppm, was normalised to 1, and the integrations of the characteristic triplets of the *rctt* conformation were measured. In all cases, the *rccc* product was observed to be the predominant configuration. There was no evidence of the *rcct* isomer in any of the crude products.

Following the reaction over time revealed the exposure time did not influence significantly influence the formation of the *rctt* isomer, as it remained constant after six minutes. This is illustrated in Figure 40, that shows the time-lapsed ^{1}H NMR spectra overlay.
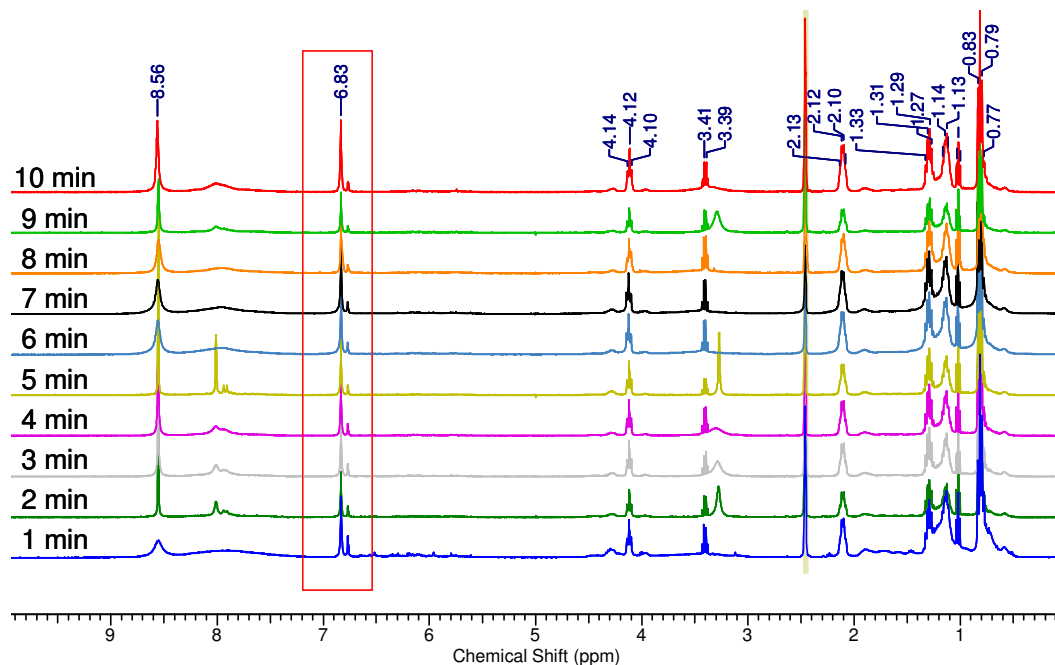
Figure 40:Effect of reaction time on the overall ^{1}H NMR spectrum of C-butyl-pyrogallol[4]arene

However, higher yields were obtained with increased reaction times, Figure 41 illustrates the relationship between time and yield, before two minutes only the linear oligomers are present and therefore yields and percentage of *rccc* could not be calculated. There is no linear relationship between time and yield over ten minutes. The overall formation of the *rccc* stereoisomer appears favoured with prolonged exposure to microwave irradiation, from 57% after two minutes irradiation to a higher yield of 70% after six minutes.
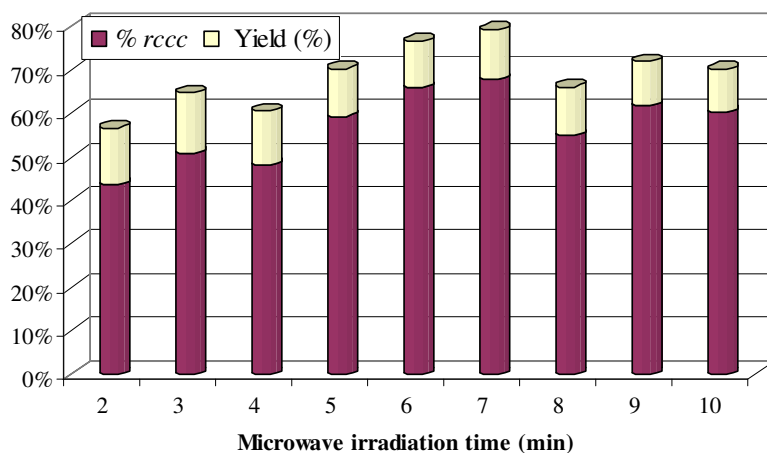
Figure 41: Overall yield (crude) and rccc stereoisomer yield depending on microwave irradiation time (min)

As shown in the characteristic region of the ^{1}H NMR spectrum (Figure 42), the macrocyclic product was only observed when the temperature was allowed to increase above 60 °C. Below these temperatures (*i.e.* 40 °C), only linear oligomers were isolated as waxy compounds that have several aromatic peaks between 6 and 6.5 ppm. As the temperature increases, the relative percentage yield of the *rccc* stereoisomer remained constant. However, when the temperature was further increased to 120 °C and above, the compound starts to decompose, maybe due to ring opening, back into the non-cyclised oligomer, this can be seen by the similarity of the ^{1}H NMR spectra for 40 °C and 140 °C.
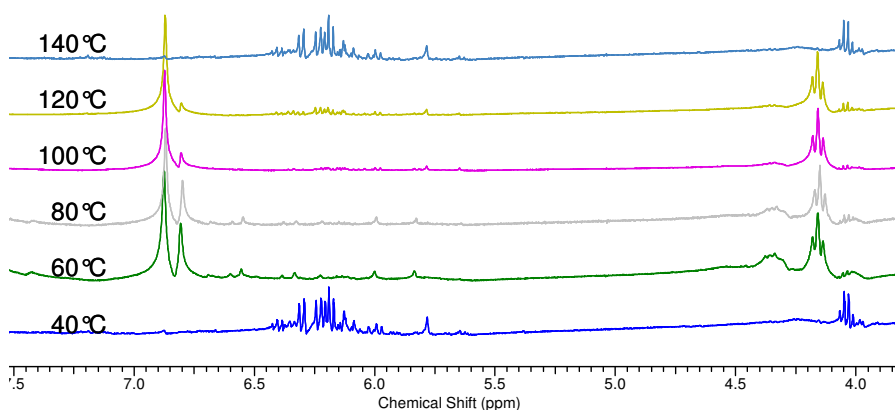
Figure 42: Effect of temperature on the characteristic region of the ^{1}H NMR spectrum of C-butyl-pyrogallol[4]arene

As the formation of the conformers is reported to be an equilibrium,[44] it can be displaced by selecting the reaction media that precipitates as the desired product (Figure 43). In order to change the reaction media, several solvents were considered. Ethyl acetate and acetonitrile are well known to favour the formation of the hexameric capsule; however, the latter could not be used in this study as it was found to form the ammonium salt in presence of strong acid such as hydrochloric acid.
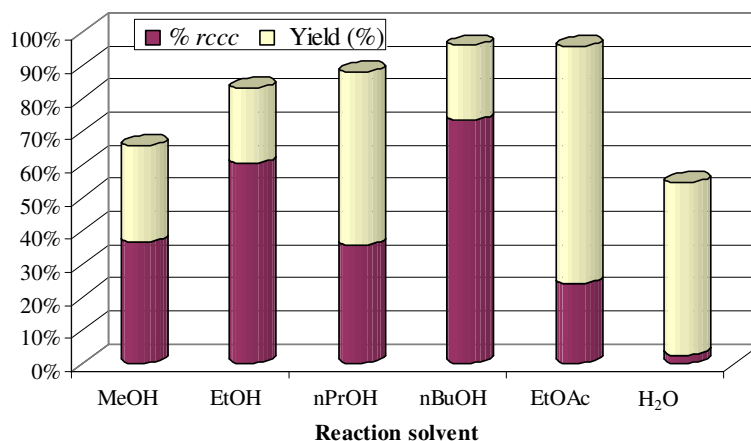
Figure 43:Overall yield (white) and % rccc (red) depending on the solvent system

As seen in Figure 44, the formation of the macrocycle is reported to proceed *via* the acetal form of the aldehyde *in situ*,[47] which subsequently reacts with the phenol, therefore a selection of alcohols were considered. Switching the solvent from ethanol to water resulted in a negligible isolated yield. This is due to the equilibrium of this condensation reaction being driven to the left, thereby preventing the reaction from going to completion. In contrast, the insolubility of the *rccc* isomer in ethanol drives the equilibrium towards the product. Remarkably, when ethyl acetate was used as the solvent system the *rccc* isomer crystallises out of the reaction media on cooling as the nanometre scale hexameric assembly but with a low yield.[82] The steric bulkiness of the acetal function was thought to play a predominant role in influencing the formation of one conformation over the other. As the length of the alcohol chain was increased from methyl to butyl, the yield of the *rccc* macrocycle was increased. Hence, by increasing the bulkiness of the acetal, the possibilities to interchange conformations were lowered. The lowest yield, obtained from propanol, may be due to a solubility issue more than its steric hindrance. The disappearance of the *rctt* isomers in the crude product is clearly visible in the overlay of the ^{1}H NMR spectra, (Figure 45) especially around 7.2 ppm.
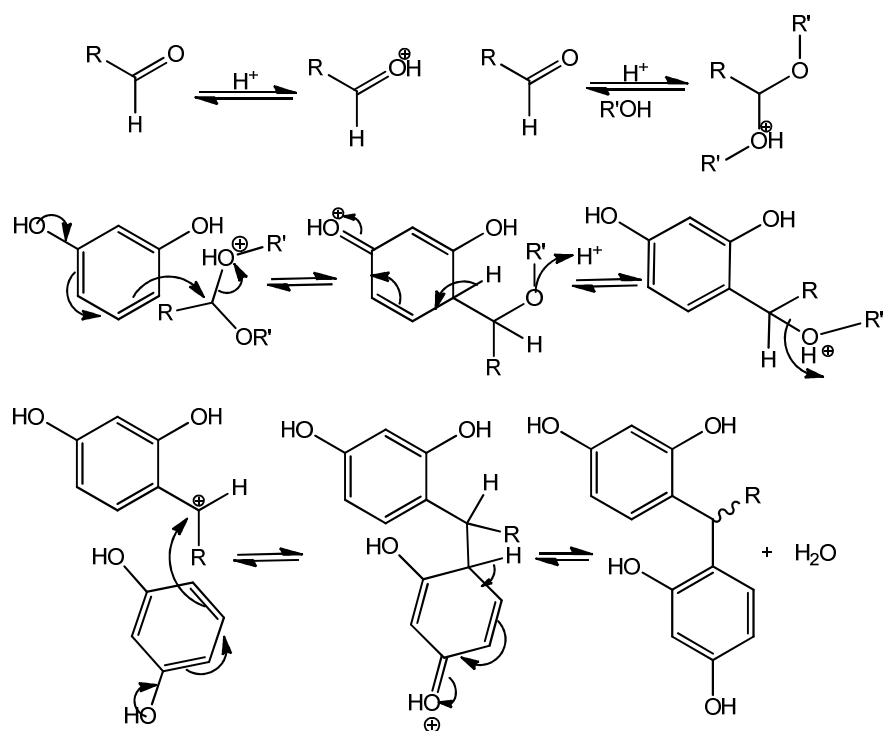
Figure 44: Proposed acetal mechanism
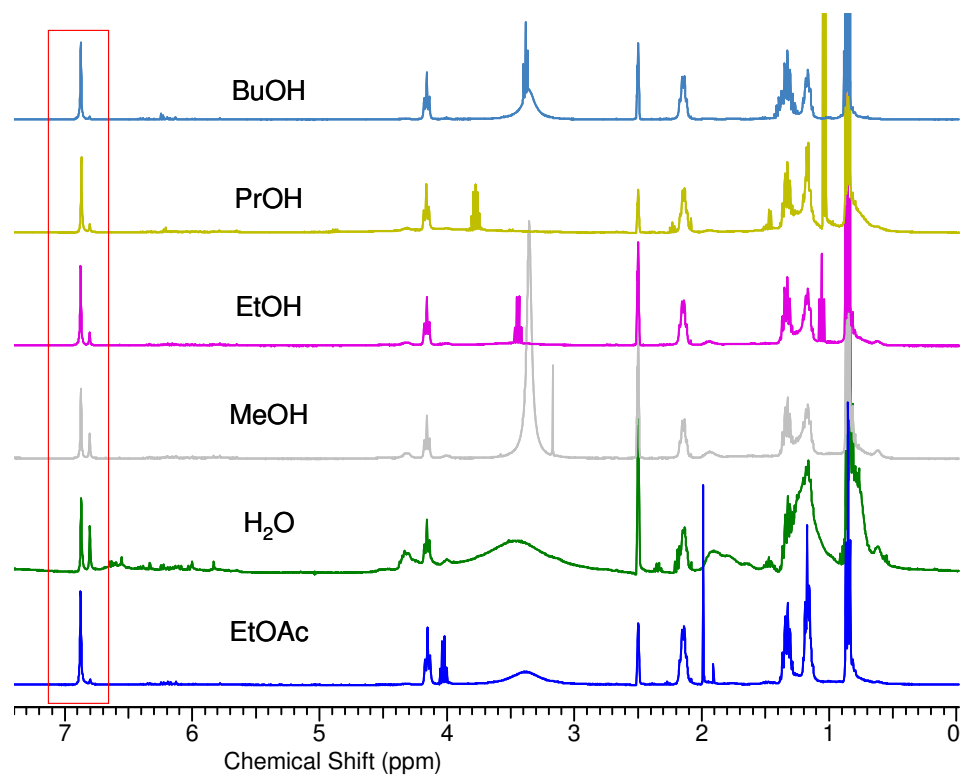
Figure 45: Effect of the solvent on the overall ^1H NMR spectrum

The solid state molecular structure obtained from slow diffusion of water into a solution of *C*-butyl-pyrogallol[4]arene in DMSO, shows that the solvent coordinates to the upper rim hydroxyl groups of the pyrogallol (Figure 46). The cone conformation of pyrogallol[4]arene is maintained by four intramolecular hydrogen bonds from 2.762 Å (O3$\cdots$O4) to 2.817 Å (O6$\cdots$O7). However, in the presence of strong polar solvent such as DMSO, the eight remaining phenolic groups are strongly hydrogen bonded to DMSO molecules that is reflected by the shortening of the hydrogen bond lengths from 2.711 Å (O2$\cdots$O14) to 2.635 Å (O7$\cdots$O16). From this X-ray study, it was deduced that this hydrogen bonding interaction could disturb the pre-organisation of the cone *rccc* stereoisomer during the condensation reaction. DMSO was therefore introduced to the reaction solvent (ethanol) to reduce the possibilities of intramolecular hydrogen bonding in the tetramer leading to the formation of the *rctt* stereoisomer. Surprisingly, the addition of DMSO had no significant effect on the overall yield or stereoisomer ratio, suggesting that the hydrogen bonding capability of the solvent has little effect on the macrocycle formation.
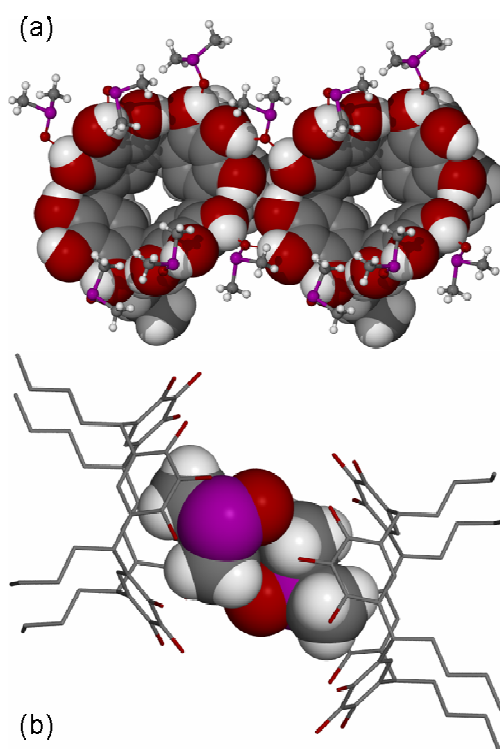
Figure 46: Molecular projection of the C-butyl-pyrogallol[4]arene DMSO clathrate: (a) top view of two rccc symmetrical cone configured macrocycles, hydrogen bonded together via two DMSO bridges, (b) 3 DMSO clathrate, hydrogens have been omitted for clarity

Substitution of the acid catalyst from hydrochloric acid to acetic acid, in the absence of any additional solvent, prevented the reaction from proceeding to the desired product. However, when *p*TSA was used as the acid catalyst in ethanol, over 70% of the *rctt* product was isolated. The addition of acetic and formic acid to a 25% hydrochloric ethanolic solution, to change the acidity and solubility, resulted in lower overall yields, whilst retaining the *rccc* conformation as the predominant stereoisomer.

To facilitate both the recycling of the catalyst and towards developing a flow reactor, a switch from homogeneous to heterogeneous conditions was investigated. Preliminary experiments involving solid acidic zeolites, including K10-montmorillonite, silicates (HMFI, HFAU), sodium mordenite (Na-MOR) as well as aluminium oxide were attempted. However, yields were far from comparable to the homogeneous acid conditions. These foulings may be caused by the heterogenous character of the catalysts. In addition, the pores sizes may restrict the access to the catalyst leading to the formation of the macrocycle or clogging the zeolites rendering them inactive, this could be potentially overcome by the use of ultrasound incorporated into the reactor design.

2. SYNTHESIS

Using this greener synthesis tuned to predominantly yield the *rccc* stereoisomer, a series of pyrogallol[4]arenes **1-4** and resorcinarenes **5-8**, with increasing pendant chain lengths were chosen as representative samples. All reactions were conducted on a gram scale and the products were characterised using ^{1}H and ^{13}C NMR techniques and MALDI-TOF mass spectrometry. In order to isolate any potential *rctt* isomer, distilled water was added to the reaction medium and the precipitate was subsequently collected and characterised. Potentially, any unreacted starting materials and solvent can then be readily recycled.

Yields and NMR chemical shifts for macrocycles **1-8** were consistent with the literature values compared to the isolated stereoisomers synthesised using traditional techniques.[82-83] There is no linear relationship between the increase of chain lengths and the overall yields; however, it is noticeable that they are usually higher for resorcin[4]arene than pyrogallol[4]arenes. It can be assumed that the presence of the extra hydroxyl group on pyrogallol may have an interfering role in the stabilisation of the aromatic ring during the cyclisation. Crystalline materials isolated from the crude reaction media were further investigated by single crystal X-ray analysis. In all cases,

the molecular structure was that of the *rccc* isomer as a solvated clathrate, with crystallographic measurements and their unit cells consistent with literature values.[44]

	R	R'	%Y	m/z [M+Na]$^+$		R	R'	%Y	m/z [M+Na]$^+$
1	OH	$(CH_2)CH(CH_3)_2$	85	799	**5**	H	$(CH_2)CH(CH_3)_2$	90	735
2	OH	$(CH_2)_2CH_3$	61	743	**6**	H	$(CH_2)_2CH_3$	96	679
3	OH	$(CH_2)_3CH_3$	62	799	**7**	H	$(CH_2)_3CH_3$	67	735
4	OH	$(CH_2)_4CH_3$	68	855	**8**	H	$(CH_2)_4CH_3$	84	791

Table 6: Microwave-assisted synthesis of calixarene macrocycles

C. AROMATIC

Aromatic resorcinarene macrocycles have received much interest in the last years, due to their ability to extract cations such as caesium, strontium,[257] lead, chromium[258] and lanthanum.[259-261] They have been investigated for their ability to extract other aromatics from water solution[262] Alt'shuler *et al.* used a different approach to form hydrated polymers,[263] and investigated their ability to react with quaternary ammonium[264] and to form cationite.[265] Phenyl-pyrogallol[4]arenes derivatives were considered as alternative compounds for lithography.[266] Their ability to form star-shaped initiators for radical polymerisation is another one of their potential uses.[267-268] Aromatic resorcinarenes have the ability to interact with biologically relevant compounds such as amino acids[269] and proteins.[270] Only a few exhibit the *rccc* conformation, like the seven resorcinarenes derivatives that were synthesised as high resolution resistant materials for supercritical CO_2 processing, which appeared to be all in the *rccc* isomers.[271] In most applications, the interactions with guest and the extraction power is driven by the all *cis* conformations. However, in 2001, the original greener method showed that it is complex to predict the isomeric ratio that will be obtained during the reaction.[54] Although the same reaction conditions were applied to for each aromatic aldehyde, Scheme 9, the reactions led to different *rccc*: *rctt* isomer ratios of 2:1 for the *o*-OH, *p*-$O(CH_2)_3CH_3$, *p*-$(CH_2)_4Br$ and *p*-NO_2 but 95:5 for the *p*-$O(CH_2)_7CH_3$.
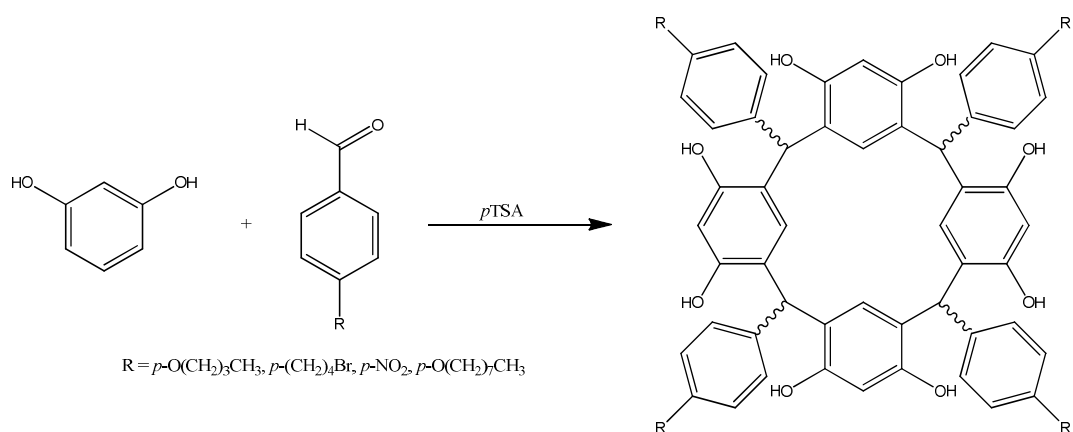
Scheme 9:Solvent-free synthesis of aromatic resorcin[4]arenes[54]

It is reported that the *rctt* isomer can be converted to the *rccc* by complexation with pentacoordinated zinc(II), even when bulky group such as benzyl and naphthyl are used.[103] The main drawback to this method is the presence of the metal that will reduce the coordination potential of the calixarenes. As it is not always easy to separate the different isomers, the selective control of the conformations is therefore needed. Hoegberg reported the first synthesis of aromatic resorcinarene in the *rccc* conformation.[256] He stated that the stereoselectivity is a result of a combination of three main factors: the conformational control *via* the non-bonded interactions within the intermediate, the reversibility of the C-C bond formation and the difference of solubility of the two macrocycles. The *rccc* is the thermodynamic product whereas the *rctt* is the kinetic product; therefore, time is thought to play an important role. An extensive study, which included a wide variety of aromatic substituted resorcinarenes, confirmed previous findings. They also drew attention to the character of the aldehyde, that may have a steric effect as well as an electron withdrawing effect *i.e.* a strong electron withdrawing effect lead mainly to the *rctt* isomer.[21] Using this traditional synthesis many aromatic derivatives have been synthesised all in the *rctt*.[257] The choice of the catalyst is essential, when using lanthanide salts of *p*-toluenesulfonic acid as the acidic catalyst seems to favour the *rctt* diastereoisomer.[260] Whereas, a new synthesis of the resorcinarene derivatives by the condensation of an aldehyde and a methoxyhydroxybenzene with another Lewis acid, $BF_3.OEt_2$, only lead to the C_{4v} conformer where all substituents are in the *cis* position.[272] Using another Lewis acid such as tin tetrachloride also led to the *rccc* isomers of octamethoxyresorcin[4]arenes in a 85% yield.[51]

1. SYNTHESIS

The selective control of the conformation was attempted, using the method that was optimised for the alkyl derivatives and aromatic footed macrocycles **9-16** were isolated. Usually the presence of a bulky group such as a benzene ring, leads to the formation of another diastereoisomer, the *rctt,* to sterically accommodate the subsituent, but as explained previously, the bulkiness is not the only factor. Methods developed by others with a different solvent such as ethoxyethanol using microwave irradiation for only two minutes was showed to favour the kinetic product *rctt*.[57] Interestingly all derivatives synthesised by Han *et al.* were also in the *rctt* conformation except for the ferrocenyl derivative that was exclusively in the *rccc*.[145] Those results led to the assumption that similar behaviour would be observed, however, the utilisation of our in-house method, when followed by a recrystallisation of the crude product from methanol-acetonitrile 1:1, showed that mainly the *rccc* isomers were present.

N	R	R'	Yield (%)	m/z $[M+Na]^+$	N	R	R'	Yield (%)	m/z $[M+Na]^+$
9	OH	C_6H_5	66	879	**13**	H	C_6H_5	72	805
10	OH	*o*-tolyl	30	935	**14**	H	*o*-tolyl	44	848
11	OH	*m*-tolyl	94	935	**15**	H	*m*-tolyl	96	848
12	OH	*p*-tolyl	87	935	**16**	H	*p*-tolyl	94	848

Table 7: Microwave-assisted synthesis of aromatic calixarene macrocycles

The ^{1}H NMR data and the crystal data obtained for a series of aromatic resorcinarenes and pyrogallolarenes showed that the all *cis* were obtained as the predominant isomers. Although not in the cone conformation due to steric hindrance as well as its reduced flexibility, if the *rccc* isomer is formed with aromatic substituents it is usually in the pinched cone (boat) conformation.[273] This conformation is rarely obtained as such even when microwave irradiation has been employed in the past. These macrocycles containing bulky pendant chains may offer interesting features such as novel inclusion complexes and new carcerands.

In addition to the mechanism of the reaction, proposed by Weinelt,[46] it can be assumed that the electrophilic cyclisation is achieved by a relatively stable benzylic carbocation, stabilised by the phenolic ring. This was confirmed by Middel,[274] as he proved that the higher electron density of methyl resorcinol increased the rate of electrophilic attack. This may explain why the aromatic resorcinarenes **13-16** gave a

better yield than the pyrogallol[4]arenes **9-12.** As the tolyl aldehydes gave better yields than the benzaldehyde reactions, it can be assumed that the presence of an aromatic substituent may increase their stability, especially if they contain *ortho* and *para* directing groups, as the electron donation is favoured by the hyper-conjugation from the methyl groups on the final canonical, as seen in Figure 47.
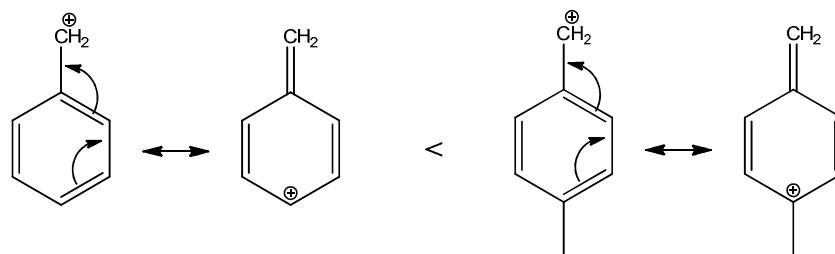
Figure 47: Stability of the carbocation due to mesomeric effect

The *o*-tolyl derivatives (**10** and **14**) were obtained in very low yield (< 44%) compared to the *meta* and *para* derivatives which is mainly due to steric hindrance. The bulkiness of the tolyl methyl group close to the methine bridge impedes the cyclisation of the oligomer, which leads not only to a lower yield but also to lower ratio of *rccc* to *rctt* isomer. Interestingly, the presence of the methyl substituent at the *meta* position leads to an increased in yield, this is due to the mesomeric effect, but still leads to the *rccc* isomer, in favour of the *rctt* isomer. The *p*-tolyl is also obtained in high yield (94%), this can be explained by the favoured stabilisation of the benzylic carbocation as well as the reduced steric hindrance.

2. CRYSTALLOGRAPHY

Suitable crystals of *C*-phenyl-pyrogallol[4]arene **9** were obtained by slow evaporation from acetonitrile, exhibiting the *rccc* boat conformation in the monoclinic space group *C*2/*m,* with a unit cell a = 20.913(3), b = 21.667(3), c = 11.3077(14) Å, β = 116.490(16)° and V = 4585.9(10) Å^3. Due to the long distances between the oxygens, 4.634 Å and 3.958 Å, the boat conformation does not allow the intramolecular hydrogen bonding that is seen in the cone conformation. This change of conformation can also be quantitavely assessed as a distortion factor (D_f) by the ratio of the minimal aromatic distance of the upper rim (4.886 Å) and the maximal separation (10.639 Å), which is 0.459 in this *rccc* conformation, as seen in Figure 48. By comparison, it is *ca*. 1.0 for the macrocyle integrated into the hexameric capsule and *ca*. 0.5 when the macrocycle is

reported in the C_{2v} conformation.[82, 275]
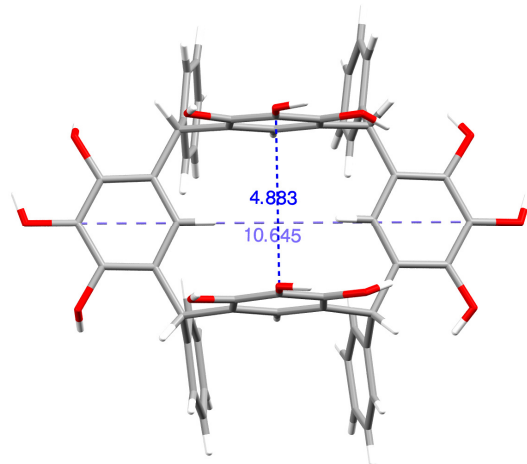
$$Df = \frac{\min aromatic}{\max aromatic} = \frac{4.883}{10.645} = 0.459$$

Figure 48: Definition of the Distortion factor (Df)

However, the boat conformation exhibited by *C*-phenyl-pyrogallol[4]arene **9** does not exhibit the C_{2v} symmetry, as the plane going through the pyrogallol ring that is involved in the intermolecular bonding, referred to as horizontal, is slightly tilted at -13.12° angle compared to the plane through the opposite horizontal pyrogallol and the four methines of the macrocycles ring as seen in Figure 49.
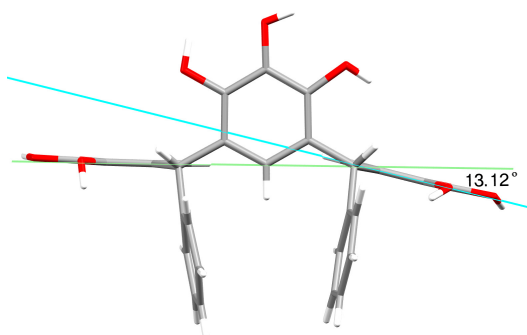
*Figure 49: C-Phenyl-pyrogallol[4]arene **9** side view*

The solvent did not participate in the hydrogen bonding network and therefore the four acetonitrile molecules contained in the unit cell have been treated as a diffuse contribution to the overall scattering without specific atom positions by the SQUEEZE function of PLATON program.[276] The *rccc* isomer enables the formation of a

intermolecular hydrogen bonded network within the upper rims with a donor acceptor distance ranging from 2.693 Å (O4···O5) to 3.005 Å (O1···O5).
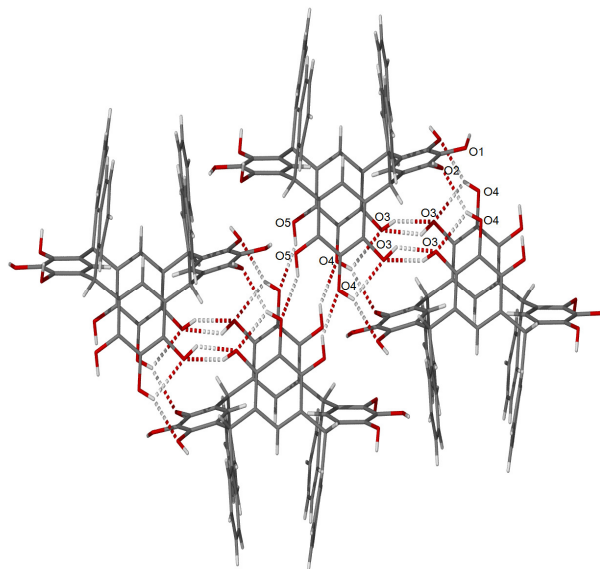
Figure 50:Hydrogen network of the rccc boat C-Phenyl-pyrogallol[4]arenes **9**

Due to the hydrophobic character of the aromatic pendant chains as well as their steric hindrance, the packing results in a hollow tubular network. This effect can be visualised by introducing planes within the packing system as shown in Figure 51. The plane across the axial pyrogallol ring of the macrocycle (in blue) is nearly at a right angle (89.91°) to the plane across the horizontal pyrogallol (in red). The inter-planar spacing within the tubes is 5.50 Å between the red planes and 4.88 Å between the blue planes.
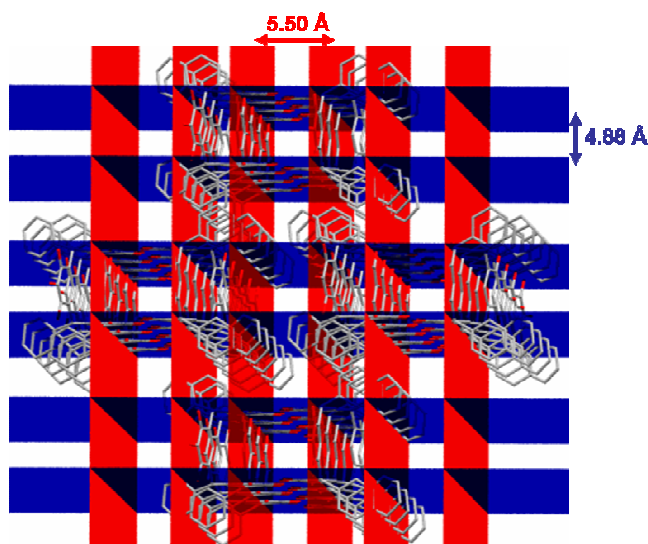
Figure 51: Plane representation of the packing system for C-Phenyl-pyrogallol[4]arene **9**

Preliminary single crystal X-ray crystallographic data for *m*-tolyl-resorcin[4]arene **15** obtained from slow diffusion of water in DMSO showed the pendant chains are also all in the *cis* position and orientated in order to minimise the steric hindrance (Figure 52). Highly polar DMSO molecules are hydrogen bonded to each resorcinolic phenol, leaving the shortest distance to another hydroxyl group over 6.73 Å, so there is no direct intermolecular hydrogen bonding, which is in accordance with others findings.[277] The hydrogen bond lengths varied from 2.577 Å (O8⋯O16) to 2.705 Å (O4⋯O15), with an average length of 2.663 Å over the eight interactions showing that their strengths are similar. The tiltings of the nearly co-planar resorcinol are in the same range, *i.e.* -6.19º and -9.37º compared to the plane constituted of the C-H groups of the macrocycle (C2-C8-C14-C20), and a distortion factor of 0.49.
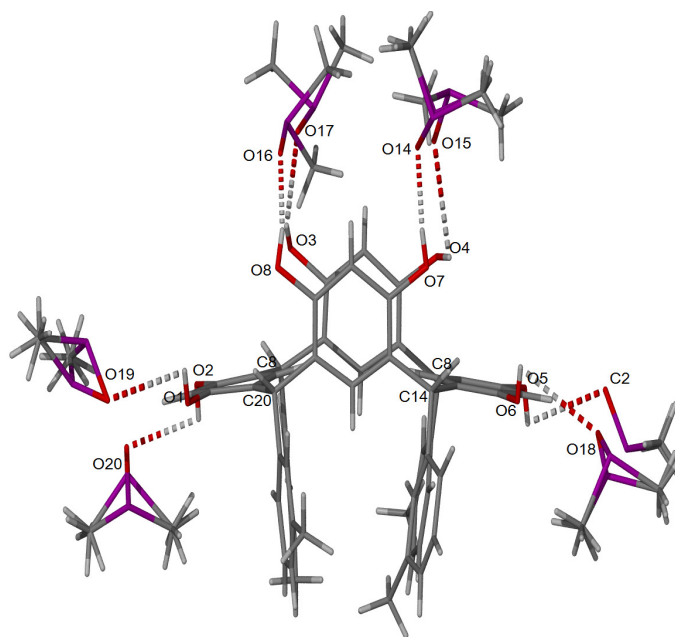
*Figure 52: m-Tolyl-resorcin[4]arene **15** hydrogen bonding interactions with DMSO.*

When DMSO is absent, an interesting packing that involved both hydrogen bonding between electronegative atoms occurs, with all the phenolic hydrogens involved and a face-to-face Ar-H⋯π interactions, this behaviour is seen in the solid state for *p*-tolyl-resorcin[4]arene **16**. The two nearly coplanar horizontal resorcinols are titled by 13.76º and 12.06° in order to maximise the strong intermolecular interactions, this results in the approach of the two perpendicular rings and therefore a reduced distortion factor of 0.39.
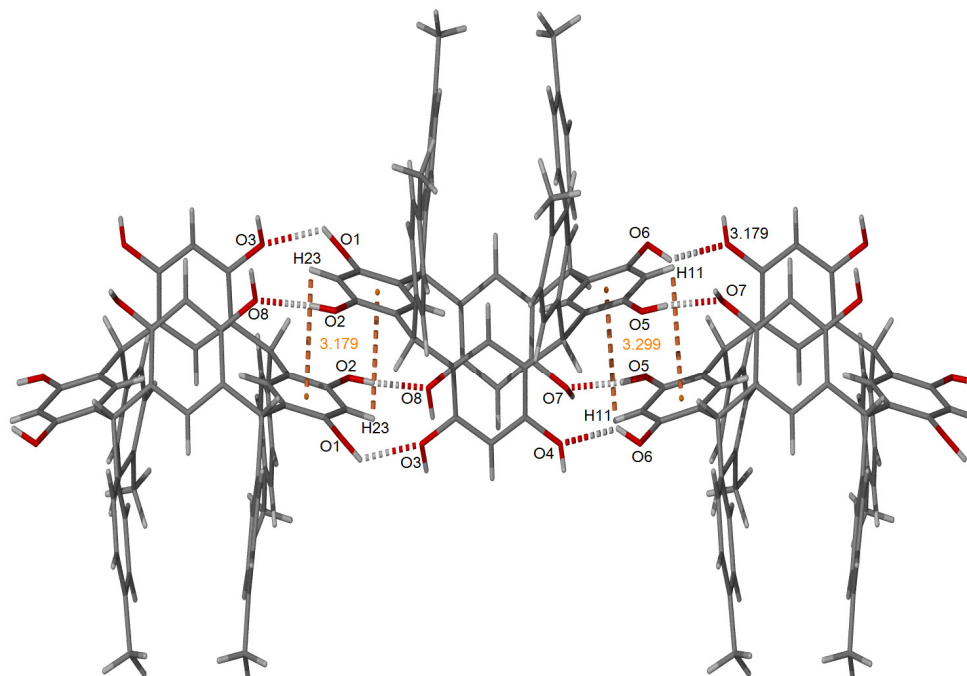
*Figure 53: Hydrogen bonding network for p-tolyl-resorcin[4]arenes **16** in the solid state*

There are eight independent hydrogen bonds holding the network together, involving all the hydroxyls from the resorcinarenes. Distances between the acceptor and the donor atoms range between 2.752 Å and 2.782 Å, (O1···O3 = 2.770 Å; O2···O8 = 2.763 Å; O4···O6 = 2.782 Å; O5···O7 = 2.752 Å). When a centroid is generated in the centre of the resorcinolic aromatic ring, it is possible to define the Ar-H···π distances (orange dotted line in Figure 53) which range between 3.299 and 3.179 Å, these relatively strong interactions due to the inductive effect of the hydroxyl groups on the benzene ring.[278]

A similar network was reported for the 'boat' conformation of *C*-methyl-resorcin[4]arene, used as a T-shaped building block when co-crystallised with pyridine. The heterocycle can break up the intramolecular hydrogen bonds that usually keep the molecule in the cone conformation.[279] As seen for the phenyl analogue **9**, the packing results in a tubular network, as represented in Figure 54, the presence of the Ar-H···π interaction, results in a tighter network noticeable by the shortening of the inter-planar spacing 5.50 Å and 4.88, to 2.65 Å and 4.64 Å, respectively.
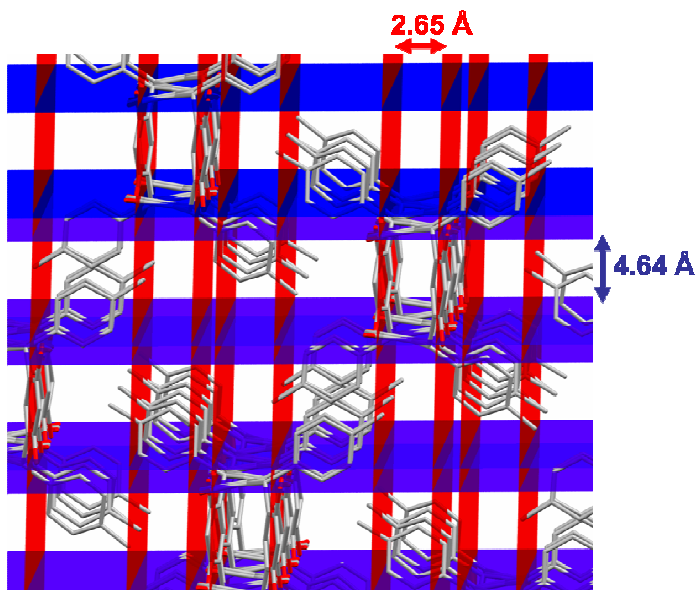
*Figure 54: Plane representation of the packing system of p-tolyl-resorcin[4]arene **16** (hydrogens have been omitted for clarity)*

As the hydrogen bonding network elongates in the *a* axis of the unit cell, the packing shows hydrophilic-hydrophobic layers with voids able to accommodate atoms with 1.2 Å radius in between the aromatic rings, shown in blue in Figure 55. By calculating the solvent accessible surface, the volume of the voids is 621.48 Å^3 occupying *ca* 19% of the unit cell volume which can explain the low density of 0.86 g.cm^{-3} of the crystals. Unfortunately, this void is smaller than what is required for hydrogen storage that should be around 2.96 Å^3 to accommodate H$_2$.[280] Nevertheless, further studies are required to investigate the structural recognition and reorganisation towards such a guest with expanded voids *via* the coordination of the hydroxyl group to various metals, leading to a new type of metal-organic framework.
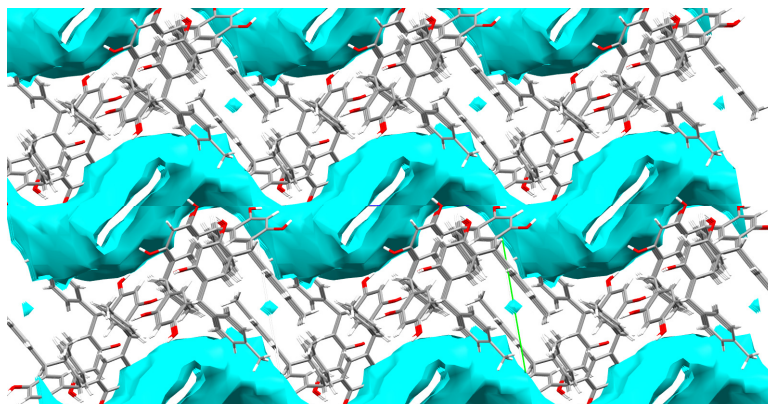
*Figure 55: Voids within the packing system of p-tolyl-resorcin[4]arene **16***

When the extra hydroxyl is present as in the case of pyrogallol, the Ar-H$^{\cdots}\pi$ interaction is replaced by a supplementary hydrogen bonding, the resulting packing system is altered and is similar to its phenyl homologue. This behaviour is seen for *m*-tolyl-pyrogallol[4]arene **11**, in the boat conformation with a distortion factor of 0.46, crystallised from methanol water (Figure 56). Preliminary single crystal X-ray crystallography data showed five intermolecular hydrogen bonds with acceptor to donor distances ranging from 2.829 Å (O6$^{\cdots}$O11) to 2.986 Å (O1$^{\cdots}$O10). The water participates to the formation of the network *via* one hydrogen bond with a length of 2.697 Å (O12$^{\cdots}$O13) which contributes to the displacement of the upper rim by 1.81 Å compared to the one below. The strongest interaction exists between the water molecules giving it a character nearly covalent with a short length of (O13$^{\cdots}$O13 = 2.326 Å) compared to the other intermolecular hydrogen.
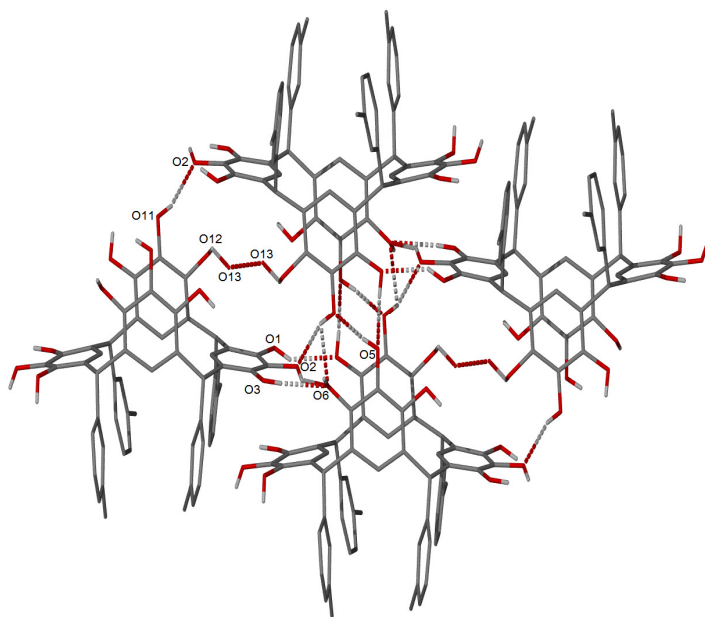
*Figure 56: Packing of the m-tolyl-pyrogallol[4]arenes **11** (hydrogens have been omitted for clarity)*

Similar behaviour is seen for *p*-tolyl-pyrogallol[4]arene **12**, in the *rccc* boat conformation with a distortion factor of 0.49. As seen in Figure 57, seven hydroxyls groups are involved in hydrogen bonds, with donor acceptor bond lengths varying from 2.739 Å (O1$^{\cdots}$O9) to 2.903 Å (O2$^{\cdots}$O10), whereas the hydroxyl from the pyrogallol ring containing O4, O5 and O6 is not involved in any hydrogen bonding, as the bond lengths with other donors exceed 3.2 Å. The solvent molecules were highly disordered and therefore the SQUEEZE program, which is designed for small moiety structures containing disordered solvent and water, was used.[276] The space filled with the

electron density was modelled as water (O13) which lies in between O2 and O11 (O2···O13 = 2.872 Å and O11···O13 = 2.807 Å) and contributes to the highest tilting of the bonded pyrogallol by 15.58°.
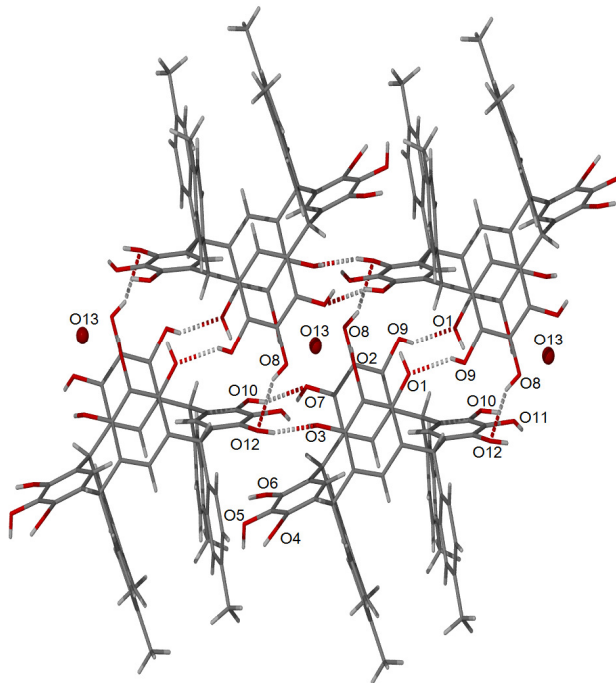
Figure 57: Packing of the p-tolyl-pyrogallol[4]arenes 12

Surprisingly, some single crystals of *p*-tolyl-resorcin[4]arene **17** obtained by slow evaporation from acetonitrile, show the *rctt* conformation in the solid state. The *rctt* was considered to be a fractional amount of the isomeric mixture that was able to be crystallised, as the NMR of the product confirmed the *rccc* as the main isomer in solution. However, it was possible to distinguish between the two crystal habits, needle and plate, which has been previously reported as isomers *rccc* and *rctt* respectively.[281] As expected the difference in conformation had a noticeable effect on the crystal packing and the hydrogen network. The chair conformation cannot lead to intramolecular bonding and therefore, only intermolecular bonding is possible. The hydrogen bonding network is mainly formed by the resorcinol perpendicular to the phenyl groups (O1···O4 = 2.763 Å). Three remaining phenols are bound to the disordered acetonitrile molecules *via* the nitrogen (O1···N2 = 2.792 Å; O2···N1 =2.862 Å; O3···N3 = 2.916 Å) which impede the formation of the aromatic hydrogen bonding. One acetonitrile lies in between two tolyl groups and contributes to the expansion of the packing in the *a* axis of the unit cell.
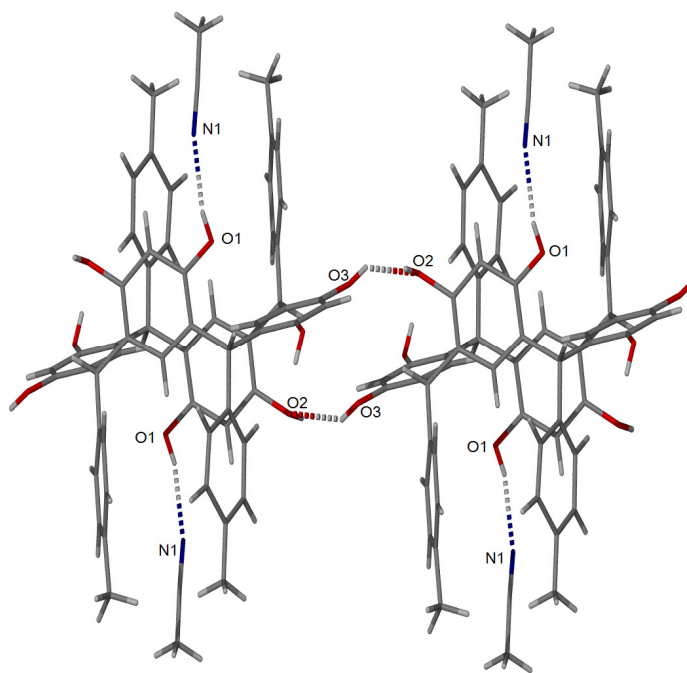
Figure 58: Hydrogen bonding network of the rctt p-tolyl-resorcin[4]arenes 17

D.HETEROCYCLIC

By combining both macrocyclic and heterocyclic chemistry, it would be possible to create a new type of inclusion complex. Due to the rapidity of the method a wide range of aldehydes could be investigated as potential starting material for these synthesis. Although some hetero-calixarenes have been reported previously, replacing the resorcinolic entities by various heterocycles such as benzofuran, benzothiophene,[299]and pyridine,[20, 79] so far only one heterocycle was attached onto the pendant chains of the calixarene macrocycle. The next compounds were investigated as a proof of principle and have opened up interesting types of compounds with many inclusion and self-assembly properties but it was not pursued any further as it was not the main focus of this project.

Inspired by the synthesis of the 2-thiophenyl-resorcin[4]arene that has been previously investigated for its ionophore ability towards chromates,[282] a novel macrocycle was synthesised by reacting *3*-thienylaldehyde with pyrogallol under microwave irradiation to give *C*-thiophen-3-yl-pyrogallol[4]arene **18**. The reaction led to a good yield due to the mesomeric effect into the heterocyclic ring. The presence of the thiophene group seems to favour the *rctt* conformation. Crystals formed by slow evaporation of deuterated DMSO exhibit the *rctt* chair conformation. Unfortunately, due to the highly disordered solvent molecules the refinement of the structure was limited, and crystallisation from other polar solvents was not successful. However, preliminary X-ray data indicates that each phenolic hydroxyl is hydrogen bonded to the oxygen of a DMSO molecule, with bond lengths varying from 2.66 Å to 2.85 Å, resulting in the bridging of the macrocycles.
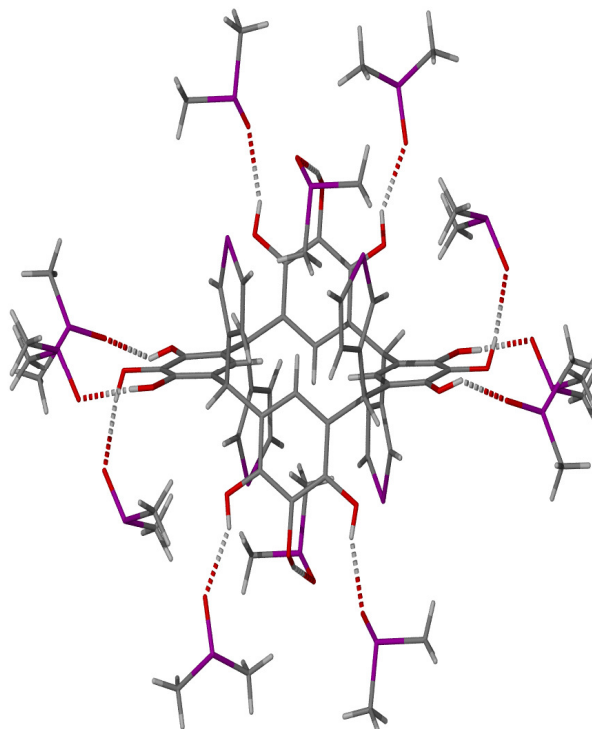
*Figure 59: Thiophene footed pyrogallol[4]arene **18** solvated with DMSO*

2. PYRIDINIUM CHLORIDE

Pyridinium is an interesting building block in supramolecular chemistry, it was previously reported that pyridine can bind to the upper rim of the calixarene to form an extended cavity,[66] and therefore it could be considered that the pyridine footed calixarene could form a tubular network and may be useful for ion transport. The only pyridinium footed resorcinarene was reported by Pirondini *et al.* where isonicotinic acyl chloride was conjugated to the hydroxyl cavitands and their coordination with various metal using the chloride salt were studied.[160] The behaviour of their pyridinium derivatives with various metals such as palladium and platinum were investigated with longer chain hydroxyl cavitands (dodecol) were formed from the alkene derivatives.[160] Using the previously described methodology, the syntheses of pyridinium footed calixarenes were attempted leading to the supposed formation of six compounds **19**-**24**, by reaction of pyrogallol and resorcinol with 2-, 3- and 4- pyridinecarboxaldehyde. The presence of the pyridine required an excess of hydrochloric acid in order to form the pyridinium salt. The crystallisation of the calixarenes were not successful, as they resulted in glassy compounds; and to date, no crystal data was obtained. The preliminary ^{1}H NMR spectra indicate the presence of the potential macrocycles, that was further confirmed by MALDI-TOF analysis, however, pure products were not isolated. The coordination of a zinc salt was attempted unsuccessfully, as well with other salt of platinum, palladium, nickel and silver. Further work will be pursued beyond this project to optimise the synthesis and the properties of those novel macrocycles as well as their self-assembly in the solid state.

CHAPTER III: POLAR FOOTED CALIXARENES

Using the method optimised for alkyl footed calixarenes, several polar footed pyrogallol[4]arenes and resorcin[4]arene were synthesised, *via* their corresponding aldehydes, masked aldehydes or acetals. The synthesis and full characterisation of molecular building blocks that demonstrate potential to self-assemble into nanometre scale scaffolds as well as covalently anchor immunogenic peptides were investigated. This study therefore focuses on targeting pyrogallol[4]arenes and resorcin[4]arenes with pendant chains showing accessible terminal groups, including primary alcohols, amines and carboxylic acids. Those macrocycles should provide viable starting materials for the addition of biologically relevant functionalities. The self-assembly of these molecular building blocks into supramolecular nanometre scale scaffolds was investigated in solid-state using X-ray crystallography and electron microscopy.

A. HYDROXY-FOOTED CALIXARENES

The first synthesis of hydroxyl-footed resorcin[4]arene was reported by Cram in 1989,[21] and was adapted later as a precursor in the synthesis of hydroxyl-footed extended cavitands as hosts, using dihydropyran and dihydrofuran as masked aldehydes.[125] Their abilities to bind to neutral guests, to form self-included capsules with metals (lanthanide) and cations (ammonium and phosphonium) have been widely investigated.[283-285] The latest research around these entities demonstrates their potential as new building blocks when transformed to water soluble phosphate footed cavitands. The addition of a single hydroxyalkyl pendant chain to the lower rim of resorcin[4]arene was achieved by mono-epoxidation of an alkene.[158] These new materials have found applications in modified stationary phases *via* of the attachment of the pendant chains to polymer supports, like cross linked polystyrene.[163]

Extended cavitands such as dendronized derivatives have been obtained *via* repeated reactions with acetonide protected bis(hydroxymethyl)propanoic acid anhydride.[286] These materials have been shown to demonstrate some interesting host-guest chemistry with applications in drug delivery, whereby the control of the guest properties is ensured by the cavity and the dendronized exterior give control of its physical properties.[287]

The alcohol functionalised resorcinarene derivatives are not restricted to their cavitands; by considering the macrocycle as a ligand Atwood *et al.* have been able to

exploit their ability to form capsules *via* the coordination of twenty-four copper (II) ions to six *C*-3-hydroxypropyl-pyrogallol[4]arenes. This assembly is isostructural to its hydrogen bonded hexameric capsule analogue with an internal volume of 1200 Å^3. It is proposed that the hydrogen bonded capsule is pre-formed prior to the insertion of the metal.[79, 100]

In the study towards the development of polar soluble nanocapsules, as potential guest transport systems, *C*-3-hydroxypropyl-pyrogallol[4]arene **25** was synthesised using the microwave-assisted method previously described, by reacting equimolar quantities of pyrogallol and 2,3-dihydrofuran in acidic ethanol (25%) at 100 ºC for 10 minutes in a 33% yield (Scheme 10). To see the effect of an additional carbon in the pendant chain, *C*-4-hydroxybutyl-pyrogallol[4]arene **26**, was synthesised using dihydro-2H-pyran in a 32% yield.[251] By utilising this new technology, the reaction times have been dramatically reduced from one week to a matter of minutes; although with marginally lower yields than the synthesis reported.[125] The work-up procedure is also reduced to a single filtration after trituration with water.
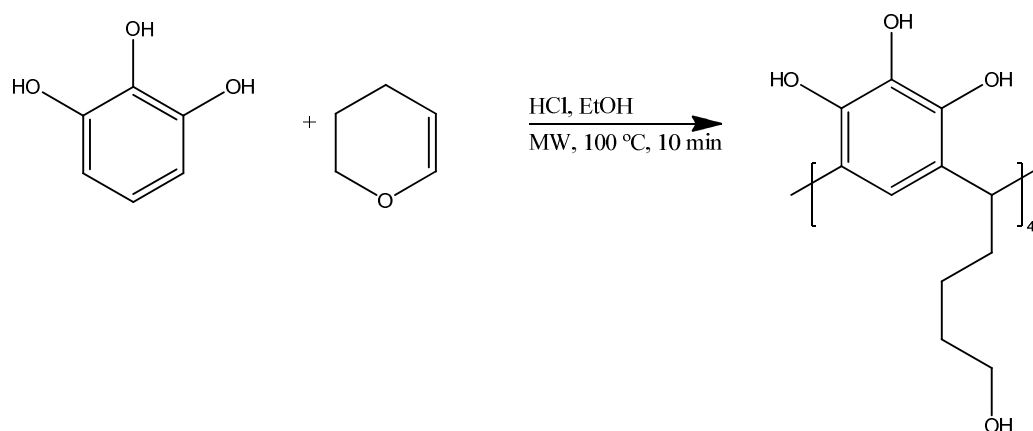
Scheme 10: Synthesis of C-4-hydroxybutyl-pyrogallol[4]arene **26**

1. C-3-HYDROXYPROPYL-PYROGALLOL[4]ARENE

Suitable crystals for single crystal X-ray crystallography were obtained directly from the reaction vessel upon cooling (Figure 60). The excess hydrochloric acid and ethanol present in the reaction media play an integral role in the hydrogen bonding network. The hydrogen bonding interaction between the chloride and a single phenolic hydrogen at the upper rim (H10$\cdots$Cl$^-$ = 2.342 Å and O10$\cdots$Cl$^-$ =3.072 Å) indicates that the chloride is in the anion form, as suggested by the computational gas phase studies.[278] Similar behaviour was seen when an ammonium cation was encapsulated

within two resorcinarene macrocycles, whereby the counteranion coordinates to the resorcinolic alcohol.[288-289]

The presence of the anion that lies in between the pendant chains, may also have a role in the hydrogen bonding of the chains as they are directed towards the inside of the cavity although O15 and O16 are close enough (2.841 Å) to form a hydrogen bond in the solid state.
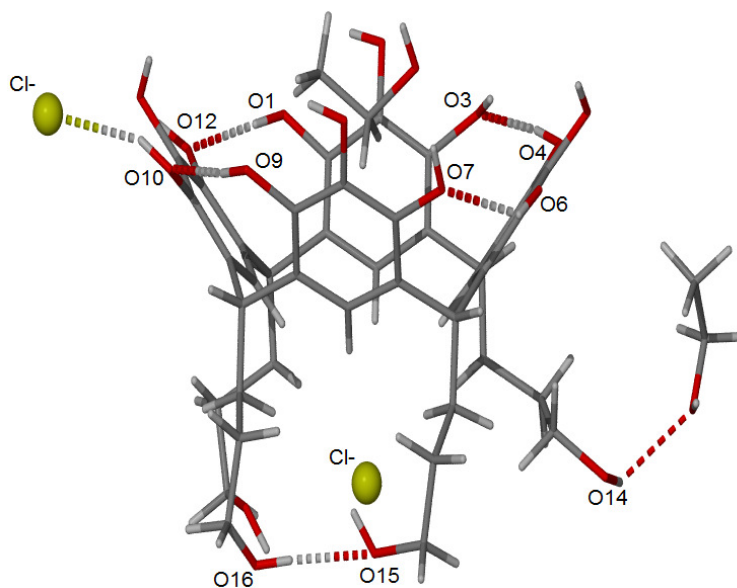
*Figure 60: C-3-hydroxypropyl-pyrogallol[4]arene **25** ethanol hydrochloride obtained from the reaction vessel*

The solid state structure of *C*-3-hydroxypropyl-pyrogallol[4]arene **25** crystallised from HCl and ethanol shows that the chloride anion is enveloped between three of the pendant propanol chains, at the annulus of the macrocycle. As shown in Figure 61, the fourth propanol chain is oriented almost perpendicularly with respect to the other three (73º) and can be seen to hydrogen bond to a single ethanol molecule (O14···O17 = 2.783 Å) and to an equivalent propanol chain on an adjacent macrocycle (green) (O14···O14 = 2.994 Å). The hydrogen bonding network is further extended *via* the interplay between this pendant propanol chain and phenolic group of a third macrocycle (O12···O14 = 2.681 Å). The third macrocycle (red) is orientated in the same direction as the first macrocycle (blue); however, the central axis are offset by 80º with respect to one another, as shown in Figure 61. These two macrocycles are further tethered *via* a hydrogen bonding interaction between the two phenolic upper rims (O2···O6 = 2.927 Å).

The two upper rims of these macrocycles are bridged by a transverse macrocycle (green) where there is a offset head-to-head hydrogen bonding network between the phenolic groups, as illustrated in Figure 61 (O2···O8 = 2.672 Å, O3···O9 = 2.899 Å, O8···O7 = 2.847 Å, O4···O11 = 2.813 Å, O7···O7 = 2.850 Å).
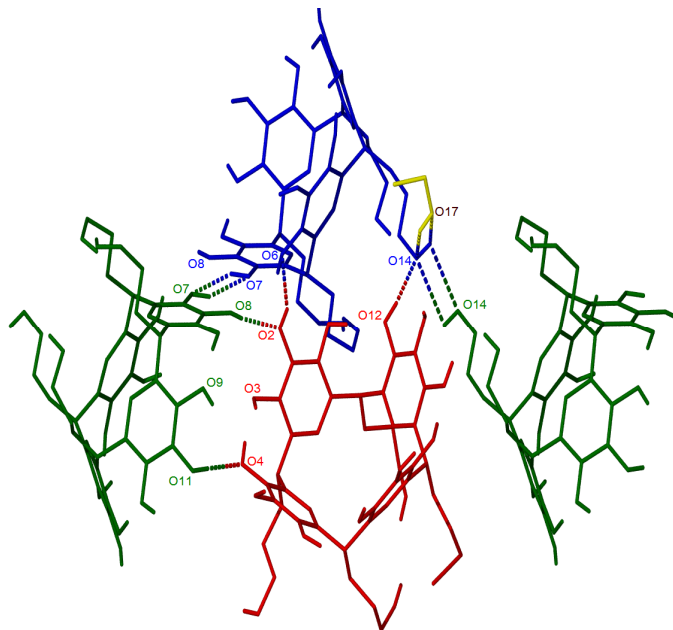
Figure 61: Interplay of the propanol chains containing O14 of C-3-hydroxypropyl-pyrogallol[4]arenes 25 (hydrogens have been omitted for clarity)

This extended hydrogen bonding network results in macrocycles packing into a pseudo hexagonal motifs along the *c* axis, represented by dotted lines in Figure 62.
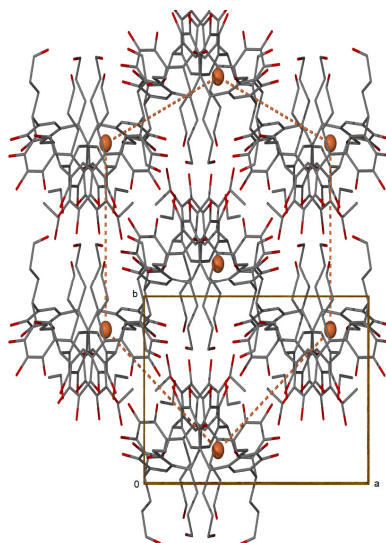
Figure 62: Pseudo hexagonal packing along the c axis of C-3-hydroxypropyl-pyrogallol[4]arenes 25 (hydrogens have been omitted for clarity)

93

The macrocyclic cavity can be seen to accept a single ethanol guest molecule (Figure 63a), that is anchored into place *via* two hydrogen bonding interactions, between the methylene hydrogens of the guest with the electron rich faces of the aromatic pyrogallol host (centroid C3 C4 C5 C6 C7 C25···H41A = 2.998 Å and centroid C15 C16 C17 C18 C19 C27···H41B = 2.698 Å).

The ethanol guest is entrapped by an offset head-to-tail open capsule, formed between the upper phenolic groups of one calixarene and the three pendant chains of a second pyrogallol[4]arene, which envelop the chloride as mentioned previously (O8···O16 = 2.892 Å) (Figure 63b). This results in the hydroxyl group of the ethanol guest forming an hydrogen bond bridge between two of the three propanol chains that make up the open capsule (O18 ··· O13 = 2.438 Å, O18···O16(A) = 2.584 Å). This second interaction of the second chain explains the disorder over two positions experienced by O16.
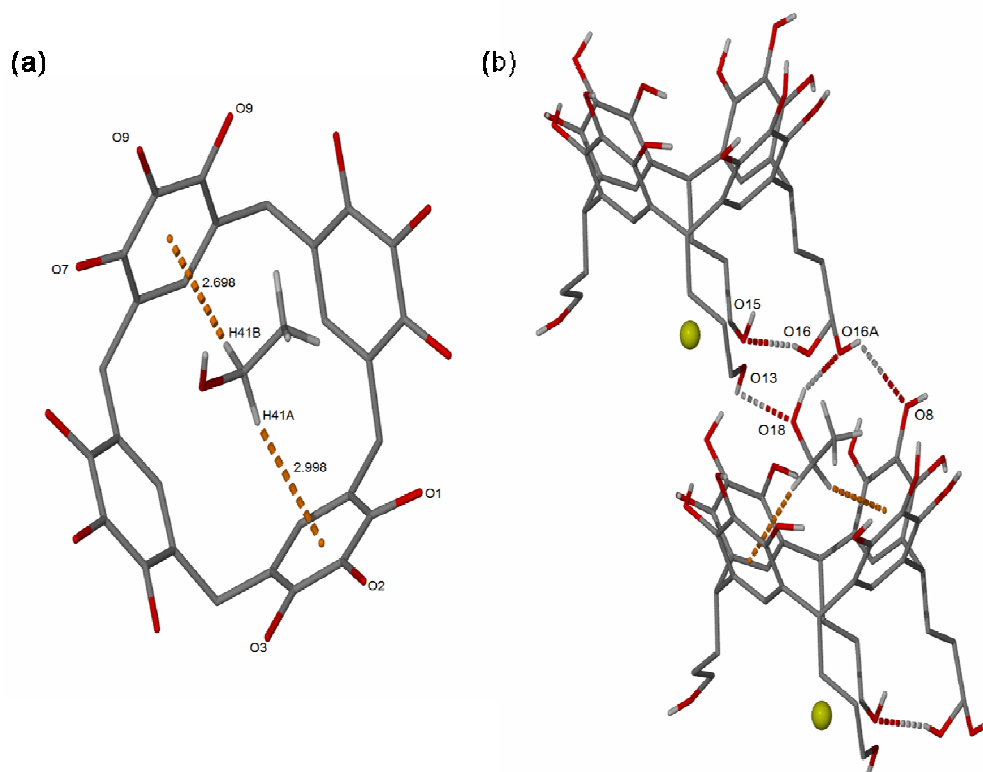
*Figure 63: Entrapment of ethanol by C-3-hydroxypropyl-pyrogallol[4]arenes **25** (a) within the cavity and (b) wih the neighboring pendant chains (hydrogens and pendant chains have been omitted for clarity)*

When the same *C*-3-hydroxypropyl-pyrogallol[4]arene **25** is crystallised from wet ethanol, a four component capsule can be seen to form and then trap two ethanol guest molecules within a cavity of *ca* 110 Å^3.[290] As shown in Figure 64, the capsule is comprised of the head-to-head arrangement of two macrocycles, seamed together *via* four phenolic hydrogen bonds (O2···O7 = 2.849 Å, O8···O3 = 2.800 Å). The two macrocycles are displaced by 4.1 Å with respect to the two C_4 axis of the two pyrogallol[4]arenes. This offset dimeric capsule is closed by two sets of two propanol chains from two independent calixarenes *via* eight hydrogen bonds with the upper rims (O1···O14 = 2.743 Å, O6···O14 = 2.726 Å, O4···O15 = 2.741 Å, O9···O15 = 2.854 Å).
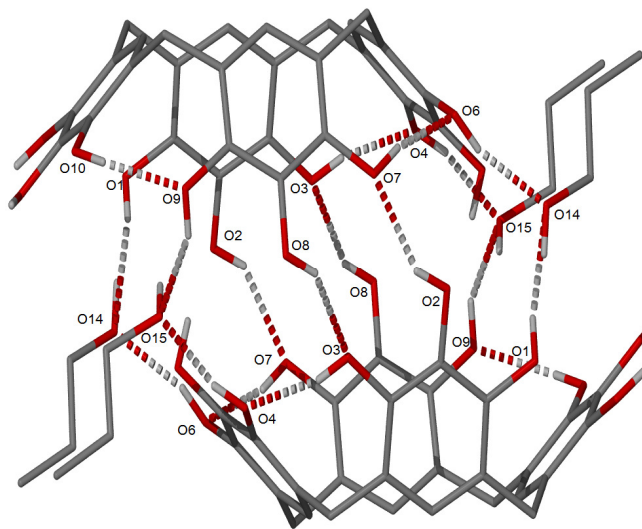
*Figure 64: Hydrogen bonding network forming the dimeric capsule comprised of two C-3-hydroxypropyl-pyrogallol[4]arenes **25** (hydrogen, upper rimss and pendant chains have been omitteded for clarity)*

As shown in Figure 65, two ethanol guest molecules occupy 87% of the available volume of the cavity. This extremely strong packing is due to the presence of two hydrogen bonds between the guest molecules and the hydrogen bonded seamed capsule (O5···O17 = 2.729 Å and O14···O17 = 2.853 Å). In addition, the ethanol guests can be seen to hydrogen bond *via* its two methylene protons to the electron rich faces of the aromatic pyrogallol host (H41A···centroid: C3 C4 C5 C6 C7 C25 = 2.454 Å and H41B···centroid: C15 C16 C17 C18 C19 C27 = 2.457 Å) as in the previously described structure containing HCl. Furthermore, there is a hydrogen bond formed between the hydroxyl group of the ethanol and the electron rich pyrogallol (H17O···centroid: C1 C21 C22 C23 C24 C28 = 2.481 Å). This causes the ethanol guest to be drawn deeper into the cavity resulting in reduced hydrogen bonds distances between the guest and the host.

Figure 65: Entrapment of ethanol within the capsule comprised of two C-3-hydroxypropyl-pyrogallol[4]arenes 25 ((hydrogens, upper rims and pendant chains have been omitted for clarity)

Adjacent macrocycles are seen to pack transversally to one another into a head-to-tail sheet network. They are held in place by hydrogen bonds involving the phenolic hydroxyls groups of one macrocycle with the alcohol chains of the next macrocycle (O4···O15 = 2.741 Å, O6···O14 = 2.727 Å, O10···O13 = 2.830 Å, O12···O16 = 3.141 Å) as shown Figure 66.

Figure 66: Head-to-tail arrangement of C-3-hydroxypropyl-pyrogallol[4]arenes 25(hydrogens have been omitted for clarity)

The ethanol and water molecules occupy the voids in the crystal lattice in between the upper rim cavity (*endo*) and the pendant chains respectively, but do not interfere with the hydrogen bonding network, so forming hydrophilic and hydrophobic bilayers. A single water molecule resides at the annulus of the macrocycles between the hydrophobic pendant chains. Unlike the chloride of the previous structure there is an absence of hydrogen bonding between the water and the pyrogallol[4]arene, with acceptor donor distances of 3.111 Å and 3.243 Å. The water is likely to repel the hydrophobic pendant chains. As the chains are unable to adopt the same structural motif as the chloride structure above, it can therefore be concluded that the disturbance of the assembly in presence of ethanol and HCl is mainly attributed to the inclusion of the chloride anion.

When wet acetone replaces wet ethanol as the crystallisation solvent for *C*-3-hydroxypropyl-pyrogallol[4]arene, the capsule is transformed into a rod-like structure; consisting of a head-to-tail arrangement. The rod-like structure contains cavities that can be seen to encapsulate one acetone molecule per calixarene; between the upper rim and the pendant propanol chains of the next calixarene. As shown in Figure 67, the acetone molecule also sits within the cavity of the upper rim with two of its methyl protons orientating towards the electron rich faces of the aromatic pyrogallol host (H42B···centroid C3 C4 C5 C6 C7 C25 = 2.696 Å and H42C···centroid C15 C16 C17 C18 C19 C27 = 2.663 Å). The guest molecule is anchored into place *via* a hydrogen bond between one of the pendant chains of the macrocycles to the carbonyl of the acetone (O14···O18 = 2.799 Å).

The pendant chain, diagonally opposite to the one attached to the guest, can be seen to form a hydrogen bond to the upper rim of the pyrogallol[4]arene that holds the guest (O11···O18 = 2.740 Å). This intermolecular hydrogen bond fastens the two macrocycles into a head-to-tail orientation, leading to the rod-like structure along the *a* axis. The tubular cavity, drawn using geometrical position is represented in blue in Figure 68.
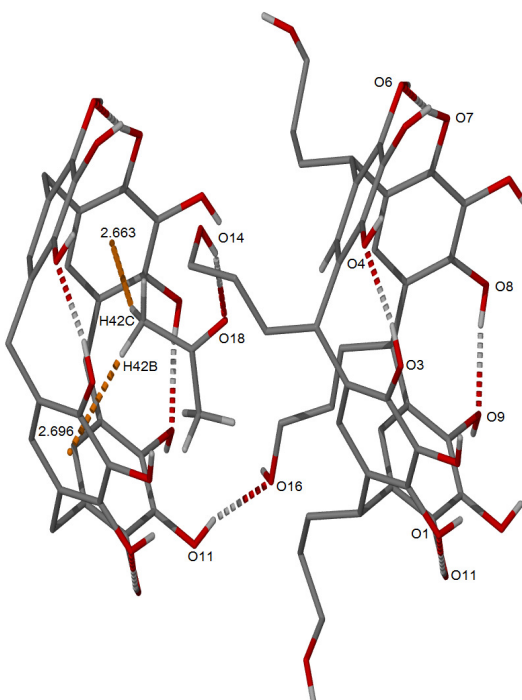
Figure 67: Entrapment of the acetone molecule within two C-3-hydroxypropyl-pyrogallol[4]arenes **25** *(hydrogens and pendant chains have been omitted for clarity)*
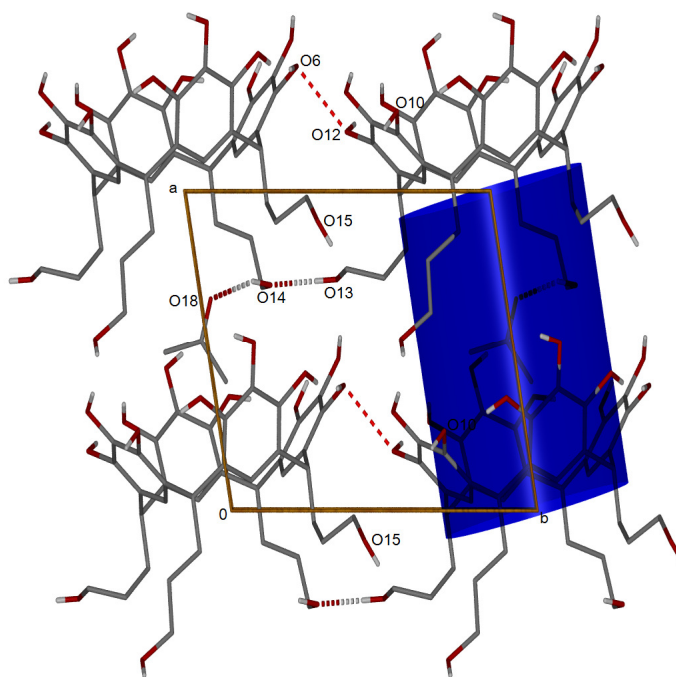
Figure 68: Tubular network formed by C-3-hydroxypropyl-pyrogallol[4]arenes **25** *view along the c axis, (hydrogens have been omitted for clarity)*

The adjacent macrocycle is also attributed to the interconnection of a parallel rod in the same direction, by the intercalation of the propanol chain nearly perpendicular to the chain containing O13; thereby integrating a discrete hydrogen bonding chain, that links to the acetone (O5···O13 = 2.640 Å, O13···O14 = 2.684 Å). This macrocycle contributes the elongation of the network along the *b* axis *via* a hydrogen bond between two adjacent phenolic groups (O6···O12 = 2.693 Å) as illustrated in Figure 69.

The alternating pattern of the tubes along the *c* axis is created by the four hydrogen bonds involving the phenolic head-to-head connections (O2···O3 = 2.702 Å and O8···O9 = 2.844 Å). These interactions are strengthened by the pendant propanol chain of the adjacent macrocycle hydrogen bonding with the upper rim of the calixarene below (O10···O15 = 2.684 Å).
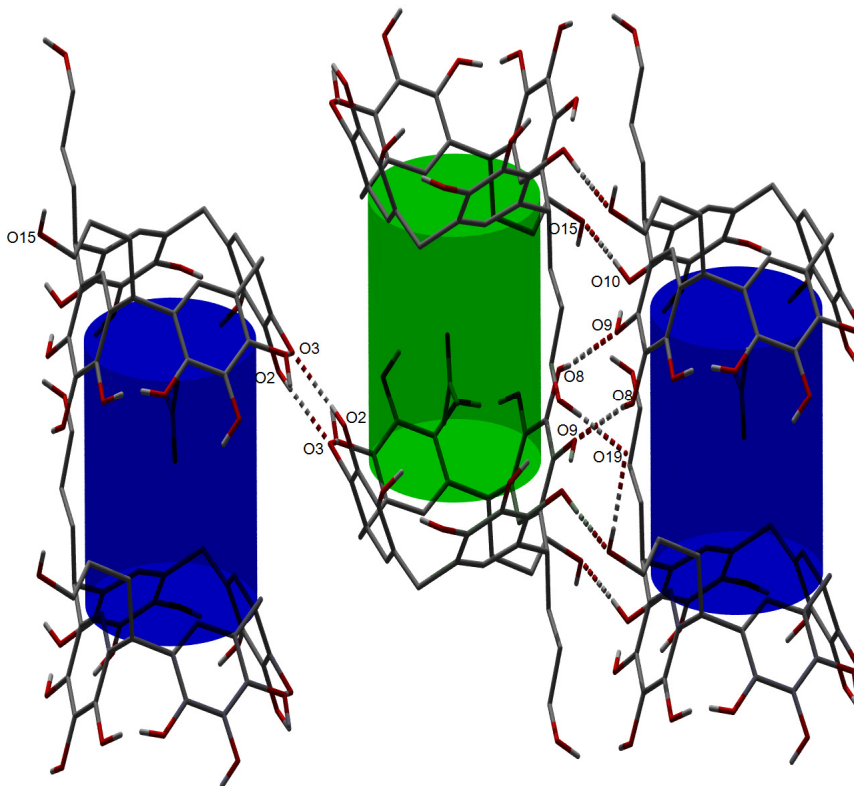
*Figure 69: Egg-box-like structure on the c axis of C-3-hydroxypropyl-pyrogallol[4]arenes **25** (hydrogens and pendant chains have been omitted for clarity)*

The macrocycle is highly hydrated, with seven hydrogen bonds involving water molecules such as H_2O17. Due to low crystal diffraction, the hydrogens were not located and the following interactions are based on the oxygen-oxygen distances and their interactions with the macrocyclic protons. The hydrogen bonding network created *via* O17, links the upper rim of three macrocycles together (O17···O1 = 2.872 Å,

O17$\cdots$O4 = 2.723 Å and O17$\cdots$O5 = 2.812 Å). The water molecule O19 also plays a role in the interconnection of those two macrocycles, by bridging the same propanol chain to another pendant chain (O15$\cdots$O19 = 2.736 Å, O19$\cdots$O16 = 2.734 Å). Although the water molecules are an intricate part of the hydrogen bonding network, they appear to be lying in channels between the tubes, as represented in Figure 70.
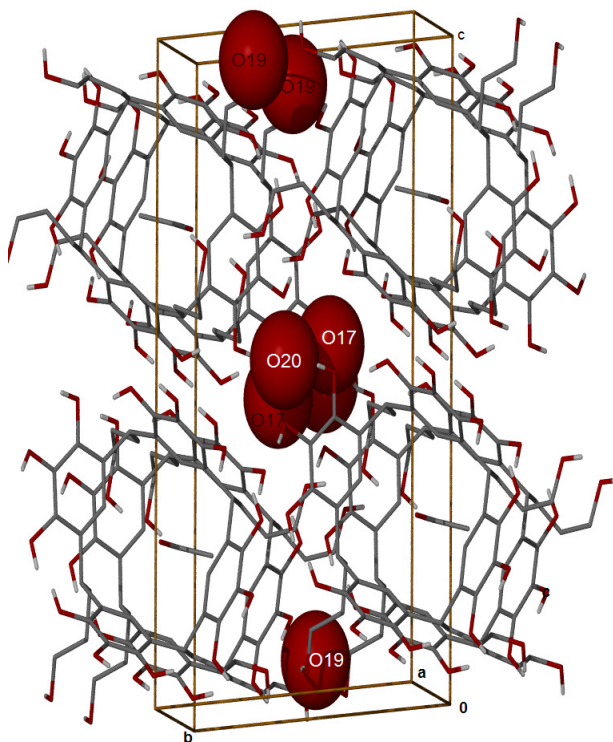
Figure 70: Water channels in the crystal packing of C-3-hydroxypropyl-pyrogallol[4]arene **25** *(hydrogens have been omitted for clarity)*

2. C-4-HYDROXYBUTYL-PYROGALLOL[4]ARENE

In accordance with the results obtained for the 3-hydroxypropyl analogues, single crystal X-ray analysis of *C*-4-hydroxybutyl-pyrogallol[4]arene **26**, which was crystallised by slow evaporation of acetone, also led to the formation of a tubular structure. Each acetone molecule sits in the cavity created by the pyrogallolarene cup and the pendants chains of the following molecule to forms a "solvent channel"; however, the acetone is not coordinated to any pendant chains as seen previously. Interestingly, its orientation within the cavity of each macrocycles varies, with an overall rotation of 90°. The crystal packing, maintained by forty hydrogen bonds, shows six molecules *i.e.* three calixarenes and three acetone molecules, in the asymmetric

unit, which fill the unit cell in the $P\bar{1}$ space group. Of the twelve hydrogen binding sites available on the upper rim of the pyrogallol[4]arene, four hydrogen donors are involved in intramolecular bonding, with average lengths between the oxygens of 2.692 Å, holding the cup into the cone conformation.
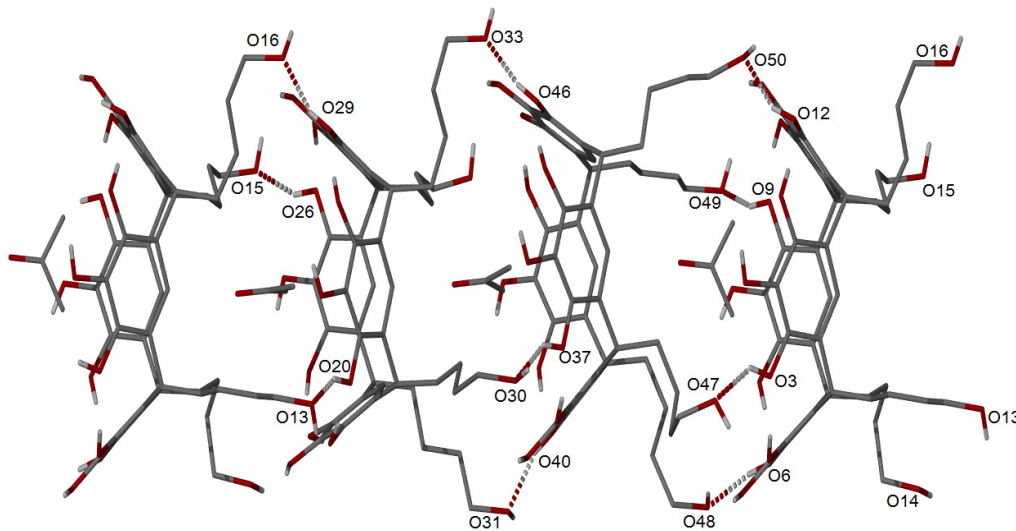
Figure 71: Hydrogen network forming the tubes made of C-4-hydroxybutyl-pyrogallol[4]arenes **26** *(hydrogens have been omitted for clarity)*

As seen in Figure 71, the pendant chains of one pyrogallol[4]arene are anchored to the upper rim of the following macrocycle, *via* three to four hydrogen bonds (

Table 8). This head-to-tail arrangement is maintained by three of the strongest intermolecular interactions of the whole packing, *i.e.* -123.5, -124.5 and -130.0 kJ.mol^{-1} [291-292].

Atom 1	Atom 2	Length (Å)	Atom 1	Atom 2	Length (Å)	Atom 1	Atom 2	Length (Å)
O13	O20	2.622	O30	O37	2.641	O47	O3	2.623
O14	O23	2.623	O31	O40	2.607	O48	O6	2.617
O15	O26	2.579	O33	O46	2.609	O49	O9	2.582
O16	O29	2.615				O50	O12	2.566

Table 8: Lengths of the hydrogen bonds interactions between the pendant chains and the upper rim

The inversion of the neighbouring tubes is generated through the upper rim interactions

leading to head-to-head disposition into an egg-box-like pattern on each side of each cup maintained by a network of fourteen hydrogen bonds (Figure 72, Table 9).
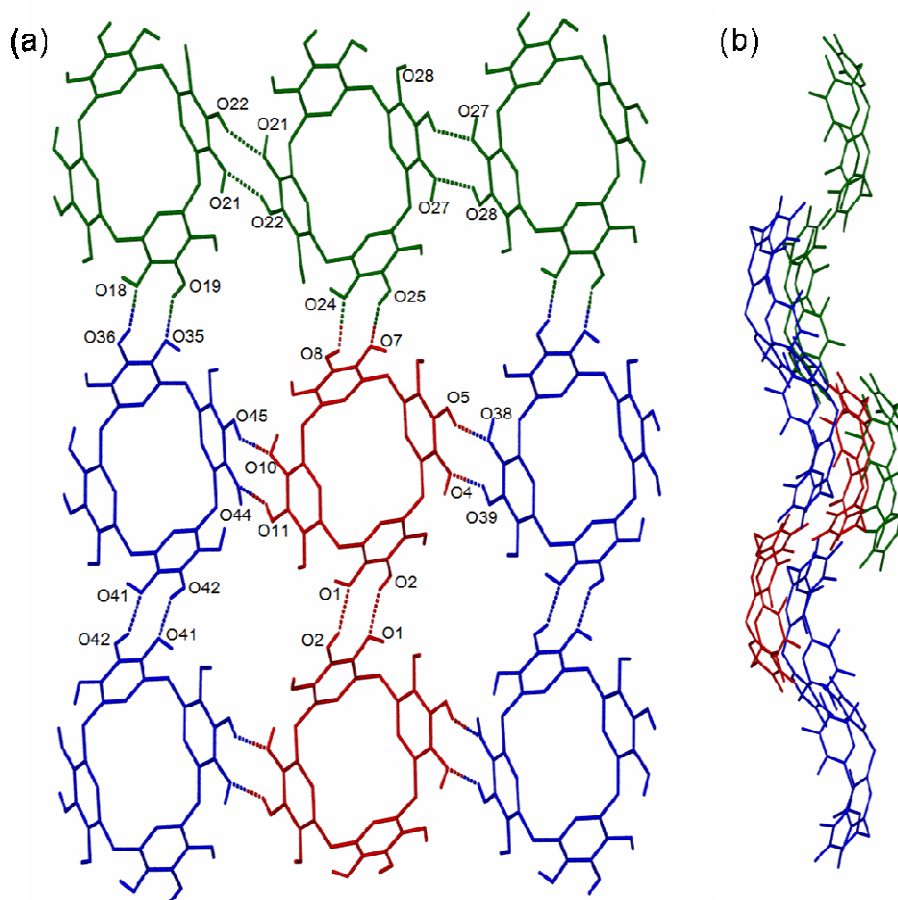
Figure 72: C-4-hydroxybutyl-pyrogallol[4]arenes' upper rims hydrogen bonding (a) leading to the egg-box-like pattern (b) (each colour represent a different macrocycle in the asymmetric unit, hydrogens and pendant chains have been omitted for clarity)

Atom 1	Atom 2	Length (Å)	Atom 1	Atom 2	Length (Å)	Atom 1	Atom 2	Length (Å)
O1	O2	2.841	O8	O24	2.804	O19	O35	2.775
O4	O39	2.708	O10	O45	2.833	O21	O22	3.138
O5	O38	2.858	O11	O44	2.861	O28	O27	2.992
O7	O25	2.757	O18	O36	2.786	O41	O42	2.754

Table 9: Upper rim hydrogen bonds lengths

Due to the absence of water molecules that were present in previous structures, the hydrogen bond network of *C*-4-hydroxybutyl-pyrogallol[4]arene **26** is strengthened by the pendant chains, resulting in a tail-to-tail arrangement in both direction of the tubes. As represented in Figure 73, these interactions occur along the (1, 1, -1) Miller plane (O14···O49 = 2.761 Å, O47···O50 = 2.957 Å, O30···O16 = 2.732 Å, O31···O32 = 2.726 Å), as well as one of its perpendicular Miller planes (10, 9, -9) (O49···O33 = 2.692 Å, O47···O31 = 2.782 Å, O15···O16 = 2.807 Å).
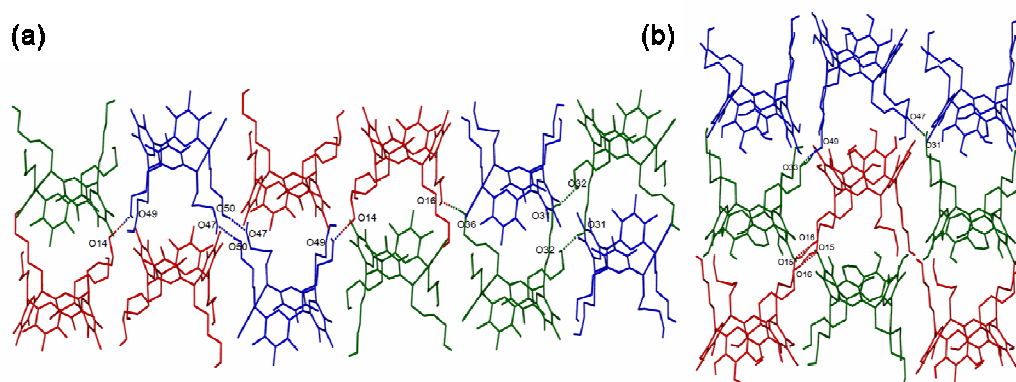
*Figure 73: Pendant chains interactions of C-4-hydroxybutyl-pyrogallol[4]arenes **26** on (a) (1, 1, -1) and(b) (10, 9, -9) Miller planes, (hydrogens have been omitted for clarity)*

When a mixture of acetone and acetonitrile (1:1) is used as crystallisation solvent, a single macrocycle, two acetonitrile and one acetone molecules are completing the asymmetric unit with $P2_1/m$ symmetry. The tubular crystal pattern created by using acetone alone as the solvent system is altered, whereby the capsule formed by the pendant chain and upper rim accommodates the acetonitrile as a guest. As seen previously, the butanol chain coordinates to the upper rim *via* hydrogen bonding interactions (O2···O9 = 3.187 Å, O4···O8 = 3.036 Å, O5···O8 = 2.836 Å) forming a rod-like structure along the *a* axis (Figure 74). However, the network is distorted by the presence of the acetonitrile and the cavity becomes permeable to guest molecules. As the pendant chains are coordinated to the central pyrogallol instead of the external one, it leads to a slight shift and tilted rods, with a displacement of 14.441 Å with respect to the two C_4 axis of the pyrogallol[4]arenes. The butanol chains also contributes to the

interconnection of the tubes by bridging the upper rims along the *c* axis *via* two hydrogen bonds (O7···O8 = 2.952 Å and O6···O8 = 2.738 Å).
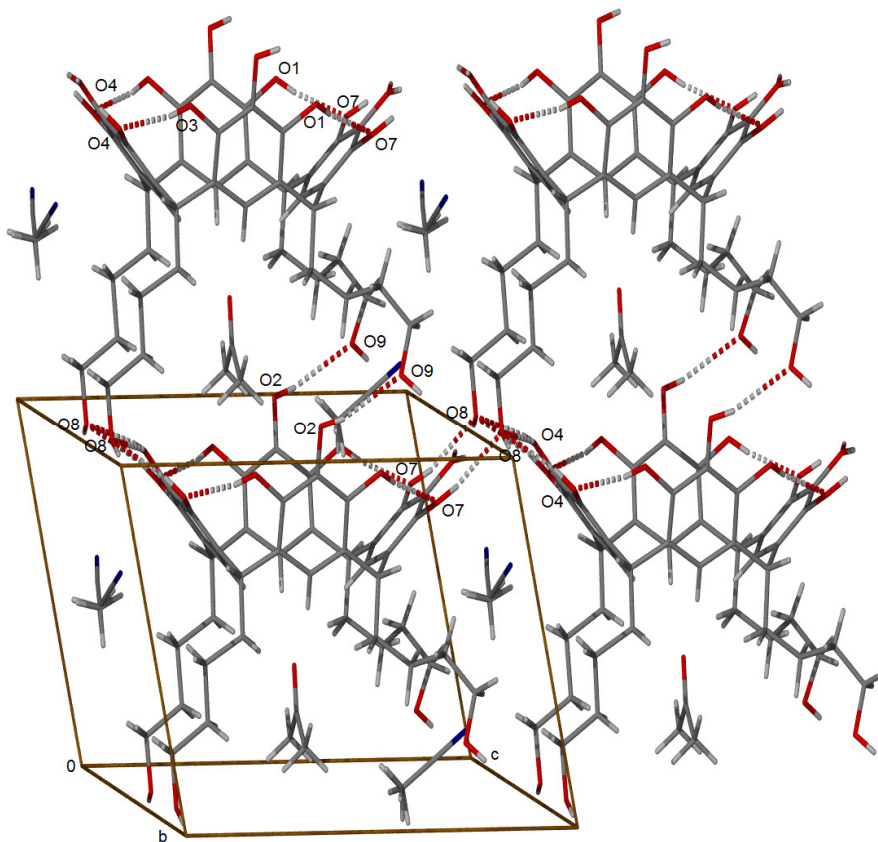
Figure 74: Packing of the titled rod formed of C-4-hydroxybutyl-pyrogallol[4]arenes along the a axis

The macrocycle is translated onto the *b* axis of the cell *via* a two fold screw axis, leading to the formation of the alternating egg-box-like pattern that enables the channel to change the directions of the rods (Figure 75). As a result, the upper rim of the translated macrocycles is anchored *via* two hydrogen bonds (O2···O3 = 2.777 Å). This interaction is reinforced by the pendant chains that are also connected (O8···O9 = 2.773 Å). Compared to the previous structures involving acetone, the guest molecule is not anchored onto the upper rim cavity. Although acetonitrile resides in between the pendant chains there is no hydrogen bonding involved (N3···O9 = 4.348 Å), therefore the involvement of the solvent is likely to be steric.
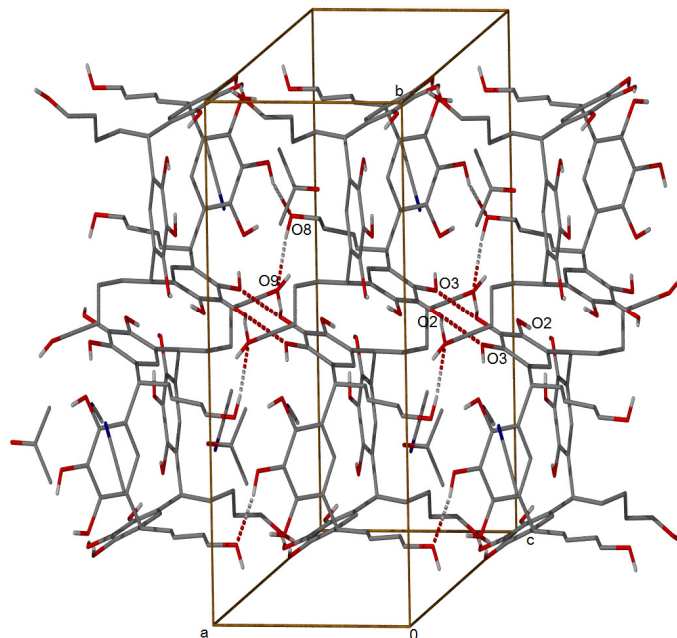
*Figure 75: Elongation of the network created by of C-4-hydroxybutyl-pyrogallol[4]arenes **26** along the b axis (hydrogens have been omitted for clarity)*

The study of the behaviour of *C*-4-hydroxybutyl-pyrogallol[4]arene **26** in the solid state when crystallised from wet acetonitrile was attempted in order to obtain the hexamer aggregate as previously reported.[81] The asymmetric unit in the *P*2*na*1 space group consists of one macrocycle, one acetonitrile that resides in between the lipophilic part of the pendant chains and two water molecules. Although crystallised from wet acetonitrile, no specific hydrogen bonding was present to form a rod-like structure, a dimeric capsule or the hexamer. The cone conformation is still maintained by the intramolecular binding (Figure 76); however, the structure exhibits a very unusual packing system. This effect is attributed to the two highly disordered water molecules that compete in the self-assembly and therefore disable the ability of a head-to-head or head-to-tail arrangement previously observed.
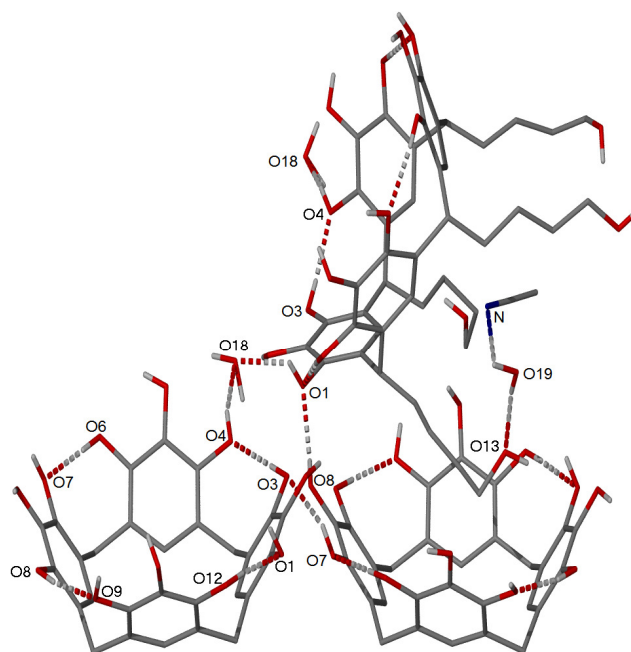
*Figure 76: Upper rim interactions of C-4-hydroxybutyl-pyrogallol[4]arenes **26** (hydrogens and pendant chains have been omitted for clarity)*

One pyrogallol[4]arene is translated *via* a two fold screw axis, this symmetry generated macrocycle is linked to the first one *via* a hydrogen bond between two phenolic hydroxyls (O1···O8 = 2.749 Å). The interconnection of these two macrocycles is reinforced by the presence of a third one, that is hydrogen bonded to the upper rim of the translated calixarene (O3···O7 = 2.7834 Å). This third macrocycle also interacts with the initial calixarene, *via* a discrete chain of hydrogen bond interactions involving a water molecule (O4···O18 = 2.707 Å and O18···O1 = 2.636 Å), as seen in Figure 76.

One of the pendant butanol chains resides in the centre of the hydrophilic part of the upper rim cavity. Although the alcohol group of this chain is pointing towards one pyrogallol face, it is not maintained by hydrogen bonding (O13···O2= 3.497 Å). Nevertheless, it is linked to the acetonitrile molecule that resides in between the lipophilic part of the four pendant chains *via* a hydrogen bonded bridge involving water (O13···O19 = 2.496 Å, O19···N = 2.950 Å). The pendant chains also contributes to the organisation of upper rim and complete the hydrogen bonding network of this crystal lattice (Figure 77). Three interactions exist between the upper rim and the pendant chains (O2···O15 = 2.743 Å, O5···O14 = 2.737 Å, O9···O14 = 2.787 Å) and one between two pendant chains themselves (O14···O16 = 2.831 Å).
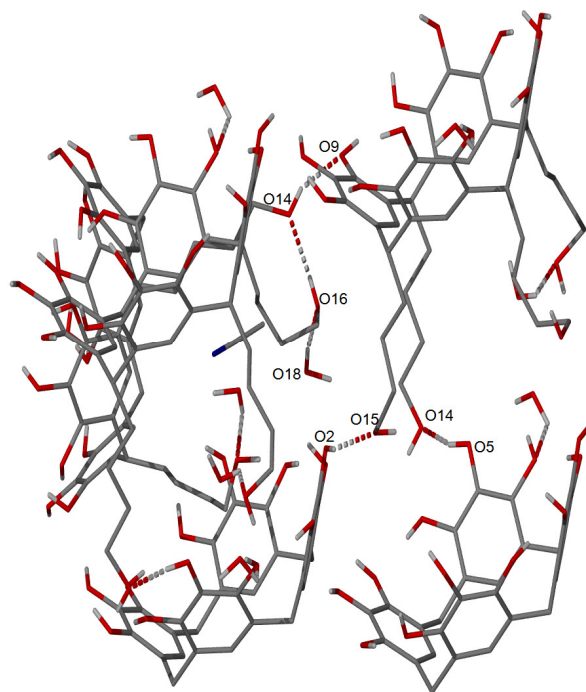
Figure 77: Involvement of the pendant chains in the packing of C-4-hydroxybutyl-pyrogallol[4]arenes 26 (hydrogens and pendant chains have been omitted for clarity)

As observed with the 3-hydroxypropyl analogues, the solvent system has an important role in the solid state, often directing the self-assembly process. The nanometre scale rods that adapt or respond to a guest (such as acetonitrile) could potentially find applications as a transport channel. The difference of the cavity volume in the presence of different guests was assessed using the computer program MCavity,[290] it shows that when only acetone is present its volume is around 92 Å^3, compared to the 128 Å^3 when acetonitrile is present. These cavities are smaller compared to the hexamer cavities of 1300 Å^3, but comparable to the 143 Å^3 cavity when forming a head-to-head dimer.[74, 293]

3. PYROGALLOL[4]ARENE METAL COMPLEX

If the pyrogallol[4]arenes aggregate on the nano-meter scale, it would favour their engulfment by the dendritic cells *via* endocytosis. Their self-assembly can be achieved through crystallisation from ethyl acetate, acetonitrile or chloroform. Unfortunately, the solubility of those macrocycles highly relies on the pendant chains functionality, which can be an issue when multi-functionalities will be present. To overcome this potential issue, the self-assembly involving chelation to metal complexes was considered, as they have shown excellent stability.[100] The crystallisations of *C*-3-hydroxypropyl-pyrogallol[4]arene with various metals, copper, gadolinium, gallium as their nitrate salts, were investigated. Unfortunately, to date, none of them resulted in crystalline materials suitable for X-ray crystallography. Attention has been turned to the zinc metal, as it was shown to have the ability to change the conformation of the macrocycle by coordinating to metal.

The first hydroxycalixarene that was coordinated to zinc, used the aminomethylated resorcin[4]arene and zinc chloride. The zinc was not directly attached to the calixarene but was intercalated in the packing, creating an cationic ligand as host for an ionic self-assembling system.[294] In 2000, zinc(II) ions were used to form loops with resorcinarene cavitands.[295] Subsequently, this work led onto different metals such as cadmium, copper as well as zinc that have shown potential to strongly bind to fullerenes C_{60}.[296] The first pyrogallol[4]arene capsule coordinated by eight zinc centres was reported in 2007. These entities were proved to be stable in both solid and liquid state entrapping one pyridine in their cavities, it was then shown that this coordination also enables the *rccc* conformation to be maintained.[103, 105, 297]

In the search for a metal organic framework, zinc pyridinium nitrate **27** $(Zn(NO_3)_2Py_3)$ was prepared by mixing zinc nitrate hexahydrate with pyridine resulting in white crystals that were then mixed in excess with *C*-3-hydroxypropyl-pyrogallol[4]arene **25** in a 1:1 mixture of acetonitrile:methanol. Upon evaporation, suitable crystals for single crystal X-ray crystallography were formed, exhibiting a very large unit cell (V= 14032.3 $Å^3$) in the *P*2$_1$/*c* space group. After data collection and structure solution, despite the resolution being very low, the preliminary single crystal refinement data showed two pyrogallol[4]arenes, in their anionic forms, self-assembled with eight zinc centres to form a dimeric capsule. The volume inside the dimer cavity is 127.6 $Å^3$, as calculated using the MCavity program.[290] Each phenolic oxygen

chelates to at least one Zn^{2+} cation, with the central phenolate anion chelating to two metal centres, with distances ranging from 2.011 Å (Zn8···O8) to 2.109 Å (Zn1···O26). As seen in Figure 78a, this arrangement leads to two pyrogallol[4]arenes being offset from one another by 45.25° about the C_{4v} axis. As shown in Figure 78b, the pyridine remains coordinated to each zinc, with distances ranging from 1.982 Å (Zn6···N5) to 2.075 Å (Zn2···N1), forming what was referred as a Pelton wheel by others.[297] If the coordinative bond was replaced by hydrogen bonding the distances range between the two closest phenolic oxygens would be from 2.886 Å to 2.966 Å.
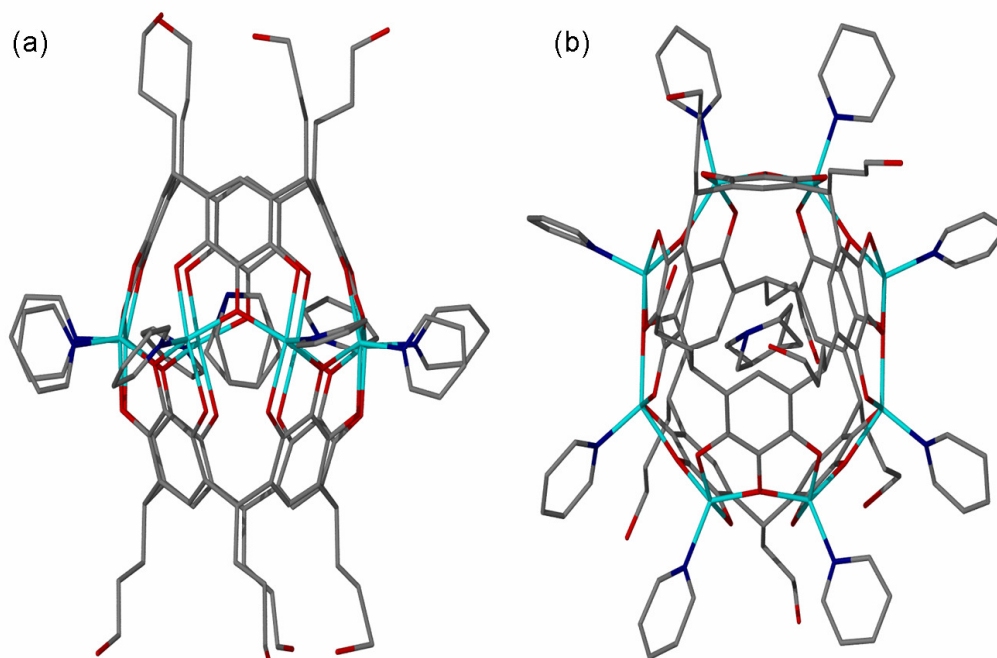
*Figure 78: C-3-hydroxypropyl-pyrogallol[4]arene bis(pyridyl) zinc (II) dimer **28** view along (a) the side and(b) from the top(hydrogens have been omitted for clarity)*

The phenolates lose their hydrogen bonding potential when coordinated to the zinc, whereas the pendant chains retain their functionality. This enable the extension of the network between capsules (O14···O29 = 2.691 Å, O15···O32 = 2.753 Å, O13···O29 = 2.775 Å), as shown in Figure 79.
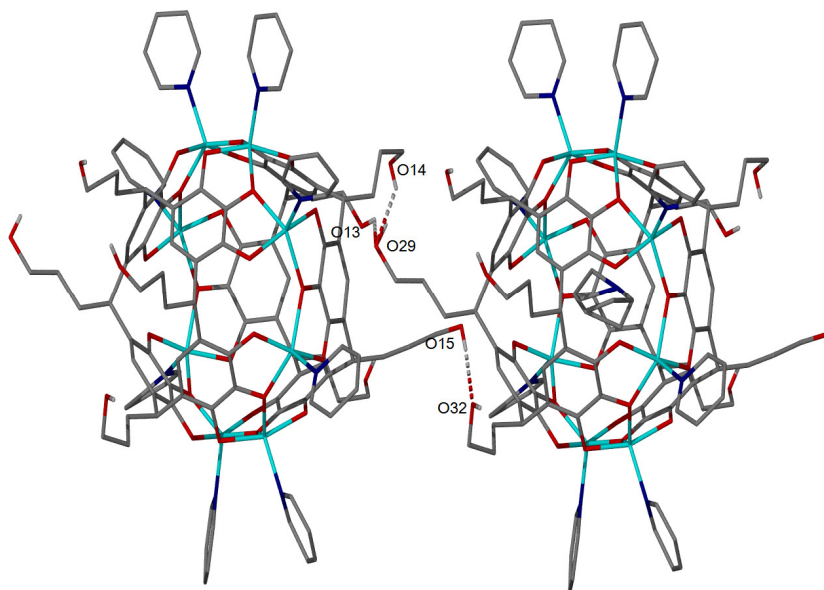
Figure 79: Hydrogen bonding interactions of the pendant chains

The stability of this new capsule in various solvents remains to be confirmed, but potentially, the further functionalisation of the lower rim could be achieved on the zinc complex. This would prove to be a useful scaffold that offers selective reversible protection of the upper rim.

4. SELF-ASSEMBLY ON THE NANOSCALE

In order to investigate the self-assembly of *C*-4-hydroxybutyl-pyrogallol[4]arene **26** into larger aggregates, on the nanoscale, a study was performed using the electron microscopy technique (TEM). When similar studies were performed, it was observed that the size and shape of the aggregates can differ depending on the solution concentration and the evaporation time.[84] The TEM image (Figure 80a) of *C*-4-hydroxybutyl-pyrogallol[4]arene **26** evaporated from an acetone and water solution (1:1, 1 mM) revealed the formation of a tubular aggregates, with width ranging from 18 to 25 nm. As seen in the solid state, several rods can interact with one another, which led to the assumption that the aggregate are the results of the assembly of eighteen to twenty-five rods in a circular manner.

The formation of spherical aggregates that have been reported previously was also attempted.[85] *C*-4-Hydroxybutyl-pyrogallol[4]arene **26** was found to be insoluble in ethyl acetate, as used in the previous studies, and this issue was overcome by using an acetone and ethyl acetate mixture (1:1, 1 mM). The TEM image obtained (Figure 80b) showed some interesting features, in a form of dumbbell-like aggregates, with a diameter of 40 nm in the spherical end part and a diameter of 15 nm in the rod-like linker. It can be assumed that the rod is formed by the entrapment of the acetone, whilst the ends of the dumbbell correspond to the aggregation of hexameric capsule. As previous studies on the alkyl footed pyrogallol[4]arene revealed that the addition of water or acetone does not interfere with the spherical aggregation, and using observations from the solid state studies, it can be concluded that the dumbbell-like aggregates are mainly caused by the polar pendant chains.
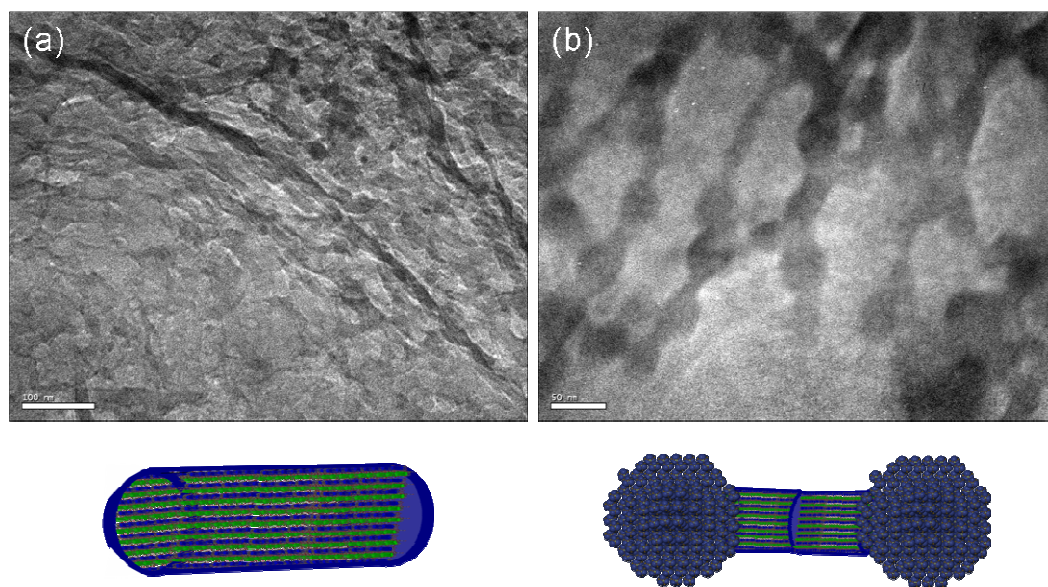
Figure 80:TEM images of C-3-hydroxypropyl-pyrogallol[4]arene aggregates from a wet acetone (a) and an acetone/ethyl acetate(b) solutions and their graphic representations

B. AMINO-FOOTED CALIXARENES

The amino group is an essential function when considering the attachment of amino acids, and it was therefore essential to use amino footed calixarenes as a starting derivative towards a peptide scaffold for immunotherapeutic vectors. The functionalisation of the pendant chains with an amino group was investigated *via* several synthetic routes. In the literature, such a compound was only reported once *via* the benzylated *C*-4-hydroxybutyl-resorcin[4]arene in a six step synthesis.[161] Such an approach was considered; however, during an investigation into the selectivity of the protection step, an alternative method became apparent. Instead, access to the amino functionality was attempted *via* the Gabriel synthesis transforming the bromine derivative obtained from the hydroxyl to an amine by reaction with potassium phthalimide (Scheme 11). Unfortunately, only the calixarene was recovered, it can be thought that the phthalimide also reacted on the unprotected phenol leading to the formation of a mixture that was not resolved.
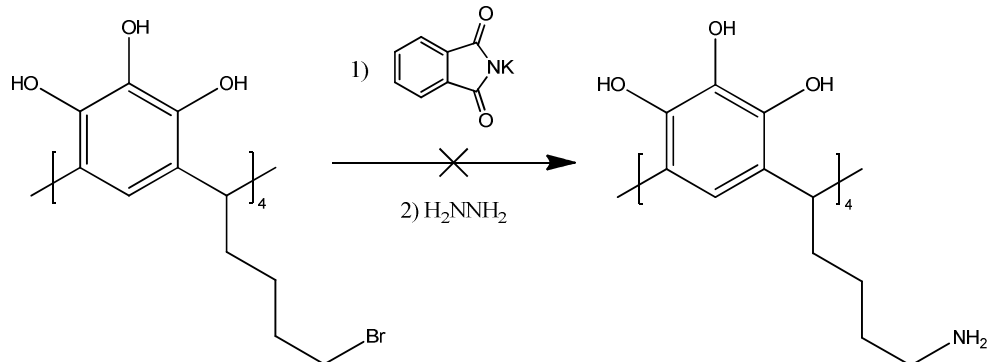
Scheme 11: Gabriel synthesis

The introduction of the amine functionality *via* the *N*-Boc-3,4-dihydro-*2H*-pyridine instead of the *2H*-dihydropyran was considered; however the presence of the Boc protecting group under acidic conditions, results in the liberation of CO_2 which was not compatible with the sealed tube microwave technique (Scheme 12). The reaction also resulted in non-cyclised oligomers when attempted under conventional heating methods.
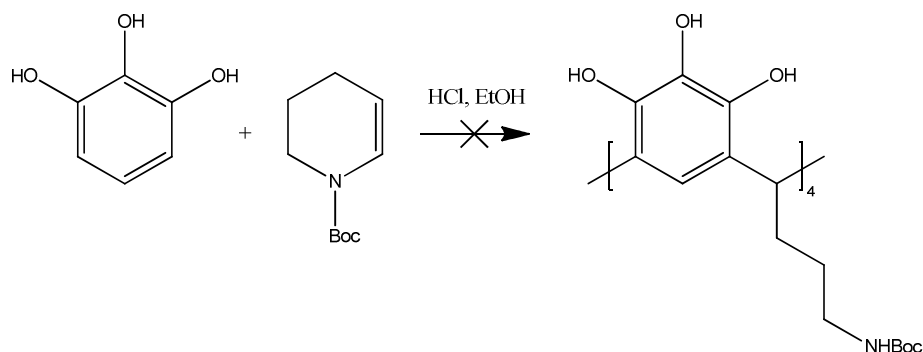
Scheme 12: Attempted synthesis of Boc protected aminopropyl-pyrogallol[4]arene

A commercially available, aminobutyraldehyde diethyl acetal was considered as a starting material for the synthesis of the calixarene. The aminobutyraldehyde offered several advantages as it is already in its protected acetal form which is thought to be an essential intermediate in the cyclocondensation process. Due to its similarities with GABA (γ-aminobutyric acid), a chief inhibitory neurotransmitter, it can be assumed that one of the metabolites of the macrocycles could be assimilated to GABA and therefore may have limited toxicity.

In view of a further selective protection of the phenolic macrocycles, the protection of the amino group was considered, with the Fmoc protecting group due to its stability in strong acidic conditions, compared with the other well-known Boc protecting group. The protected amine was synthesised **33** (44 %) and condensed with pyrogallol. The only product **34** obtained (13%) showed some unexpected features. Although reactants were used in equimolar amounts, the tetramer was not obtained. Instead a product formed of a single pyrogallol ring and two five membered nitrogen containing rings, was obtained as a single enantiomer (Scheme 13).
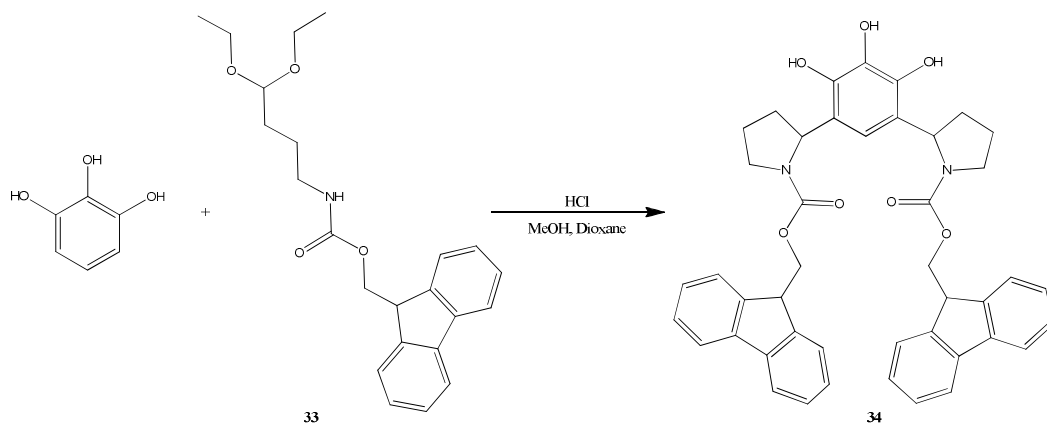
Scheme 13: Synthesis of bis((9H-fluoren-9-yl)methyl)2,2'-(4,5,6-trihydroxy-1,3-phenylene)dipyrrolidine-1-carboxylate 34

It can be assumed that the presence of a longer chain, *i.e.* made of more than six carbons, is necessary between the Fmoc group and the methine bridge. Therefore, a linker is required to not only favour the formation of the tetramer in a cone conformation but also provide more freedom and less steric hindrance to elongate the pendant chains with other entities.

Suitable crystals for X-ray analysis of bis((9H-fluoren-9-yl)methyl)2,2'-(4,5,6-trihydroxy-1,3-phenylene)dipyrrolidine-1-carboxylate **34** were isolated from the reaction mixture (Figure 81). The two Fmoc groups are nearly parallel to each other (angle *ca* 5º). The packing is formed *via* two interaction types, the first being the hydrogen bonding between the phenolic group in the *ortho* position of the pyrogallol and the carbonyl group from the Fmoc. With strong interactions, indicated by relatively short distances between hydrogen donors and acceptors it enables the translation of the molecule along the *a* axis (O1···O6 = 2.739 Å and O3···O5 = 2.726 Å).
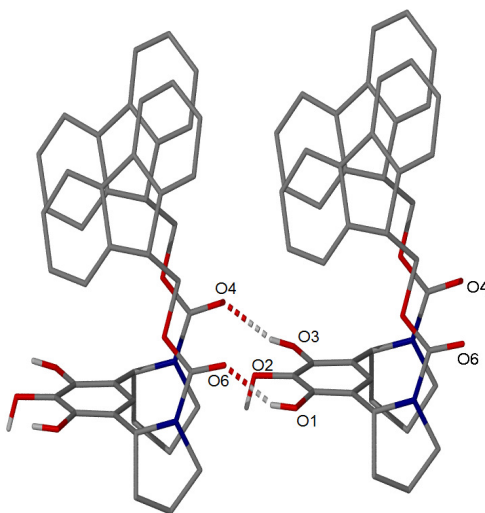
*Figure 81: Hydrogen bonding between two bis((9H-fluoren-9-yl)methyl)2,2'-(4,5,6-trihydroxy-1,3-phenylene)dipyrrolidine-1-carboxylates **34** (hydrogens have been omitted for clarity)*

The second interaction involves a tilted edge-to-face Ar-H···π bonding between one hydrogen of the Fmoc and the face of the pyrogallol with a 75º angle (centroid 1: C1 C2 C3 C4 C5 C6···H41 = 3.187 Å, centroid 2: C45 C46 C47 C48 C49 C50···H85 = 3.152 Å,). The combination of those interactions involving the two chiral molecules that form the asymmetric unit results in the formation of an helical type packing (Figure 82).
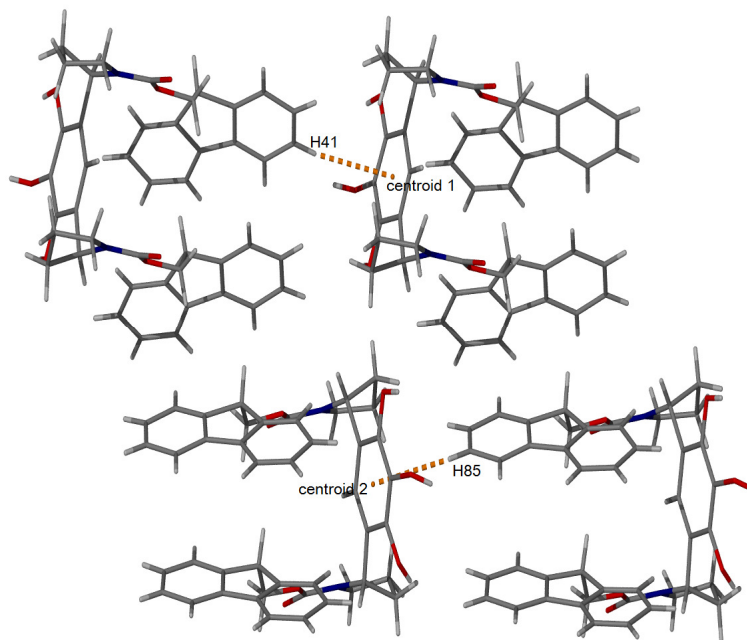
Figure 82: Helicated packing of bis((9H-fluoren-9-yl)methyl)2,2'-(4,5,6-trihydroxy-1,3-phenylene)dipyrrolidine-1-carboxylates **34**

The unprotected aminobutyraldehyde diethyl acetal was therefore reacted with resorcinol and pyrogallol. In order to maintain the acetal functionality, a microwave and grinding methods using *p*TSA as a catalyst were considered but were shown to be unsuccessful for the formation of aminoalkyl-pyrogallol[4]arene. It can be assumed that under those reaction conditions, a cyclised compound is formed in similar fashion to the solid phase synthesis of piperazine using the aminobutyraldehyde acetal and catalytic of *p*TSA in DCM.[298]

Using the method described previously, equimolar quantities of aminobutyraldehyde diethyl acetal and the appropriate phenol were reacted in a mixture of hydrochloric acid and dioxane (25%) at 100 ºC for 10 minutes under microwave irradiation. Two new water soluble macrocycles, *C*-3-aminopropyl-pyrogallol[4]arene **35** and *C*-3-aminopropyl-resorcin[4]arene **36** were synthesised as their hydochloride salts in a single step, with reasonably low yield, 10% and 26% respectively. Although in the protected acetal form, the presence of a strong acid can catalyse the reaction of the aldehyde and the amine functionality, therefore forming an imine, which explains the reduced yields. Ammonium cations have been widely investigated as guests with alkyl-footed pyrogallol[4]arenes and resorcin[4]arenes. In solution, they can act as guest in the hexameric capsule. The pyrogallol[4]arene is selective over neutral amine, such as

115

trihexylamine, compared to resorcin[4]arene that encapsulate both amines and ammounium cations.[90] It has been proved that the ratio of ammonium is highly important in its encapsulation within the hexameric capsule and its presence does not impede the self-assembly.[94, 299] In the encapsulation study of tetraethylammonium cation by alkyl footed resorcin[4]arene derivatives it was found that the counterion does not play any role in the process; however, its nature may change the inclusion of the water molcule in the capsule.[86] In the solid state, tetraalkylammonium cations can only be encapsulated by both resorcin[4]arene and pyrogallol[4]arenes in dimeric capsules, as revealed by several crystal structures.[289, 300-301] Solid state analysis for both *C*-3-aminopropyl-pyrogallol[4]arene **35** and *C*-3-aminopropyl-resorcin[4]arene **36** compounds showed the significance of the counter anion. The chloride anion, from the hydrochloric acid, plays an essential role in the self-assembly as it is involved in the hydrogen bonding network on both the upper and lower rim.

1. *C*-3-AMINOPROPYL- PYROGALLOL[4]ARENE HYDROCHLORIDE **35**

Suitable crystals for X-ray analysis of *C*-3-aminopropyl-pyrogallol[4]arene **35** were obtained by slow evaporation of a methanolic solution. The cone conformation is maintained *via* four intramolecular hydrogen bonds between eight phenolic hydroxyls (O4···O3 = 3.018 Å, O6···O7 = 2.708 Å, O9···O10 = 2.987 Å and O1···O12 = 2.715 Å). The ammonium pendant chains can be compared to the trialkylammonium cations that have been considered as guests in a dimeric complex of *C*-methyl-pyrogallol[4]arenes.[302] However due to steric hindrance the usual self-assembly created by the direct interactions of two upper rim cannot be achieved by *C*-3-aminopropyl-pyrogallol[4]arene **35**. Instead, the upper rim of the macrocycle coordinates *via* hydrogen bonds to the solvent (O2···O14 = 2.946 Å, O3···O14 = 2.919 Å, O8···O15 = 2.602 Å, O7···O16 = 2.595 Å), as well as the chloride anion (O1···Cl2 = 2.860 Å, O5···Cl4 = 2.855 Å). The short distances between one phenolic hydrogen and the chloride (O11···Cl5 = 2.445 Å, H11O···Cl5 = 1.632Å) give the strong bond a covalent character. These distances are much shorter than the ones previously reported (3.057-3.072Å).[302] The chloride anion also acts as a linker between the methanol and the upper rim forming a bridge (Cl4···O15 = 3.066 Å, Cl2···O16 = 3.446 Å). Two of the remaining phenolic hydroxyls hydrogen bond directly to the adjacent macrocycle (O4···O11 = 2.806 Å, O10···O5 = 2.754 Å) leading to a head-to-head assembly along the *a* axis (Figure 83).
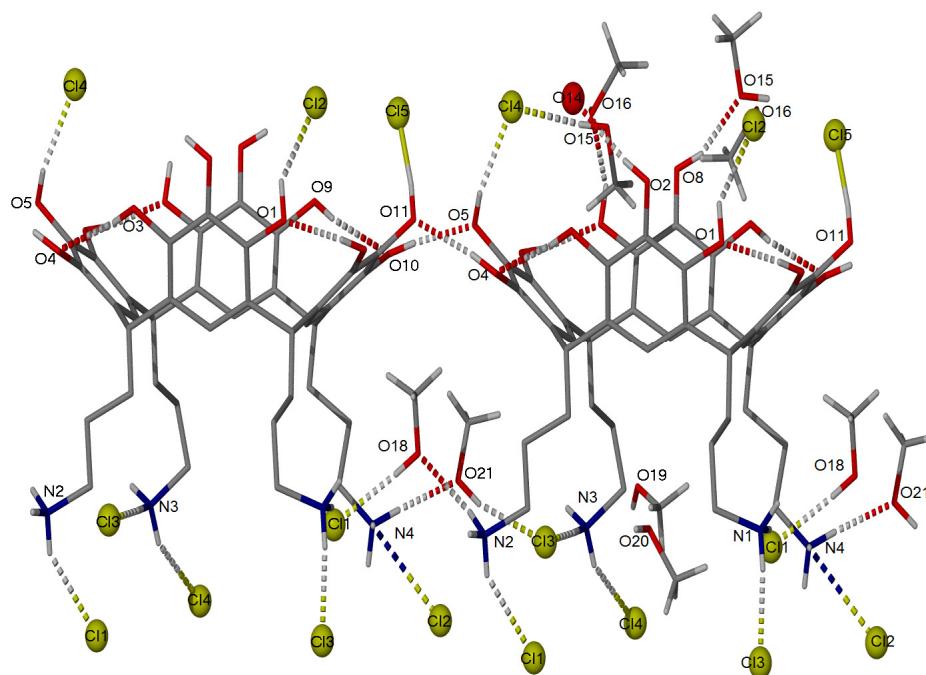
*Figure 83: Hydrogen bonding of the upper rim and chloride interaction with the pendant chains of C-3-aminopropyl-pyrogallol[4]arenes **35**.HCl, (hydrogens have been omitted for clarity)*

As seen in Figure 83, the ionic interactions that exist between the ammonium group and the chlorides have moderate hydrogen bonding properties. Each cation interacts with at least one halide anion (N1···Cl3 = 2.940 Å, N2···Cl1= 3.100 Å, N2···Cl5 = 3.024 Å N3···Cl4=3.027 Å, N3···Cl5= 3.024 Å and N4··· Cl2= 3.026 Å). Surprisingly, although two chlorides reside in between the pendant chains, there is only one interaction with the ammonium (N3···Cl3= 3.306 Å) as the other distances exceed the sum of their van der Waals radii ($r_{Cl}+r_N$ = 3.31Å < N1···Cl1=3.486 Å, N4···Cl1= 3.478 Å, N2···Cl3=4.158 Å). Two of the methanol molecules that surround the pendant chains constitute a bridge with a chloride anion (O21···Cl3 = 3.104 Å, O21···N4 = 2.831 Å, O18 ···Cl1 = 3.046 Å, O18 ···N2 = 2.718 Å). Two distorted methanol are trapped inside the space created by the four pendant chains but do not coordinate with any of them.
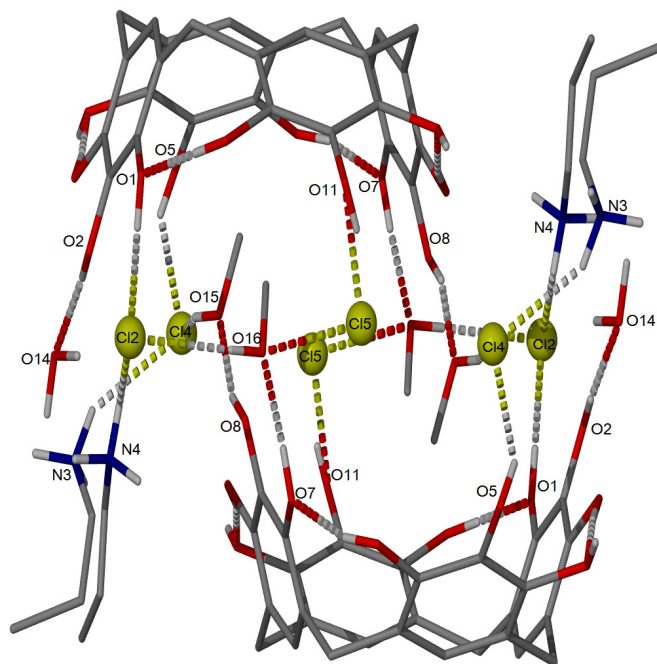
*Figure 84: Hydrogen bonding generating the dimeric complex formed from C-3-aminopropyl-pyrogallol[4]arenes **35**, HCl and methanol,(hydrogens and pendant chains have been omitted for clarity)*

The combined effect of these ionic interactions and the hydrogen bonded one involving the chloride and the solvent, with both the pendant chains and the upper rim, leads to the formation of an offset bridged dimer involving a tridendate chloride anion (N4···Cl2···O1 = 108.05º, N4···Cl2···O21 = 54.53º, O21···Cl2···O1 = 149.61º) Figure 84.[303]

As shown in Figure 85, the offset head-to-head dimeric semi-closed capsule with a calculated internal volume of *ca* 240 $\mathring{A}^3$ is locked by the hydrogen bonding between the upper rim and the guest molecules, as well as the pendant chains of adjacent capsules (O6···N3 = 2.789 $\mathring{A}$ and O12···N1 = 2.868 $\mathring{A}$). This results in another tricoordinate chloride center (N3···Cl4···O5 = 118.65º, N3···Cl4···O15 = 114.87º, O5···Cl4···O15 = 107.34º).
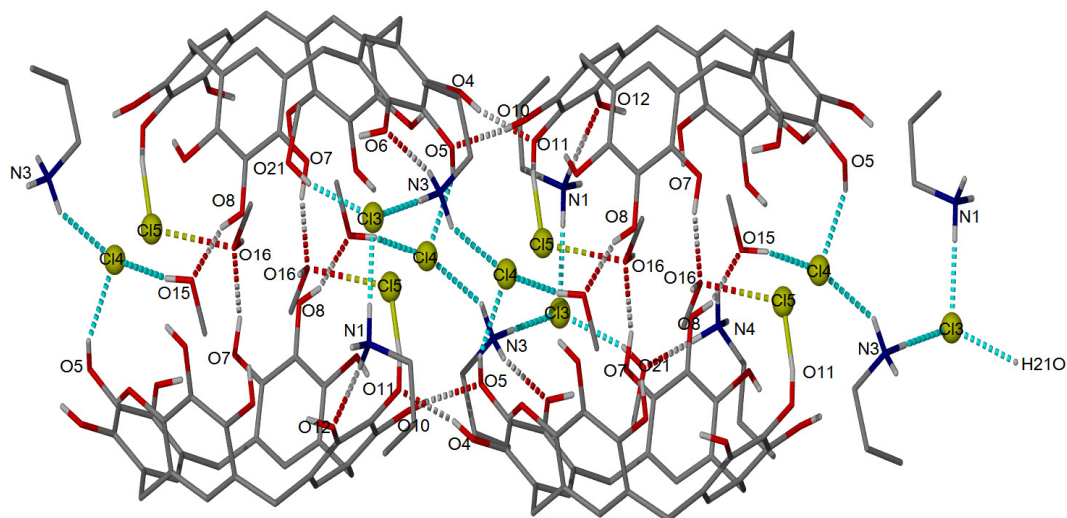
Figure 85: Connection of the dimeric complex formed from C-3-aminopropyl-pyrogallol[4]arenes 35, HCl and methanol,(hydrogens and pendant chains have been omitted for clarity)

2. *C*-3-AMINOPROPYL-RESORCIN[4]ARENE HYDROCHLORIDE **36**

Two suitable crystals for single crystal X-ray analysis of *C*-3-aminopropyl-resorcin[4]arene **36** hydrochloride were obtained by slow evaporation of a methanolic solution. The two sets of data showed $P\bar{1}$ crystal symmetry. However, they show different isolated polymorphs. It appears that the second structure could be less stable than the first one due to rapid solvent loss resulting in a high disorder of the macrocycle core.

In the first structure, the asymmetric unit consists of one methanol molecule, five chloride anions and one *C*-3-aminopropyl-resorcin[4]arene **36** in a flatened cone conformation (Df = 0.65). In line with other ammonium complexes previously described,[289] this conformation is ensured by two intramolecular hydrogen bonds (O1···O8 = 2.845 Å and O4···O5 = 2.864 Å) out of the four possible combinations (O2···O3 = 3.261 Å and O6···O7 = 3.190 Å). The resorcinol rings are therefore slighly tilted towards those intramolecular interactions creating a distortion in the macrocyclic core, which does not adopt the perfect C_{4v} symetry anymore, where the average intramolecular hydrogen bonds length is 2.787 Å. The thirty-two interactions necessary to form the packing rely on the presence of the chloride anion. The only two direct hydrogen bonds involve the methanol molecule (N2···O9 = 2.833 Å and N3···O9 = 2.775 Å), that bridges two pendant chains of the same macrocycle together (Figure 86).
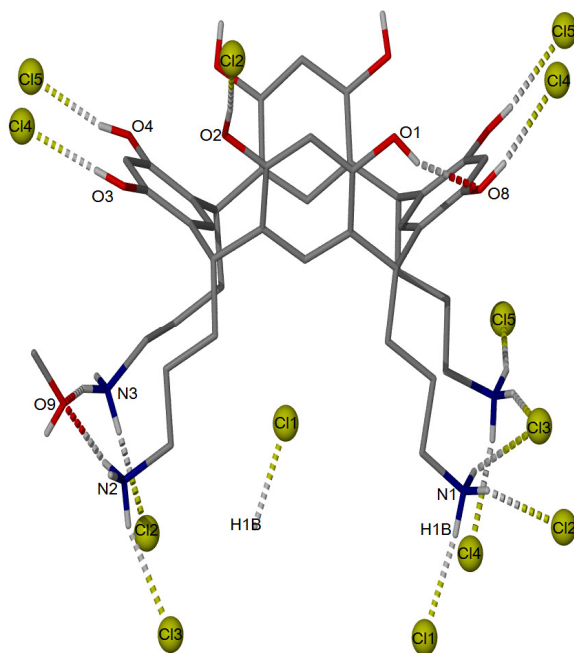
Figure 86: Direct hydrogen bonding with the asymmetric unit of C-3-aminopropyl-resorcin[4]arene 36, HCl and methanol, (hydrogens have been omitted for clarity)

Like its pyrogallol[4]arene analogue, two *C-C*-3-aminopropyl-resorcin[4]arenes **36** form an offset dimer (Figure 87) that originates from three available hydrogens on the ammonium cation of one pendant chain (N4···Cl4 = 3.081Å, N4···Cl5 = 3.209Å, N4···Cl3 = 3.116Å) combined with the tricoordinate chloride counteranion (Cl4). These interactions also take part in the extension of the system in a perpendicular direction of the dimer. As the macrocycle is inverted, a link is formed between the upper rim and the pendant chains. The absence of four hydroxyl groups on the upper rim that are seen in its pyrogallol analogue has an effect on the self-assembly. As the head-to-head arrangement of the upper rims of the resorcinarene with the adjacent macrocycle along the *b* axis is achieved *via* a chloride bridge, whereby the anion coordinates to the upper rim of two adjacent macrocycle *via* hydrogen bonding network (O3···Cl4 = 3.075 Å, Cl4···O8 = 3.071 Å, O4···Cl5 = 2.977 Å, Cl5···O7 = 2.997 Å). Those dimeric capsules resemble the inclusion of a large ammonium cation with methyl-resorcin[4]arene with similar bond lengths (O···Cl- = 2.91 to 3.11 Å), which is contributed to steric hindrance.[289, 300]
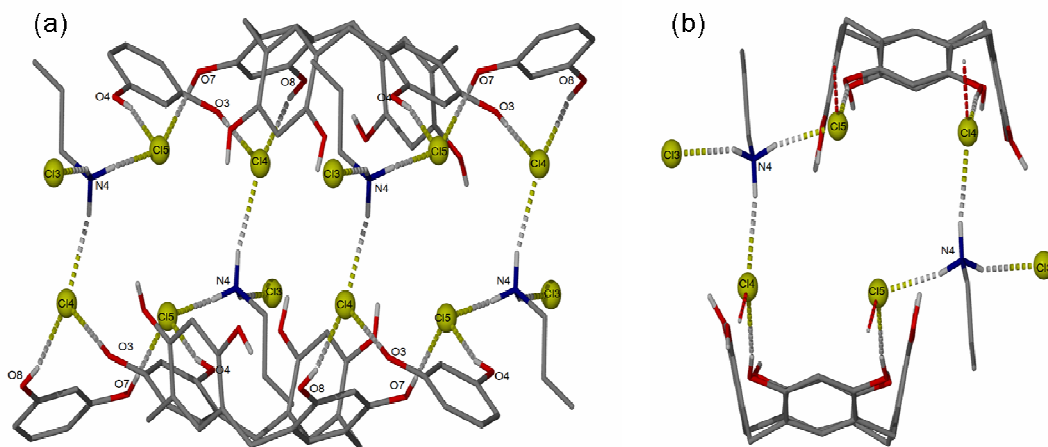
*Figure 87: Offset dimeric complex of C-3-aminopropyl-resorcin[4]arenes **36**, HCl and methanol, (a) along the b axis and (b) along the a axis,(hydrogens and pendant chains have been omitted for clarity)*

As seen in Figure 88, the dimer is locked by the incorporation of pendant chains from adjacent capsules within the same plane. This bridging also occurs with the nearly parallel resorcinol with one of the ammonium chains from *C*-3-aminopropyl-resorcin[4]arene **36** (O2$\cdots$Cl2 = 2.983 Å, Cl2$\cdots$N1 = 3.107Å).
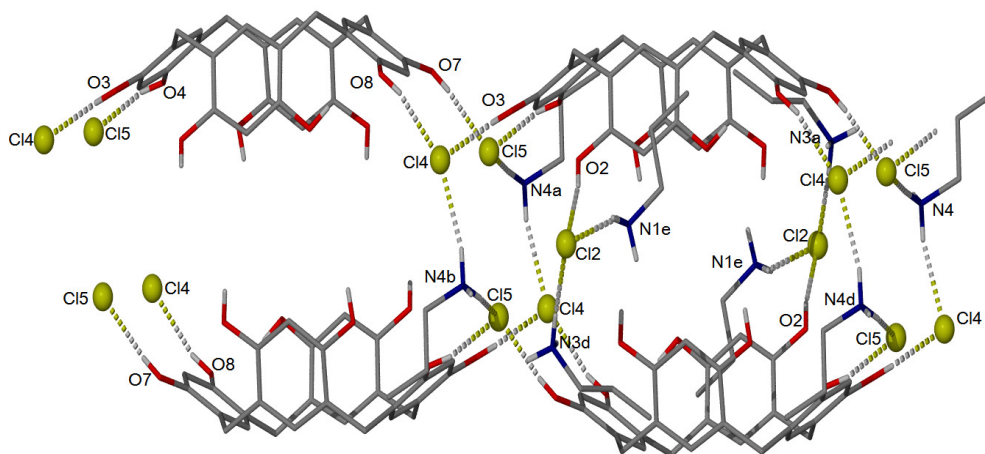
*Figure 88: Interactions of other pendant chains with the dimeric complex formed by C-3-aminopropyl-resorcin[4]arenes **36**, HCl and methanol, (hydrogens and pendant chains omitted for clarity)*

The pendant chains of the two macrocycles translated in the *b* axis are connected *via* a bridging methanol molecule that is linked to a chloride anion (O9···Cl3 = 3.157 Å). In turn, this then interacts with two ammonium ions from the pendant chains of an adjacent resorcin[4]arene (Cl3···N1= 3.213 Å, Cl3···N4= 3.116 Å), as seen in Figure 89.
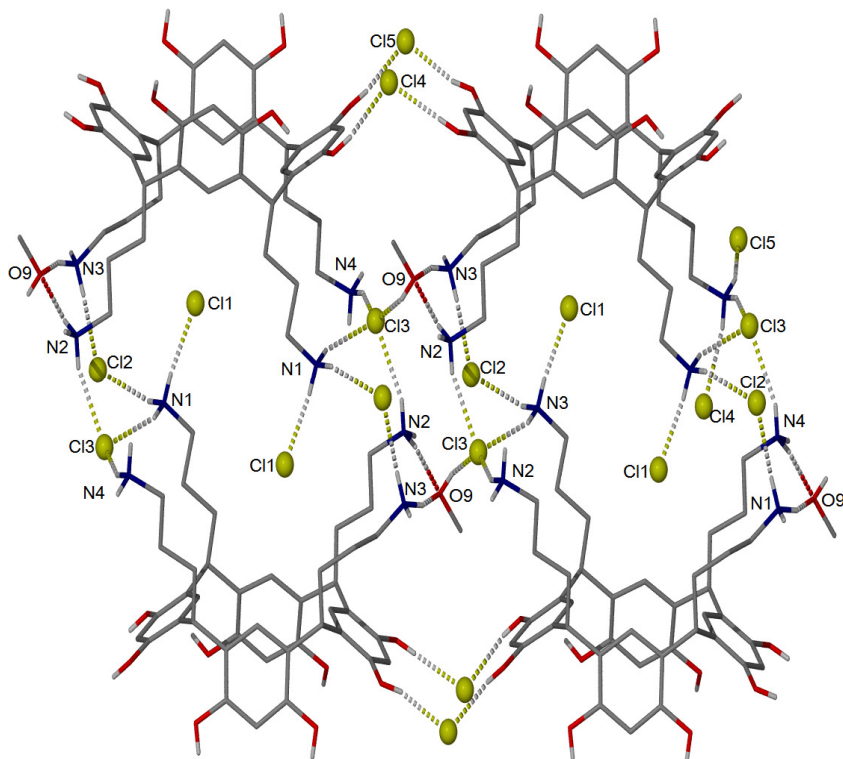
Figure 89: Interconnection of the pendant chains of C-3-aminopropyl-resorcin[4]arenes **36** *(hydrogens omitted for clarity)*

The chloride that resides at the annulus of the lower rim of the macrocycle, within the pendant chain, is locked into position *via* an interaction with one of the pendant chains that ensure the tail-to-tail arrangement (Cl1···N1 = 3.066 Å). One highly coordinated choride is responsible for the agglomeration of all the pendant chains together and thereby maintains the framework (Cl3···N1 = 3.213 Å, Cl3···N2 = 3.279 Å, Cl3···N3 = 3.273 Å, Cl3···N4 = 3.116 Å, Cl3···H9O = 2.437 Å).

In the second structure, despite involving the same macrocycle and the same solvent system, the packing differs. Two *C*-3-aminopropyl-resorcin[4]arenes, eight chloride anions and disordered solvent molecules (predicted to be two water molecules using the SQUEEZE program) consitute the asymetric unit.[276]

The macrocycles are in a boat-like conformation (Df= 0.53 and 0.54) due to the presence of only one intramolecular H-bond between the phenolic hydrogen (O1···O8 = 2.826 Å). This conformation results in a set of two nearly coplanar resorcinol (133.84º and 138.63º) and two nearly parallel resorcinol units (11.67º and 10.13º).

The ammonium terminus of one of the pendant chain resides at equidistance of the two, almost parallel, resorcinols (O2···N8 = 2.970 Å, N8···O5 = 2.897 Å, O10···N4 = 2.955 Å, N4···O13 = 2.9910 Å). The ammonium cation is also stabilised by its electrostatic interaction with the highly electronegative π electron cloud of the coplanar resorcinol ring that it is sitting on (N4···centroid: C49 C50 C51 C52 C53 C66 = 3.191 Å and N8···centroid: C9 C10 11 C12 C13 C26 = 3.143 Å). These distances are shorter than the one reported for the inclusion acetylcholine trimethylammonium moiety in *C*-ethyl-resorcin[4]arene, where the shortest distance is 3.31 Å.[304] As shown in Figure 90, these interactions led to the formation of a herringbone-like stacking of the macrocycles.
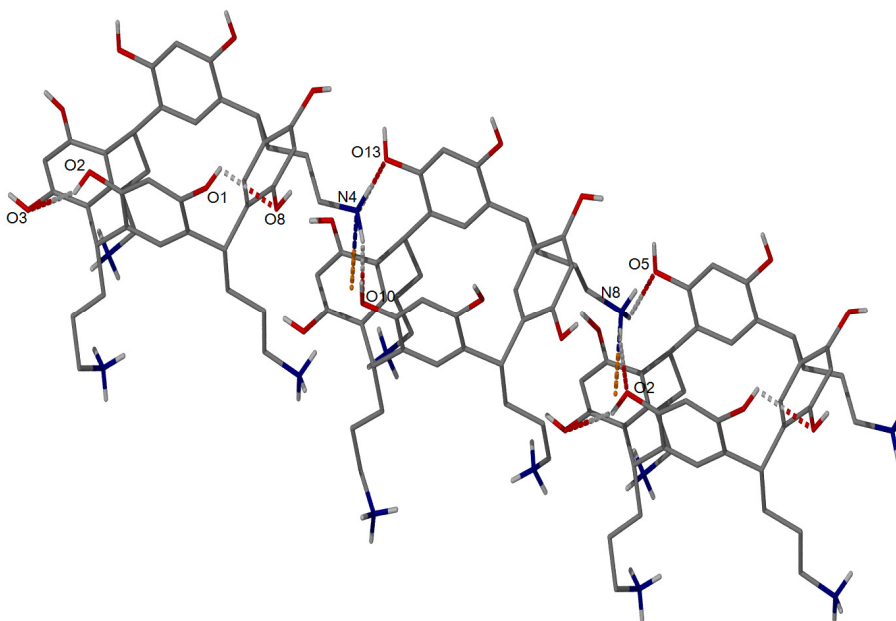
*Figure 90: Herringbone-like stacking of C-3-aminopropyl-pyrogallol[4]arenes **35** (hydrogen have been omitted for clarity)*

The presence of the guest and its attraction towards the ring create an electron pulling effect on the macrocycle. This results in a distortion of its core, as seen in the following diagram based on the x-ray results, Figure 91. The aromatic core is distorted in the herringbone polymorph, loosing the symmetry within the macrocyclic backbone

(light blue) compared to the highly symmetrical C_{4v} cone conformation (dark blue) and the previously observed C_{2h} boat conformation (red).
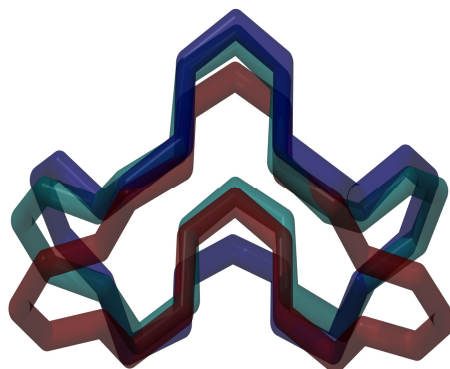
Figure 91: Representation of the distortion of the macrocyclic core compared to the cone and boat conformations.

There is no direct hydrogen bonding between the upper rims; however, they are linked together *via* water molecule bridges (O13$\cdots$O17 = 2.870 Å, O12$\cdots$O17= 2.337 Å). Each ammonium cation is coordinated to a chloride anion, this can lead to the interconnection of the pendant chains of two macrocycles (Cl2$\cdots$N3 = 3.195 Å, Cl2$\cdots$N2= 3.163 Å, Cl2$\cdots$N1 = 3.144 Å and Cl5$\cdots$N5 = 3.101 Å, Cl5$\cdots$N7 = 3.176 Å). The chloride anion that coordinates with the upper rim of the macrocycles and the ammonium cation enables the formation of the network (Cl1$\cdots$N1 3.156 Å, Cl1$\cdots$O10 = 3.003 Å, Cl4$\cdots$N2= 3.268 Å, Cl4$\cdots$O11 = 3.083 Å, Cl6$\cdots$N6 = 3.225 Å, Cl6$\cdots$O3 = 3.036 Å and Cl8$\cdots$N3 = 3.145 Å, Cl8$\cdots$O9 = 3.001 Å). Compared to the previous structure, due to the presence of the ammonium chains within the cavity, the chloride anion cannot participate to the formation of the dimeric capsule but allows the formation of head-to-tail arrangement (Figure 92).

It can be assumed that the upper rim interactions are maintained *via* the solvent molecules, as they are not hydrogen bonded to the pendant chains. The solvent accessible volume is 124.44 Å^3 representing 2.5% of the unit cell. Considering the molecular volume of methanol to be 34.5 Å^3, three molecules of methanol will potentially occupy these voids, situated on top of the resorcinol opposite to the π-bonded ammonium.
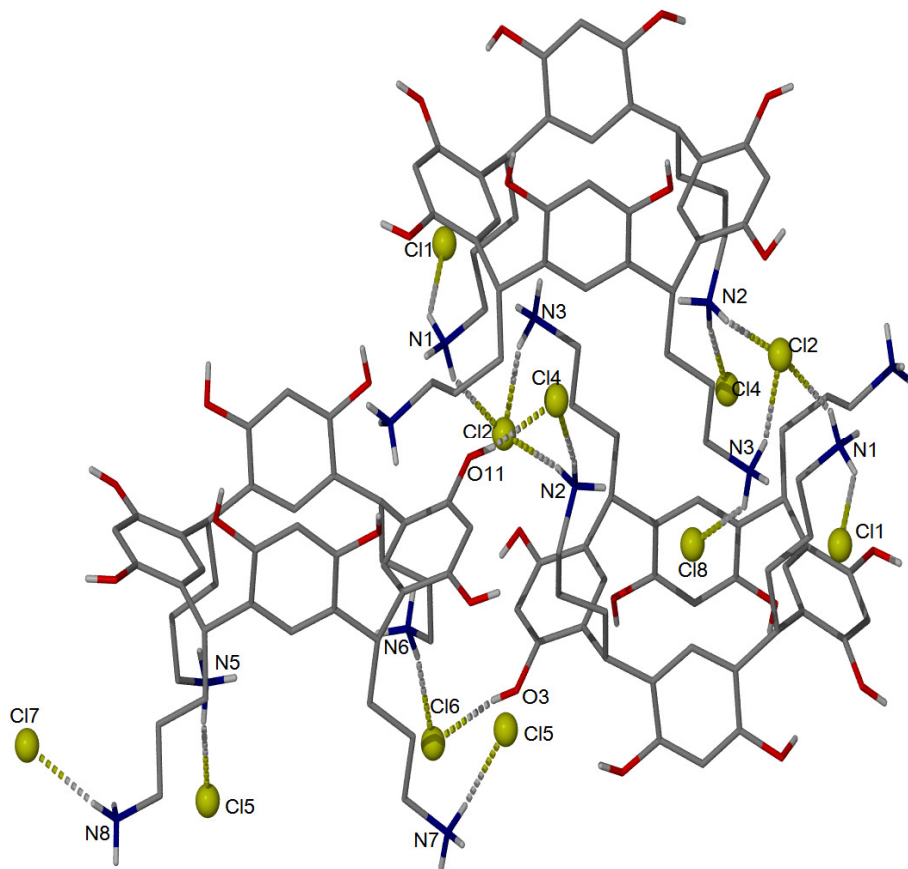
*Figure 92: Chloride involvement in the packing of C-3-aminopropyl-pyrogallol[4]arenes **35** (hydrogens and pendant chains omitted for clarity)*

The study of the behaviour of polar pyrogallol[4]arenes and resorcin[4]arenes in the solid state showed some interesting features, with an array of three dimensional frameworks. The effect of changing the crystallisation solvent is considerable and should not be dismissed in the study of the self-assembly towards the nano-vectors. Further studies should be included in both solid and liquid state. In addition the stability of the hydrogen bonded capsule should be investigated in presence of biological component such as protein and antibodies, as well as physiological serum. The use of metal coordination should also be investigated in more detail.

CHAPTER IV: TOWARDS BIOLOGICALLY ACTIVE CALIXARENES

Functionalities such as amines and carboxylic acids are widely used in covalent bio-conjugation and are essential in the investigation towards biologically active calixarenes. As described in the introduction chapter, most of the research done previously by others on these types of molecules was pursued on alkylated calixarenes, which cannot be readily functionalised with peptides. It was therefore necessary to introduce a functional group that would be easily transformed. It was thought that the precursors presented in the previous chapter could be easily conjugated to other biologically relevant functionalities such as amino acids, peptides, and further down the line, proteins and DNA. To achieve the full functionalisation several synthetic routes were attempted. Firstly, the transformation of the hydroxyl group was considered by esterification but required the selective protection of the upper rim. Secondly, the transformation of the starting calixarene was attempted showing good potential, a more reliable method using a combination of polymer bound reagent and microwave irradiation was developed towards attaching peptides. This enabled the preliminary attachment of one amino acid, a small peptide, and an elongated polyethylene chain. Unfortunately, this part of the project has proved to be more challenging than expected mainly due to purification difficulties. Although purification methods using C-18 reverse phase chromatography were developed on the HPLC, the fraction collection did not always lead to pure samples in sufficient quantities for full characterisation and further work.

A. SELECTIVE PROTECTION

Most functionalisations of the pendant chains presented in the literature are achieved on cavitands, whereby the phenolic alcohols are protected and not accessible for hydrogen bonding. Although their conversion back to the unprotected calixarenes may be possible using selective reactants such as boron tribromide, it has not been reported as these materials are mainly used for their exceptional encapsulation properties.

To achieve the further functionalisation of the hydroxyl footed pyrogallol[4]arene macrocycles, it was thought that a selective protection of the hydroxyl groups, either phenolic or or the primary alcohol was required. The acidity of the phenolic group (pKa 5.1 for pyrogallol) is much higher than the primary alcohol group (pKa ca 15) and therefore is more accessible to electrophilic substitution, resulting in selective reactions at the upper rim. These properties can be exploited using the experimental conditions in order to favour the chemoselectivity.[305-306] Complete esterification of all phenolic groups of alkyl footed resorcin[4]arenes and pyrogallol[4]arenes with 2-bromo-isobutyryl bromide, using pyridine was achieved in the research to make novel star shaped initiators for controlled radical polymerisation of styrene.[267] Several protecting groups were considered and led to various levels of substitutions, summarised in Table 10.

	Method	Subst.
Acetylation **37**	Acetyl chloride, pyridine Pyridine, acetic anhydride	mixture
Pivalation **38**	Pivaloyl chloride, potassium hydroxide or diisopropyldiethylamine or triethylamine	mixture
Tosylation **39**	Tosyl chloride, triethylamine	unresolvable
Boc protection **40**	Boc anhydride, DMAP	16/12
Benzylation **41**	Benzyl bromide, sodium iodide, potassium carbonate	mixture
Methylation **42**	Methyl iodide, potassium carbonate	12/12

Table 10: Attempted protections of hydroxyalkyl-pyrogallol[4]arene (subst. represent the substitution level of the hydroxyls (12 being the upper rim, 16 being the upper rim and the pendant chains)

Previous derivatisations of the alkyl footed pyrogallolarenes' upper rims by complete tosylation and partial mesylation were reported.[307] Similar behaviours were expected during the protection of its alcohol derivative, *C*-4-hydroxybutyl-pyrogallol[4]arene **26**. When attempted, only the 4-methylbenzenesulfonic acid was recovered so another method was therefore considered within this project.

The reaction of the phenolic alcohol with acyl chloride, *via* the use of pivalate as a protecting agent is widely used.[158, 169] Unfortunately, when attempted selective protection was not achieved either by the reaction of acyl chloride nor pivaloyl

chloride, using conventional heating methods or under microwave irradiation. The microwave irradiation enables the protection step to be reduced from four days to ten minutes using acetic anhydride in pyridine with an alkyl footed pyrogallol[4]arene.[57, 307] This protection led to an unresolvable mixture when used with its hydroxyl analogue.

For the synthesis of bergenin derivatives, a class of trihydroxybenzoic acid glycosides, the selective protection of the phenolic groups was achieved by benzylation using potassium carbonate as a base and benzyl bromide in a mixture of acetone and DMF.[308] Similar conditions were used for the benzylation of *C*-4-hydroxybutyl-pyrogallol[4]arene **26**, but the product was seen to decompose into a black tar. It was supposed that substitution of the upper rim would be partial, *i.e.* only eight out of the twelve phenols would be substituted due to the steric hindrance of the benzyl bromide. By reducing the steric hindrance, using methyl iodide, the selective protection of the upper rim was achieved in a 40 % yield.
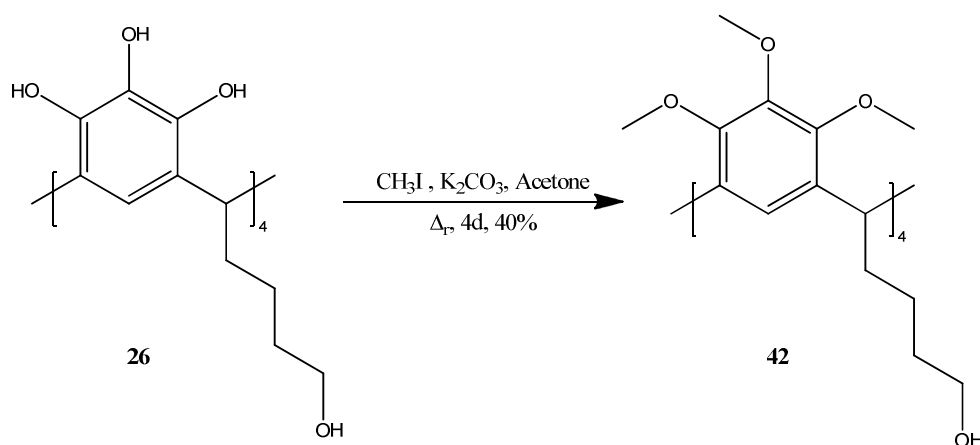
Scheme 14: Synthesis of C-4-hydroxybutyl-dodecamethylpyrogallol[4]arene **42**

It is reported that the base is most likely to deprotonate one set of four of the eight available phenols in resorcin[4]arene, which are more acidic than the second set, due to the formation of the hydrogen bonds.[125] The pendant alcohol chains could potentially react with the excess bridging reagent, which diminishes the yield of cavitands. This effect could also account for the low yield obtained in the methylation.

Suitable crystals for X-ray analysis of *C*-4-hydroxybutyl-dodecamethoxypyrogallol[4]arene **42** were obtained by slow evaporation of an acetonitrile solution. Due to the partial loss of its hydrogen bonding potential, the cone conformation is transformed to a boat, with a distortion factor of *Df* = 0.40. The resulting structure showed an altered behaviour in the crystalline phase that can

only be held by the interplay of the pendant chains (O13···O14 = 2.497 Å, O16···O16 = 2.626 Å , O16···O13 = 2.642 Å and O14···O15 = 2.646 Å).
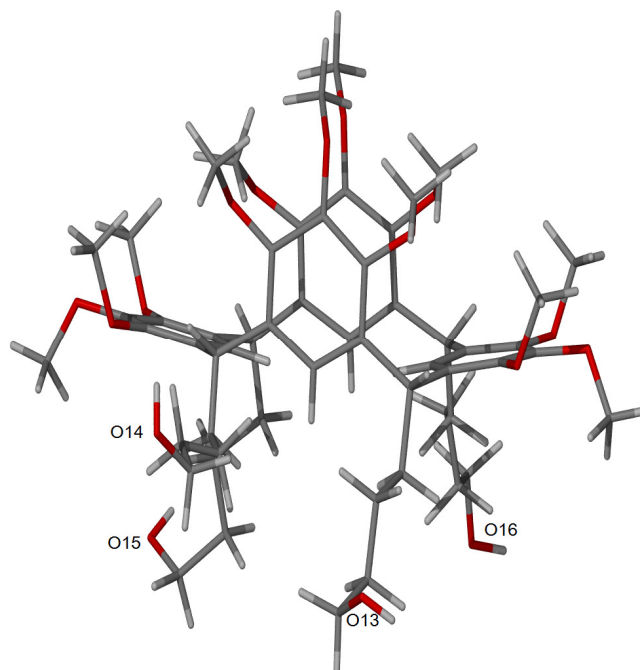
Figure 93: Asymetric unit of C-4-hydroxybutyl-dodecamethoxypyrogallol[4]arene **42**

The reaction of 1,2,3-trimethoxybenzene and 1,3-dimethoxybenzene with equimolar amounts of valeraldehyde was also attempted, using hydrochloric acid as a catalyst. However, it did not lead to any reaction, showing the necessity of the electron donation of the hydroxyl group to the aromatic ring to ensure the electrophilic substitution. The *tris*-Boc-protected pyrogallol was therefore considered as a potential starting material instead of pyrogallol. But the strong acidic condition resulted in the liberation of gas that was caused by its deprotection. The cyclisation may occur in the presence of another catalyst such as *p*-TSA or $BF_3.OEt_3$, or the use of another acidic resistant protecting group. Nevertheless, their presence may impede the formation of the cone conformer.

B. FUNCTIONALISATION OF THE PENDANT CHAINS

1. PYROGALLOL[4]ARENE PRECURSORS

a) Halogenated hydroxycalix[4]arene

Halogenated hydroxycalixarenes can be obtained by simple condensation of halogenated aldehydes with either resorcinol or pyrogallol.[21, 147] However, when the synthesis of analogues with shorter chain lengths, *i.e.* methyl or ethyl were attempted, an insoluble polymer that could not be resolved was produced. This behaviour has only been reported previously when reacting the phthalimide derivatives.[148] It was thought that the nature of the acetal, as a dioxolane that is highly reactive was the main factor; however, when repeated with a diethyl acetal similar results were observed.
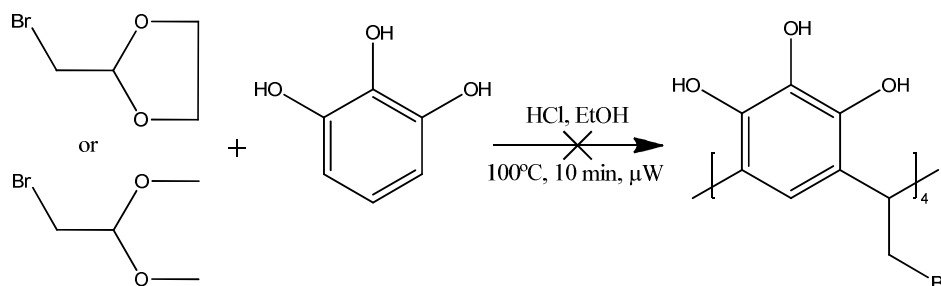
Scheme 15: Attempted synthesis of bromomethylpyrogallol[4]arene

The formation of the polymer was therefore attributed to the presence of the bromine as well as the chain length. Under acidic conditions, the substitution may occur at both *ortho* and *para* positions of the phenolic hydroxyl, therefore forming a bakelite-like structure or the oligomer. A similar phenomenon was observed when another chloro substituted aldehyde was used, inferring that the presence of a strong electronegative atom such as chlorine or bromine adjacent to the acetal may impede the stabilisation of the intermediate carbocation. Another method was therefore considered to access the brominated compound, utilising hydroxyl footed pyrogallol[4]arenes as a starting material. The brominated pendant chains could be further transformed to other functionalities, including amines and thiols.[152] The bromination of the calixarenes' pendant chains has been reported by using triphenylphosphine and tetrabromomethane on the *C*-4-hydroxybutyl-methoxy-resorcin[4]arene.[151] Inspired by Stoll, who functionalised the upper rim of the cavitands,[139] phosphorous tribromide was chosen as the brominating agent and resulted in the *C*-4-bromobutanyl-pyrogallol[4]arene **43**

being obtained in a 65% yield. This synthetic route has an advantage over the previous protocols, as it does not require any prior protection of the upper rim. This selectivity toward aliphatic alcohols is achieved by the nature of the substitution, indeed the bromination occurs *via* an S_N2 mechanism that cannot be achieved on aromatic phenols.
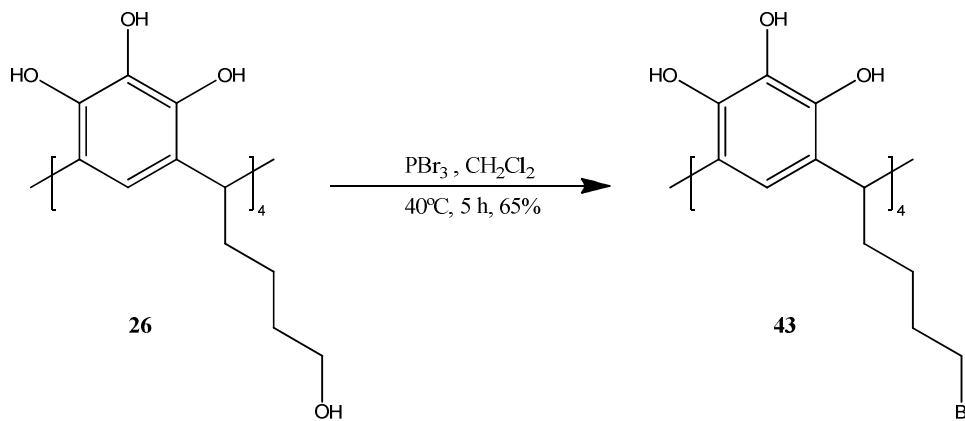
Scheme 16: Synthesis of C-bromobutanyl-pyrogallol[4]arene 43

b) Carboxylic acid footed calixarene

Octamethyl ether tetracarboxylic acid resorcin[4]arenes were obtained by from a reaction of 2,4-dimethoxycinnamate with $BF_3.OEt_2$ as a Lewis acid catalyst, followed by a hydrolysis step.[50] These only examples of ester footed resorcinarenes were then transformed to the corresponding acids and to a chiral "bridged basket" by linking the pendant chains together by reaction of acyl chloride and dialcohols.[179] However, the synthesis of these types of macrocycles can lead to a mixture of isomers involving several isomers and therefore an alternative method was applied.
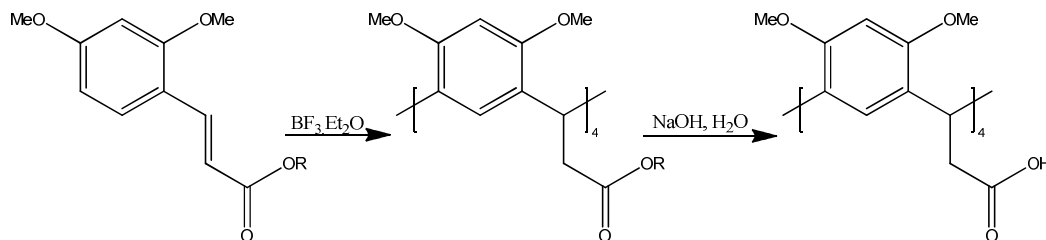
Scheme 17: Synthesis of resorcin[4]arenes octamethyl ether tetraester

It has been shown that in presence of a base, even a weak one, the esterification reaction is favoured at the phenolic alcohol; however, in presence of acetylating catalysts such as pyridine and DMAP the chemoselectivity can be lost.[305] The

elongation of the pendant chains with a carboxylic acid end was therefore attempted by reacting *C*-3-hydroxypropyl-pyrogallol[4]arene **25** and *C*-3-aminopropyl-pyrogallol[4]arene **35** with acetic, glutaric and succinic anhydrides.

$R= CH_3, (CH_2)_2, (CH_2)_3$
$R'= CH_3, (CH_2)_2COOH, (CH_2)_3COOH$
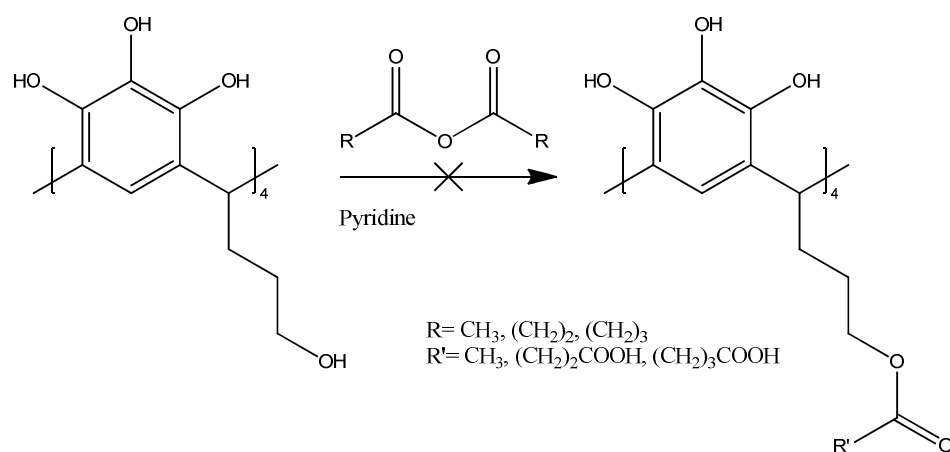
Scheme 18: Reaction of C-3-hydroxypropyl-pyrogallol[4]arene with anhydrides

It was found that all selectivity was also lost, even in the absence of the base. The mass spectra analysis showed a polymer-like distribution of the peaks with mass difference in between peaks of 101. It can therefore be assumed that acetylation also occurs at two phenolic alcohols, possibly resulting in a cyclised diester at the upper rim. In contrast, an esterification using an acidic catalyst such as *p*TSA or sulphuric acid, should have favoured the reaction of the primary alcohols, but the product was seen to decompose when heated. However, when the aminopropylresorcina[4]arene was reacted with succinic anhydride, it appears that the reaction is favoured, but the pure product was not isolated.

In order to introduce the carboxylic acid prior to the formation of the macrocycle a commercially available acetal was considered. The acid catalysed cyclocondensation of ethyl-3,3-diethoxypropionate with pyrogallol was attempted, leading to the formation of a non-resolvable mixture. In view of previous results, the small chain length between the aldehyde and the ester group may interfere in the stabilisation of the intermediate carbocation. It can also be assumed that electrophilic addition also occurs at the ester bond, forming a polymer. The ester itself may well be competing with the acetal, as it can be hydrolysed under acidic conditions, however, this effect may drive the equilibrium to the right favouring the macrocycle formation. In order to assess the role of the carboxylic acid in the reaction, 4-formylbenzoic acid was reacted with

132

pyrogallol under microwave irradiation, forming predominantly the *rctt* chair (80%) conformation in a 86% yield. This high ratio of *rctt* may be due to the fact that the starting aldehyde is sparingly soluble in the acidic ethanolic solution and may therefore displace the reaction towards the formation of the kinetic product.
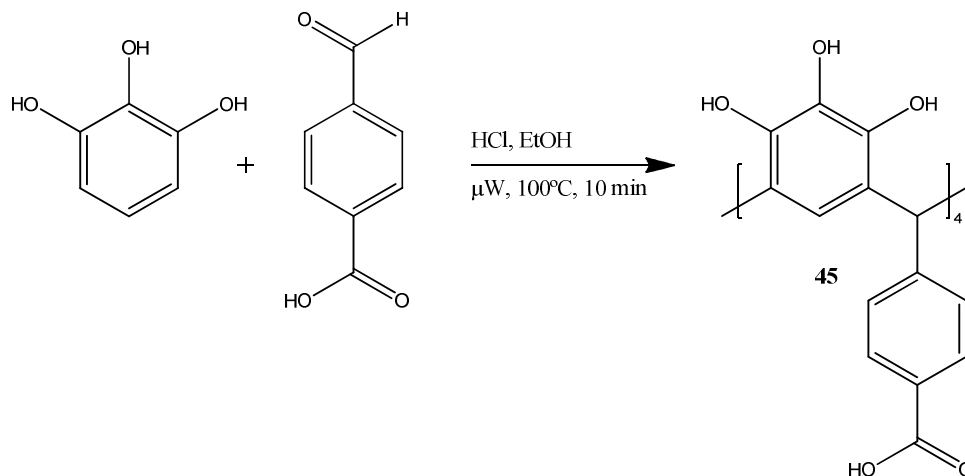
*Scheme 19: Synthesis of 4-benzoic-pyrogallol[4]arene acid **45***

As the method used was tuned for the formation of the *rccc* for the aliphatic and aromatic analogues, it can be assumed that the formation of the *rctt* isomers is probably due the presence of the aromatic carboxylic acid, therefore its presence has an effect in the cyclisation process. Suitable crystals for single crystal X-ray analysis were obtained from deuterated dimethyl sulfoxide, which is highly disordered within the crystal.
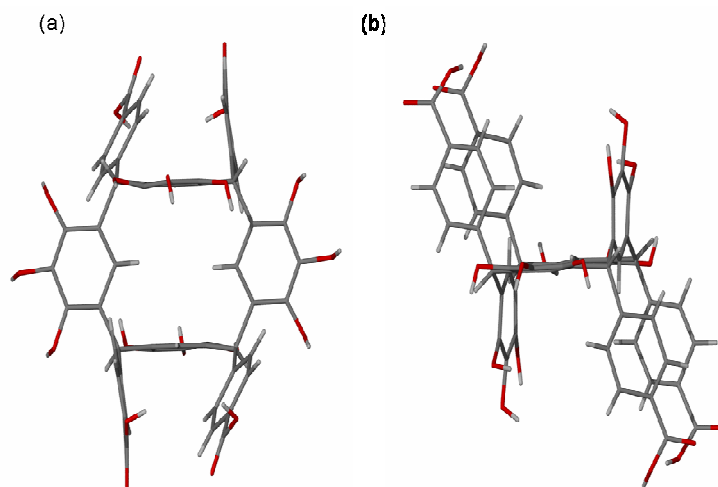
Figure 94: rctt 4-benzoic-pyrogallol[4]arene acid view from (a) top and (b) side

2. ATTACHMENT OF ONE AMINO ACID

With a wide selection of macrocycles prepared from the variety of commercially available acetals, many coupling reactions were attempted to attach a relevant amino acid or linker onto the macrocycles' pendant chains. In order to avoid the selective protection of the upper rim and the potential solubility issue, the functionalisation of the acetal was envisaged first. A protected amino acid, Fmoc-(tBuO)glutamic acid, was coupled to aminobutyraldehyde *via* a DIC/HOBt coupling in an 84% yield. Unfortunately, when reacted with pyrogallol under acidic conditions, the condensation did not lead to the tetramer.
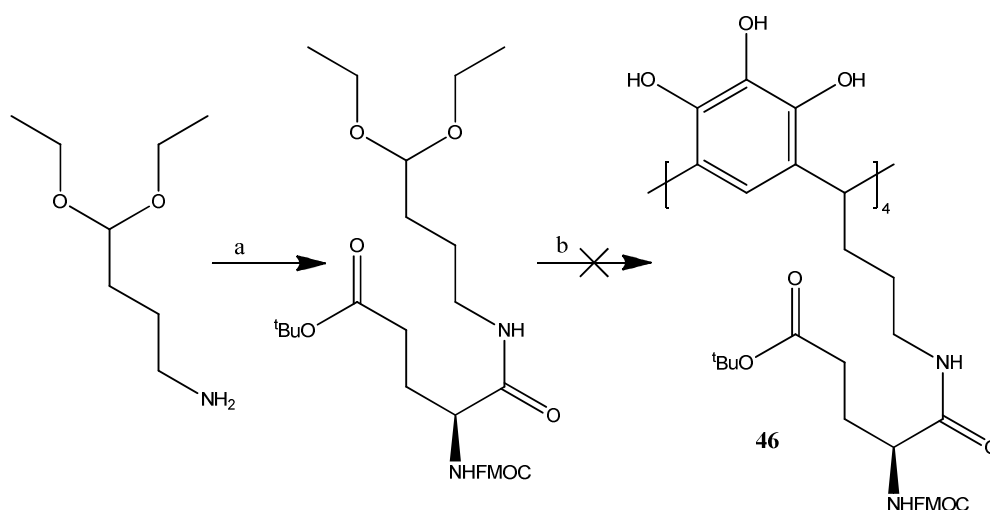
Scheme 20: Transformation of the aminobutyraldehyde diethylacetal; a) PS-DCC, PS-DIEA, b)Pyrogallol, HC, EtOH, 100 ºC, 10min, µW

Similar results were obtained when other linkers were used, such as *N*-protected aminocaproic and aminoundecanoic acids. It was therefore decided that the extension of the pendant chains should be pursued *via* attachment to the cyclised macrocycle instead. A bifunctional linker such as gluteraldehyde was also considered. However, the absence of selectivity during the Schiff base formation, will result in a polymer-like structure that may include several calixarenes together and therefore was not pursued further. Instead, the coupling reaction between an amine and a carboxylic acid in the presence of a non protected phenol was considered as it was reported that it did not interfere.[176]

Several reactions were therefore attempted on aminopropyl macrocycles, using various coupling agents combined with different bases, activators and protected amino acids to avoid any side reactions. This results are summarised in Table 2. Although most reactions succeeded in yielding the calixarene, the purification, in particular the removal of the side products, including the urea and base, was challenging. This was particularly problematic due to the unpredicted solubility issues of the target calixarenes. The hydrophilic nature of the upper rim, also proved to be a problem when trying to separate out the pure products by HPLC.

Macrocycle	Amino Acid	Coupling Agents
RsC_3NH_2	Boc-Ala	DCC, DMAP
RsC_3NH_2	Boc-Ala	EDC.HCl, DIEA
RsC_3NH_2	Boc-Ala	DIC, HOBt
RsC_3NH_2	Boc-Ala	DIC, DIEA **47**
RsC_3NH_2	Boc-Ala	DIC, DIEA, HOBt
RsC_3NH_2	Fmoc-Asp(OtBu)	DIC, Pyridine
RsC_3NH_2	Boc-Ala	DIEA, HOBt, NHS
RsC_3NH_2	Boc-Ala	DIEA, NHS
RsC_3NH_2	Fmoc-Ala	PS-DCC, DIEA **48**
PgC_3NH_2	Ac-cysteine	PS-DCC, PS-DIEA

Table 11: Attempted coupling of aminoacids to the macrocycle

The attachment of butyloxylcarbonyl protected alanine was successful when reacted with *N,N'*-diisopropylcarbodiimide (DIC, 5 eq.), Hünig's base (DIEA, 4 eq.) and aminopropylresorcin[4]arene (RsC_3NH_2, 1 eq.), with and without 1-hydroxybenzotriazole. However, the yields were very low (< 5%) and only traces of the desired compound could be identified by ^{1}H NMR. Moreover, the removal of both *N,N'*-diisopropylurea and diisopropylethylamine was difficult and sufficient material was not recovered for full analysis *via* reversed phase HPLC. Nevertheless the MALDI analysis, which has sensitivity up to the ng/mL, showed that one fraction contained the tri-Boc-ala-aminopropylresorcin[4]arene.

In order to avoid the presence of the side product, generated by the coupling agent, *i.e.* *N,N'*-diisopropylurea (DICU) or *N,N'*-dicyclohexylylurea (DCU), polymer bound reagents were considered. This method has been shown to be highly useful when working on small scales as they can be removed by simple filtration.[309] In addition, this valuable technique can also be combined with microwave irradiation. The tetra-substituted Fmoc protected alanine aminopropylresorcin[4]arenes were obtained by combining PS-DCC and microwave irradiation at 100 °C for five minutes, with and without HOBt. Although the yields obtained were low (< 1%), comparable to the liquid phase reaction, the absence of HOBt led to a higher ratio of the fully substituted compound according to the mass spectrometry analysis. In order to check the effect of the base, the attachment of protected aspartic acid to aminopropylpyrogallol[4]arene was attempted using only resin bound reagents PS-DCC and PS-DIEA, coupled with microwave irradiation at 100 ºC for 20 minutes. According to the mass spectra analysis, the reaction contained a mixture of unreacted starting material and mono-functionalised calixarene, but was not isolated for further analysis.

3. ATTACHMENT OF STEALTH MOLECULES

The attachment of a long pegylated chain would extend the size of the particle as well as improve the solubility in water. The attachment of a pegylated chain was attempted using DIC coupling in solution, although the ^{1}H NMR data indicates the presence of the calixarenes, the purification was challenging due to solubility issues. This was overcome by the use of a polymer bound coupling agent which faciliated the purification process. Therefore the attachment of a succinyl functionalised PEG chain has been successfully achieved, as indicated by ^{1}H NMR.
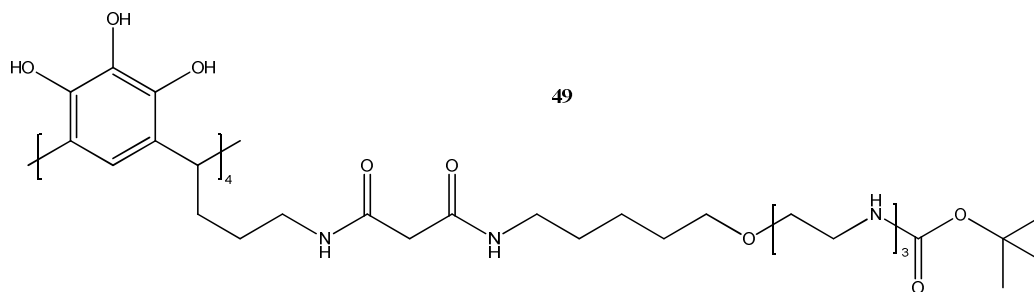
Figure 95: Pegylated macrocycle

The mutation of p53, which is the most common abnormality found in 50% of human cancers, is expressed in twelve out of eighteen primary uveal melanomas.[310] This key human antigen is essential in the pathway involving the control of apoptosis and cell cycle arrest. Due to its over expression in many cancers, it is a target of choice for immunotherapy. Therefore, peptides derived from the oncogenic protein p53 were chosen as model antigens and were synthesised using the microwave-assisted SPPS method.

Peptide synthesis first appeared in 1882, and this well-known process was revolutionised in 1959 by Bruce R. Merrifield when he introduced the concept of an insoluble support.[311] Today, solid phase peptide synthesis (SPPS), employing a variety of functionalised resins derived from Merrifield's resin, is the most widely used method. Used in combination with microwave irradiation, it leads to a more efficient and rapid synthesis of pure peptide.[312]
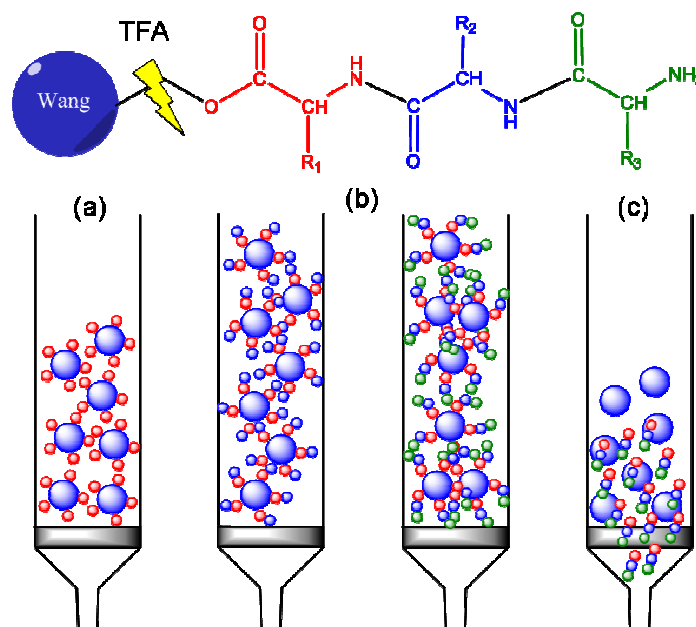
Figure 96: SPPS synthesis

The synthesis is based on protection, deprotection and coupling methods, all on a solid polymeric support, combined with microwave irradiation. Wang resin, a modified Merrifield resin, is the most commonly used resin due to its mild cleavage requirements. As represented in Figure 96, the peptides are synthesised on the

Wang resin preloaded with a Fmoc protected amino acid on the *C*-terminus (Figure 96a). The amino acid is then deprotected with piperazine and coupled with the carboxylic acid of the following amino acid in the sequence, using O-benzotriazole-*N,N,N',N'*-tetramethyl-uronium-hexafluoro-phosphate (HBTU), DIEA / NMP as a coupling reagent (Figure 96b). When the sequence is completed, the resin is cleaved with an appropriate acidic mix (*e.g.* TFA) and the peptide precipitated in diethyl ether (Figure 96c).

The attachment of the cleaved peptide to the calixarene was considered using solution phase chemistry, but this method was limited to peptides sequences with no functional side chains, as their protection groups are designed for removal in the cleavage step. Asp-Ala-Ala-Ala (6eq.) was reacted with aminopropylresorcin[4]arene (1 eq.) in the presence of PS-DCC without any base **50**, which resulted in no substitution as indicated by the MALDI analysis. The attachment using the unbound Ala-Ala-Ala-p53(108-122) unprotected peptide **51** (MW= 1873.01g.mol^{-1}, 2 eq.) to C-3-aminopropyl-pyrogallol[4]arene **35** (1 eq.) using polymer bound reagent PS-DCC (8.eq) and PS-DIEA (6 eq.) was subsenquently attempted. The resulting solid that was obtained was used for MS analysis. It revealed the presence of a mixture containing the free peptide *m/z* = 1874.01 [M]$^+$ and 1897.91 [M + Na]$^+$. Another peak at *m/z* = 2603.31 corresponds to the mass of a single peptide chain and one calixarene. However, this would lead to a m/z ratio of 2637.01, the difference of mass could potentially correspond to the loss of two hydroxyls groups, indicating that the peptide was attached at three sites on the macrocycle. The spectra also revealed a *m/z* = 3428.68 corresponding to the mass of two pyrogallol[4]arene covalently bound to one single peptide. Although this method proved that the peptide could be covalently attached, it is not selective enough and does not enable the controlled growth onto all pendant chains. Therefore, another approach was considered, whereby the peptides grafted onto the Wang resin was synthesised until completion and then attached to the macrocycle.

As an alternative, the calixarene linkage was therefore attempted on the resin bound protected peptide. In order to couple the functional feet of the calixarenes onto the peptide linked to the resin, it was necessary to introduce a carboxylic function or introduce a linker such as succinic or glutaric anhydride onto the resin.

In an attempt to optimise the conjugation method, small peptides containing three alanines were first considered. The tri-alanine epitope is a sequence available

for trypsin-like cleavage site; associated with the proteosome and therefore could constitute an excellent linker between the calixarene and the peptide of interest.[245] In order to induce more flexibility between the resin bound peptide and the calixarene pendant chain, dodecanedioic acid was used as a lipophilic spacer. Unfortunately, when the spacer bound resin was reacted with either aminopropyl pyrogallol[4]arene or the aminopropyl resorcin[4]arene, the functionalisation was not complete as indicated by MALDI mass spectrometry. The NMR results also showed trace of both peptide and undecanedioic acid, indicating that the didodecanedioic acid tends to react with the peptide preferentially, resulting in a peptidic dimer.

The direct coupling of the carboxylic footed pyrogallol[4]arene was also attempted using similar methods, although it was thought to be restrained by its chair conformation. All syntheses led to a complex mixture with similar mass to the expected compounds however, this could not be resolved. Generally it corresponded to both di- and tri- substituted calixarenes and none of the fully substituted compound was obtained. This was thought to be induced by the flexibility and therefore the accessibility of the peptides residue towards the pendant chains. As seen in the previous chapter, the solvent and the nature of the pendant chain play an essential role on self-assembly in the solid state, it can be assumed that this effect is also present in solution and may impede the funtionalisation reaction.
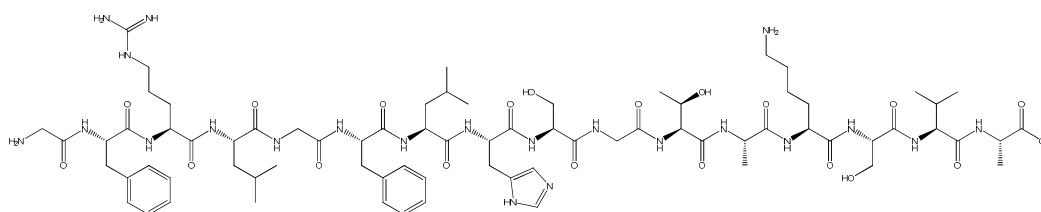
Scheme 21: p53(108) sequence Gly-Phe-Arg-Leu-Gly-Phe-Leu-His-Ser-Gly-Thr-Ala-Lys-Ser-Val-Ala

The immunogenic peptides, p53(108) was synthesised using the SPPS method and was then modified using glutaric anhydride in order to attach the aminopropylpyrogallol[4]arene. Only one compound was isolated, with 74 % purity as evaluated by HPLC. According to the MALDI analysis, only the non-conjugated modified peptide was recovered **52**. Similar results were obtained when a longer

sequence was used. Ala-Ala-Ala-p53(108)-Ala **51** was also synthesised using the SPPS method, according to the MALDI spectrum, the sequence was successfully synthesised (m/z = 1861.97, $[M]^+$ and 1882.95, $[M+K]^+$) and small part of the peptide was still Fmoc protected (m/z = 2083.03, $[M+Fmoc]^+$), showing the importance of the deprotection step within the synthesis. Piperazine deprotection should be performed prior to the cleavage step as its use in solution phase can also be challenging. These results also indicated that the coupling is independent of the amino acid and could be caused by the coupling agent.

Although HBTU seems to be the coupling agent of choice for amino acids to form peptides, DIC appears to be more efficient when coupling to other amines.[313] The solid supported carbodiimide was also expected to be a efficient reagent. Unfortunately, the polymer bound coupling was not efficient when applied to the peptide bound resin, due to accessibility of the reagent within the pores of the polymer.

Inspired by Merrifield's work and the peptide synthesis just realised, a novel solid supported method involving pyrogallol[4]arene macrocycle was considered. This method could offer the accessibility to a simplified method that could give a way to a wide range of compounds in the high throughput range thereby leading to a synthetic automated process. This tool would be highly desirable for the biological screening assay, by mean of grafting the peptide directly onto macrocycles, leading to potential peptides library.

C. SOLID SUPPORTED SYNTHESIS

When the Wang resin was used as a solid support in the peptide synthesis, the structure of the linker, hydroxymethylphenol (HMP), was attractive. Its similarity to the *C*-hydroxybutyl-resorcin[4]arene and *C*-hydroxybutyl pyrogallol[4]arene, due the presence of both phenolic and alkyl alcohol functional groups, led to the consideration that the calixarenes could be covalently bound to the resin (Figure 97). The work on selective protection showed that the benzyl chloride of the Merrifield resin could selectively react with phenolic hydroxyl on the upper rim of the calixarene. This method could potentially overcome the problem encountered during the attachment of long peptide onto the pendant chains of the calixarenes.

The concept of functionalising polymeric resins with calixarene derivatives has been considered by others for various different purposes. The ability of the

phenolates to substitute chlorine, has also been considered as a potential pathway for the attachment of this class of macrocycles onto commercially available resins.[314-315] These useful new materials have been investigated for the extraction of metals,[164, 316-317] especially in two-phase extraction systems.[318] Calixarenes have been previously transformed by attaching polymerisable groups to give access to a novel high performances polymeric materials for photolitography.[319] Macrocycle based polymers were obtained by condensation of calix[4]resorcinarene with formaldehyde, to asses their ion-exchange capacities.[265] A polymeric matrix immobilised resorcin[4]arene was used to immobilised palladium in order to catalyse hydrogenation.[320] More recently, calixarenes have been attached to TentaGel resin and tested in solid-phase synthesis by condensation of thymine unit onto the upper rim.[321] The emergence of solid phase organic chemistry (SPOC), due to its ease of purification was therefore an attractive concept.
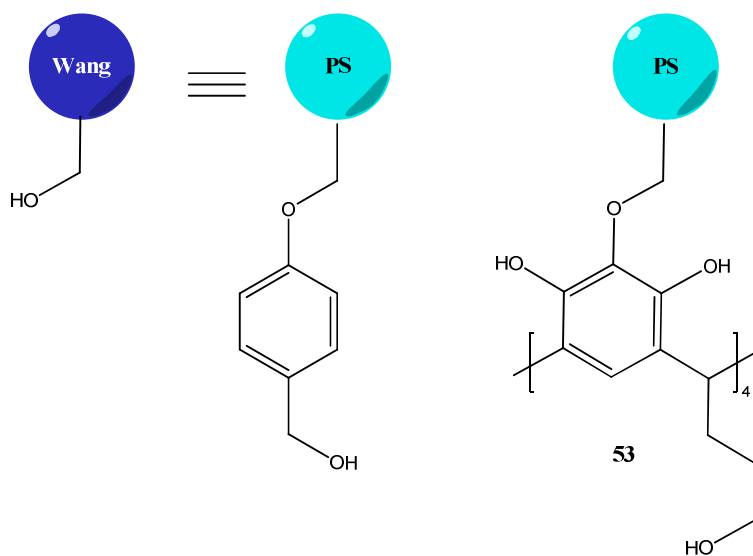
Figure 97: Similarities of HMP linker and C-4-hydroxybutyl-pyrogallol[4]arene

The degree of incorporation of any linker to a polymeric support correlates not only with the substitution but also with its swelling capability.[322] It has been shown that more than 99 % of the reactive sites on a resin are in the microporous interior of the bead. These become accessible during the swelling process and the pore sizes are large enough to accommodate the 10 Å diameter calixarene.

1. ATTACHMENT ONTO THE RESIN

The linkage of phenols on Merrifield resin has been widely studied, involving a different bases. Benzyloxybenzylamine (BOBA) is linked to Merrifield resin by reacting sodium hydroxide in dimethylsulfoxide for twenty hours.[323] Phenolate can be obtained by heating a slurry of sodium hydride in tetrahydrofuran to reflux for over sixteen hours.[314] Sodium hydride is a strong base that has been previously used to attach alkyl alcohol to polystyrene resins.[324] As the use of sodium hydride may impede the selectivity when other alcohols are present it should be avoided when selectivity is sought.[325] In order to obtain a selective functionalisation, several bases were considered, it was thought that a weaker base would be more selective and therefore sodium hydroxide and sodium hydride were avoided. In addition, some pyrogallol[4]arenes were seen to decompose under strong basic conditions. Several phenols were attached to a Merrifield resin by reacting phenols with sodium methoxide in dimethylacetamide for sixteen hours.[326] Although proving that the phenols reacted faster than the hydroxybenzyl alcohol, it could not be used with the calixarenes due to solubility issue but could be reevaluated with other solvent systems, or a step-wise addition approach. Caesium carbonate can be used with *N*-methylpyrrolidone at 150 °C in a microwave reactor for five minutes, to prepare Wang resin, giving better results than the traditional use of potassium carbonate and potassium iodide.[327] Potassium carbonate was considered in order to deprotonate the phenolic hydroxyls of the calixarenes. Although the substitution occurred, the method offers some disadvantages. The drawbacks of the method were the solubility of the base as well as the presence of three different phases. A phase transfer catalyst, *tert*-butyl ammonium chloride, was added to overcome the solubility problem but only resulted in partial attachment. In order to minimise the number of phases, weaker liquid bases including diisopropylethylamine, triethylamine and pyridine were also tried. Diisopropylethylamine is the only base that is able to deprotonate the phenols, without forming a quaternised amine with the chlorine which may sterically hinder the substitution. According to the IR analysis, the use of pyridine resulted in the maximum substitution. The results of this study are summarised in Table 12. The functionalisation of the polymer has yet to be optimised, nevertheless it enabled the project to carry on to the proof-of concept of pyrogallol[4]arene substituted resin.

Base considered	Outcome
Sodium methoxide	Solubility issue
Potassium carbonate Caesium carbonate	Limited substitution due to a three phase reaction
Diisopropylamine/NMP	No substitution
Tritehylamine	Weak substitution
Pyridine dried on potassium hydroxide	Partial substitution **54**

Table 12: Bases considered for the attachment to the resin

Infrared is a useful tool to assess functional changes, especially when groups have characteristic bands such as carbonyl are used. Since the emergence of the resin in organic synthesis, several infrared techniques have been optimised to obtain the maximum information with the minimum amount of sample, moving away from the traditional use of potassium bromide discs preparation of the sample. Diffuse reflectance FTIR (DRIFT) enables the reduction of the amount of sample required and single bead analysis is now possible.[328] When all available methods, such as single bead, beam condenser Macro-ATR, Macro-Raman and KBr methods were compared, it was found that they all give similar results.[329] With the Wang resin, several characteristic peaks are observable with all methods except Raman, a sharp band at 3573 cm^{-1} and a broad band at 3449 cm^{-1} attributed to the free and intra-resin hydrogen bonded hydroxyl groups, and a strong CH_2-OH bending vibration at 1232 cm^{-1}.

The analysis of the functionalisation was performed using a Perkin -Elmer AT-FTIR. By comparing the unsubstituted Merrifield resin, the *C*-3-hydroxypropyl-pyrogallol[4]arene and the substituted resin, comparable changes are observable. Different sample preparations were attempted either using the beads directly, the ground beads, potassium bromide disks with varying concentration of the sample and a pressed disk of the resin. However, the best spectrum was obtained when using the beads directly. Although the spectral baselines were distorted, it was still possible to observe the main changes that account for successful substitutions.

As shown in Figure 98, the disappearance of the C-Cl band at 1262-1266 cm^{-1} present in the unsubstituted Merrifield resin is observed when the substitution occurred. The three main bands for the pyrogallol[4]arene substituted resin are visible at

3181, 1692 and 1303 cm^{-1}, indicating the presence of hydrogen bonded hydroxyls considered as phenols. The appearance of the characteristic bands of the pyrogallol[4]arene confirm its presence, as it was shown previously when other calixarenes were used.[314]
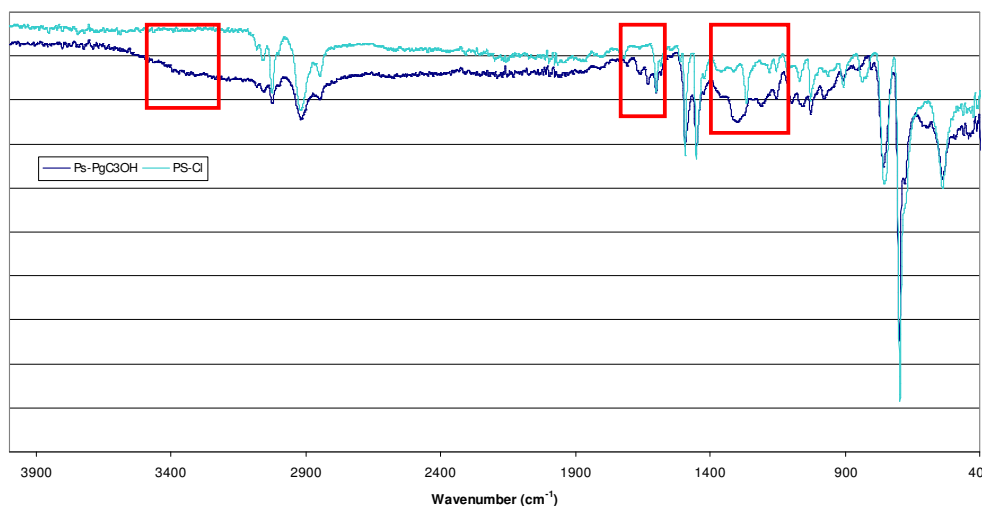
Figure 98: Comparison between the PS-Cl and PS-PgC$_3$OH

The quantification of the substitution was determined by Volhard's method (Scheme 22). The chloride ion concentration was obtained by titration of the unreacted silver ions, from a standard silver nitrate solution, with a potassium thiocyanate solution, using ferric ammonium sulphate in an acidic solution as a coloured indicator. Generally, a known amount of resin is reacted with a base such as methylmorpholine to displace the chloride. Pyridine was used for the substitution, as it can be directly assessed by titration of the reaction washes. As previously reported, this method may show some inconsistency and therefore should be used in combination with other analytical methods.[330]
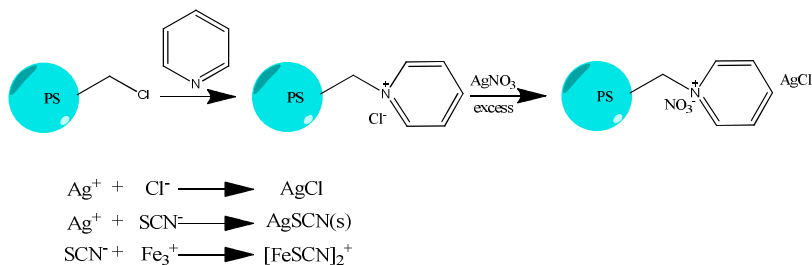
Scheme 22: Volhard's titration

144

SEM also gives an important insight into the nature of the polystyrene beads, their size and consistency. The size of the commercial polystyrene beads was found to be not homogenous within the sample, varying from 50 - 100 µm, as seen in Figure 99.
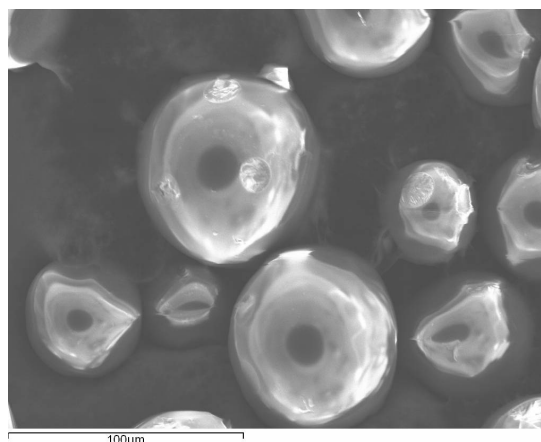
Figure 99: SEM image of the pyrogallol[4]arene resin beads

Although it is not quantitative, SEM can also be used as an elemental analysis useful tool to compare the functionalised resin with the starting material. In order to see a significant difference, elements with high K_α values, such as sulphur, were introduced to the resin bound macrocycle. In order to check the functionalisation occurs at either the phenolic or the aliphatic alcohols, the resin was reacted with methanesulfonyl chloride. The resulting resin was washed and analysed by SEM-EDX.
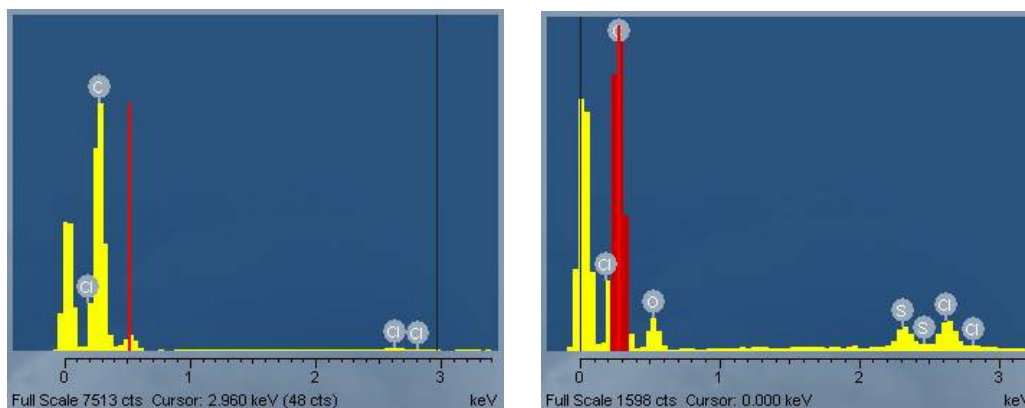
Figure 100: SEM-EDX of the PS-Cl and PS-PgC$_3$OSO$_2$CH$_3$

As seen in Figure 100, although chlorine still appears on the beads surface, showing the attachment was not complete, sulphur is also present on the surface of the beads confirming the presence of the macrocycles.

The presence of the pyrogallol[4]arene on the polystyrene resin was also assessed by ATR-IR. The hydroxyl stretch of the phenols (3362 cm^{-1}) is still present proving that the hydroxyl groups are on the surface on the beads as shown in Figure 101.
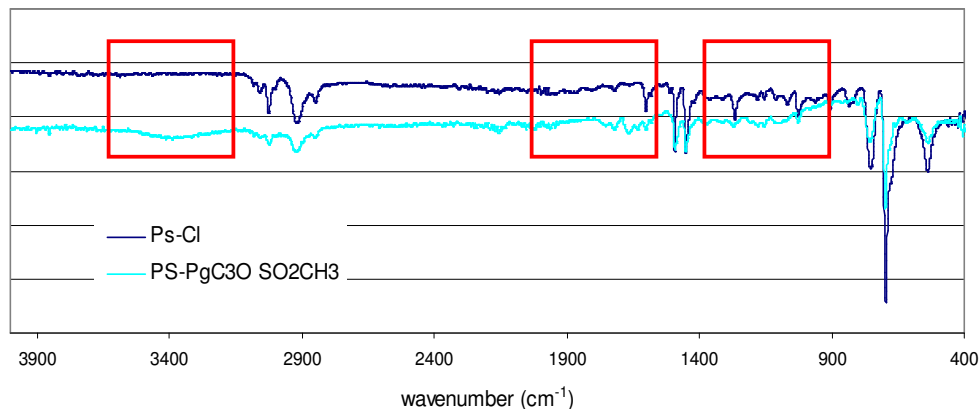
Figure 101: IR PS-Cl and PS-PgC$_3$OSO$_2$CH$_3$, red boxes highlight the comparable regions of the spectra to Figure 97

2. CLEAVAGE OF THE MACROCYCLE

Once the attachment of the macrocycles onto the resin was efficiently assessed, the retrieval of the product and subsequently its cleavage was developed. In the search for the solid-supported synthesis of steroids it has been shown that stannic chloride (SnCl$_4$) is effective for the cleavage of phenolic compound from Merrifield resin.[325-326] Wang resin is one of the solid supports of choice for solid-phase peptide synthesis due to its ease of removal by treatment with acid such as trifluoroacetic acid can also act as a deprotecting agent. It was therefore considered first due to its lower toxicity and higher ease of use. For pyrogallol[4]arene functionalised resin, the cleavage was thought to occur at a different point than the Wang resin. As the phenolic alcohols are directly attached to the methylene group of the Merrifield resin, it decreases the mesomeric effect within the aromatic ring. The TFA-cleaved product has been seen to form a derivative, in the *ortho* position of the phenol;[326] however, due to the calixarene structure, this position is not available for the rearrangement and therefore was avoided.
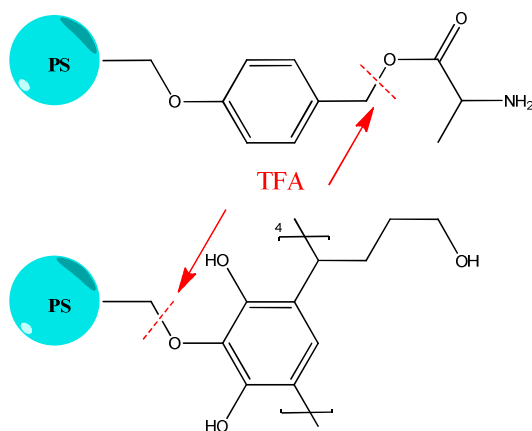
Figure 102: TFA cleavage site on Wang resin and pyrogallol[4]arene resin

When PS-PgC$_3$OH was treated with a TFA solution (95 %) for two hours at room temperature, the resulting product, after evaporation and trituration in water, was isolated as the pure *C*-3-hydroxypropyl-pyrogallol[4]arene as analysed by NMR. In order to identify the nature of the remaining alcohol, near-IR was attempted, although the main differences were observable in the visible IR shifts.
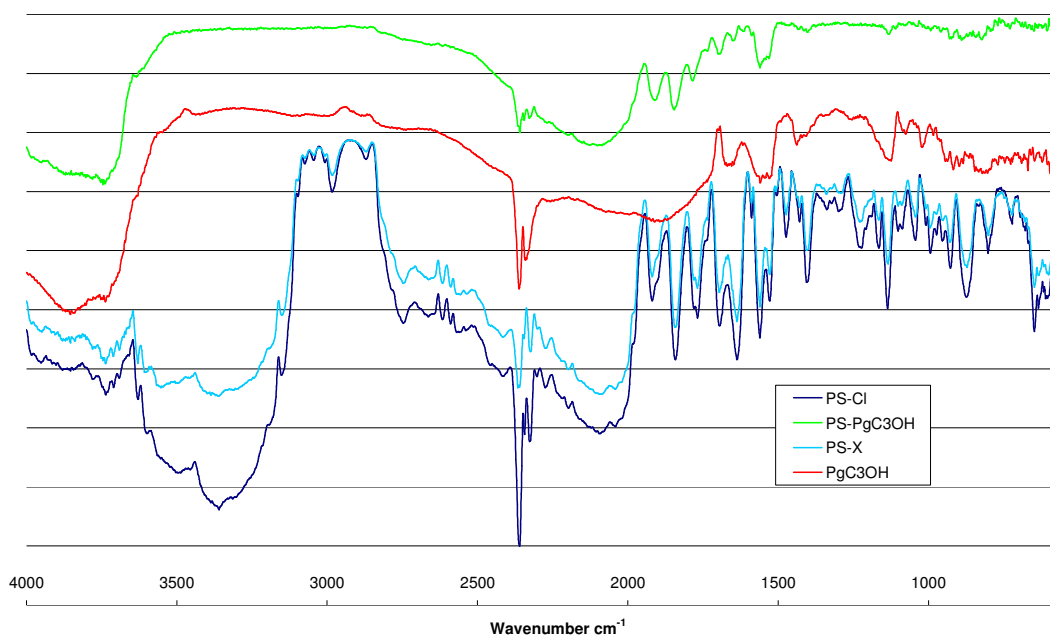
Figure 103: IR spectra of unsubstituted resin (PS-Cl), the free C-3-hydroxypropyl-pyrogallol[4]arene (PgC$_3$OH) and the substituted resin before cleavage (PS-PgC$_3$OH) and after (PS-X)

147

When comparing the IR spectra, in Figure 103, it is noticeable that the calixarene functionalised resin has the same spectrum as the free macrocycle. The comparison of the Merrifield resin and the cleaved resin also proved that the cleavage occurred.

3. FUNCTIONALISATION OF THE PYROGALLOL[4]ARENE RESIN

In the search for pegylated Merrifield resin and its attachment to cyclodextrin (CD), it has been shown that there are advantages to use a mono-functional linker 1,6-hexamethylene diisocyanate (HMDI), that can be reacted stepwise onto the alcohol chain of the PEG and the alcohol of the CD. This functional change is visible in IR by the introduction of a carbonyl.[331] This method was employed to confirm that the remaining hydroxyl chains of the pyrogallol[4]arene were available to react and was confirmed by IR. However, one drawback is that the carbamate linker may be cleaved by the TFA mix and consequently it could not be used for further functionalisation.[332]

Esterification has been achieved using ten equivalents of acid pre-treated with DIC (5 eq.) in DMF for five minutes, followed by the addition to a mixture of the resin with DMAP as a catalyst. The use of the microwave irradiation not only increased the yield but also reduced the amount of acid required to achieve the maximum substitution in a minimum time (7 minutes, 100 W). Interestingly it has been shown that the use of a closed vessel can lead to a rearrangement of the DIC urea, leading to lower yield. HOBt (5eq.) has been shown to increase the esterification yield when used in combination with DCC (5eq.) and DMAP (1 eq.).[333-334] The efficacy of this reported method was assessed by introducing the sulphur *N*-acetylcysteine *via* a DIC coupling. The IR results in Figure 104 showed the presence of the pyrogallol[4]arene on the resin, but the low content of carbonyl peak indicate the low substitution.
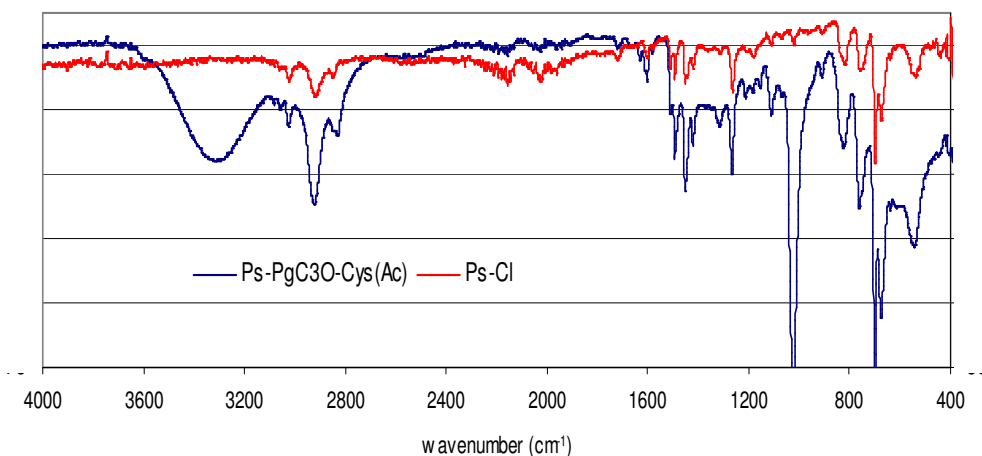
Figure 104: IR spectra of unsubstituted resin (PS-Cl) and the substituted resin before cleavage (PS-PgC3OCys(Ac))

The SEM-EDX results showed the presence of the sulphur on the surface of the beads, implying a successful functionalisation (Figure 105).
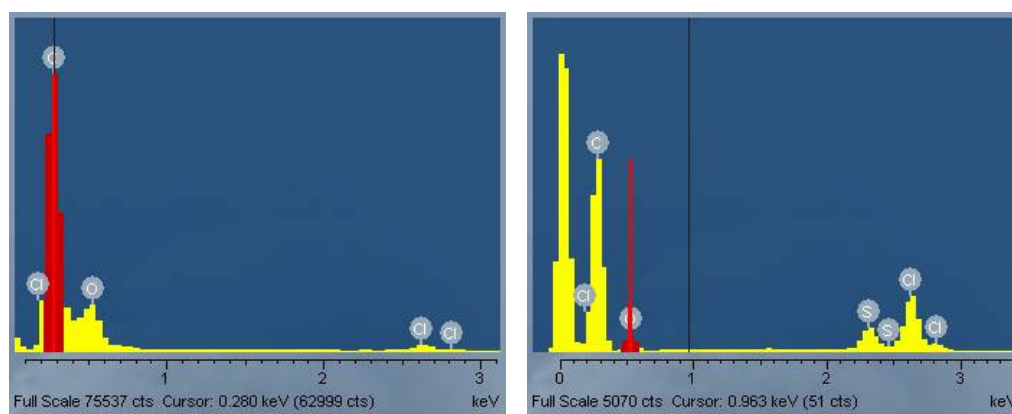
Figure 105: SEM EDX Spectra of (a)PS-Cl 200-400(b) PS-PgC$_3$OCys(Ac)

The analysis of the substitution was also assessed by UV, by determining the Fmoc-chromophore liberated in the supernatant following the cleavage with piperazine. As the Fmoc concentration is directly correlated to the substitution level, it can be compared to commercially available substituted resins that are used for peptide synthesis. In view of the further functionalisation of the resin with amino acids and peptides, it would also be a useful tool for monitoring the reaction.

The functionalisation of the pyrogallol[4]arene resin was then extended to a small peptide. *Tri*-alanine peptide was grafted to the pyrogallol[4]arene resin *via* a DIC coupling. The MALDI analysis of both starting pyrogallol[4]arene and the peptido-pyrogallol[4]arene revealed that three *tri*-alanine peptidic chains were successfully attached onto the calixarene. These results demonstrate the feasibility of this novel synthetic process but still require further investigation to confirm the attachment onto the pendant chains.

Further analyses, such as TGA, are required to assess the substitution as well as the efficiency of the methods. The good swelling properties of the resin result in the formation of a gel that can be analysed by NMR either directly[324] or by an insert.[335] Although working on a solid phase, it has been shown that ^{13}C NMR can be used to analyse Merrifield resin using a conventional spectrometer, by enhancing the signal to noise ratio and decreasing the resolution.[268, 336] As ^{13}C NMR has also been proved efficient on a pegylated resins,[57, 334] this analytic method should be optimised in future work. In addition, this type of solid supported work could be extended to chlorotrityl resin, as it is known to react readily with phenols,[337] and can be readily cleaved with TFA. Silyl chloride linkers have been proved to attach effectively primary and secondary alcohols as well as phenols to Merrifield resin.[338] Improvement of the cleavage step could be achieved by microwave irradiation; the use of a cleavage mix of 1:1 TFA/DCM, for three hours can results in low yield,[339] but this can be improved by microwave heating for thirty minutes at 500 W at 75 °C.[340] Recently, a method using microwave irradiation reported the efficient cleavage of peptide by reacting a mixture of TFA/TIS/H$_2$O (95 : 2.5 : 2.5) at room temperature for 15 minutes followed by a fifteen minutes   irradiation (30 W) at 50 °C.[341] Other cleavage mix involving trifluoromethanesulfonic acid (TfOH) and trimethylsilyl triflate (TMSOTf) could also be attempted as they appear to be more effective with than TFA at cleaving hydroxybenzamide.[323] Hydrochloric acid could also be used but can sometimes lead to unexpected residues.[327]

CHAPTER V: CALIXARENES DERIVATIVES IN BIOLOGICAL SYSTEM

As mentioned previously, the pyrogallol[4]arene derivatives have been less extensively studied than their calix[4]arene analogues. Because the macrocycle will be considered for immunisation in the future, it is therefore necessary to investigate their toxicity before using them as immunotherapeutic vectors. Potentially the macrocycles that have been functionalised with peptides will be employed but as a starting point, pyrogallol[4]arenes alone were investigated for toxicity and inertness *in vitro*. This work involves heamolytic properties on red blood cells and their effect on dendritic cells. The latter was assessed by studying the effect of varying concentration of the lead macrocycle on the viability and proliferation of the cells. Preliminary studies, including haemolytic properties and cytotoxicity studies did not show any toxicity at the workable concentrations.

A. INTRODUCTION

Phenol derived calix[4]arenes (Figure 106a) have received most attention for their interactions with various biological systems and Coleman has performed pioneering work in assessing their cytotoxy, by showing their lack of haemolytic properties unlike many other polyphenols.[19, 342] The low toxicity of calixarenes combined with their complexing ability provide promising use as vectors in pharmacology.[343-344] They can therefore stabilise medicines, prolong their effects of and decrease their side effects creating a new convenient medicinal form. Sulfonation of these compounds gives access to *para*-sulfonato-calix[n]arenes (Figure 106b), that have been widely studied, mainly by Coleman and co-workers, who presented a review of their biochemistry and biodistribution.[345-346] Combined with drugs, their biological activities are quite widespread as they have been shown to have anti-viral, anti-bacterial and antithrombotic activities as well as the ability to inhibit enzymes such as *L*-lysyl oxidase, which is up-regulated in tumours to increase metastasis.[347] Phosphonated calixarene derivatives (Figure 106c) also show good promise as anticancer agents. Their efficacy and non-toxicity have been confirmed by using high doses from 10 to 40 mg of calix[4]arene per take of pharmaceutical salt.[348]
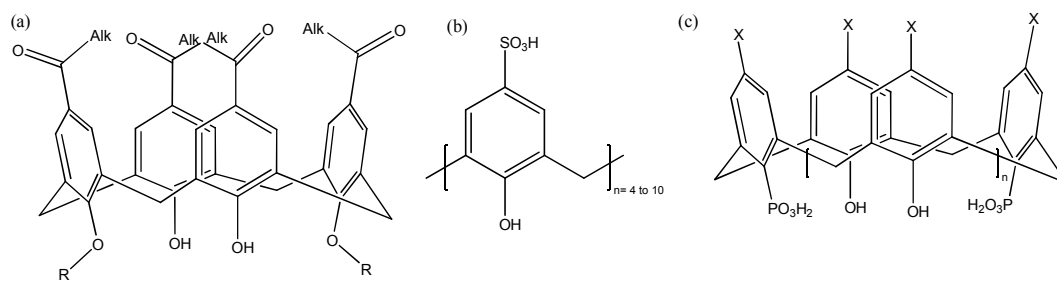
Figure 106: (a) General formulae of the amphiphilic calixarenes, Alk=CH₃(CH₂)n with n= 4,6,8,10 and R= H, PO(OEt)₂or PO(OH)₂[1], (b) para-sulfonato-calix[n]arene and (c) patented phosphonated calix[n]arene

Tert-butyl-calix[4]arene covalently bound to an antifungal drug, amphotericin (Figure 107a) was shown to have an antifungal activity that is ten times less toxic than the unbound drug.[349]
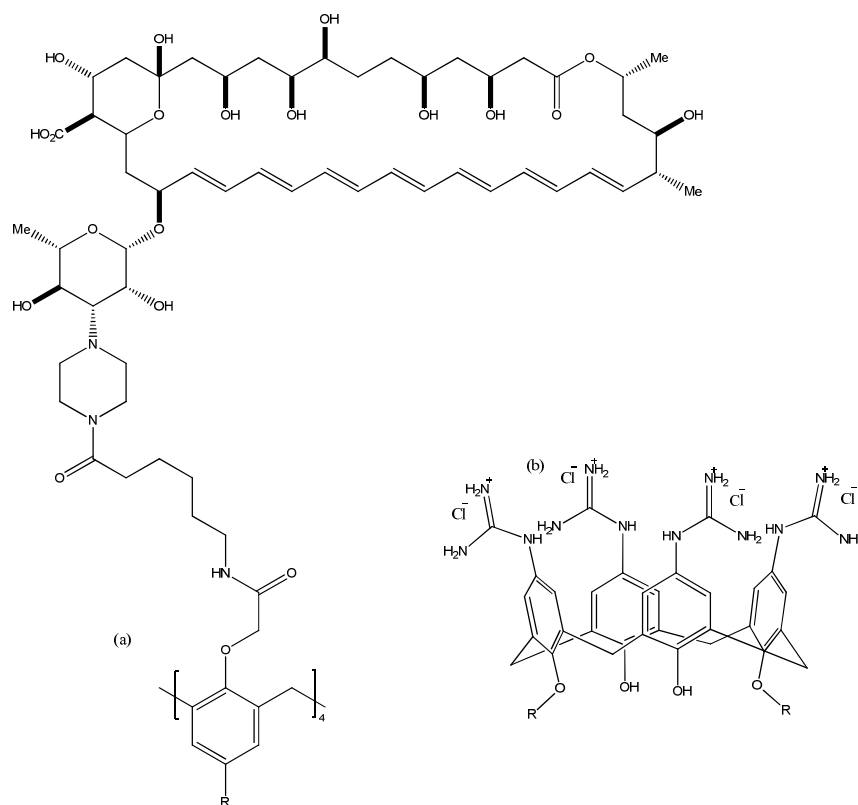
Figure 107: (a) Amphotericin B-calix[4]arene conjugate, R=H or t-Bu[349], (b) Guanidinium calixarene derivative R =hexyl, propyl, methyl[350]

Water soluble guanidinium calixarene derivatives (Figure 107b) have been made by reacting the amine derivative with *N,N'-di(tert*-butoxycarbonyl)thiourea in the presence of mercury (II) chloride. Their ability to bind to plasmid DNA in the

millimolar concentration range without any toxicity can be exploited in the condensation of DNA to perform cell transfection.[350] The toxicity of those derivatives was assessed by using a MTT assay, a cell proliferation and viability assay based on the reduction of a yellow tetrazole (MTT, 3-(4,5-dimethylthiazol-2-yl)-diphenyl tetrazolium bromide) within living cell mitochondria; no toxicity was found up to 25 µM.[351] They showed promise as an antibacterial agent in several studies.[352-354] Similar derivatives have shown comparable broad spectrum and lower cytotoxicity compared to commercially available agents, leading to the conclusion that they have a place as an adjuvant for antimicrobial chemotherapy or disinfection.[355]

Ureidocalix[8]arenes were shown to modulate C6 glioma cell proliferation and were proposed as an anticancer agent (Figure 108a).[356] In order to rule out their apoptotic effect, flow cytometry analysis after staining by propidium iodide and the MTT cell proliferation assay were performed. Pegylated calix[n]arenes, Figure 108b, not only enhance the innate defence mechanism in murine macrophages by mediation of an *L*-arginine dependent mechanism of activation but are also effective in MHC class II. It has also been assessed that the optimal chain length for high antimicrobial activities is PEG-6.[357]
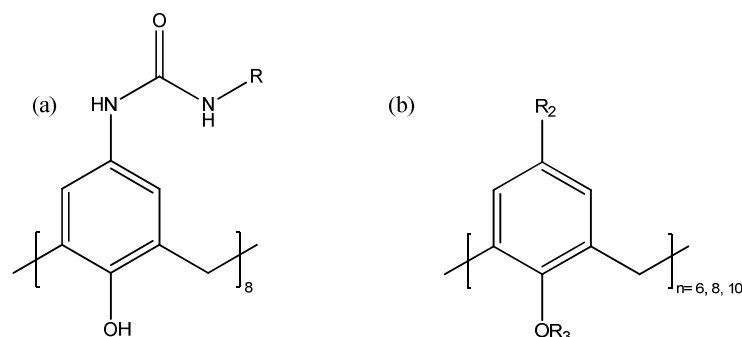
Figure 108: (a) Ureidocalix[8]arene, R=GlcNAc, butyl, H [356]; (b) Pegylated calix[n]arene, [357] R_2 = C_4H_8 or C_8H_{17}, R_3= H or $(CH_2CH_2O)_{n=6\ to\ 12}$

N-Acetyl-*D*-glucosamine substituted calix[4]arenes (Figure 109a) were used as a stimulator of NK-cell mediated antitumour immune response, showing better response than *N*-acetyl-*D*-glucosamine substituted dendrimers that are conventionally used.[358] Glycomimetic antigens, based on carbohydrated calix[4]arene attached to antigenic peptides, were evaluated as part of an anticancer vaccine (Figure 109b). After immunisation, an increase in efficacy was found for the one conjugated to calix[4]arene compared to the monovalent antigen.[359]
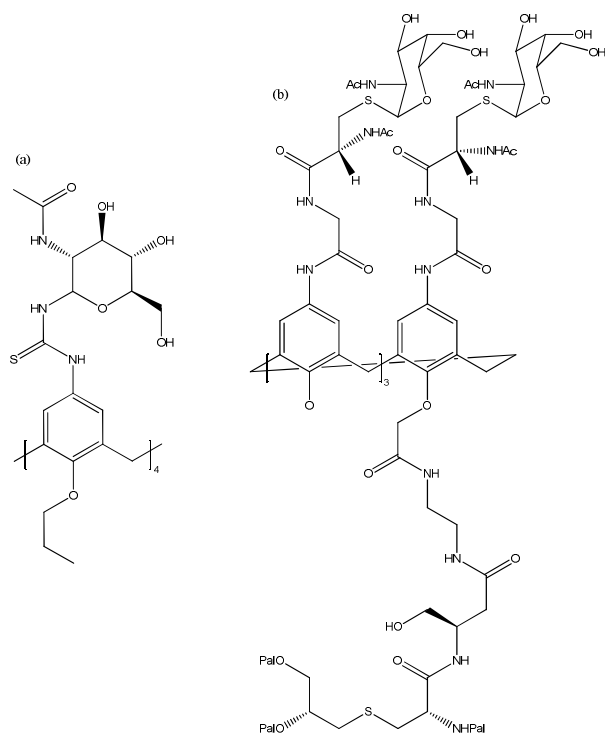
Figure 109: Glycosylated calix[4]arene: (a) N-Acetyl-D-glucosamine substituted (b) carbohydrated calix[4]arene attached to antigenic peptides

Cyclohexapeptidomimetic calix[4]arene derivatives were first reported for their antiangiogenic and antitumour properties,[360] and then patented as growth factor binding compounds.[361] Other antimicrobial peptide mimetics based on calixarenes have the potential to treat diseases, neutralise endotoxins, inhibit endothelial cell proliferation and act as angiogenic factors (Figure 110a).[362-363] Their ability to inhibit the binding of vascular endothelial growth factor to its receptor was proved both *in vitro* and *in vivo* in a nude mouse xenograft model.[364] Towards the development of calix[4]arene-based radiotherapeutic agents, Grote Gansey *et al.* studied the conjugation to biomolecules such as human or mouse serum albumin (HSA/MSA) and an antibody directed against a pregnancy hormone was chosen as a model tumour specific antibody mAb-506A. Their functionality remained inherent when up to six equivalents of calixarenes were attached and did not lead to any immunogenic response (Figure 110b).[365]
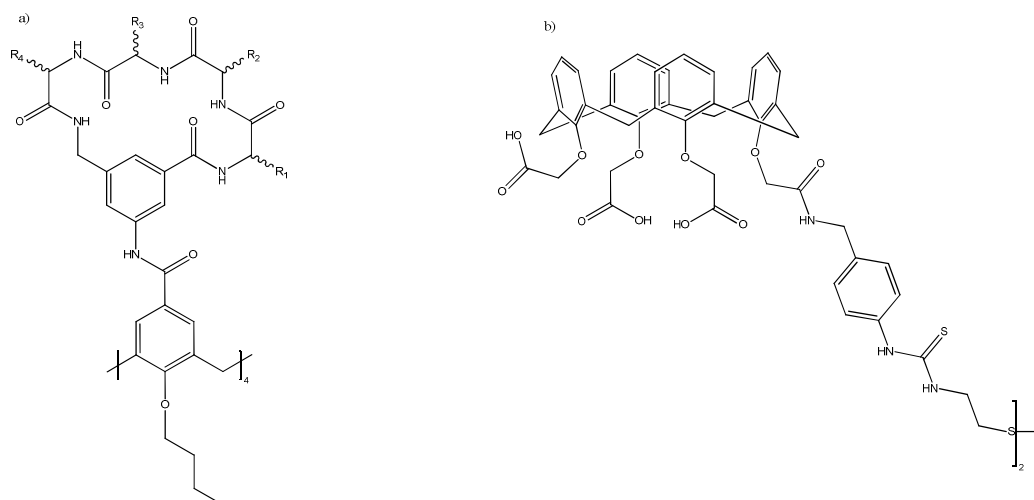
Figure 110: Peptidic calix[4]arene

Nucleotide-calix[4]arene conjugates have shown excellent water solubility and preliminary studies assessed their ability to inhibit DNA replication *in vitro* (Figure 111).[366]
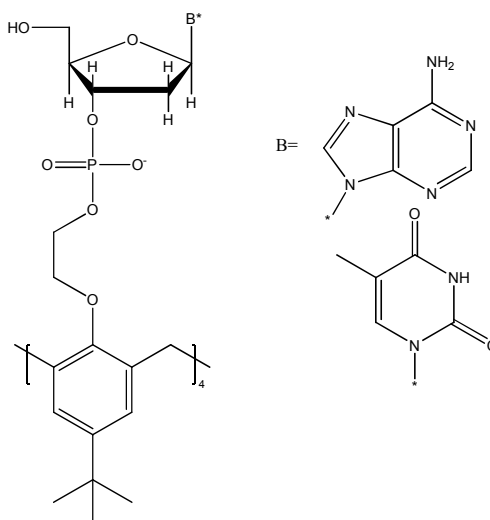
Figure 111: Nucleotide calix[4]arene conjugate[366]

Amino-functionalised calix[4]arene pentamers, represented in Figure 112, also exhibit DNA binding with reduced toxicity, emphasizing their potential as a gene transfection agent.[367]
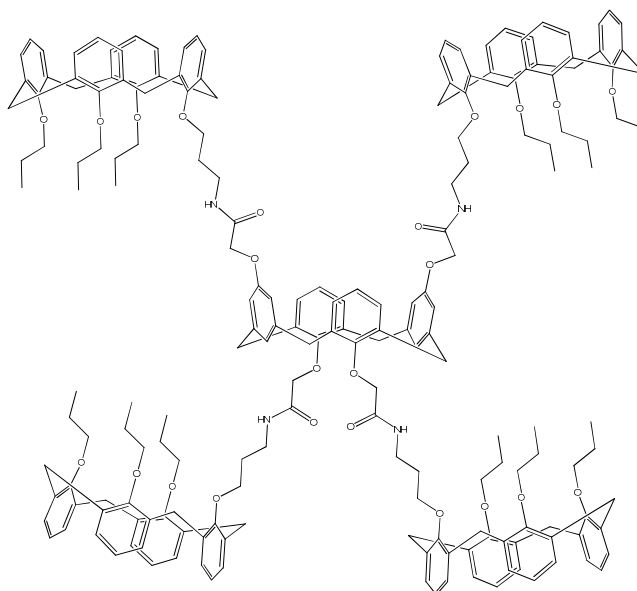
Figure 112: Calix[4]arene pentamer[367]

Most reported biological studies related to calixarenes macrocycles concentrated on the *tert*-butylphenol derivatives, and studies including their hydroxyl derivatives, *i.e.* resorcin[4]arene and pyrogallol[4]arene, have received less attention.[252] Resorcinol, the resorcinarene precursor, when incorporated into some drugs, is thought to have particular structural characteristics that contributes to the increased potency and activity of medicine.[368] One of the simplest and most commonly used classes of resorcinol derivatives are the resorcinolic lipids, identified from numerous plants, fungi and bacteria and thought to play a defensive role as antimicrobial and antifungal agents.[369-370] Their antiseptic properties are associated with their low surface tension which enables the compounds to penetrate membranes, and their chemical reactivity is associated with the two hydroxyl groups.[371] The antiseptic properties of hexyl-resorcinol are exploited in several commercially available treatments such as sprays and gargles, *e.g.* Beecham's throat plus and Strepsils Extra Lozenges. Substituted resorcinol derivatives can also exhibit depigmental action and have proved to be effective in the inhibition of tyrosinase, an enzyme known to catalyse the production of melanine.[372]
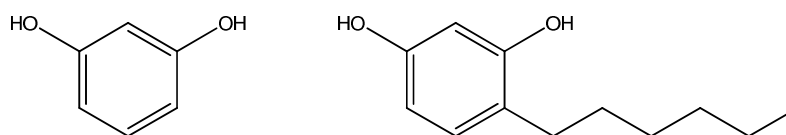
Figure 113: Resorcinol and hexyl-resorcinol

These antiseptic properties seem to be retained in the tetrameric form, as fluorinated substituted resorcin[4]arene have been purposely used to coat medical devices such as stents.[373] Prolyl bearing lipophilic resorcin[4]arenes (Figure 114), that self-assemble into solid-lipid nanoparticles, can be modified on the surface to maximize the interaction with specific antibodies for drug targeting.[374]
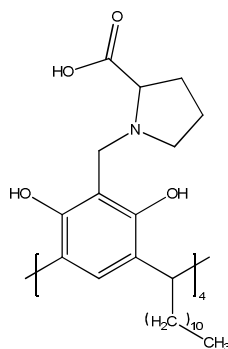
Figure 114: Prolyl bearing lipophilic resorcin[4]arene

The ability of calixarene derivatives, in particular alkyl and aryl resorcinarene derivatives, for use as excipients for active substances, was evaluated in 2006 by Wolf.[375] The protein localised into the eukaryotic cell nuclei, histone, can bind to resorcinarenes *via* hydrogen bonding and cluster effects.[376-379]
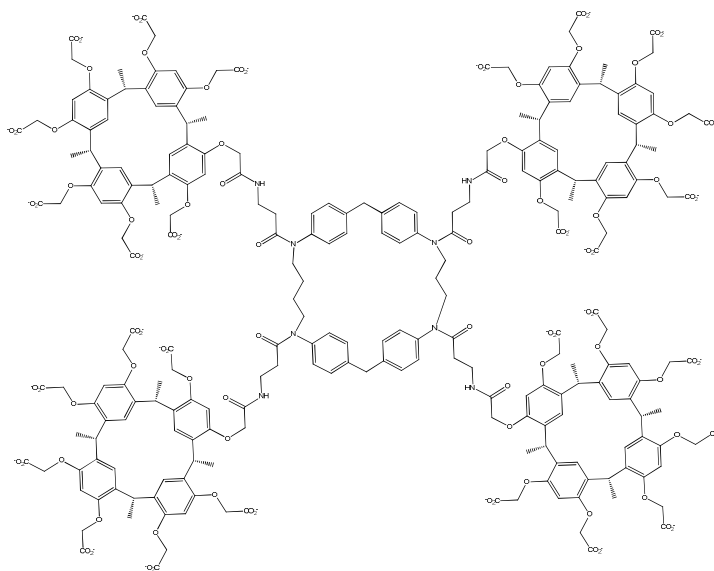
Figure 115: Histone binding resorcinarene cluster[38]

Glycosylated dendrimers, based on resorcinarene, have also been applied to biological systems.[380-381] When the phenoxy groups are replaced by saccharides, the lipophilic chains take over the self-assembly in the transformation of nanoparticles into an "artificial virus".[382] Their potential as vectors was assessed in hepatic cells (Figure 116).[383] Glycosylated resorcinarenes bound to DNA form virus-like particles, with decreased toxicity, capable of receptor-mediated hepatocyte targeting.[384] An artificial bi-stable resorcinarene host guest system was engineered to mimic a biological protein-DNA interaction which was controlled and switched by UV light.[385]
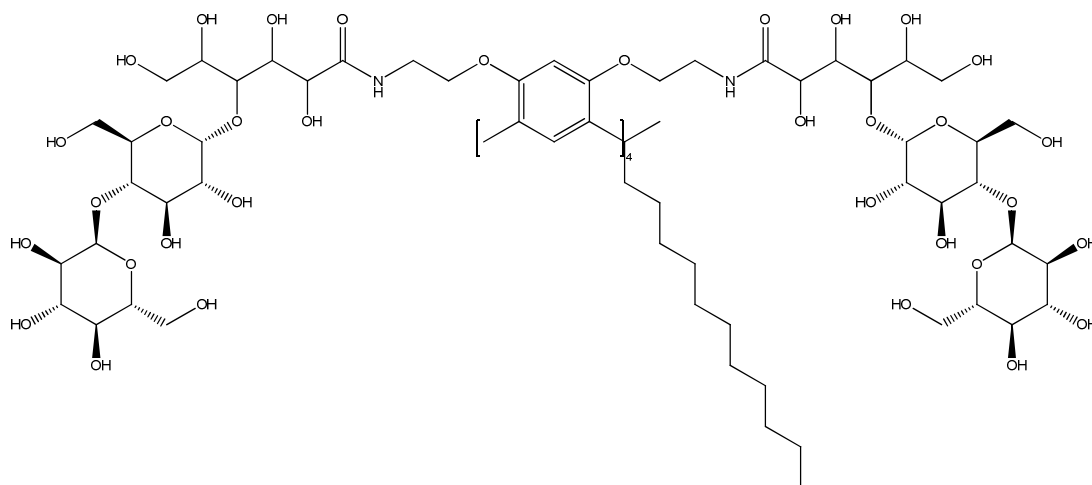
Figure 116: Glycosylated lipophilic resorcin[4]arene[382]

Studies exposed the ability of calixarenes to interact with the immune system with only little toxicity, showing good promise in terms of the pyrogallol[4]arenes derivatives. As pyrogallol is a biologically active compound and is used in biology to assess peroxidase activity, it could be expected to show little to no toxicity.[386] However, pyrogallol can be seen to have an inhibiting effect *in vitro* on the growth of juxtaglomerular cells.[387] It can also induce hepatocytoxicity in both mice and humans resulting in liver damage, as indicated by the levels of hepatic injury markers such as serum transaminase and bilirubin.[388]

Although the mechanism of pyrogallol is considered different to catechol and phenol interactions in the formation of reactive oxygen species (ROS) which can be responsible for DNA damage,[389] the pyrogallol[4]arenes reduce the oxidation properties by locking the benzene positions four and six due to the methine bridge.

In 1995, hundreds of calixarene derivatives were patented as part of a pharmaceutical preparation with antibacterial, antifungal, anticancer and anti-HIV activity. Interestingly, the *p*-fluorotolyl-propanoate-pyrogallol[4]arene potassium salt (Figure 117a) showed a low EC_{50} on the micromolar range.[390]

In order to assess the effect of the extra hydroxyls on the phenolic rings, the amino footed pyrogallol[4]arene (PgC_3NH_2, Figure 117b), known to be water soluble in its hydrochloric salt form, was considered. As this macrocycle will be the base to any peptidic derivatives in this study, it was essential to assess its effect on its own before seing its combined effect.

(a)

X = H, C_1-C_4 alk, NH_2
Y = OH or OCH_2COOCH_3
n=5-15

(b)

35
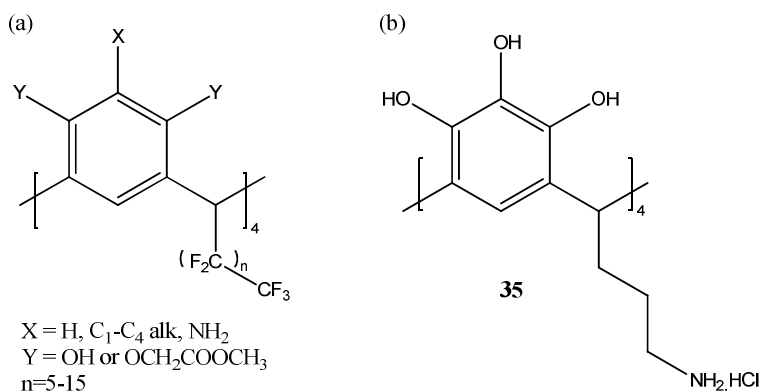
Figure 117: (a) Antimicrobial macrocycle and (b) C-3-aminopropyl-pyrogallol[4]arene 35

As the pyrogallol[4]arene will be considered as a vector for peptide delivery, it was essential to see its effect first when put in contact with blood, then its effect on dendritic cells that would be the cells targeted for immunisation. In general, the concentration of the tested calixarene was calculated depending on the amount of peptide used. In a typical immunisation experiment, 100 µg of peptides MHC class I, consisting of ten amino acids with an average weight of 1000 $g.mol^{-1}$, was used per injection per take. This is equivalent to 10 µmol per take as the ratio of calixarene to peptide is one to four, making the maximum dose of calixarene per take 2.5 µmol.

B. PYROGALLOL[4]ARENE *IN VITRO*

1. HAEMOLYTIC PROPERTIES

The haemolytic properties of the *C*-3-aminopropyl-pyrogallol[4]arene **35** were assessed in order to evaluate its effect on blood, using a similar method to the one reported by Coleman.[391] The test consisted of monitoring the lysis of the red blood cells when treated with increasing concentrations of calixarenes. For this quantitative colourimetric determination of the haemoglobin release, Drabkin's reagent was used, as it oxidises the iron from the heme, which can then coordinate to cyanide forming cyanmethemoglobin which has an absorbtion band at 540 nm by UV-vis. This comparative test was performed on washed erythrocytes extracted from freshly drawn human blood anti-coagulated using EDTA, to reduce the effect of other cells present in blood such as leukocytes and thrombocytes.

The total haemolysis was obtained when the red blood cells were subjected to hypotonic stress by incubating them in water. The percentage of haemolysis is the ratio of the absorbance of sample with the calixarenes, corrected with the negative control and absorbance positive control, as shown in Equation 1.

Equation 1:% Haemolysis

$$\% \ Haemolysis = \frac{A_{540nm} \ of \ sample \ with \ calixarene - A_{540nm} \ of \ PBS}{A_{540nm} \ of \ sample \ with \ water - A_{540nm} \ of \ PBS} \times 100$$

The first experiment was performed using the extract of sample directly. As the red haemoglobin absorbs at 450 nm, it can have an impact on the readings at 540 nm. Therefore, the samples should also be centrifuged before being added to the Drabkin's reagent, in order to minimise any false positive results.

The *C*-3-aminopropyl-pyrogallol[4]arene **35** was only sparingly soluble in PBS, therefore to increase solubilisation DMSO was added and maintained at less than 10% DMSO. This was thought to affect the cells as DMSO was previously seen to induce haemolysis. [392-394] However it did not have an effect over an incubation time of 30 minutes. As seen in Figure 118, the haemolysis increased considerably with increasing concentration of pyrogallol[4]arene. There is no significant haemolytic effect below 1 mM with the maximum value of 42% at 10 mM and the 50% haemolysis is

extrapolated to 11 mM. Those haemolytic percentage values are much higher than the ones obtained for the *para*-sulfonato calix[*n*]arenes where the maximum response of 30% was obtained for a concentration of 200 mM.[391]
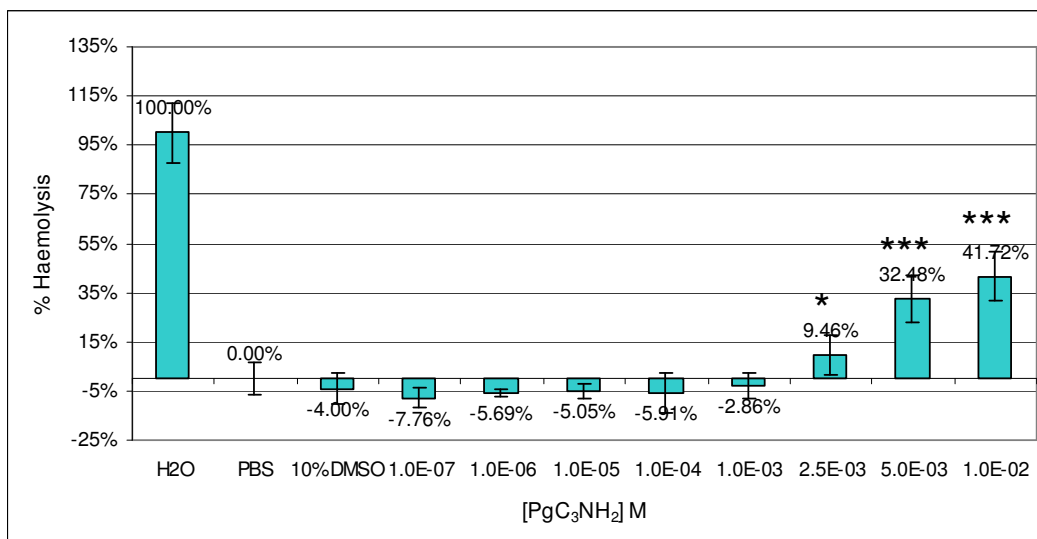
Figure 118: Haemolysis percentage relative to the overall concentration of of C-3-aminopropyl-pyrogallol[4]arene 35 after an incubation of 30 minutes, the data are represented by the mean value (n=2) ± SD, all p values <0.01 relative to untreated cells.

Those preliminary results allowed for the optimisation of the methods, nevertheless the experiment should be repeated with three different donors in a wider concentration range in order to obtain the HC50. In addition, the compound could be dissolved in another solvent that does not induce haemolysis. The results were therefore encouraging to continue using the macrocycle with cells such as dendritic cells.

2. CYTOTOXICITY ON DENDRITIC CELLS

a) Generation of Dendritic Cells

Dendritic cells were generated from bone marrow of HLA-DR4 immunologically naive mice, using a well-established technique, adapted from Inaba *et al.*[395] Briefly, bone marrow was flushed from mice hind limbs, extracted and washed several times and then cultured with a specific growth factor (GM-CSF), and a synthetic analogues of ds-RNA (Poly-IC). The cells were washed on day two and four, to remove any non-adherent cells. A week after the collection of the cells, the cells were harvested and used for further test. Although this method is effective, it uses 24 well-plates, which can restrict the growth and the washing step that can be problematic. It has

been shown that the growth of a pure population of dendritic cells is affected by a lower plating density, a prolonged culture period and a reduction of the GM-CSF dose.[396] Therefore, an alternative method of culturing dendritic cells in Petri dishes was attempted (method B). [397] The cultures were further split into two, to compare the maturation induced by LPS on dendritic cells.

Based on cell count on harvest day, this new method (B) showed similar results with respect to the production of immature dendritic cells and improved results in the production of mature dendritic cells. However, the cell count is not sufficient to estimate the purity of the population as it can include other cells such as granulocytes, but can be assessed by their surface marker expression using flow cytometry analysis. In order to phenotype the dendritic cells and recognise myeloid dendritic cells, the positive expression of both MHC class II and CD11c were checked. CD86 is a surface marker that is at high levels in PBMC and DC and at low levels in resting B cells and T lymphocytes. Its levels increase as it is a marker of preliminary maturation that has been induced using LPS. The results of the flow cytometry analysis are presented below in Figure 119.
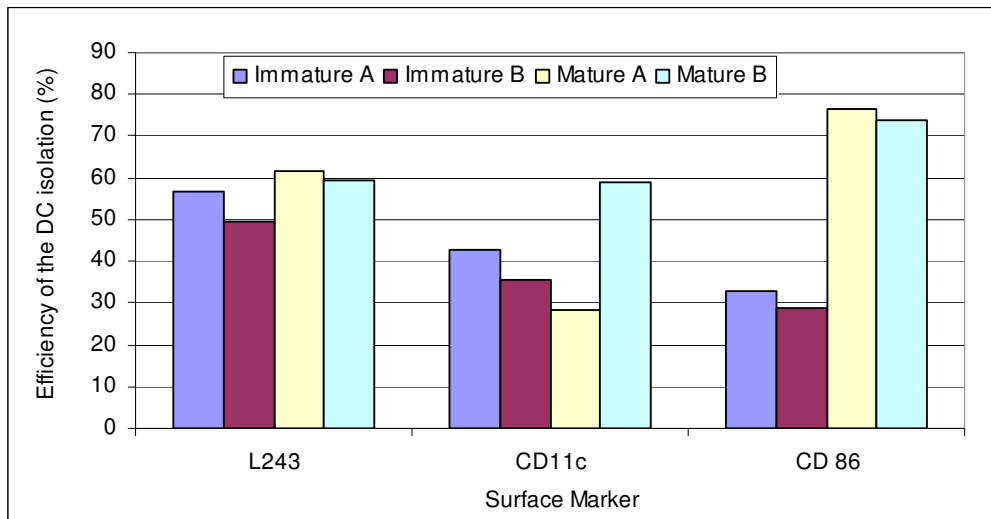
Figure 119: Effect of the BMDC generation method on the cell surface markers expression, Method A adapted from Inaba et al.[395], Method B adapted from Lutz et al.[396]

As seen in Figure 119, within the four subtypes, 50% (at most 61%) of the population is MHC II and CD11c positive. These values indicate that when using both techniques, the population contains other non dendritic cells. This issue could be overcome using cell enrichment tools such as CD11c magnetic beads.[398] In terms of

maturation, CD86 was used to asses the degree of maturity and by its expression it appears that both methods led to similar results. CD86 is a surface marker that is at high levels in PBMCs and DCs and at low levels in resting B cells and T lymphocytes. More recently another surface marker CD83 appeared to be more specific to DCs.[399] In addition, the use of double staining with a multi-colour flow cytometer would allow assessment of the exact population that is expressing both CD86, MHC II and CD11c, showing the integrity of the dendritic cells. These tests should also be performed in combination with one another, after incubation with the calixarene to see if they can induce the maturation and the expression of MHC I. This indicates that both techniques are valuable and can be considered for further experimentations that consist of assessing the viability of the cells when in contact with a pyrogallol[4]arene solution.

b) Viability depending on the ATP levels

The toxicity and inertness of *C*-3-aminopropyl-pyrogallol[4]arene **35** and *C*-3-aminopropyl-resorcin[4]arene **36** were also assessed *in vitro* on dendritic cells that were cultured using the method previously described. A cell viability bioluminescent test has been performed using the ViaLight® HS Kit measuring the adenosine triphosphate (ATP) levels. As ATP is a crucial co-enzyme that contributes to the transport of energy within a living cell, any form of cell injury results in rapid decrease in cytoplasmic ATP levels. This assay is based on the reaction of an enzyme, Luciferase, which is oxidised in presence of ATP, that catalyses the emission of light. This assay has been proved efficient in cell viability assessement.[400-401]

Equation 2: From ATP to light

$$ATP + Luciferin + O_2 \xrightarrow[Mg^{2+}]{Luciferase} Oxyluciferin + AMP + PP_i + CO_2 + LIGHT$$
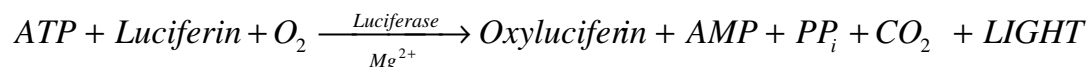
After a twenty-four hours incubation period with different concentrations of calixarene derivatives, diluted in the culture medium, a nucleotide releasing agent was added to each well and left to react for ten minutes. The ATP monitoring reagent was then added and the light was measured using a luminometer. The luminescence was then compared to the untreated cells that were considered as a 100 % release of ATP.

As shown in Figure 120, the ATP release is relatively stable from nano-molar to micro-molar concentrations, with similar values to the non-treated (control) cells.

Generally, the resorcinol and pyrogallol derivatives follow the same trend. However, this changes at a concentration of 0.5 mM, with a rise in luminescence observed for the pyrogallol[4]arene derivative, which may be caused by the conjugated character of the macrocycles.
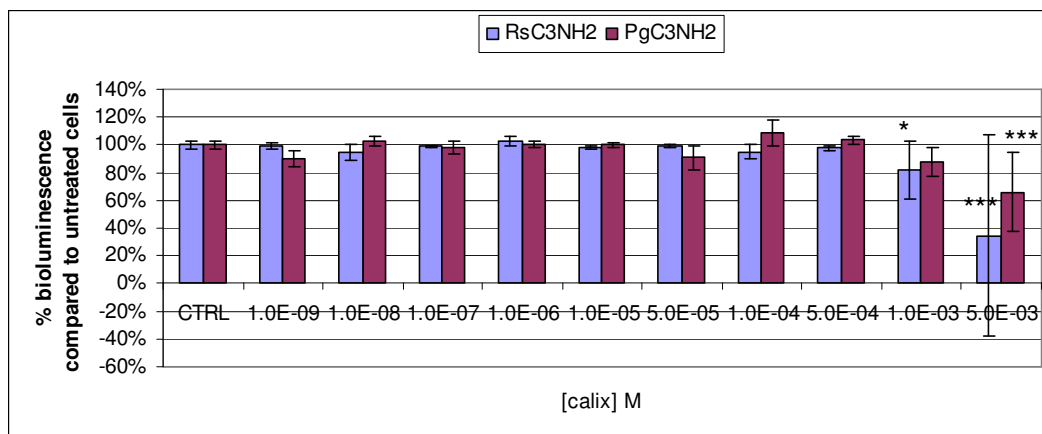
*Figure 120: Percentage of cytoplasmic ATP release relative to the untreated cells depending on the concentration of C-3-aminopropyl-pyrogallol[4]arene **35** and C-3-aminopropyl-resorcin[4]arene **36** (in mol/L), mean values (n=2) ±SD, p values are relative to the untreated cells*

The ToxiLight® Bioassay, a non-destructive bioluminescent cytotoxicity assay, was used to indirectly quantify the release of adenylate kinase (AK) from damaged cells.[402] This assay follows the same principle as the one previously described, as it involves the reaction of adenosine diphosphate (ADP) with AK that is released by damaged cells, followed by the reaction with Luciferase that enables measurement of the ATP.

Equation 3: Role of AK

$$Mg^{2+}ADP + ADP \xrightarrow{\quad AdenylateKinase \quad} Mg^{2+}ATP + AMP$$

The quantification of the light was performed relative to the untreated cells, depending on the calixarene concentration in the culture media. This assay only requires the use of the cell culture supernatant and therefore it can be performed at different time-points. In this case twenty-four hours and a week later, it was performed on the same cells that were washed with calixarene containing media. The results show some unexpected features, such as those seen in Figure 121, indicating reduced cell damage with increasing concentrations and time for both the pyrogallolarene and

164

resorcinarene. This suggests that they could be non-toxic at workable concentrations. This effect is likely to be caused by the high concentration of calixarene or the cell culture media. If it were to damage the cells, they would likely be washed away, resulting in a decrease of ATP within the media.
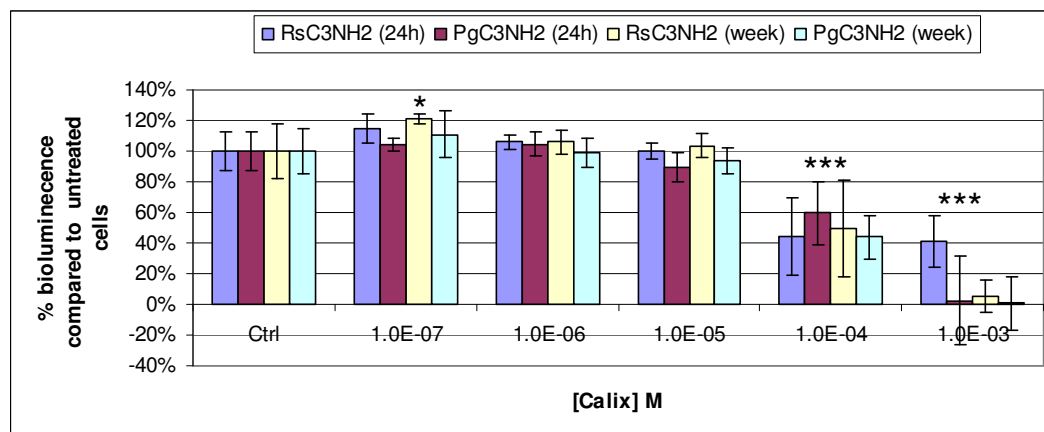
*Figure 121: Percentage of ATP release relative to the untreated cells depending on the concentration of C-3-aminopropyl-pyrogallol[4]arene **35** and C-3-aminopropyl-resorcin[4]arene **36** after 24hours and a week (in mol/L), mean values (n=2) ±SD.*

The effect of the calixarenes on the dendritic cell growth can also be observed by optical microscopy, as illustrated in Figure 122. At a 1 mM concentration of PgC_3NH_2, the cells appeared totally lysed and only fragments remained. At 0.1 mM, cells are still present but their morphology indicates that they have been subjected to a stress that impedes their proliferation. At a concentration below 10 μM, the *C*-3-aminopropyl-pyrogallol[4]arene **35** is seen to have no effect on the dendritic cells as their morphology is very similar to the untreated cells (ctrl) suggesting that they are still viable.
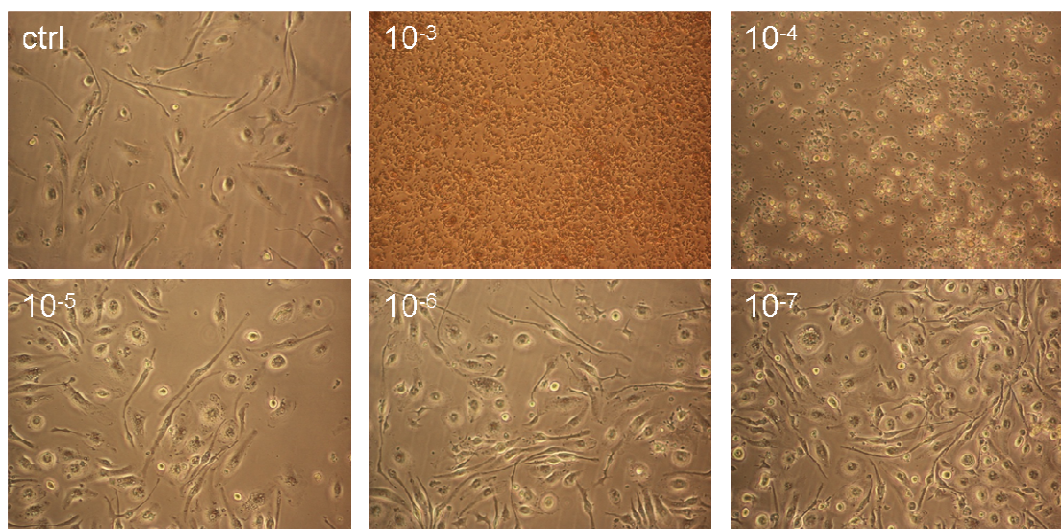
Figure 122: Photomicrographs (x10) of dendritic cells cultured with different concentration of C-3-aminopropyl-pyrogallol[4]arene (PgC₃NH₂) (M) incubated for 24 hours.

c) Proliferation assay using propidium iodide

Propidium iodide (PI) is a fluorescent agent that can intercalate with the DNA of cells with permeable membranes, damaged or dead cells and does not react with living healthy cells. Combined with the Elispot technology, it can be used to estimate the cell viability. Fixed numbers of dendritic cells were cultured with various concentrations of *C*-3-aminopropyl-pyrogallol[4]arene **35** for 1 hour and 24 hours, before the percentage of PI positive cells compared to the total cell count was assessed. In view of the results, PI was incorporated in all cells, even in the absence of pyrogallol[4]arene. The ability of the dendritic cells to engulf external antigens, induces a certain permeability to the cells which may explain the incorporation of PI. Nevertheless, the PI assay can be used to assess the proliferation rather than toxicity or cell damage.

As seen in Figure 123, the results obtained after one hour appears to be less reproducible, which may be induced by the external stress caused to the cells. However, the results appear more reproducible after an incubation of 24 hours; it seems that the calixarene has no significant effect compared to the untreated cells below 0.5 mM.
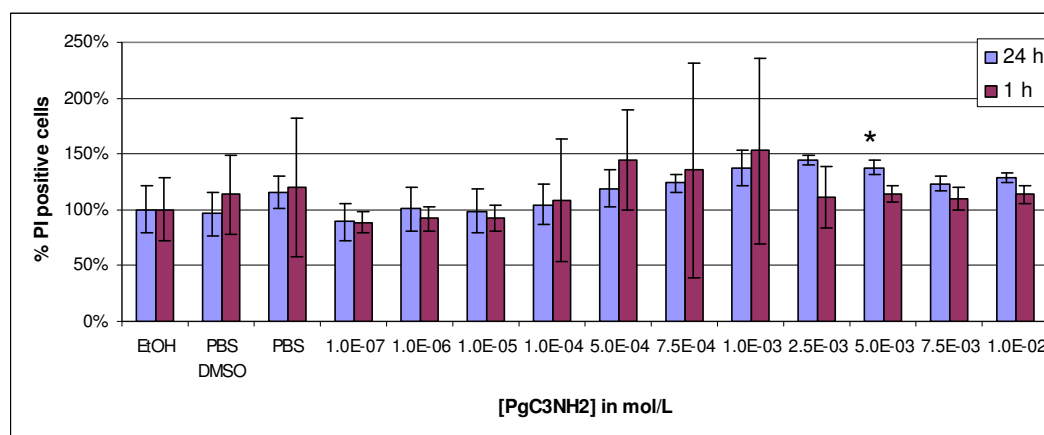
Figure 123:Percentage of PI positive cells depending on the concentration of calixarene in mol/L after 1 hour and 24 hour, represent by the mean (n=2) ±SD, p<0.05.

These method developments have been performed for all viability assays, with preliminary data indicating that the calix[4]arene macrocycles do not cause cell death at workable concentrations below 0.5 mM. These tests are part of a proof of concept but cannot be conclusive; they need to be repeated in order to obtain full statistical analysis. It is essential to perform several tests to assess the toxicity of any new compounds, including viability, proliferation, functionality and integrity of the cells. Solutions of calixarenes, containing no cells should also be used in the assays in order to avoid any false positives.

Future work should include extensive studies on the ability of the calixarenes, both as a precursor and as part of the vaccine formulation, to induce the maturation of the dendritic cells in addition to their cytoxicity studies. The attachment of biologically active material could be applied to bigger entities such as proteins and DNA, which would increase the potential as a drug delivery scaffold. Although preliminary studies have been performed for these types of molecules they need to be extended before proving to be safe for use as a vector in the vaccine form. They have to be safe, traceable and soluble offering definitive advantages over the other available systems that have already been approved by the FDA and MHRA.

CHAPTER VI: CONCLUSION AND FUTURE WORK

The formulation of the peptide nano-scaffold vaccine could potentially contain multifunctional capsules that have the capacity to use both the class I and the class II pathways, as well as carry traceable markers such as fluorescein. This will enable the production of both an adaptive and innate immune response, therefore preventing tumour recurrence. Although the major objective of the project: to engineer a novel pyrogallol[4]arene based vector towards the delivery of immunogenic peptides to dendritic cells was not wholly achieved, the investigation into potential nano-scaffolds for these peptides has been examined with some success.

As mentioned in the introduction of Chapter V; *tert*-butyl phenol based calixarene have previously shown promise in several biological applications. Until this study resorcin[4]arene and pyrogallol[4]arene calixarene analogues have not been explored. It can be expected that the peptide containing nano-scaffolds have similar toxicity to their polar precursors. However, those studies remain to be completed, and will be required for each potential vector, prior to any *in vivo* studies. The preliminary cytotoxicity studies indicate that both the potential precursors of the vectors, *i.e. C*-3-aminopropyl-pyrogallol[4]arene **35** and *C*-3-aminopropyl-resorcin[4]arene **36** have minimal toxicity on both red blood cells and dendritic cells. Although it appears that the viability of the cells is conserved, it is necessary to investigate the effect that larger aggregates may have. In view of many studies involving nanometre scale materials, it is understood that the nano-size may have a beneficial effect on dendritic cells and further studies should be performed investigating their effect on the cell maturation. The potential metabolites that would be generated by the scaffolds could be investigated by using artificial proteosomes or an animal study.

The major challenge of the project was to selectively biofunctionalise the pendant chains of the macrocycles. Although selective protections were investigated it did not lead to the target materials in sufficient quantities to fully characterise them and test their bioavailabilities. By having access to a plethora of commercially available acetals and aldehydes, the biofunctionalisation was attempted prior to the cyclocondensation of the macrocycles. This synthetic pathway proved to be somewhat more complicated than expected. The complex nature of the cyclisation process that is multifactorial, requires the optimisation of several conditions to achieve the desired

macrocycles in the desired cone conformation. Firstly, the starting material, *i.e.* the aldehyde, was required to have for the functional groups at least three carbons away from the carbonyl group in order to increase the cyclisation process. If the aldehyde is aromatic, it requires the presence of substituent that would favour the stabilisation of a carbocation. The choice of solvent is also fundamental in order to achieve the formation of thermodynamic compounds.

Utilising new greener techniques for preparation of pyrogallol[4]arenes, that employ microwave radiation has led to an improved efficiency by reducing considerably the reaction time. It is now possible to gain a rapid access to a library of materials and optimise the reactions condition towards the targeted compounds. The microwave synthesis allowed the production of a library of aliphatic and aromatic compounds, and also demonstrated the possibility to extend this to heterocyclic aldehydes. The only restriction to a wide range of novel macrocycles, is the availability of the starting aldehydes, that could be investigated further. The synthesis of commercially unavailable lead aldehydes will therefore be the subject of further studies.

The study into the self-assembly of the nanoscale capsules from these functionalised macrocycles requires further exploration in order to understand the effect of the subsistent on the self-assembly process. The interaction of the macrocycles can be seen on the nanoscale and it would be interesting to see how the presence of the peptide could interfere or favour the self-assembly process. Peptides are known to self-assemble due to the availability of a high number of hydrogen donors and acceptors, which contributed to protein folding. Since the capsule sizes are on the nanoscale this will have an impact on their interaction with the dendritic cells. It would be interesting to see that effect and compare the immune response.

In terms of the optimisation of the microwave method, still more can be achieved whereby the method to synthesise the aromatic macrocycles could be further refined to obtain a total control over the various stereoisomers. The crystal data indicate that the *rccc* form can be isolated from the reaction mixture, but unfortunately, it is not homogenous. In view of these findings, it can be concluded that the control of the stereoisomer production is multifactorial and therefore its total control can be challenging. The choice of the reaction conditions is very important; however, the electronic properties of the starting material have an effect as well as its steric

hindrance. As the synthesis of non-functionalised macrocycle was not the main focus it was not investigated deeper but will be the study of future work.

The self-assembly of the macrocycle, is highly influenced by the solvent as shown in chapter III. This effect can be exploited and tuned towards further applications, but may also lead to complications. If the macrocycles were to be found to change their potential to self-assemble into a capsule, it may be necessary to lock them into place using other methods *e.g.* coordination with a metal such as copper or gadolinium. This may also be achieved by covalently binding the upper rims together using alkyl dihalides.

The solubility of the biofunctionalised macrocycles may also be problematic, as experienced during this project it can be challenging to selectively functionalise the pendant chain in order to obtain a fully functionalised macrocycle. Even if the functionalisation occurs, it can be difficult to isolate. It appears that the solubility character of the macrocycles is highly influenced by the pendant chains and therefore the non-bound amino acid and peptides. In addition, the macrocycles have the ability to entrap starting materials such as peptides within its pendant chain. In order to overcomes some of these problems, the addition of PEG to the macrocycles will need further investigation and optimisation.

Solid phase functionalisation of the macrocycles could potentially overcome the solubility issues incurred previously. However, due to time constraints, only the feasibility studies have been achieved at this stage and it remains to be proved that only the phenolic groups of the calixarene are bound to the solid support. This could potentially be addressed by using Fmoc-protected amino acid grafted onto the starting aldehyde. In addition, this would enable the detection of the degree of functionalisation by UV titration of the deprotected Fmoc. The peptide can then be synthesised onto the resin and fluorophores can also be included.

The inclusion of a fluorophore on the pendant chain terminus would be a very useful tool for the investigation of the calixarene *in vitro,* whereby, the engulfment of the macrocycles by the dendritic cells could be followed by the use of fluorescence microscopy. If a cleavage site was to be included and the fluorescent peptide was not completely cleaved, it would be possible to follow the presentation of the peptides onto the cells surface. By attaching other fluorophores onto the macrocycle core, it could be possible to follow this process within the cell. By understanding this uptake

mechanism, it could possible to target the DCs that would trigger this cascade of events leading to the presentation of the peptide to other macrophages.

If the nanovectors were to be realised and fully characterised, several studies into assessing the potential future use of the calixarenes for immunotherapeutic purposes should be considered, using the well-established protocol to assess peptide immunogenicity. First, it would be necessary to compare both in-house synthesised and commercially bought p53 peptides. Then the effect of the vectors should be assessed by comparing the immunological response of the peptide alone and the peptide-calixarene complex. Finally the effect of the calixarenes should be compared to the traditional adjuvant IFA in order to potentially remove it.

CHAPTER VII: EXPERIMENTAL

A. GENERAL INFORMATION

All chemicals were used as received by the suppliers (SigmaAldrich, Acros, AlfaAesar) unless stated otherwise. All other solvents were used as supplied (Laboratory, Analytical or HPLC grade), without prior purification. Microwave experiments were performed on CEM Discover®-SP microwave (CEMCorporation, UK), dynamic with temperature or pressure control, 30 second pre-stirring, power max function (simultaneous air cooling). Peptides syntheses were carried out on CEM Discover®-SPS Microwave peptide synthesiser (CEMCorporation, UK).

Thin layer chromatographies were performed on glass plates coated with silica and C60 silica. Flash chromatography was performed using BIOTAGE SPX2.0 (Biotage, UK). High performance liquid chromatography were performed on a HPLC Agilent 1100 series (Agilent, UK) using a Hypersil Gold C18 column (ThermoFisher, UK), 250 mm, 5 µm particle size using HPLC grades solvents (ThermoFisher, UK).

Nuclear magnetic resonance (NMR) spectra were recorded on a JEOL ECX 400, (JEOL, USA) spectrometer internally referenced to TMS in the deuterated solvent stated; ^{1}H (400 MHz) and ^{13}C proton decoupled 100 MHz. All chemical shifts (δ) are quoted in ppm and coupling constants (*J*) in Hz. Residual signals from the solvents were used as an internal reference.

Mass spectra were obtained upon an APCI Platform spectrometer, Shimadzu Axima CFR+3 (Shimadzu, Japan) and Bruker Ultraflex3 (Bruker Corporation, Germany) MALDI-TOF mass spectrometer using a raster mode and a 1000 averages, using CHCA as a matrix with only molecular ions and major peaks reported.

Single crystal analyses were performed at on the Oxford Diffraction Xcalibur, Sapphire3, the EPSRC X-ray crystallography service at the University of Southampton and Daresbury synchrotron laboratory. The structure was solved and refined using the programs SHELXS-97[403] and SHELXL-97[404] respectively. The program X-Seed[405] was used as an interface to the SHELX programs and POVRAY[406] to prepare the figures.

Infrared spectra were recorded on a Perkin-Elmer Spectrum 100 Fourier transform spectrophotometer with a diamond attenuated total reflectance (ATR) sampling accessory (PerkinElmer, UK).

UV-vis spectrometry was achieved on a JASCO V530 (Jasco, USA) TEM images were generated on a JEOL JEM-2010, accelerating voltage 200 keV, tungsten filament, electron beam current 10 µA; using a Gatan SC1000 ORIUS CCD camera. SEM were performed on JEOL JSM-A840A scanning electron microscope (SEM), (Jeol Ltd, UK).

B. CHAPTER II

1) *C*-Alkyl-pyrogallol[4]arene and *C*-alkyl-resorcin[4]arene 1-8
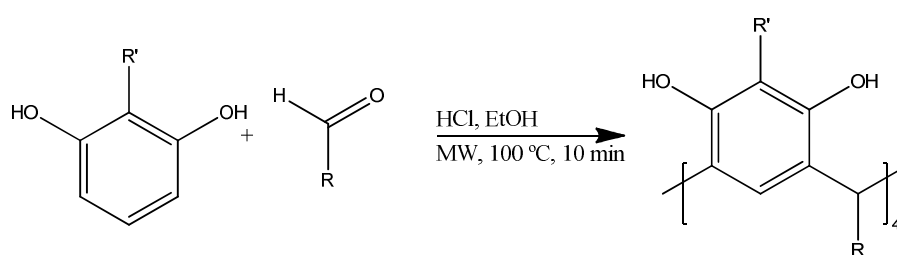
The aldehyde of choice (R = $(CH_2)CH(CH_3)_2$, $(CH_2)_2CH_3$, $(CH_2)_3CH_3$, $(CH_2)_4CH_3$, 1 eq., 4 mmol) was added to a solution of pyrogallol (R'= OH) or resorcinol (R'= H) (1 eq. 4 mmol) in ethanol (2 mL) and concentrated HCl (37%, 500 µL) contained in a CEM pressure vial (10 mL). After pre-stirring (30 sec), the mixture was heated (100 ºC) by microwaves (100 W, PowerMax) for 10 min. Upon cooling to room temperature, the *rccc* product crystallised from solution, whereupon it was collected by vacuum filtration as the pure product, yields are summarised in the following table. ^{1}H NMR, ^{13}C NMR and MS for all of the isolated products are consistents with the literature values from synthesised using conventional heating methods.[82-83]

	R	R'	%Y	m/z $[M+Na]^+$		R	R'	%Y	m/z $[M+Na]^+$
1	OH	$(CH_2)CH(CH_3)_2$	85	799	**5**	H	$(CH_2)CH(CH_3)_2$	90	735
2	OH	$(CH_2)_2CH_3$	61	743	**6**	H	$(CH_2)_2CH_3$	96	679
3	OH	$(CH_2)_3CH_3$	62	799	**7**	H	$(CH_2)_3CH_3$	67	735
4	OH	$(CH_2)_4CH_3$	68	855	**8**	H	$(CH_2)_4CH_3$	84	791

2) *C*-Butyl-pyrogallol[4]arene 3
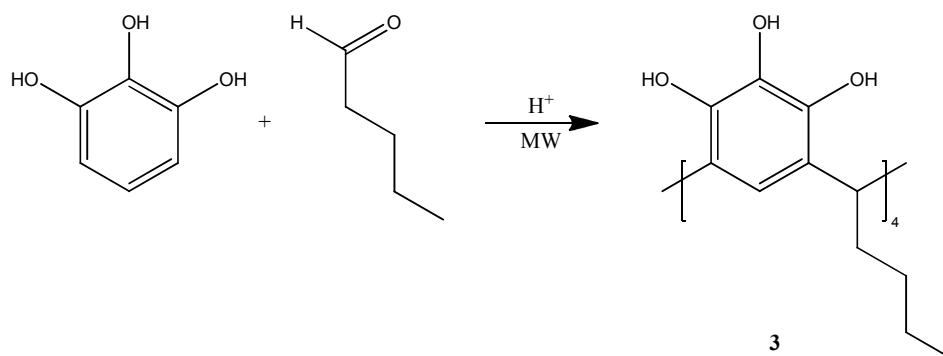
Valeraldehyde (1 eq., 4 mmol, 425 µL) was added to a solution of pyrogallol (1 eq. 4 mmol, 0.504 g) in an appropriate solvent (1.5 mL) and concentrated HCl (37%, 500 µL) contained in a CEM pressure vial (10 mL). After pre-stirring (30 sec), the mixture was heated (Figure 42), by microwaves (100 W, PowerMax) for a given time (Figure 40) after which the mixture was added directly into cold water (5 mL), collected by vacuum filtration and washed with water (2 mL x 3) and used crude for NMR analysis.

C-butyl-pyrogallol[4]arene (*rccc*): ^{1}H NMR (400 MHz, d_6-DMSO) δ = 8.60 (br. s, 12H, OH), 6.88 (s, 4 H, ArH), 4.15 (t, ^3J = 7.9 Hz, 4H, C$_1$H), 2.15 (q, ^3J = 7.9 Hz, 8 H, C$_2$H$_2$), 1.16 (quin, ^3J = 7.9 Hz, 8 H, C$_3$H$_2$), 1.33 (m, 8 H, C$_4$H$_2$), 0.85 (t, ^2J = 7.3 Hz, 12 H, C$_5$H$_3$) ppm. ^{13}C NMR (101 MHz , d_6-DMSO) δ = 139.5, 132.8, 124.5, 113.5, 33.7, 32.6, 30.2, 22.1, 14.2 ppm. MALDI-TOF *m/z* for C$_{44}$H$_{56}$O$_{12}$ calcd. 776.38, found 799.07 [M+Na][+].

Time (min)	T(°C)	Solvent	Yield (%)	*rccc* [a] (%)	Time (min)	T(°C)	Solvent	Yield (%)	*rccc* [a] (%)
1			Oligomer [b]		40			Oligomer [b]	
2			57	77	60			Oligomer [b]	
3			65	79	5	80	EtOH	77	85
4			60	80	120			Decompose [b]	
5	100	EtOH	73	83	140			Decompose [b]	
6			76	86			MeOH	56	66
7			79	86			*n*PrOH	40	88
8			66	83	5	100	*n*BuOH	76	96
9			72	86			EtOAc	25	96
10			70	86			H$_2$O	56	4

Suitable crystals were obtained by slow evaporation of deuterated DMSO, crystal data for *C*-butyl-pyrogallol[4]arene **3** DMSO clathrate: $C_{55}H_{89}O_{17.50}S_{5.50}$, $M = 1206.59$ g mol^{-1}, triclinic, space group $P\bar{1}$ (No. 2), $a = 12.7282(3)$ Å, $b = 13.3196(2)$ Å, $c = 19.2932(3)$ Å, $\alpha = 104.3940(10)°$, $\beta = 97.5090(10)°$, $\gamma = 99.0330(10)°$, $V = 3079.26(10)$ Å^3, $T = 120(2)$ K, $Z = 2$, $D_c = 1.301$ g cm^{-3}, $\mu = 0.272$ mm^{-1}, $F_{000} = 1294$, crystal size = $0.19 \times 0.17 \times 0.08$ mm^3, $R1 = 0.0780$, $wR2 = 0.1859$, *GooF* = 1.015 Crystallographic data in have been deposited with the Cambridge Crystallographic Data Centre as supplementary publication no CCD 755190

3) *C*-Phenyl-pyrogallol[4]arene 9
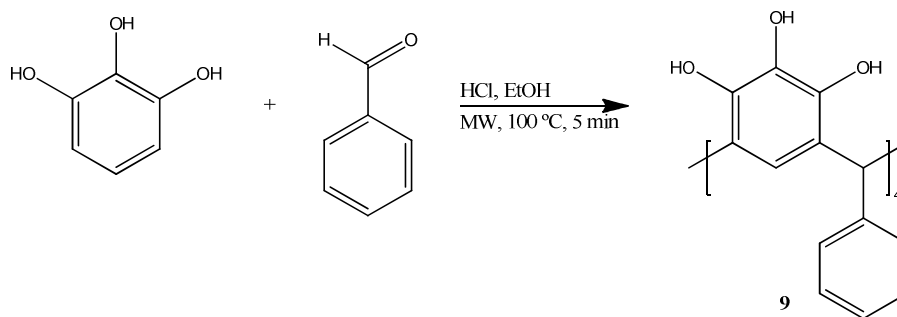
Benzaldehyde (1 eq., 4 mmol, 405 µL) was added to a solution of pyrogallol (1 eq. 4 mmol, 0.504 g) in ethanol (1.5 mL) and concentrated HCl (37%, 500 µL) contained in a CEM pressure vial (10 mL). After pre-stirring (30 sec), the mixture was heated (100 ºC) by microwaves (100 W, PowerMax) for 10 min. Upon cooling to room temperature, the *rccc* product crystallised from solution, whereupon it was collected by vacuum filtration and washed with water (2 mL x 3) to obtain red solid (0.565 g, 6.69 x 10^{-4} mol, 66 %).

^{1}H NMR (400 MHz, d_6-DMSO) δ = 8.51 (s, 12H, OH), 6.92 (t, ^2J=7.3Hz, 8H, C_{10}H), 6.83 (t, ^2J=7.3Hz, 4H, ArC_{11}H), 6.60 (d, ^2J=7.3Hz, 8H, C_9H), 5.99 (s, 4H, ArC_lH), 5.66 (s, 4H, C_7H) ppm. ^{13}C NMR (101 MHz, d_6-DMSO) δ = 152.5, 145.7, 128.9, 128.6, 127.1, 126.9, 124.5, 120.6, 102.0 ppm. MALDI-TOF *m/z* for $C_{52}H_{40}O_{12}$ calcd. 856.25, found 879.25 [M+Na]$^+$

Crystal data for *C*-phenyl-pyrogallol[4]arene **9** *rccc*: $C_{52}H_{40}O_{12}$, $M = 856.84$, $0.18 \times 0.09 \times 0.09$ mm^3, monoclinic, space group $C2/m$ (No. 12), $a = 20.913(3)$, $b = 21.667(3)$, $c = 11.3077(14)$ Å, $\beta = 116.490(16)°$, $V = 4585.9(10)$ Å^3, $Z = 4$, $D_c =$

175

1.241 g/cm^3, F_{000} = 1792, Xcalibur, Sapphire3, MoK$_\alpha$ radiation, λ = 0.71073 Å, T = 150(2)K, $2\theta_{max}$ = 50.0º, 11089 reflections collected, 4146 unique (R_{int} = 0.0625). Final $GooF$ = 0.977, $R1$ = 0.0925, $wR2$ = 0.2211, R indices based on 1959 reflections with I >2sigma(I) (refinement on F^2), 305 parameters, 0 restraints. Lp and absorption corrections applied, μ = 0.088 mm^{-1}.

4) *C-o*-Tolyl-pyrogallol[4]arene 10
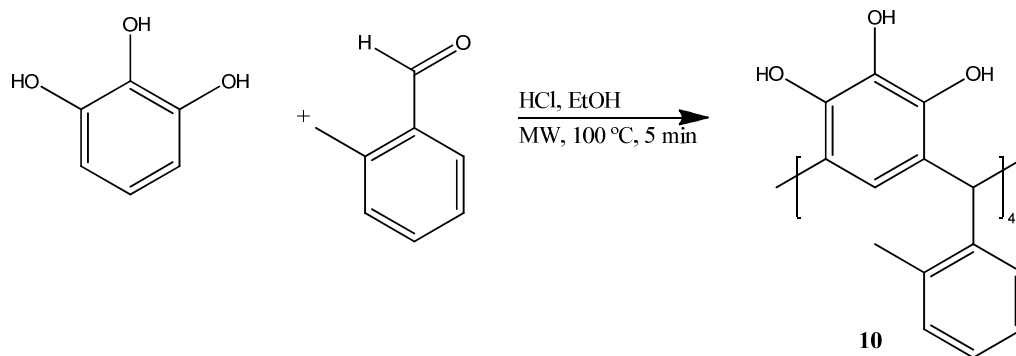
10

  o-Tolyl-aldehyde (1 eq., 4 mmol, 368 μL) was added to a solution of pyrogallol (1 eq. 4 mmol, 0.504 g) in ethanol (1.5 mL) and concentrated HCl (37%, 500 μL) contained in a CEM pressure vial (10 mL). After pre-stirring (30 sec), the mixture was heated (100 ºC) by microwaves (100 W, PowerMax) for 10 min. Upon cooling to room temperature, a solid precipitated from solution, whereupon it was collected by vacuum filtration and washed with water (2 mL x 3) to obtain a brown solid (0.275 g, 3.01 x 10^{-4} mol, 41%) of which the *rccc* isomer is (50%).

^{1}H NMR (400 MHz, CDCl$_3$) δ_H = 6.90 (t, ^3J = 3.8 Hz, 8H, ArC$_l$H), 6.69 - 6.36 (m, 4H, AA'XX'), 6.26-5.99 (m, 4H, AA'XX'), 4.635 (s, 4H, CH), 1.12 (12 H, CH$_3$) ppm. ^{13}C NMR (101 MHz, CDCl$_3$) δ = 148.7, 140.6, 139.8, 134.2, 123.5, 123.3, 120.0, 118.6, 95.6, 59.8, 37.8, 23.6 ppm. MALDI-TOF *m/z* for C$_{56}$H$_{48}$O$_{12}$ calcd. 912.31, found 935.97 [M+Na]$^+$.

5) *C-m*-Tolyl-pyrogallol[4]arene 11
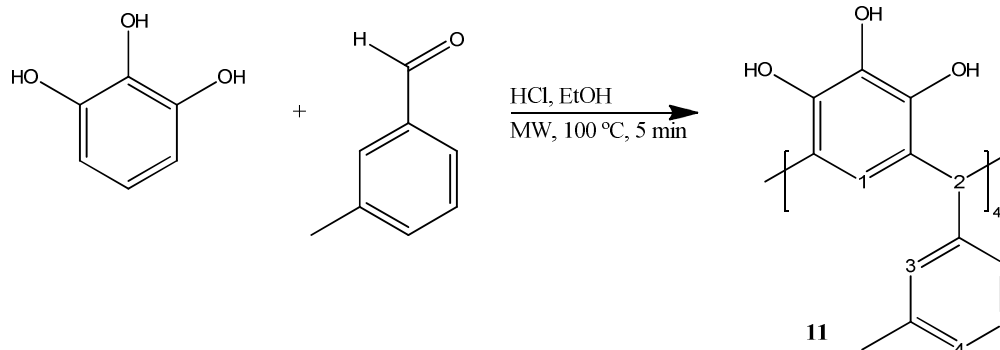
11

m-Tolyl-aldehyde (1 eq., 4 mmol, 471 µL) was added to a solution of pyrogallol (1 eq. 4 mmol, 0.504 g) in ethanol (1.5 mL) and concentrated HCl (37%, 500 µL) contained in a CEM pressure vial (10 mL). After pre-stirring (30 sec), the mixture was heated (100 ºC) by microwaves (100 W, PowerMax) for 10 min. Upon cooling to room temperature, the *rccc* product crystallised from solution, whereupon it was collected by vacuum filtration and washed with water (2 mL x 3) to obtain a pink solid (0.857g, 9.69 x 10^{-4} mol, 96%).

^{1}H NMR (400 MHz, CDCl$_3$) δ = 6.16 - 5.96 (m, 4H, C$_5$H), 5.96 - 5.84 (m, 4H, C$_6$H), 5.81 (br. s., 4H, C$_4$H), 5.77 - 5.48 (m, 4H, C$_3$H), 5.15 (s, 4H, C$_1$H), 4.97 (br. s, 4H, C$_2$H), 1.26 (br. s., 12H, CH$_3$) ppm. ^{13}C NMR (101 MHz, CDCl$_3$) δ = 150.9, 143.7, 138.9, 134.2, 127.9, 124.2, 123.7, 119.3, 100.7, 39.8, 19.7 ppm. MALDI-TOF *m/z* for C$_{56}$H$_{48}$O$_{12}$ calcd. 912.31, found 935.97 [M+Na]$^+$.

Preliminary crystal data for *m*-tolyl-pyrogallol[4]arene *rccc*: C$_{56}$H$_{48}$O$_{13}$, M = 928.94, yellow block, triclinic, $0.10 \times 0.05 \times 0.02$ mm^3, space group $P\bar{1}$ (No. 2), a = 11.3087(7), b = 11.6653(8), c = 19.9865(14) Å, α = 92.610(5), β = 102.904(5), γ = 108.740(6)°, V = 2414.0(3) Å^3, Z = 2, D_c = 1.278 g/cm^3, F_{000} = 976, Xcalibur, Sapphire3, MoK$_\alpha$ radiation, λ = 0.71073 Å, T = 173(2)K, $2\theta_{max}$ = 58.7°, 19468 reflections collected, 8097 unique (R_{int} = 0.3778). Final *GooF* = 1.281, R1 = 0.1652, *wR*2 = 0.4065, R indices based on 2652 reflections with I >2sigma(I) (refinement on F^2), 638 parameters, 0 restraints. Lp and absorption corrections applied, μ = 0.091 mm^{-1}.

6) *C-p-Tolyl-pyrogallol[4]arene* 12
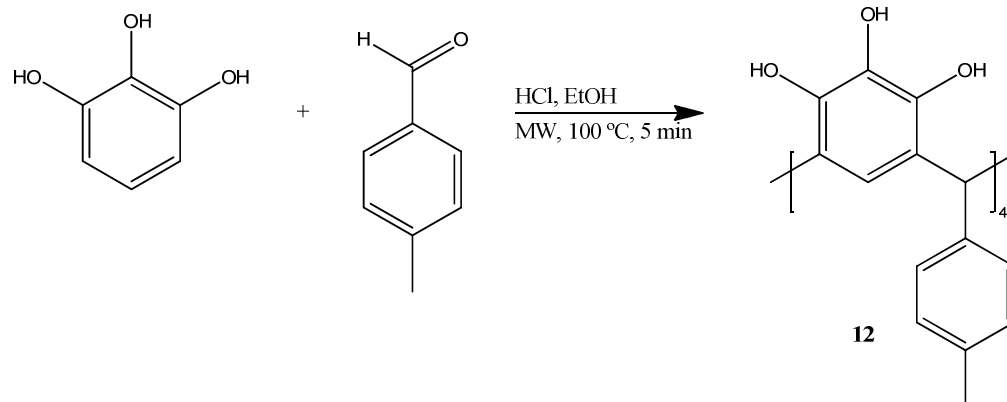
p-Tolyl-aldehyde (1 eq., 4 mmol, 472 µL) was added to a solution of pyrogallol (1 eq. 4 mmol, 0.504 g) in ethanol (1.5 mL) and concentrated HCl (37%, 500 µL) contained in a CEM pressure vial (10 mL). After pre-stirring (30 sec), the mixture was heated (100 °C) by microwaves (100 W, PowerMax) for 10 min. Upon cooling to room temperature, the *rccc* product crystallised from solution, whereupon it was collected by vacuum filtration and washed with water (2 mL x 3) to obtain a pink solid, (0.857 g 9.38 x 10^{-4} mol, 94%)

^{1}H NMR (400 MHz, CDCl$_3$) δ_H =6.95 (d, ^2J= 7.8 Hz, AA'XX', 8 H), 6.82 (d, ^2J= 7.8 Hz, AA'XX', 8 H), 6.43 (s, 4 H, ArH), 5.32 (s, 4 H, CH), 1.41 (s, 12H, CH$_3$) ppm. ^{13}C NMR (101 MHz, d_6- CDCl$_3$) δ= 150.8, 140.9, 138.9, 127.0, 125.9, 119.2, 100.5, 39.6, 19.1 ppm; MALDI-TOF *m/z* for C$_{56}$H$_{48}$O$_{12}$ calcd. 912.31, found 935.97 [M+Na]$^+$

Crystal data for p-tolyl-pyrogallol[4]arene: 2(C$_{56}$H$_{48}$O$_{12}$)O, *M* = 1841.89, colourless block, 0.14 × 0.06 × 0.02 mm^3, monoclinic, space group *P*2$_1$/*n* (No. 14), *a* = 11.2436(8), *b* = 22.0850(15), *c* = 21.1825(17) Å, β = 92.624(4)°, *V* = 5254.4(7) Å^3, *Z* = 2, *D*$_c$ = 1.164 g/cm^3, *F*$_{000}$ = 1936, Bruker-Nonius Roper CCD camera on goniostat, MoK$_\alpha$ radiation, λ = 0.71073 Å, *T* = 173(2)K, 2θ_{max} = 53.5°, 57148 reflections collected, 11152 unique (*R*$_{int}$ = 0.1657). Final *GooF* = 1.004, *R*1 = 0.1137, *wR*2 = 0.2936, *R* indices based on 4051 reflections with I >2sigma(I) (refinement on *F*^{2}), 625 parameters, 0 restraints. Lp and absorption corrections applied, μ = 0.082 mm^{-1}.

7) *C-P*henyl-resorcin[4]arene 13
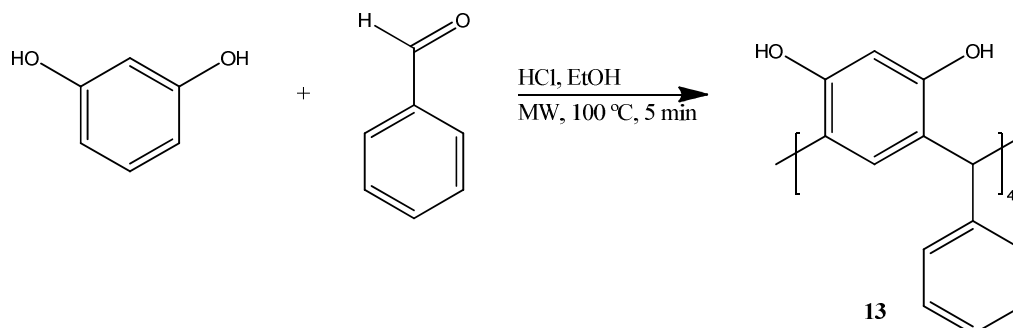
Benzaldehyde (1 eq., 4 mmol, 405 μL) was added to a solution of resorcinol (1 eq. 4 mmol, 0.440 g) in ethanol (1.5 mL) and concentrated HCl (37%, 500 μL) contained in a CEM pressure vial (10 mL). After pre-stirring (30 sec), the mixture was heated (100 ºC) by microwaves (100 W, PowerMax) for 10 min. Upon cooling to room temperature, the *rccc* product crystallised from solution, whereupon it was collected by vacuum filtration and washed with water (2 mL x 3) to obtain a orange solid (0.570 g, 7.19 x 10^{-4} mol, 72 %)

^{1}H NMR (400 MHz, d_6-DMSO) δ = 8.51 (s, 8H, OH), 6.92 (s, 4H, ArC$_1$H), 6.81 (d, ^2J=7.3 Hz, 8H, C$_{10}$H), 6.71 (d, ^2J=7.3 Hz, 8H, C$_9$H), 6.58 (m, 4H, C$_{11}$H), 6.09 (s, 4H, ArC$_4$H), 5.60 (s, 4H, C$_7$H) ppm. ^{13}C NMR (101 MHz, d_6-DMSO) δ= 152.5 145.7, 128.9, 128.6, 127.1, 126.9, 124.5, 120.6, 102.0 ppm. MALDI-TOF m/z for C$_{52}$H$_{40}$O$_8$ calcd. 792.27, found 815.27 [M+Na]$^+$.

8) *C-o*-Tolyl-resorcin[4]arene 14
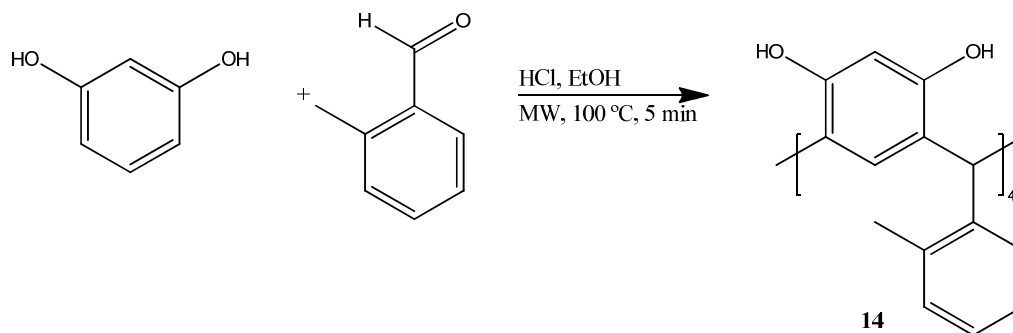
o-Tolyl-aldehyde (1 eq., 4 mmol, 368 μL) was added to a solution of resorcinol (1 eq. 4 mmol, 0.440 g) in ethanol (1.5 mL) and concentrated HCl (37%, 500 μL) contained in a CEM pressure vial (10 mL). After pre-stirring (30 sec), the mixture

was heated (100 ºC) by microwaves (100 W, PowerMax) for 10 min. Upon cooling to room temperature, the product precipitated from solution, whereupon it was collected by vacuum filtration and washed with water (2 mL x 3) to obtain a yellow brown solid (0.375 g, 4.42 x 10^{-4} mol, 44%) of which the *rccc* isomer is (50%) according to the NMR.

^{1}H NMR (400 MHz, d_6-DMSO) δ = 8.53 (s, 4 H, OH), 8.43(s, 4 H, OH), 6.80 (t, ^3J = 7.3 Hz, 4 H, AA'XX'), 6.70 (m, ^3J = 7.3 Hz, 8 H, ArCH), 6.49 (s, 4 H, ArCH), 6.30 (d, J = 6.2 Hz, 4 H ArCH, AA'XX'), 6.10 (s, 4 H, ArCH), 5.66 (s, 4 H, CH), 1.72 (s, 12 H, CH$_3$) ppm. ^{13}C NMR (101 MHz, d_6-DMSO) δ = 152.6, 152.4, 144.3, 135.2, 129.2, 124.4, 124.4, 120.5, 118.9, 18.7 ppm. MALDI-TOF *m/z* for $C_{56}H_{48}O_8$ calcd. 848.33, found 848.33 [M]$^+$.

9) *C-m*-Tolyl-resorcin[4]arene 15
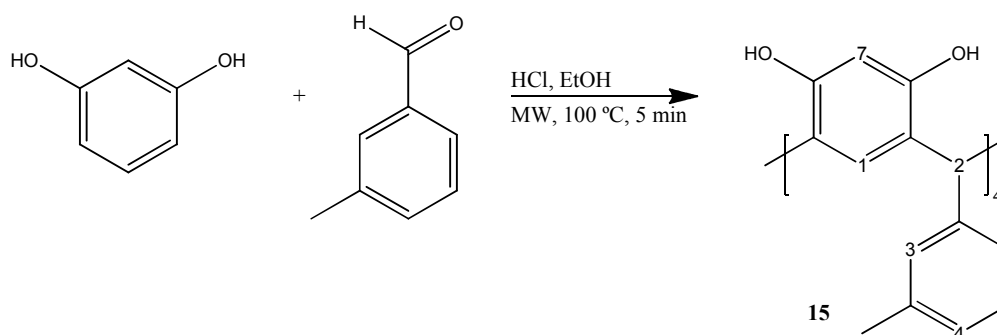
m-Tolyl-aldehyde (1 eq., 4 mmol, 471 μL) was added to a solution of resorcinol (1 eq. 4 mmol, 0.440 g) in ethanol (1.5 mL) and concentrated HCl (37%, 500 μL) contained in a CEM pressure vial (10 mL). After pre-stirring (30 sec), the mixture was heated (100 ºC) by microwaves (100 W, PowerMax) for 10 min. Upon cooling to room temperature, the *rccc* product crystallised from solution, whereupon it was collected by vacuum filtration and washed with water (2 mL x 3) to obtain a brown solid (0.794 g, 9.46 x 10^{-4} mol, 94%).

^{1}H NMR (400 MHz , CDCl$_3$) δ = 6.11 (t, ^3J = 7.4 Hz, 4 H, C$_5$H), 5.98 (d, ^3J = 7.3 Hz, 4 H, C$_6$H), 5.87 (d, ^3J = 7.4 Hz, 4 H, C$_4$H), 5.79 (s, 4 H, C$_3$H), 5.47 (s, 4 H, C$_7$H), 5.39 (s, 4 H, C$_1$H), 4.91 (s, 4 H, C$_2$H), 1.34 (s, 12 H, CH$_3$)

^{13}C NMR (101 MHz, d_6-DMSO) δ= 144.9, 143.0, 138.5, 137.0, 131.2, 129.6, 125.8, 126.1, 124.8, 124.7, 39.2, 19.6 ppm; MALDI-TOF *m/z* for $C_{56}H_{48}O_8$ calcd. 848.33, found 848.33 [M]$^+$

Preliminary crystal data for *m*-tolyl-resorcin[4]arene *rccc* DMSO solvate*:* $C_{56}H_{48}O_8.6(C_2H_6SO)$, $M =$, Yellow block, $0.65 \times 0.41 \times 0.34$, triclinic, space group $P\bar{1}$ (No. 2),), $a = 13.235(3)$, $b = 13.610(3)$, $c = 22.988(5)$ Å, $\alpha = 89.161(17)$, $\beta = 84.311(18)$, $\gamma = 72.655(18)°$, $V = 3932.7(14)$ Å^3, $Z = 4$, $D_c = 1.245$ g/cm^3, $F_{000} = 1568$, Xcalibur, Sapphire3, MoKα radiation, $\lambda = 0.71073$ Å, $T = 173(2)$K, $2\theta_{max} = 57.2°$, 32596 reflections collected, 17264 unique ($R_{int} = 0.1941$). Final *GooF* = 0.933, $R1 = 0.1699$, *wR2* = 0.4018, *R* indices based on 3893 reflections with I >2sigma(I) (refinement on F^2), 437 parameters, 0 restraints. Lp and absorption corrections applied, $\mu = 0.288$ mm^{-1}
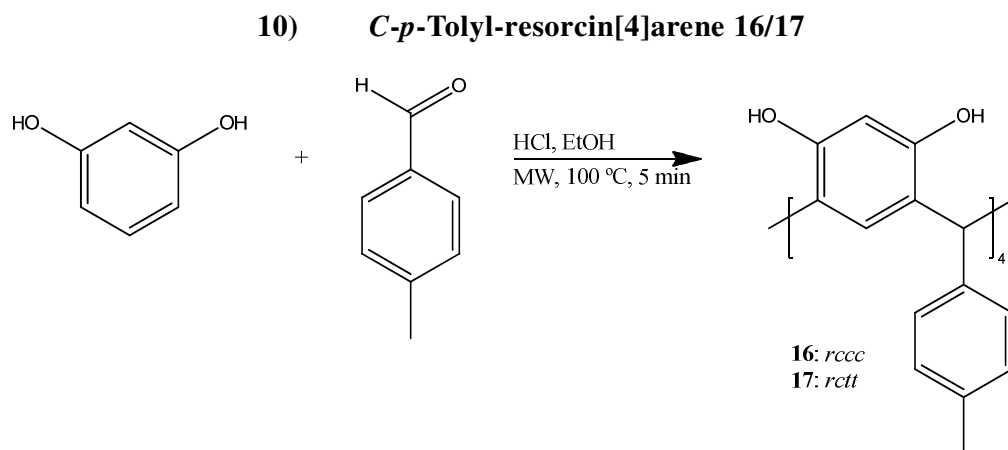
10) *C-p-Tolyl-resorcin[4]arene 16/17*

16: *rccc*
17: *rctt*

p-Tolyl-aldehyde (1 eq., 4 mmol, 472 µL) was added to a solution of resorcinol (1 eq. 4 mmol, 0.440 g) in ethanol (1.5 mL) and concentrated HCl (37%, 500 µL) contained in a CEM pressure vial (10 mL). After pre-stirring (30 sec), the mixture was heated (100 ºC) by microwaves (100 W, PowerMax) for 10 min. Upon cooling to room temperature, the *rccc* product crystallised from solution, whereupon it was collected by vacuum filtration and washed with water (2 mL x 3) to obtain a red solid (0.738 g, 8.66 x 10^{-4} mol, 87%).

^{1}H NMR (400 MHz, d_6-DMSO) δ = 5.98 (d, ^3J = 7.8 Hz, 8 H), 5.86 (d, ^3J = 7.8 Hz, 8 H), 5.46 (s, 4 H, C_7H), 5.34 (s, 4 H, C_1H), 4.96 (s, 4 H, CH), 1.49 (s, 12H, CH$_3$) ppm.
^{13}C NMR (101 MHz, d_6-DMSO) δ= 140.3, 131.9, 129.8, 127.1, 127.0, 126.3, 120.0, 46.8, 19.1 ppm; MALDI-TOF *m/z* for $C_{56}H_{48}O_8$ calcd. 848.33, found 848.33 [M]$^+$

Crystal data for *p*-tolyl-resorcin[4]arene *rccc*: $C_{56}H_{48}O_8$, $M = 848.94$, yellow fragment, $0.08 \times 0.04 \times 0.02$ mm^3, triclinic, space group $P\bar{1}$ (No. 2), $a =$

13.3943(10), b = 14.5076(10), c = 17.4518(11) Å, α = 99.329(4), β = 100.179(4), γ = 90.615(4)°, V = 3291.0(4) Å^3, Z = 2, D_c = 0.857 g/cm^3, F_{000} = 896, Bruker-Nonius APEX II CCD camera on goniostat, MoK$_\alpha$ radiation, λ = 0.71073 Å, T = 120(2)K, $2\theta_{max}$ = 53.4°, 1597107 reflections collected, 11488 unique (R_{int} = 0.1148). Final $GooF$ = 0.946, R1 = 0.1042, $wR2$ = 0.2643, R indices based on 4766 reflections with I >2sigma(I) (refinemel on F^2), 589 parameters, 0 restraints. Lp and absorption corrections applied, μ = 0.057 mm^{-1}.

Preliminary crystal data for *p*-tolyl-resorcin[4]arene acetonitrile *rctt*: $C_{56}H_{48}O_8 \cdot 4(CH_3CN)$, M = 1066.94, Yellow block, 0.16 × 0.09 × 0.02 mm^3, triclinic, space group $P\bar{1}$ (No. 2), a = 11.678(2), b = 11.836(2), c = 11.902(3) Å, α = 85.132(18), β = 62.42(2), γ = 84.296(17)°, V = 1449.6(5) Å^3, Z = 2, D_c = 1.255 g/cm^3, F_{000} = 580, Xcalibur, Sapphire3, MoK$_\alpha$ radiation, λ = 0.71073 Å, T = 173(2)K, $2\theta_{max}$ = 58.1°, 13812 reflections collected, 7763 unique (R_{int} = 0.1408). Final $GooF$ = 0.980, R1 = 0.1304, $wR2$ = 0.3258, R indices based on 1530 reflections with I >2sigma(I) (refinement on F^2), 327 parameters, 0 restraints. Lp and absorption corrections applied, μ = 0.077 mm^{-1}.

11) *C*-Thiophen-3-yl-pyrogallol[4]arene 18
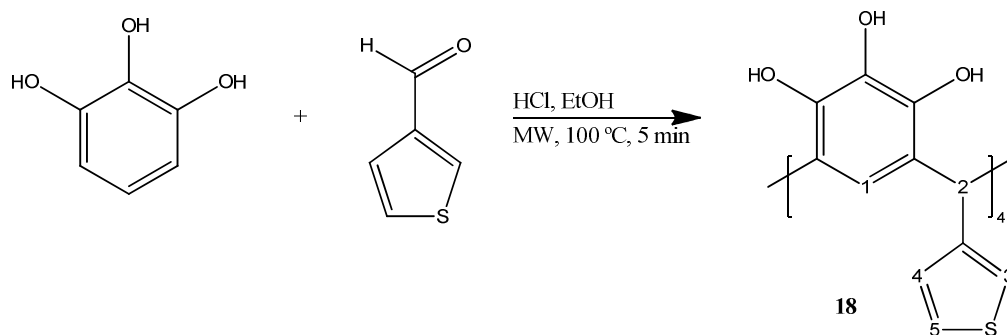
3-Thienylaldehyde (1 eq., 4 mmol, 375 µL) was added to a solution of pyrogallol (1 eq. 4 mmol, 0.504 g) in ethanol (1.5 mL) and concentrated HCl (37%, 500 µL) contained in a CEM pressure vial (10 mL). After pre-stirring (30 sec), the mixture was heated (100 °C) by microwaves (100 W, PowerMax) for 10 min. Upon cooling to room temperature, a solid precipitated from solution, whereupon it was collected by vacuum filtration and washed with water (2 mL x 3) to obtain a grey solid (0.230 g, 2.61 x 10^{-4} mol, 26%).

^{1}H NMR (400 MHz , d_6-DMSO) δ = 7.03 (dt, ^4J = 1.9, 5 Hz, 4 H, C_5H), 6.36 (dd, J = 0.8, 5.0 Hz, 4 H, C_4H), 6.24 (m, 2 H, ArC$_1$H), 5.95 (br. s, 4 H, C_3H), 5.69 (m, 4 H, C_2H), 5.36 (s, 2 H, ArC$_1$H) ppm ^{13}C NMR (101 MHz , d_6-DMSO) δ = 44.02, 120.70, 120.85, 122.07, 123.93, 128.86, 141.96, 142.33, 145.58 ppm, MALDI-TOF m/z for $C_{44}H_{32}O_{12}S_4$ calcd. 880.08, found 903.44 [M+Na]$^+$ Elemental analysis for $C_{44}H_{32}O_{12}S_4$ calcd: C, 59.99; H, 3.66; found: C, 56.27; H, 2.19.

Crystal data for C-Thiophen-3-yl-pyrogallol[4]arene: $C_{32}H_{41.50}O_{11.50}S_7$, M = 834.57, colourless block, $0.05 \times 0.07 \times 0.13$ mm^3, triclinic, space group $P\bar{1}$ (No. 2), a = 12.0585(6), b = 16.0631(8), c = 20.9249(8) Å, α = 99.314(4), β = 103.039(4), γ = 90.589(4)°, V = 3891.9(3) Å^3, Z = 4, D_c = 1.424 g/cm^3, F_{000} = 1750, Xcalibur, Sapphire3, MoK$_\alpha$ radiation, λ = 0.71073 Å, T = 173(2)K, $2\theta_{max}$ = 46.5°, 50598 reflections collected, 11169 unique (R_{int} = 0.1294). Final $GooF$ = 1.045, $R1$ = 0.1305, $wR2$ = 0.2686, R indices based on 6675 reflections with I >2sigma(I) (refinement on F^2), 954 parameters, 0 restraints. Lp and absorption corrections applied, μ = 0.462 mm^{-1}.

12)   *C*- Pyridin-2-yl-pyrogallol[4]arene 19
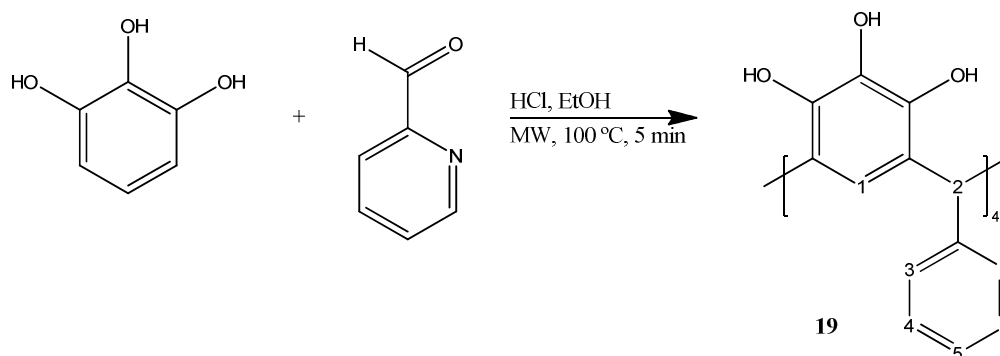
2-Pyridinecarboxaldehyde (1 eq., 4 mmol, 381 µL) was added to a solution of pyrogallol (1 eq. 4 mmol, 0.504 g) in ethanol (1.5 mL) and concentrated HCl (37%, 500 µL) contained in a CEM pressure vial (10 mL). After pre-stirring (30 sec), the mixture was heated (100 ºC) by microwaves (100 W, PowerMax) for 5 min. After which, concentrated HCl (37%, 500 µL) was added to the mixture and reacted for further 5 min. Upon cooling to room temperature, the product precipitated from solution, whereupon it was collected by vacuum filtration and washed with cold ethanol (2 mL x 3) to obtain a waxy crude solid (0.40 g).

^{1}H NMR (400 MHz, d_6-DMSO) δ = 8.88 (br. s., OH), 8.64 (m, 4 H, C$_6$H), 8.34 (m, 4 H, C$_4$H), 7.77 (m, 4 H, C$_5$H), 7.33 (m, 4 H, C$_3$H), 6.25 (m, 4 H, C$_1$H), 5.97 (m, 4 H, CH) ppm. MALDI-TOF *m/z* for C$_{48}$H$_{36}$N$_4$O$_{12}$ calcd. 860.23, found 861.02 [M+H]$^+$.

13)   *C*- Pyridin-3-yl-pyrogallol[4]arene 20
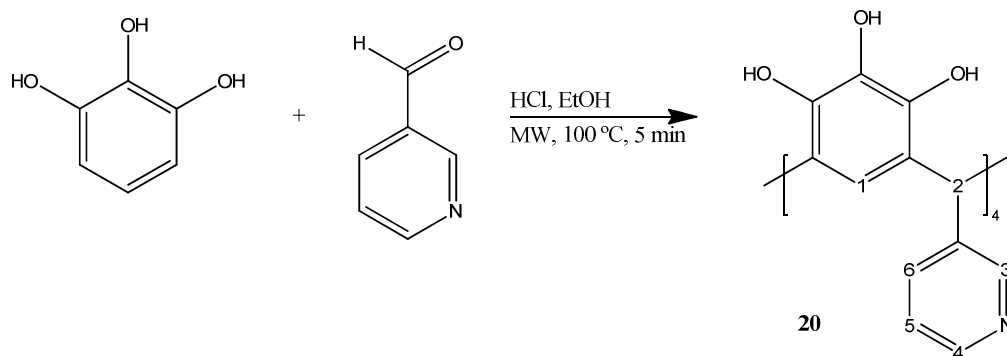
3-Pyridinecarboxaldehyde (1 eq., 4 mmol, 376 µL) was added to a solution of pyrogallol (1 eq. 4 mmol, 0.504 g) in ethanol (1.5 mL) and concentrated HCl (37%, 500 µL) contained in a CEM pressure vial (10 mL). After pre-stirring (30 sec), the mixture was heated (100 ℃) by microwaves (100 W, PowerMax) for 5 min. After which, concentrated HCl (37%, 500 µL) was added to the mixture and reacted for further 5 min. Upon cooling to room temperature, the product precipitated from solution, whereupon it was collected by vacuum filtration and washed with cold ethanol (2 mL x 3) to obtain a yellow crude solid (0.996 g).

^{1}H NMR (400 MHz, d_6-DMSO) δ = 8.71 - 8.56 (m, 4 H, C$_4$H), 8.51 - 8.22 (m, 4 H, C$_3$H), 8.06 - 7.78 (m, 8 H, C$_6$H+ C$_5$H), 6.22 (m, 4 H, C$_1$H), 5.77 - 5.51 (m, 4 H, C$_2$H) ppm. MALDI-TOF *m/z* for C$_{48}$H$_{36}$N$_4$O$_{12}$ calcd. 860.23, found 861.02 [M+H]$^+$.

14)   *C*- Pyridin-4-yl-pyrogallol[4]arene 21
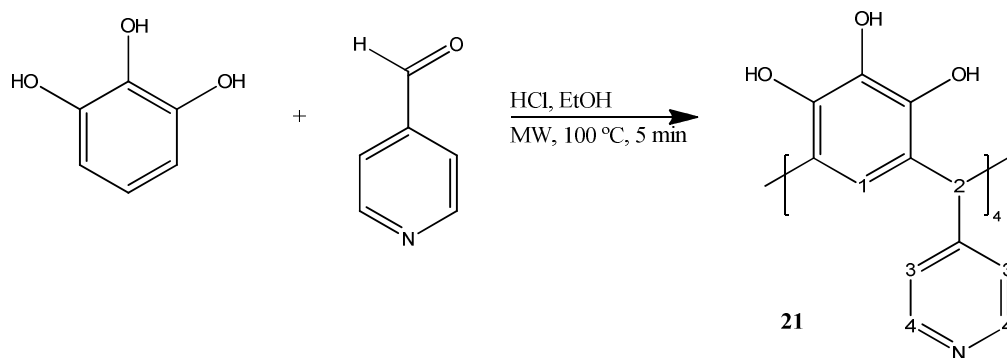
4-Pyridinecarboxaldehyde (1 eq., 4 mmol, 378 µL) was added to a solution of pyrogallol (1 eq. 4 mmol, 0.504 g) in ethanol (1.5 mL) and concentrated HCl (37%, 500 µL) contained in a CEM pressure vial (10 mL). After pre-stirring (30 sec), the mixture was heated (100 ºC) by microwaves (100 W, PowerMax) for 5 min. After which, concentrated HCl (37%, 500 µL) was added to the mixture and reacted for further 5 min. Upon cooling to room temperature, the product precipitated from solution, whereupon it was collected by vacuum filtration and washed with cold ethanol (2 mL x 3) to obtain a orange crude solid (0.948 g).

^{1}H NMR (400 MHz, d_6-DMSO) δ = 8.65 (m, 8 H, C_3H), 7.47 (m, 8 H, C_4H), 6.20 (m, 4H, C_1H), 5.85 (m, 4 H, CH) ppm. MALDI-TOF m/z for $C_{48}H_{36}N_4O_{12}$ calcd. 860.23, found 861.02 [M+H]$^+$.

15)   *C*- Pyridin-2-yl-resorcin[4]arene 22
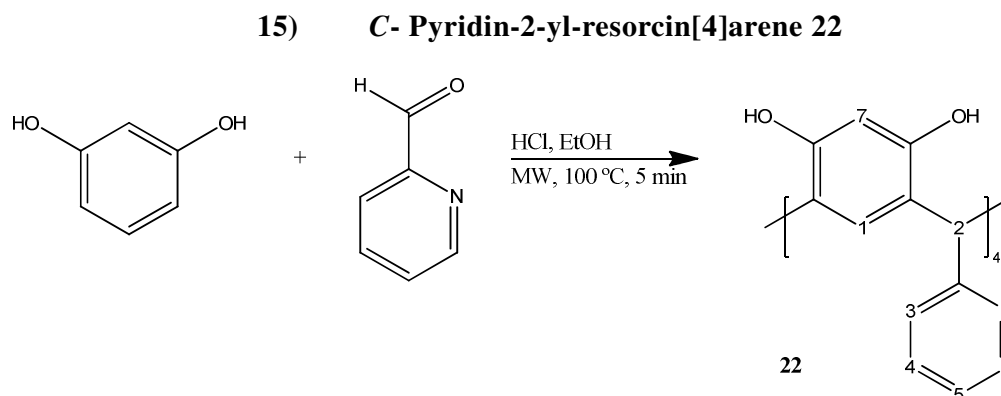
2-Pyridinecarboxaldehyde Pyridin-2-yl aldehyde (1 eq., 4 mmol, 381 µL) was added to a solution of resorcinol (1 eq. 4 mmol, 0.440 g) in ethanol (1.5 mL) and concentrated HCl (37%, 500 µL) contained in a CEM pressure vial (10 mL). After pre-stirring (30 sec), the mixture was heated (100 ºC) by microwaves (100 W, PowerMax) for 5 min. After which, concentrated HCl (37%, 500 µL) was added to the mixture and reacted for further 5 min. Upon cooling to room temperature, the product precipitated from solution, whereupon it was collected by vacuum filtration and washed with cold ethanol (2 mL x 3) to obtain a crude yellow solid (0.652 g).

^{1}H NMR (400 MHz, d_6-DMSO) δ = 8.73 - 8.51 (m, 4 H, C_6H), 8.49 - 8.26 (m, 4 H, C_4H), 7.88 - 7.66 (m, 4 H, C_5H), 7.63 - 7.38 (m, 4 H, C_2H), 6.67 - 6.37 (m, 4 H, C_1H), 5.95 - 5.66 (m, 4 H, CH) ppm. MALDI-TOF m/z for $C_{48}H_{36}N_4O_8$ calcd. 796.25, found 797.04 [M+H]$^+$

16)   *C*- Pyridin-3-yl-resorcin[4]arene 23
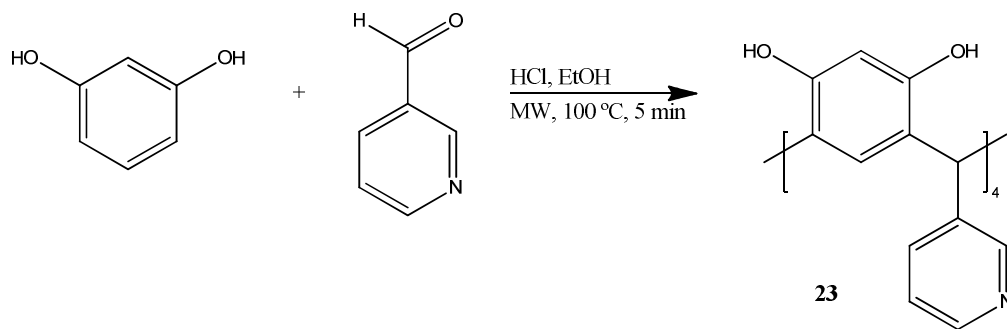
3-Pyridinecarboxaldehyde (1 eq., 4 mmol, 376 µL) was added to a solution of resorcinol (1 eq. 4 mmol, 0.440 g) in ethanol (1.5 mL) and concentrated HCl (37%, 500 µL) contained in a CEM pressure vial (10 mL). After pre-stirring (30 sec), the mixture was heated (100 ºC) by microwaves (100 W, PowerMax) for 5 min. After which, concentrated HCl (37%, 500 µL) was added to the mixture and reacted for further 5 min. Upon cooling to room temperature, the product precipitated from solution, whereupon it was collected by vacuum filtration and washed with cold ethanol (2 mL x 3) to obtain a crude yellow solid (0.884 g).

^{1}H NMR (400 MHz, d_6-DMSO) δ = 9.76 (m, OH), 8.66 (m, 4 H, C_4H), 8.39 (m, 4 H, C_3H), 7.81 (m, 4 H C_6H), 7.53 (m, 4 H, C_5H), 6.60 - 6.30 (m, 8 H, C_1H + C_7H), 5.81 - 5.75 (m, 4 H, CH) ppm. MALDI-TOF *m/z* for $C_{48}H_{36}N_4O_8$ calcd. 796.25, found 797.32 [M+H]$^+$.

17)   *C*- Pyridin-4-yl-resorcin[4]arene 24
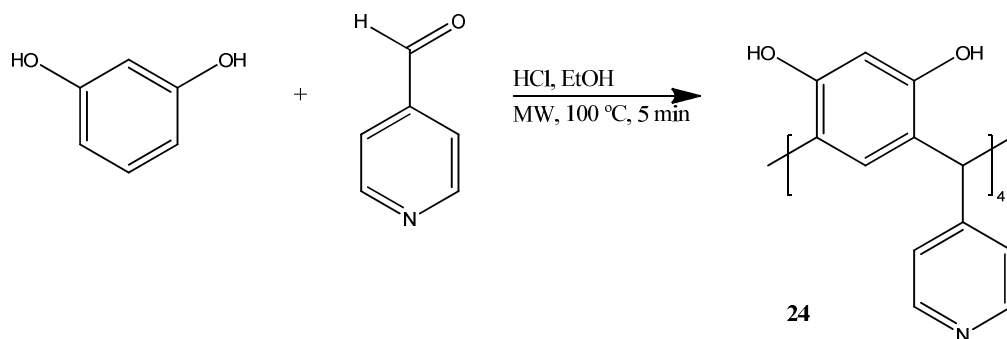
4-Pyridinecarboxaldehyde (1 eq., 4 mmol, 378 µL) was added to a solution of resorcinol (1 eq. 4 mmol, 0.504 g) in ethanol (1.5 mL) and concentrated HCl (37%, 500 µL) contained in a CEM pressure vial (10 mL). After pre-stirring (30 sec), the mixture was heated (100 ºC) by microwaves (100 W, PowerMax) for 5 min. After

which, concentrated HCl (37%, 500 µL) was added to the mixture and reacted for further 5 min. Upon cooling to room temperature, the product precipitated from solution, whereupon it was collected by vacuum filtration and washed with cold ethanol (2 mL x 3) obtain a beige crude solid (0.884 g).

^{1}H NMR (400 MHz, d_6-DMSO) δ = 9.56 (br. s., 8H, OH), 8.72 (m, 8 H, C$_3$H), 7.49 (m, 8 H, C$_4$H), 6.59 (m, 4 H, C$_7$H), 6.21 - 6.10 (m, 4 H, C$_1$H), 5.56 (m, 4 H, CH) ppm. MALDI-TOF m/z for C$_{48}$H$_{36}$N$_4$O$_8$ calcd. 796.25, found 797.02 [M+H]$^+$.

C. CHAPTER III

18)   *C*-3-Hydroxpropyl-pyrogallol[4]arene 25
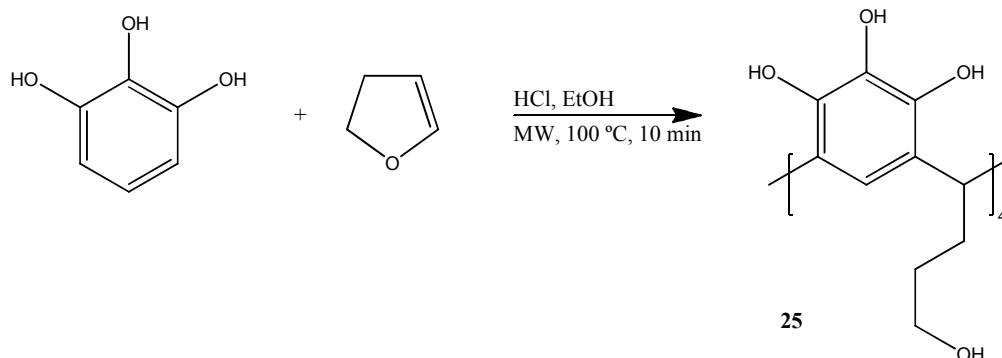
2,3-Dihydro-pyran (1.0 eq., 4 mmol, 302 µL) was added to a solution of pyrogallol (1 eq. 4 mmol, 0.504 g) in ethanol (1.5 mL) and concentrated HCl (37%, 500 µL) contained in a CEM pressure vial (10 mL). After pre-stirring (30 sec), the mixture was heated (100 ºC) by microwaves (100 W, PowerMax) for 10 min. Upon cooling to room temperature, the product crystallised from solution, whereupon it was collected by vacuum filtration and washed with cold ethanol to obtain a pink crystalline solid (0.277g, 0.33 mmol, 33%).

^{1}H NMR (400 MHz, d_6-DMSO) δ = 6.87 (s, 4H, ArC$_1$H), 4.13 (t, ^3J=7.8 Hz, 4H, C$_7$H), 2.15 (m, 8H, C$_{11}$H$_2$), 1.44 (m, 8H, C$_{10}$H$_2$), 1.18 (m, 8H, C$_9$H$_2$) ppm. ^{13}C NMR (101 MHz, d_6-DMSO) δ = 139.5, 132.9, 124.5, 113.5, 61.0, 33.7, 32.6, 29.2 ppm. MALDI-TOF m/z for C$_{40}$H$_{48}$O$_{16}$ calcd. 784.29, found 807.32 [M+Na]$^+$. IR (ν ATR): 3250, 2926, 1689, 1609, 1457, 1284, 1197, 1094, 1031, 972, 506 cm^{-1}.

Crystal data for *C*-3-hydroxpropyl-pyrogallol[4]arene ethanol hydrochloride: $2(C_{40}H_{48}O_{16})$ $2(C_2H_6O)$ $CH4O$ $2(Cl)$, $M = 1760.61$, colourless, block, $0.49 \times 0.29 \times 0.12$ mm^3, monoclinic, space group $P2_1/c$ (No. 14), $a = 10.3676(10)$, $b = 18.003(2)$, $c = 22.7013(17)$ Å, $\beta = 91.344(9)°$, $V = 4236.1(7)$ Å^3, $Z = 2$, $D_c = 1.380$ g/cm^3, $F_{000} = 1864$, Xcalibur, Sapphire3, Mo Kα radiation, $\lambda = 0.7107$ Å, $T = 173(2)$K, $2\theta_{max} = 57.5°$, 22931 reflections collected, 9719 unique ($R_{int} = 0.0676$). Final *GooF* = 1.093, *R*1 = 0.1113, *wR*2 = 0.3191, *R* indices based on 4975 reflections with I >2sigma(I) (refinement on F^2), 579 parameters, 0 restraints. Lp and absorption corrections applied, $\mu = 0.167$ mm^{-1}.

Crystal data for *C*-3-hydroxpropyl-pyrogallol[4]arene ethanol hydrate: $(C_{40}H_{48}O_{16})$ (C_2H_6O) H_2O, $M = 848.87$, colourless, block, $0.30 \times 0.22 \times 0.17$ mm^3, triclinic, space group $P\bar{1}$ (No. 2), $a = 12.1034(11)$, $b = 13.3287(8)$, $c = 14.0589(12)$ Å, $\alpha = 85.637(6)$, $\beta = 65.052(9)$, $\gamma = 79.177(6)°$, $V = 2019.8(3)$ Å^3, $Z = 2$, $D_c = 1.396$ g/cm^3, $F_{000} = 904$, Xcalibur, Sapphire3, Mo Kα radiation, $\lambda = 0.7107$ Å, $T = 173(2)$K, $2\theta_{max} = 57.7°$, 19654 reflections collected, 10609 unique ($R_{int} = 0.0603$). Final *GooF* = 0.843, *R*1 = 0.0616, *wR*2 = 0.1153, *R* indices based on 3113 reflections with I >2sigma(I) (refinement on F^2), 567 parameters, 0 restraints. Lp and absorption corrections applied, $\mu = 0.109$ mm^{-1}.

Crystal data for *C*-3-hydroxpropyl-pyrogallol[4]arene Acetone Water: $(C_{40}H_{48}O_{16})$ $2(C_3H_6O)$ H_2O, $M = 882.86$, colourless cubic, $0.15 \times 0.13 \times 0.06$ mm^3, triclinic, space group $P\bar{1}$ (No. 2), $a = 9.0689(5)$, $b = 12.1833(6)$, $c = 20.4988(10)$ Å, $\alpha = 91.570(4)$, $\beta = 92.234(4)$, $\gamma = 101.876(4)°$, $V = 2213.3(2)$ Å^3, $Z = 2$, $D_c = 1.325$ g/cm^3, $F_{000} = 936$, Xcalibur, Sapphire3, MoK$_\alpha$ radiation, $\lambda = 0.71073$ Å, $T = 150(2)$K, $2\theta_{max} = 50.0°$, 14427 reflections collected, 7751 unique ($R_{int} = 0.0446$). Final *GooF* = 0.959, *R*1 = 0.0727, *wR*2 = 0.1973, *R* indices based on 3795 reflections with I >2sigma(I) (refinement on F^2), 583 parameters, 0 restraints. Lp and absorption corrections applied, $\mu = 0.105$ mm^{-1}.

19)   *C*-3-Hydroxybutyl-pyrogallol[4]arene 26

26
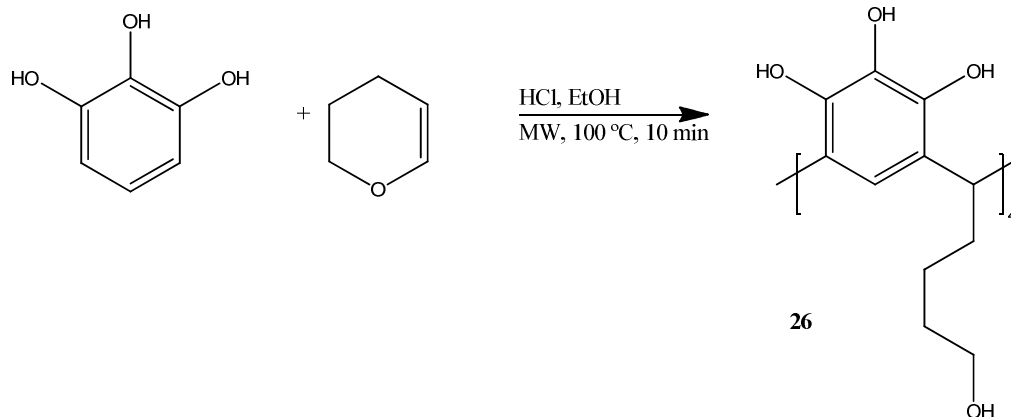
3,4-Dihydro-2H-pyran (1.0 eq., 4 mmol, 365 µL) was added to a solution of pyrogallol (1 eq. 4 mmol, 0.504 g) in ethanol (1.5 mL) and concentrated HCl (37%, 500 µL) contained in a CEM pressure vial (10 mL). After pre-stirring (30 sec), the mixture was heated (100 ºC) by microwaves (100 W, PowerMax) for 10 min. Upon cooling to room temperature, the product crystallised from solution, whereupon it was collected by vacuum filtration and washed with cold ethanol to obtain a pink crystalline solid (0.268 g, 0.32 mmol, 32%).

^{1}H NMR (400 MHz, d_6-DMSO) δ = 8.64 (s, 8H, OH), 8.08 (s, 4H, OH), 6.89 (s, 4H, ArC$_I$H), 4.13 (t, ^3J= 7.8 Hz, 4H, C$_7$H), 3.35 (m, 8H, C$_{11}$H$_2$), 2.14 (m, 8H, C$_{10}$H$_2$), 1.44 (m, 8H, C$_8$H$_2$), 1.18 (m, 8H, C$_9$H$_2$) ppm. ^{13}C NMR (101 MHz, d_6-DMSO) δ =139.5, 132.8 124.5, 113.5, 61.0, 33.7, 32.6, 30.7, 24.3 ppm. MALDI-TOF *m/z* for C$_{44}$H$_{56}$O$_{16}$ calcd. 840.36, found 840.91 [M]$^+$.

Crystal data for *C*-4-hydroxybutyl-pyrogallol[4]arene **26** acetone clathrate: (C$_{44}$H$_{56}$O$_{16}$) (C$_3$H$_6$O), *M* = 898.97, colourless rod, 0.10 × 0.02 × 0.02 mm^3, triclinic, space group *P*Ī (No. 2), *a* = 18.13(2), *b* = 18.45(2), *c* = 23.83(4) Å, *α* = 108.74(2), *β* = 107.06(2), *γ* = 100.91(2)°, *V* = 6853(16) Å^3, *Z* = 6, *D*$_c$ = 1.307 g/cm^3, *F*$_{000}$ = 2880, Bruker SMART APEX2 CCD diffractometer, synchrotron radiation, λ = 0.6939 Å, *T* = 120(2)K, 2θ_{max} = 48.8°, 50280 reflections collected, 24034 unique (*R*$_{int}$ = 0.0942). Final *GooF* = 1.007, *R*1 = 0.0865, *wR*2 = 0.2264, *R* indices based on 10912 reflections with I >2sigma(I) (refinement on *F*^{2}), 1779 parameters, 9 restraints. Lp and absorption corrections applied, μ = 0.099 mm^{-1}.

Crystal data for *C*-4-hydroxybutyl-pyrogallol[4]arene **26** acetonitrile acetone solvate: $(C_{44}H_{56}O_{16})$ 2(CH_3CN) (C_3H_6O), M = 1004.06, colourless block, $0.30 \times 0.18 \times 0.1$ mm^3, monoclinic, space group $P2_1/m$ (No. 11), a = 9.6489(3), b = 18.2583(9), c = 14.4414(4) Å, β = 104.706(2)°, V = 2460.83(16) Å^3, Z = 2, D_c = 1.355 g/cm^3, F_{000} = 1070, Bruker-Nonius Roper CCD camera on goniostat, MoK radiation radiation, λ = 0.71073 Å, T = 120K, $2\theta_{max}$ = 53.0°, 27400 reflections collected, 5244 unique (R_{int} = 0.0764). Final *GooF* = 1.026, $R1$ = 0.0864, $wR2$ = 0.2232, R indices based on 3147 reflections with I >2sigma(I) (refinement on F^2), 364 parameters, 0 restraints. Lp and absorption corrections applied, μ = 0.109 mm^{-1}.

Crystal data for *C*-4-hydroxybutyl-pyrogallol[4]arene **26** acetonitrile hydrate: 2($C_{44}H_{56}O_{16}$) 2(CH_3CN) H_2O, M = 1797.90, colourless block, $0.30 \times 0.30 \times 0.30$ mm^3, orthorhombic, space group $Pna2_1$ (No. 33), a = 18.875(4), b = 15.211(3), c = 14.964(3) Å, V = 4296.3(15) Å^3, Z = 2, D_c = 1.390 g/cm^3, F_{000} = 1916, Bruker SMART APEX2 CCD diffractometer, Synchrotron radiation, λ = 0.6939 Å, T = 120(2)K, $2\theta_{max}$ = 53.0°, 27665 reflections collected, 8675 unique (R_{int} = 0.0628). Final *GooF* = 1.051, $R1$ = 0.0620, $wR2$ = 0.1736, R indices based on 8269 reflections with I >2sigma(I) (refinement on F^2), 625 parameters, 5 restraints. Lp and absorption corrections applied, μ = 0.106 mm^{-1}.

20) Zinc complex: C-3-hydroxypropyl-pyrogallol[4]arene bis(pyridyl) zinc (II) dimer 28
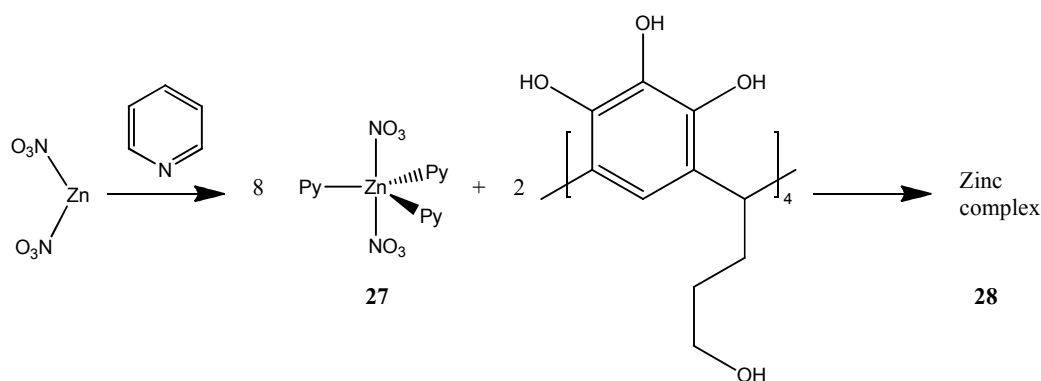
Zinc nitrate hexahydrate (1 eq., 21 mmol, 6.4 g) was dissolved in pyridine dried over potassium hydroxide pellets (3.6 eq., 77 mmol, 6 mL), the reaction mixture was heated at 60 ºC for 30 min and left to cool at room temperature, upon evaporation

the zinc pyridine complex (Zn(NO$_3$)$_2$Py$_3$) **27** crystallised in near quantitative yield. The zinc pyridine (4.1 eq., 2.62 mmol, 1.121 g) was added to *C*-hydroxypropyl-pyrogallol[4]arene **25** (1 eq., 6.41 x 10^{-4} mol, 0.500 g) in methanol (2 mL). The solution was heated until dissolution and was left to evaporate. After a week, crystals suitable for X-ray crystallography were obtained.

Crystal data for squeezed C-3-hydroxypropyl-pyrogallol[4]arene bis(pyridyl) zinc (II) dimer: 2(C$_{40}$H$_{36}$O$_{16}$) 9(C$_5$H$_5$N) 8(Zn) C$_2$H$_4$, *M* = 2773.18, 0.04 × 0.08 × 0.10 mm^3, yellow block, monoclinic, space group *P*2$_1$/*c* (No. 14), *a* = 17.0144(6), *b* = 29.7554(10), *c* = 31.9759(11) Å, *β* = 119.910(3)°, *V* = 14032.3(8) Å^3, *Z* = 4, *D*$_c$ = 1.313 g/cm^3, *F*$_{000}$ = 5676, Xcalibur, Sapphire3, MoK$_\alpha$ radiation, λ = 0.71073 Å, *T* = 173(2)K, 2θ_{max} = 55.5º, 126244 reflections collected, 30515 unique (*R*$_{int}$ = 0.0971). Final *GooF* = 1.377, *R*1 = 0.1277, *wR*2 = 0.2805, *R* indices based on 16373 reflections with I >2sigma(I) (refinement on *F*^{2}), 1578 parameters, 4 restraints. Lp and absorption corrections applied, *μ* = 1.414 mm^{-1}.

21)   2-((1,3-Dioxolan-2-yl)methyl)isoindoline-1,3-dionyl-pyrogallol[4]arene 30
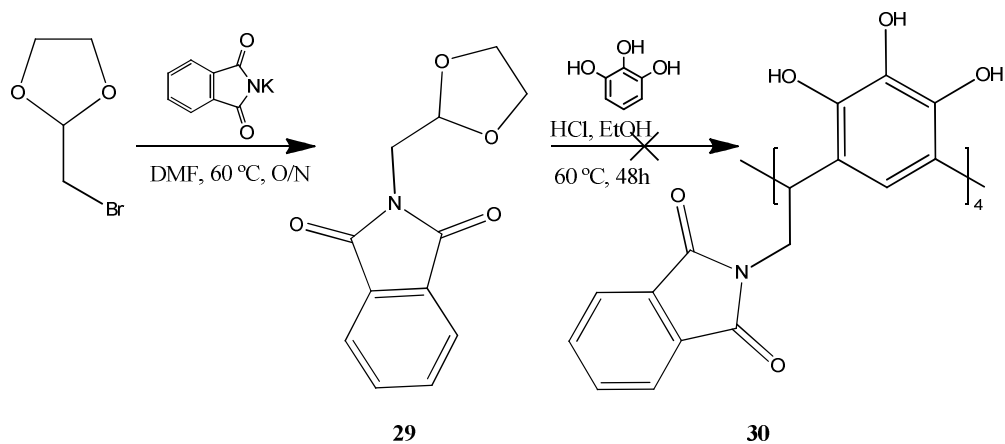
A mixture of potassium phthalimide (1.5 eq., 14.48 mmol, 2.68g) and 2-(2-bromoethyl)-1,3-dioxolane (1.0 eq., 9.6 mmol, 1 mL) was stirred in DMF (20 mL) at 60°C overnight. Water (100 mL) was added and the reaction mixture was extracted with chloroform (3x75 mL). The combined organic phases were washed with water (100 mL), dried over magnesium sulphate and evaporated under vacuum. The resulting crystals (1.01 g, 4.3 mmol, 31%) were dried under vacuum.

The crude 2-(2-(1,3-dioxolan-2-yl)ethyl)isoindoline-1,3-dione was dissolved in ethanol (1 mL) and added to a solution of pyrogallol (1 eq., 4.3 mmol, 0.542g) in ethanol (500 µL) and concentrated HCl (37%, 500 µL). The reaction mixture was stirred at room temperature (2 hours) and then heated for 5 days (65 ºC). The product could not be identified or isolated.

22)   2-(2-(1,3-Dioxolan-2-yl)ethyl)isoindoline-1,3-dionyl-pyrogallol[4]arene 32
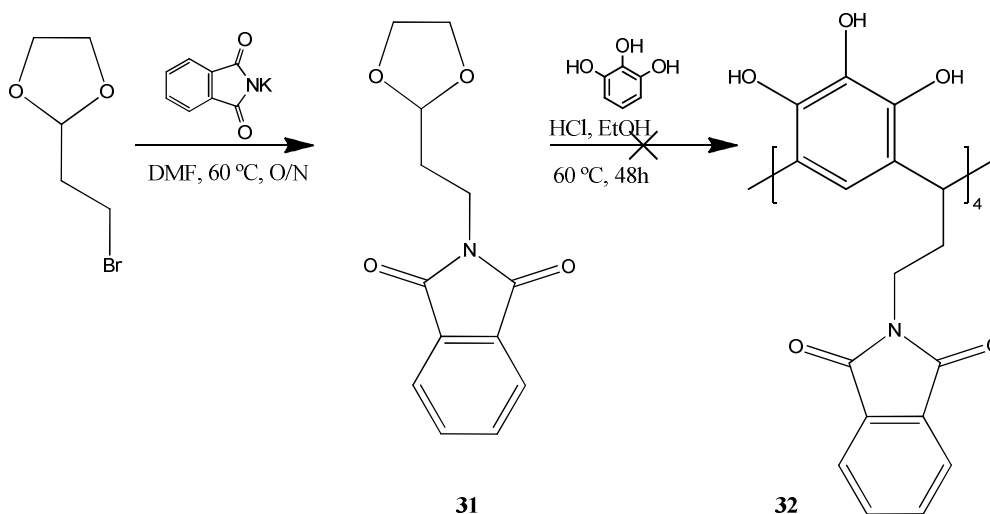
A mixture of potassium phthalimide (1.2 eq., 12 mmol, 2.23 g) and 3-(3-bromopropyl)-1,3-dioxolane (1.0 eq., 10 mmol, 1.20 mL) was stirred in DMF (20 mL) at 60°C overnight. Water (100 mL) was added and the reaction mixture was extracted with chloroform (3 x 75 mL). The combined organic phases were washed with water (100 mL), dried over magnesium sulphate and evaporated under vacuum. The resulting crystals (2.81 g, 11.3 mmol, 94%) were dried under vacuum and used without further purification.

The crude 2-(2-(1,3-dioxolan-2-yl)ethyl)isoindoline-1,3-dione was dissolved in ethanol (1 mL) and added to a solution of pyrogallol (1 eq., 4.3 mmol, 0.542g) in ethanol (500 µL) and concentrated HCl (37%, 500 µL). The reaction mixture was stirred at room temperature (2 hours) and then heated for 5 days (65 ºC). The product could not be identified or isolated.

23)   Bis((9H-fluoren-9-yl)methyl)2,2'-(4,5,6-trihydroxy-1,3-phenylene)dipyrrolidine-1-carboxylate 34
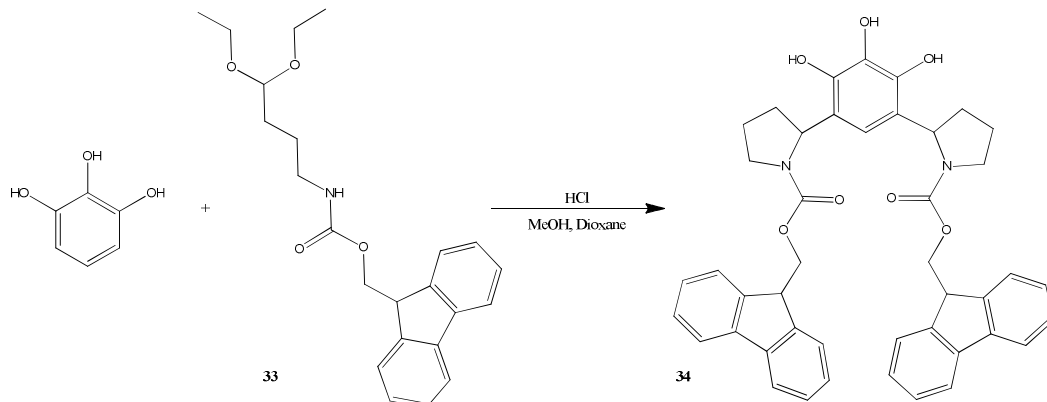
Under nitrogen, to a solution 9-fluorenylmethyl chloroformate (1.0 eq., 5.78 mmol, 1.5 g) in THF (25 mL) was added 4-aminobutyraldehyde diethyl acetal (1.0 eq., 5.78 mmol, 1 mL) and *N,N*-diisopropylethylamine (1.0 eq., 5.78 mmol, 1 mL). The solution was stirred at room temperature for 12 hours, water (150 mL) was then added and the mixture was extracted with diethyl ether (3 x 50 mL). The combined organic phases were washed with water (100 mL), dried over magnesium sulphate and evaporated. The resulting oil was purified by flash chromatography (1 EtOAc/ 1 Hex R_f = 0.62) to obtain 0.98g (2.5 mmol, 44 %) of pure (9H-fluoren-9-yl)methyl (4,4-diethoxybutyl)carbamate.

^{1}H NMR (400 MHz, d_6-DMSO) δ = 7.88 (d, ^3J =7.4 Hz, 2 H), 7.68 (d, ^3J =7.4 Hz, 2 H), 7.42 (t, ^3J =7.4 Hz, 2 H), 7.30 (d, ^3J =7.4 Hz, 2 H), 4.33 (t, ^3J =5.7 Hz, 1 H), 4.28 (d, ^3J = 7 Hz, 1 H, CHFmoc), 3.59 (m, 8 H, CH$_2$), 2.96 (m, 4 H), 1.08 (t, J = 7.0 Hz, 6 H, CH$_3$) ppm. ^{13}C NMR (101 MHz, d_6-DMSO) δ =156.1, 143.9, 140.7, 127.6, 127.1, 126.6, 125.1, 101.9, 65.1, 64.5, 46.7, 30.6, 24.7, 15.30 ppm.

Under nitrogen, to a solution of (9H-fluoren-9-yl)methyl (4,4-diethoxybutyl)carbamate (1 eq., 2.77 mmol, 1.09 g) in ethanol (5 mL) was added dropwise over 30 min a solution of pyrogallol (1 eq., 2.77 mmol, 0.35 g) in a 25% HCl ethanolic mixture. The reaction mixture was stirred at room temperature overnight and then heated at 40°C for 4 hours. Upon cooling, the resulting precipitate was filtered, washed with ice-cold ethanol and crystallised from acetonitrile/water to yield to yellow needles (0.25 g, 0.3 mmol, 13 %).

Crystal data for bis((9H-fluoren-9-yl)methyl)2,2'-(4,5,6-trihydroxy-1,3-phenylene)dipyrrolidine-1-carboxylate: $C_{44}H_{40}N_2O_7$, M = 708.78, colourless block, 0.56 × 0.38 × 0.18 mm^3, triclinic, space group $P2_1$ (No. 4), a = 8.4426(4), b = 17.5344(8), c = 12.6136(6) Å, α = 90.00, β = 104.534(3), γ = 90.00°, V = 1807.51(15) Å^3, Z = 2, D_c = 1.302 g/cm^3, F_{000} = 748, Bruker-Nonius Roper CCD camera on goniostat, MoK$_\alpha$ radiation, λ = 0.71073 Å, T = 120(2)K, $2\theta_{max}$ = 52.0°, 18915reflections collected, 6940 unique (R_{int} = 0.03447). Final $GooF$ = 1.083, $R1$ = 0.1349, $wR2$ = 0.3500, R indices based on 6330 reflections with I >2sigma(I) (refinement on F^2), 482 parameters, 1 restraints. Lp and absorption corrections applied, μ = 0.088 mm^{-1}.

24)   *C*-3-Aminopropyl-pyrogallol[4]arene 35
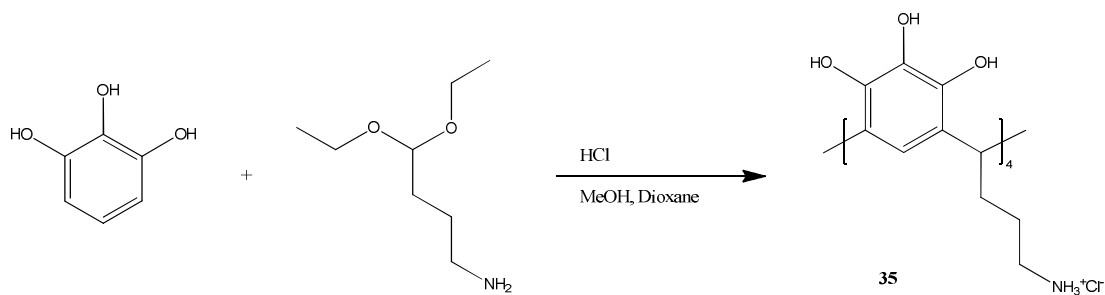
4-Aminobutyraldehyde diethyl acetal (1.0 eq., 4 mmol, 711 µL) was added to a solution of pyrogallol (1 eq. 4 mmol, 0.504 g) in dioxane (2.4 mL) contained in a CEM pressure vial (10 mL). Concentrated HCl (37%, 0.6 mL) was then added. After pre-stirring (30 sec), the mixture was heated (100 ºC) by microwaves (100 W, PowerMax) for a given time (10 min). Upon cooling to room temperature, the waxy solid formed was was collected by vacuum filtration and washed with cold dioxane (2 mL). The resulting solid was then heated in methanol (5 mL) for 2 hours, yielding in pink crystals that were collected by vacuum filtration (76 mg, 0.1 mmol, 10%).

^{1}H NMR (400 MHz, d_6-DMSO) δ = 8.62 (s, OH), 8.06 (s, OH), 6.92 (s, 4H, ArC$_l$H), 4.16 (t, ^3J =19.33 Hz, 4H, C$_7$H), 2.82 (t, ^3J =17.32 Hz, 8H, C$_{10}$H$_2$), 2.32 (m, 8H, C$_8$H$_2$), 1.47 (m, 8H, C$_9$H$_3$) ppm. ^{13}C NMR (101 MHz, d_6-DMSO) δ = 139.8, 132.9, 123.9, 113.6, 33.9, 30.3, 26.0 ppm. MALDI-TOF m/z for $C_{40}H_{52}N_4O_{12}$ calcd: 780.36 found: 781.11 [M+H]$^+$; 803 [M+Na]$^+$.

Crystal data for *C*-3-aminopropyl-pyrogallol[4]arene **35** hydrochloride salt: $2(C_{44}H_{56}Cl_4N_4O_{12})$ 2(Cl) 2O, pink block, M = 2244.65m $0.32 \times 0.24 \times 0.18$ mm^3, triclinic, space group $P\bar{1}$ (No. 2), a = 13.652(3), b = 13.737(3), c = 17.278(4) Å, α = 90.87(3), β = 109.05(3), γ = 109.85(3)°, V = 2851.8(14) Å^3, Z = 1, D_c = 1.3207 g/cm^3, F_{000} = 1188, Xcalibur, Atlas, Gemini ultra, Cu Kα radiation, λ = 1.5418 Å, T = 173(2)K, $2\theta_{max}$ = 156.9, 17293 reflections collected, 12242 unique (R_{int} = 0.0240). Final *GooF* = 1.075, *R*1 = 0.0781, *wR*2 = 0.2426, *R* indices based on 7731 reflections with I >2sigma(I) (refinement on F^2), 713 parameters, 3 restraints. Lp and absorption corrections applied, μ = 0.280 mm^{-1}.

25) **C-3-Aminopropyl-resorcin[4]arene 36**
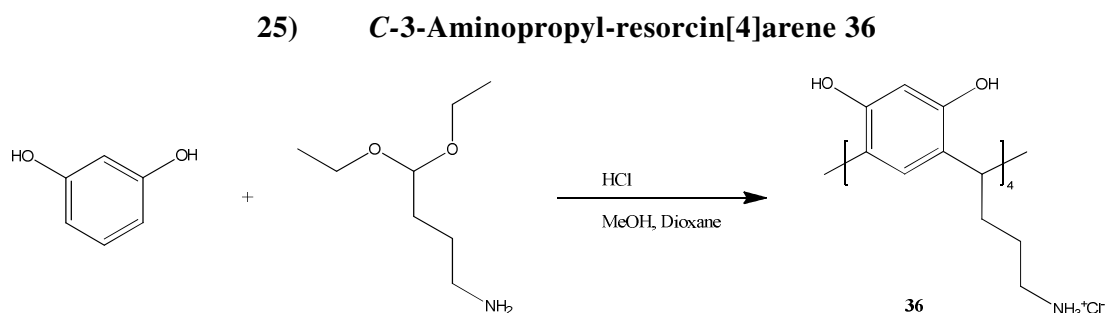
Under nitrogen, resorcinol (1.0 eq., 25 mmol, 2.75 g) was dissolved in ethanol (15 mL) and stirred for 30 min and hydrochloric acid (37%, 3.75 mL) was added. After 30 min stirring, 4-aminobutyraldehyde diethyl acetal (1.0 eq., 25 mmol, 4.32 mL) was added dropwise over one hour. The reaction mixture was stirred at room temperature for 2 hours, at 45°C for 15 hours and 60°C for 12 hours. The yellow solid formed upon cooling was collected by vacuum filtration and recrystallised from methanol (5 mL) to yield to a yellow powder (1.16 g, 1.6 mmol, 26 %).

^{1}H NMR (400 MHz, d_6-DMSO) δ = 6.82 (s, 4H, ArC$_1$H), 6.18 (s, 4H, ArC$_4$H), 4.22 (t, ^3J =7.8 Hz, 4H, C$_7$H), 2.88 (t, ^3J =7.8 Hz, 8H, C$_{10}$H$_2$), 1.93 (q, ^3J = 19.08 Hz, 8H, C$_8$H$_2$), 1.49 (m, 8H, C$_9$H$_3$) ^{13}C NMR (101 MHz, D$_2$O) δ: 151.9, 125.9, 123.5, 102.9, 48.9, 39.4, 33.7, 31.1, 25.1 ppm. MALDI-TOF *m/z* for $C_{40}H_{52}N_4O_8$ calcd. 716.86, found 738.91 [*M*+Na]$^+$.

Crystal data for *C*-3-aminopropyl-resorcin[4]arene **36** hydrochoride salt: $(C_{40}H_{56}N_4O_8)$ 5(Cl) (CH_4O), $M = 930.18$, colourless plate, $0.18 \times 0.15 \times 0.03$ mm^3, triclinic, space group $P\bar{1}$ (No. 2), $a = 12.4545(2)$, $b = 14.9875(3)$, $c = 16.6760(3)$ Å, $\alpha = 105.6440(10)$, $\beta = 99.7590(10)$, $\gamma = 105.2270(10)°$, $V = 2793.80(9)$ Å^3, $Z = 3$, $D_c = 1.106$ g/cm^3, $F_{000} = 982$, Bruker-Nonius APEX II CCD camera on goniostat , MoK$_\alpha$ radiation, $\lambda = 0.71073$ Å, $T = 120(2)$K, $2\theta_{max} = 55.3°$, 55916 reflections collected, 12668 unique ($R_{int} = 0.0568$). Final *GooF* $= 1.052$, $R1 = 0.0970$, $wR2 = 0.2508$, *R* indices based on 9082 reflections with I >2sigma(I) (refinement on F^2), 562 parameters, 0 restraints. Lp and absorption corrections applied, $\mu = 0.306$ mm^{-1}.

Crystal data for *C*-3-aminopropyl-resorcin[4]arene **36** hydrochloride salt: $C_{40}H_{56}O_{8.20}N_4Cl_{3.70}$, $M = 855.25$, colourless fragment, $0.20 \times 0.15 \times 0.10$ mm^3, triclinic, space group $P\bar{1}$ (No. 2), $a = 15.6853(2)$, $b = 18.1004(3)$, $c = 21.7168(4)$ Å, $\alpha = 65.4010(10)$, $\beta = 74.2660(10)$, $\gamma = 65.5410(10)°$, $V = 5066.45(14)$ Å^3, $Z = 4$, $D_c = 1.121$ g/cm^3, $F_{000} = 1810$, Bruker-Nonius Roper CCD camera on goniostat, MoK$_\alpha$ radiation, $\lambda = 0.71073$ Å, $T = 120(2)$K, $2\theta_{max} = 50.0°$, 100168 reflections collected, 17814 unique ($R_{int} = 0.0891$) Final *GooF* $= 1.046$, $R1 = 0.0842$, $wR2 = 0.2083$, *R* indices based on 12634 reflections with I >2sigma(I) (refinement on F^2), 1057 parameters, 0 restraints. Lp and absorption corrections applied, $\mu = 0.264$ mm^{-1}.

26)   *C*-4-Hydroxybutyl-dodecacetyloxypyrogallol[4]arene 37
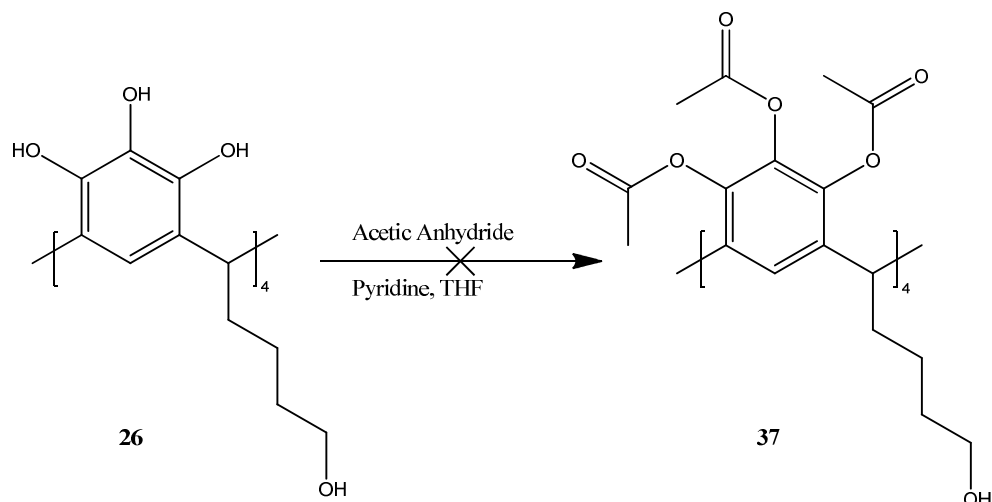
To a solution of *C*-hydroxybutyl-pyrogallol[4]arene **26** (1 eq., 2.5 x 10^{-4} mol, 0.210 g) in THF (1.25 mL) contained in a CEM pressure vial (10 mL), acetic anhydride (13.1 eq., 3.2 mmol, 310 µL) and pyridine (3 eq., 7.6 x 10^{-4} mol, 0.3 mL) was added. After pre-stirring (30 sec), the mixture was heated (140 ºC) by microwaves (200 W, PowerMax) for 5 min. Upon cooling, a yellow solid precipitated which was collected by vacuum filtration and washed with water (2 x 3 mL). The solid was recrystallised from ethanol to give a white solid (0.188 g) containing an unresolvable mixture.

27) *C*-**4-Hydroxypropyl-dodecapivaloyl-pyrogallol[4]arene 38**
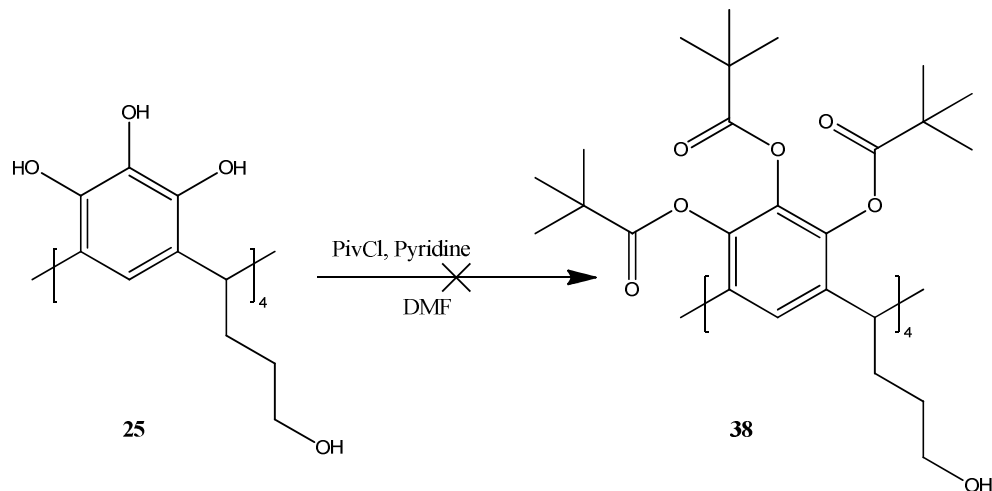
To a stirred solution of *C*-hydroxypropyl-pyrogallol[4]arene **25** (1 eq., 2.5 mmol, 2g) in DCM (100 mL), at 0 ℃, was added triethylamine (24 eq., 61.1 mmol, 8.56 mL) followed by pivaloyl chloride (16 eq., 40.7 mmol, 5 mL) and catalytic amount of DMAP (0.2 g). The reaction mixture was warmed up to room temperature and stirred for 15 hours. After which it was quenched by the careful addition of a saturated solution of ammonium chloride (25 mL) and stirred for 1 hour. The solution was washed with water (2 x 100 mL) and brine (100 mL). The organic phase was collected, dried over magnesium sulfate and evaporated under vacuum, but was seen to decompose.

28) *C*-**4-Hydroxybutyl-tosylpyrogallol[4]arene 39**
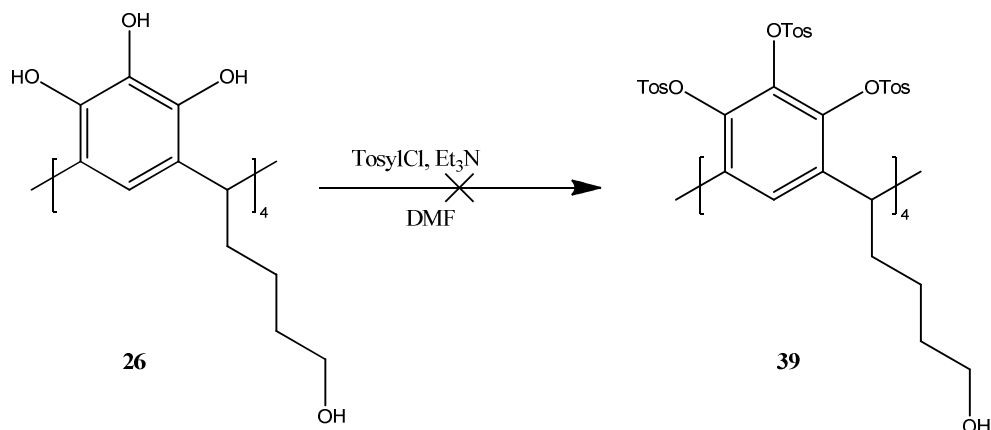
Under nitrogen, to a solution of *C*-hydroxybutyl pyrogallol[4]arene (1 eq., 5 mmol, 4.25g) in acetonitrile (250 mL), was added triethylamine (22 eq., 0.11 mol, 15 mL) and stirred at 80 ℃ for 1 hour. Tosyl chloride (20 eq., 0.1 mol, 19.20 g) in acetonitrile (50 mL) was added dropwise over 15 min. The reaction mixture was heated to reflux for 6 hours, the product was seen to decompose to a black tar. Upon cooling, the solid formed was collected by vacuum filtration was found to be 4-methylbenzenesulfonic acid.

29) *C*-**4-Hydroxypropyl-dodecaboc-pyrogallol[4]arene 40**
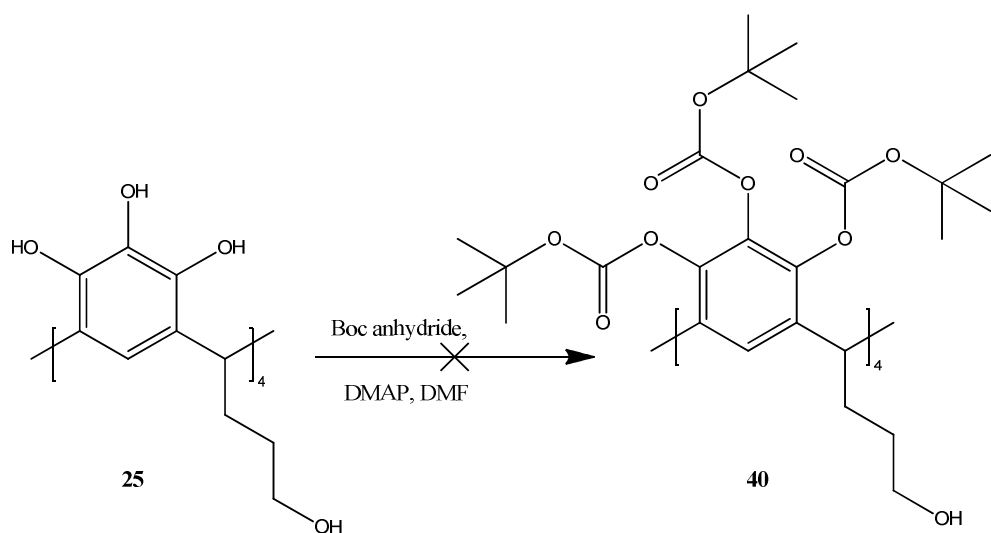
To a solution of *C*-hydroxypropyl-pyrogallol[4]arene **25** (1 eq., 4.3 mmol, 3.4g) in THF (50 mL) was added portionwise *di-tert*-butyl dicarbonate (14 eq., 60.5 mmol, 13.2g) and a catalytic amount of DMAP (0.2 g). The reaction mixture was stirred at room temperature for 18 hours, evaporated under vacuum. The resulting solid was dissolved in ethyl acetate (80 mL) and washed with water (2 x 40 mL) and sodium hydroxide (2M, 40 mL). The organic phase was dried over magnesium sulfate and evaporated under vacuum; to give a white solid that appears to contain a mixture of compounds that were not further purified.

30) *C*-4-Hydroxybutyl-dodecabenzyloxypyrogallol[4]arene 41
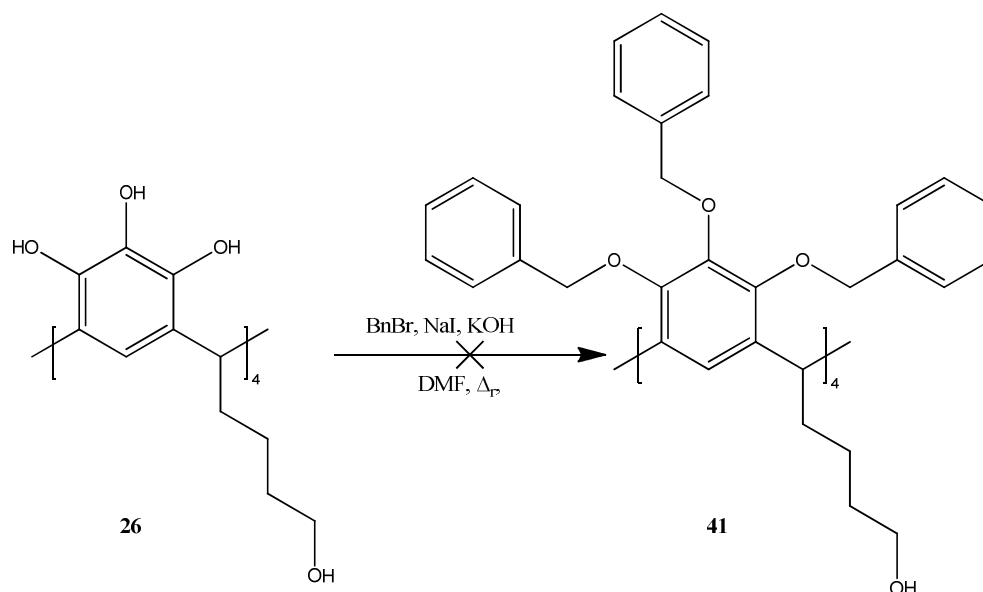
Under nitrogen, to a solution of *C*-4-hydroxybutyl-pyrogallol[4]arene **26** (1.0 eq., 10 mmol, 8.4 g) in DMF (120 mL) potassium hydroxide (20 eq., 0.2 mol, 15.61 g) was added and the mixture was stirred at room temperature for 1 hour. In an ice bath, to a solution of sodium iodide (13.2 eq., 0.132 mol, 13.2 g) in DMF (25 mL) was added dropwise benzyl bromide (13.2 eq., 0.132 mol, 15.66 mL). After complete dissolution, the benzyl iodide solution was added dropwise to the pyrogallol[4]arene solution over 1 hour. The reaction mixture was heated under reflux. The reaction mixture was evaporated under vacuum and the product was seen to decompose into a black tar.

31) *C*-4-Hydroxypropyl-dodecamethoxypyrogallol[4]arene 42

OH

HO — OH

CH₃I , K₂CO₃, Acetone

Δᵣ, 4d, 40%

26   **42**

OH   OH
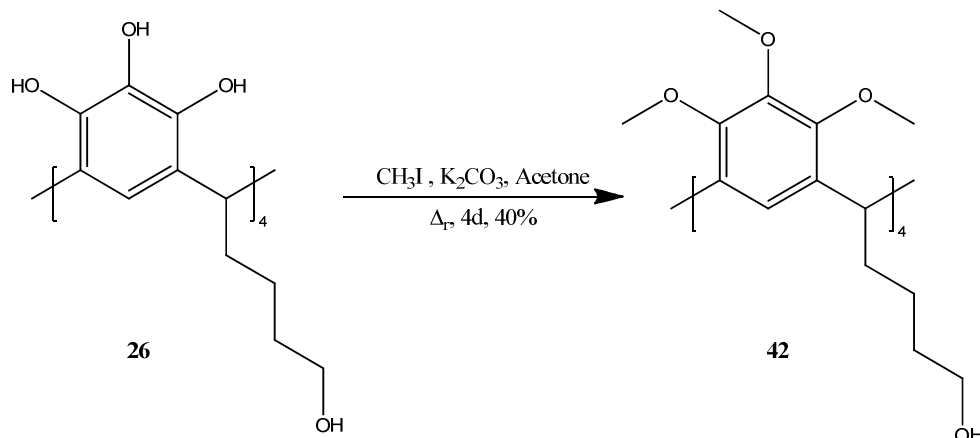
Under nitrogen, a mixture of *C*-4-hydroxybutyl-pyrogallol[4]arene **26** (1.0 eq., 5 mmol, 4.2 g) and dried potassium carbonate (2.9 eq., 14.5 mmol, 2g) in acetone (300 mL) was stirred at room temperature for one hour. Methyl iodide (12.2 eq., 61 mmol, 3.8 mL) was added dropwise over one hour and the mixture was heated under reflux for four days. The reaction mixture was filtered and washed with acetone. The filtrate was evaporated and the residue was dissolved in a mixture of dichloromethane and water (300 mL). The aqueous phase was acidified with 1N HCl until the pH reached 1. The aqueous phase was extracted with DCM (3 x 100 mL) and the combined organic phases were washed with water (100 mL) and dried over dry magnesium sulphate, before being evaporated to dryness. The resulting solid was recrystallised from acetonitrile to give yellow crystals (2.016 g, 2 mmol, 40% yield).

^{1}H NMR (400 MHz, CDCl₃) δ = 6.40 (s, 4H, ArC$_I$H), 4.46 (t, ^3J= 7.8 Hz, 4H, C$_7$H), 1.81 (m, 8H, C$_8$H), 1.58 (m, 8H, C$_{10}$H$_2$) 1.41 (m, 8H, C$_9$H$_2$), 0.83 (s, 36H, OCH₃) ppm. ^{13}C NMR (101 MHz, CDCl₃) δ =149.5, 145.9, 133.3, 120.1, 62.8, 60.3, 60.1, 36.5, 35.3, 32.7, 24.4 ppm. MALDI-TOF *m/z* for C₅₆H₈₀O₁₆ calcd. 1008.54, found 1009.54 [*M*+H]$^+$.

Crystal data for *C*-4-hydroxybutyl-dodecamethoxypyrogallol[4]arene: C₅₆H₈₀O₁₆, *M* = 1009.20, colourless slab, 0.32 × 0.22 × 0.11 mm³, monoclinic, space group *P*2₁/*c* (No. 14), *a* = 13.96(6), *b* = 15.04(4), *c* = 22.30(10) Å, *β* = 92.49(16)°, *V* = 4678(32) Å³, *Z* = 4, *D*$_c$ = 1.433 g/cm³, *F*$_{000}$ = 2176, MoK$_α$ radiation, λ = 0.71073 Å, *T* = 120(2)K, 2$θ_{max}$ = 50.0°, 18445 reflections collected, 7705 unique (*R*$_{int}$ = 0.0719). Final *GooF* = 1.042, *R*1 = 0.1010, *wR*2 = 0.2820, *R* indices based on 5430 reflections

with I >2sigma(I) (refinement on F^2), 677 parameters, 3 restraints. Lp and absorption corrections applied, $\mu = 0.104$ mm^{-1}.

32)   *C*-**4-Bromobutanyl- pyrogallol[4]arene 43**
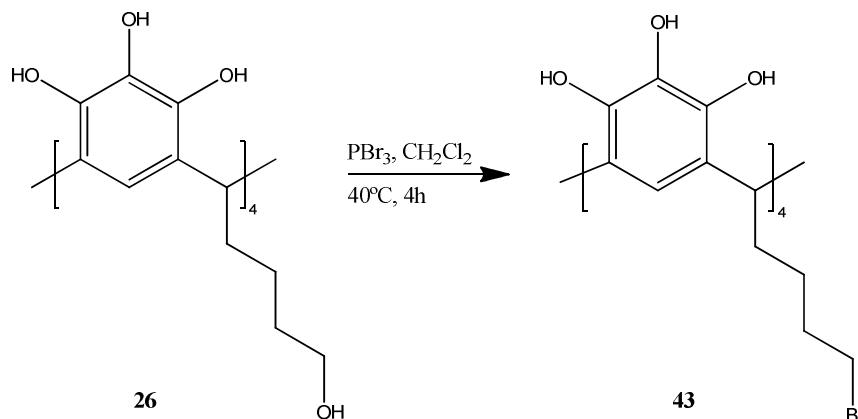
Under nitrogen, *C*-4-hydroxybutyl-pyrogallol[4]arene **26** (1.0 eq., 5 mmol, 4.2 g) was dissolved in DCM (30 mL) at cooled down at 0°C. Phosphorous tribromide (1.3 eq., 6.6 mmol, 6.6 mL) was added dropwise over 10 min and the mixture was stirred until it reached room temperature (1.5 hr). The reaction mixture was stirred at 40 °C over 5 hours. The reaction mixture was then evaporated under vacuum and the resulting oil was sonicated in water (30 mL) for 15 min, filtered and dried under vacuum to obtain a pink solid (3.50 g 3.2 mmol, 65%).

^{1}H NMR (400 MHz, d_6-DMSO) δ = 8.64 (s, 8H, OH), 8.08 (br. s., OH), 6.88 (s, 4H, ArC$_1$H), 4.13 (m, 4H, C$_7$H), 2.16 (m, 8H, C$_{11}$H$_2$), 1.84 (m, 8H, C$_{10}$H$_2$), 1.43 (m, 8H, C$_8$H$_2$) 1.20 (m, 8H, C$_9$H$_2$) ppm. ^{13}C NMR (101 MHz, d_6-DMSO) δ =139.5, 132.8, 124.6, 113.5, 61.0, 33.7, 32.6, 30.7, 24.3 ppm. HPLC purity >90%. t_R=1.409. ESI-MS for C$_{44}$H$_{52}$Br$_4$O$_{12}$ calcd. 1092.02, found 1091, 1093, 1095 *m/z*: [*M*+H, Br ratio]$^+$.

33) *C*-3-Succinylaminopropyl-resorcin[4]arene 44
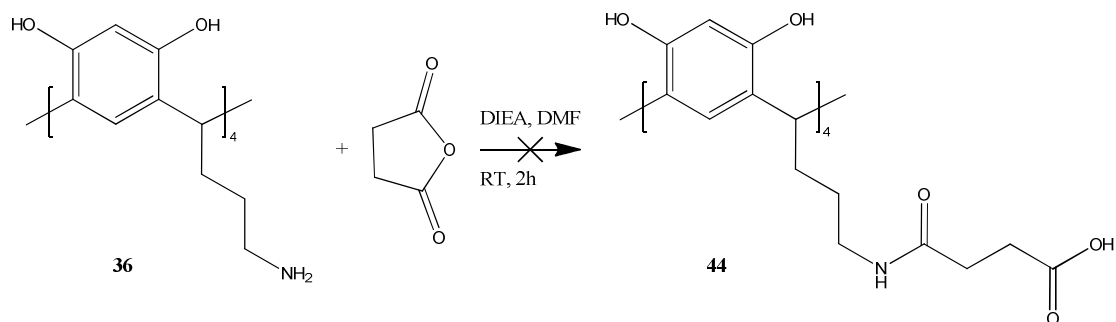
Under nitrogen, *C*-3-aminopropyl-resorcin[4]arene **36** (1.0 eq., 50 mg, 7×10^{-4} mol) and succinic anhydride (4 eq., 3×10^{-4} mol, 30 mg,) and DIEA (4×10^{-4} mol, 70 µL) were dissolved in DMF (2 mL) and stirred at room temperature for 2 hours. The solid formed by trituration with methanol (2 mL) was filtered and dried under vacuum to give a powder (30 mg) but the pure product was not isolated.

^{1}H NMR (400 MHz, CD$_3$OD) δ : 7.39 (s, 4H, ArC$_1$H), 6.18 (s, 4H, ArC$_4$H), 4.26 (t, ^3J =8.1 Hz, 4H, C$_7$H), 3.55 (m, 8H, C$_{10}$H$_2$), 3.25 (t, ^3J =7.1 Hz, 8H, C$_{10}$H$_2$), 3.02 (q, ^3J =7.1 Hz, 8H, C$_{12}$H$_2$), 2.91(s, 2H), 2.62 (q, ^3J =15.7 Hz, 12H, C$_{13}$H$_2$), 2.31 (m, 8H,C$_9$H$_3$), 1.24 (m, 2H) ppm.^{13}C NMR (101 MHz, CD$_3$OD) δ : 175.9, 174.2, 153.1, 141.6, 125.6, 55.8, 43.7, 40.5, 34.7, 30.6, 29.7, 18.6, 17.1, 13.1 ppm. MALDI-TOF *m/z* for C$_{56}$H$_{68}$N$_4$O$_{24}$ calcd.: 1181.15 , found: 1140 [*M*+K]$^+$.

34) *C*-4'carboxyphenyl-pyrogallol[4]arene 45
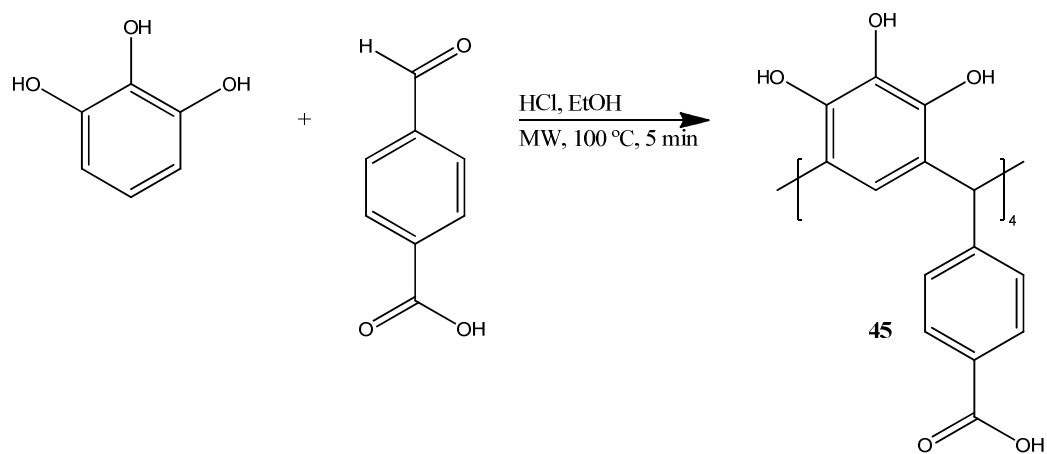
In a CEM pressure vial (10 mL), pyrogallol (1.0 eq., 4 mmol, 0.504 g) and 4-formylbenzoic acid (1.0 eq., 4 mmol, 711 µL) were dissolved in ethanol (1.5 mL). Concentrated HCl (37%, 500 µL) was then added and the mixture was subjected to microwave irradiation (100 W, PowerMax) for 10 min at 100 ºC. Upon cooling, a solid product formed from solution which was then collected by vacuum filtration and washed with water (3 x 2 mL) to obtain a pale pink solid (0.88 g, 0.86 mmol, 86%), the NMR indicate the presence *rctt* (80%) and the *rccc* (20%).

rccc: ^{1}H NMR (400 MHz, d_6-DMSO) δ = 12.39 - 12.14 (b. s, 1 H, COOH), 7.46 (d, ^3J = 8.1 Hz, 2 H, ArH$_4$), 6.79 (d, ^3J = 8.1 Hz, 2 H, ArH$_3$), 5.97 (s, 0.5 H, ArH$_1$), 5.81 (s, 1 H, CH), 5.10 (s, 0.5 H, ArH$_1$) ppm.

rctt: ^{1}H NMR (400 MHz, d_6-DMSO) δ = 12.39 - 12.14 (b. s, 4 H, COOH), 7.46 (d, ^3J = 8.4 Hz, 8 H, ArH$_4$), 6.69 (d, ^3J = 8.4 Hz, 8 H, ArH$_3$), 5.98 (s, 2 H, ArH$_1$), 5.71 (s, 4 H, CH), 5.11 (s, 2 H, ArH$_1$) ppm.

^{13}C NMR (101 MHz, d_6-DMSO) δ = 166.9, 152.7, 142.4, 139.7, 132.2, 128.2, 121.1, 120.6, 46.0 ppm. MALDI-TOF *m/z* for $C_{56}H_{40}O_{20}$ calcd. 1032.21, found 1055.28 $[M+Na]^+$

Crystal data for *C*-4'carboxyphenyl -pyrogallol[4]arene *rctt* acid DMSO clathrate, $C_{40}H_{20}O_{16}S_{10}$, M = 1077.16, 0.026 × 0.085 × 0.138 mm^3, pink block, triclinic, space group $P\bar{1}$ (No. 2), a = 12.0838(13), b = 13.9326(18), c = 15.430(2) Å, α = 111.106(12), β = 99.481(10), γ = 103.207(10)°, V = 2270.5(5) Å^3, Z = 2, D_c = 1.576 g/cm^3, F_{000} = 1096, MoK$_\alpha$ radiation, λ = 0.71073 Å, T = 173(2)K, $2\theta_{max}$ = 50.0º, 19405 reflections collected, 7982 unique (R_{int} = 0.1728). Final *GooF* = 1.342, $R1$ = 0.2208, $wR2$ = 0.4296, *R* indices based on 1816 reflections with I >2sigma(I) (refinement on F^2), 277 parameters, 0 restraints. Lp and absorption corrections applied, μ = 0.556 mm^{-1}.

35)   Fmoc glutamic aminopropyl pyrogallol[4]arene 46
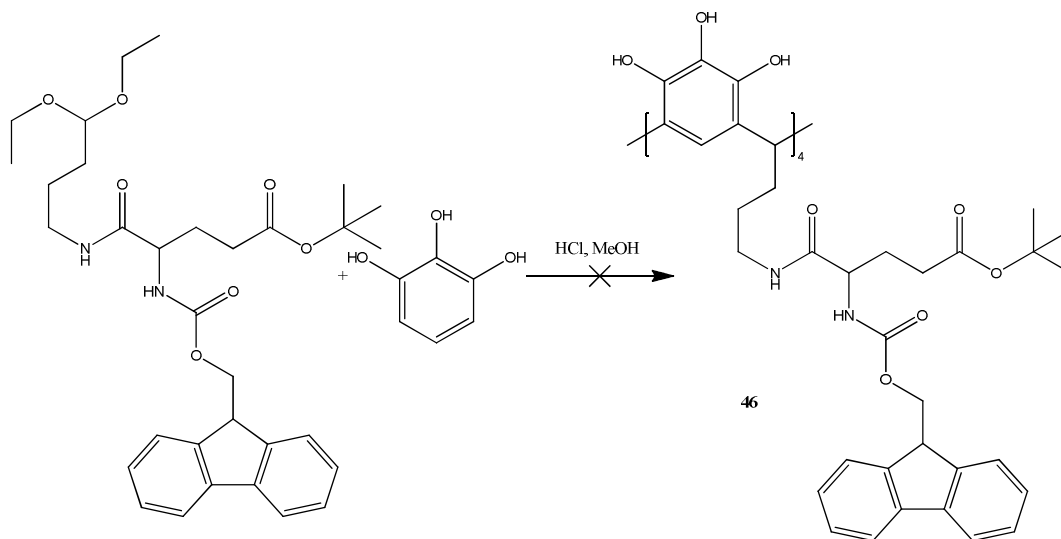
In a CEM pressure vial (10 mL)., PS-DCC (1.1 eq., 2.2 x 10^{-4} mol, 165 mg) PS-DIEA (1.1 eq., 2.2 x 10^{-4} mol, 59 mg) and Fmoc-glutamic acid *t*-butyl ester (1.1 eq., 2.2 x 10^{-4} mol, 93 mg) were stirred in DMF (1.5 mL) at room temperature for 30 min. Aminobutyraldehyde (1 eq., 2 x 10^{-4} mol, 36 μL) was added and the mixture was subjected to microwave irradiation for 5 min at 100 ℃ (100 W). The mixture was filtered and washed with DMF (2 x 1 mL) and evaporated. The resulting in a yellow wax, which was dissolved in methanol (1.5 mL) with pyrogallol (1.0 eq., 2 mmol, 0.252 g). Concentrated HCl (37%, 500 μL) was then added and the mixture was subjected to microwave irradiation (100 W, PowerMax) for 10 min at 100 ℃. The macrocycle could not be isolated.

36)   *C-tert*-Butyl (1-(butylamino)-1-oxopropan-2-yl)carbamate-resorcin[4]arene 47
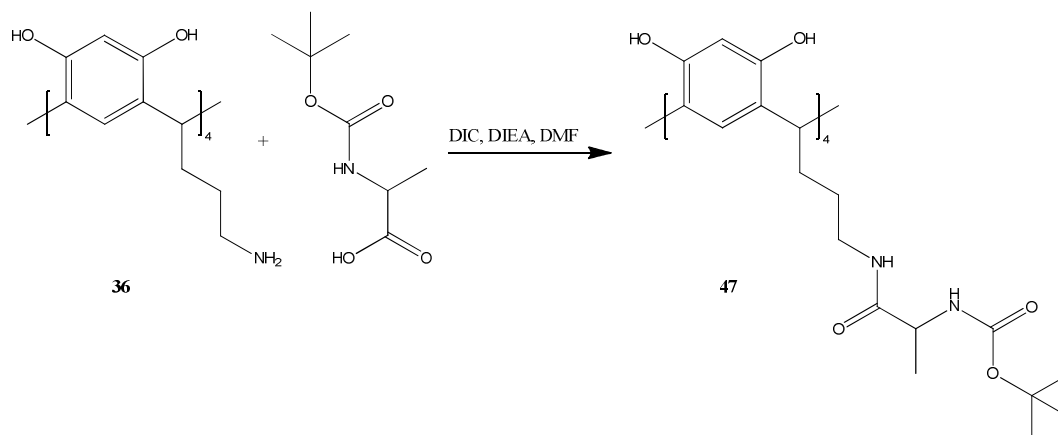
        N-Boc-alanine (5 eq., 1 mmol, 0.19 g,) and *C*-3-aminopropyl-resorcin[4]arene **36** (1 eq., 2×10^{-4} mol, 148 mg) were dissolved in DMF (3 mL). DIC (6 eq., 1.2 mmol, 180 µL) and DIEA (4 eq., 8×10^{-4} mol, 130 µL) were added and the mixture was stirred at room temperature for 24 hours. After trituration with methanol, the precipitate was collected under vacuum and analysed by NMR to show trace of the expected compound. ^{1}H NMR (400 MHz, d_6-DMSO) δ = 8.84 (s, 8H) , 7.70 (s, 4H), 7.07 (s, 4H), 6.70 (s, 4H), 6.09 (s, 4H), 4.16 (t, ^3J =8.2 Hz, 4H,), 3.86 (m, 4H), 3.02 (m, 12H), 1.97 (m, 8H), 1.23 (m, 32H), 1.09 (m, 8H) ^{13}C NMR $(CD_3)_2SO$ $δ_C$ (ppm): 172.6, 163.6, 154.3, 151.9, 123.9, 79.5, 54.6, 49.1, 43.4, 42.5, 41.5, 27.5, 22.3, 21.1, 20.5, 20.1, 18.6, 11.9 MALDI-TOF *m/z* for $C_{72}H_{104}N_8O_{20}$ calcd.: 1401.64, found: 1402.78 $[M+H]^+$

37)   *C*-3-(9H-fluoren-9-yl)methyl (1-(butylamino)-1-oxopropan-2-yl)carbamate-resorcin[4]arene 48
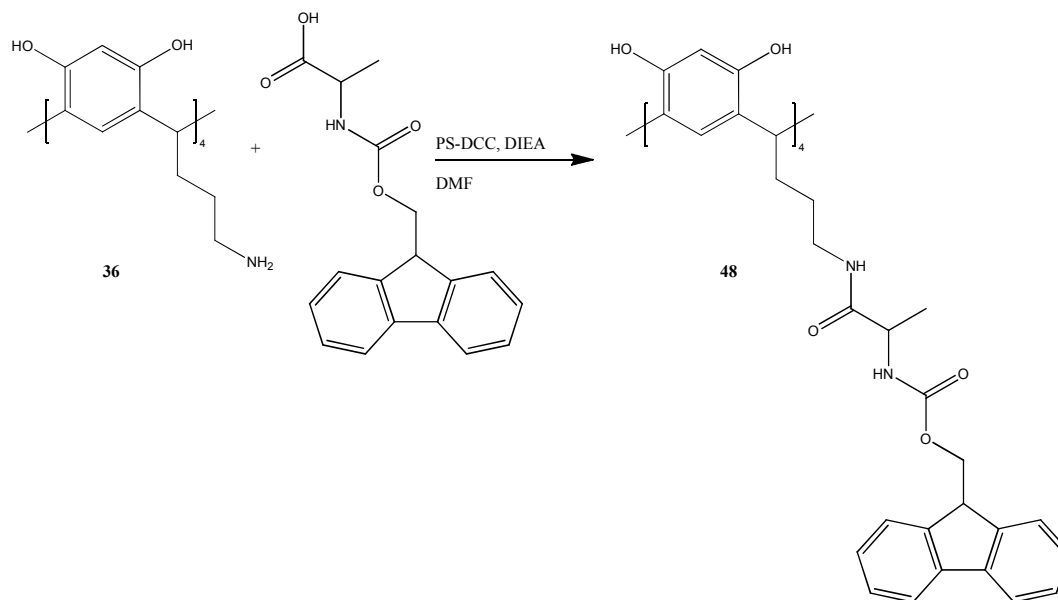
Method 1: In a CEM pressure vial (10 mL)., Fmoc-alanine (6 eq., 3.5 x 10^{-4} mol, 0.109 g) and PS-DCC (4.5 eq., 2.7 x 10^{-4}, 201 mg) and HOBt (6.1 eq., 3.7 x 10^{-4}, 201 mg) were stirred in DCM/DMF mixture (1:1, 1 mL). *C*-3-aminopropyl-resorcin[4]arene **36** (1.0 eq., 6 x 10^{-5} mol, 42 mg) and of DIEA (1.0 eq., 6 x 10^{-5}, 10 µL) were added with DCM/DMF mixture (1:1, 1 mL). the mixture was subjected to microwave irradiation (100 W, PowerMax) for 10 min at 100 ºC. After filtration under vacuum, the resin was washed with DMF (2 mL). The solution was evaporated to dryness and triturated with methanol/diethyl ether (1:1, 2 mL) and used for analysis. MALDI-TOF *m/z* for $C_{112}H_{112}N_8O_{20}$ calcd. 1890.2, found 1911.01 [M+Na]$^+$

Method 2: In a CEM pressure vial (10 mL), Fmoc-alanine (6 eq., 3.5 x 10^{-4} mol, 0.109 g) and PS-DCC (4.5 eq., 2.7 x 10^{-4}, 201 mg) were stirred in DCM/DMF mixture (1:1, 1 mL). *C*-3-aminopropyl-resorcin[4]arene **36** (1.0 eq., 6 x 10^{-5} mol, 42 mg) and DIEA (1.0 eq., 6 x 10^{-5}, 10 µL) were added with DCM/DMF mixture (1:1, 1 mL). The mixture was subjected to microwave irradiation (100 W, PowerMax) for 10 min at 100 ºC. After filtration under vacuum, the resin was washed with DMF (2 mL). The solution was evaporated to dryness and triturated with methanol/diethyl ether (1:1, 2 mL) and used for analysis. MALDI-TOF *m/z* for $C_{112}H_{112}N_8O_{20}$ calcd.: 1890.2, found: 1911.01 [M+Na]$^+$

38)   Pegylated *C*-3-aminopropylpyrogallol[4]arene 49
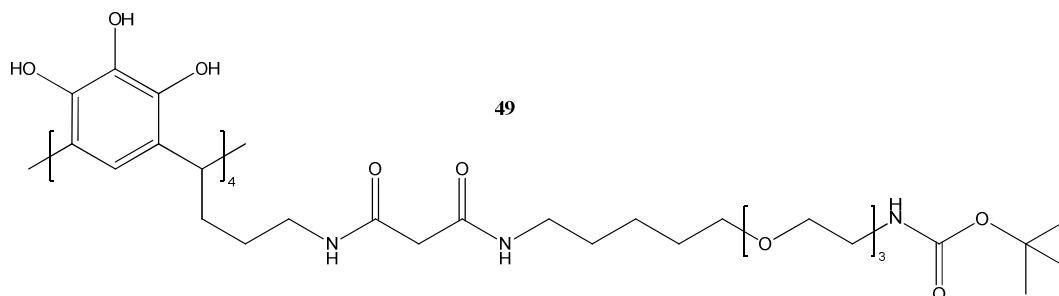
In a CEM pressure vial (10 mL)., 2,2-dimethyl-4,21-dioxo-3,8,11,14-tetraoxa-5,20-diazatricosan-23-oic acid (6 eq., 2.9 x 10^{-4} mol, 125 mg) and PS-DCC (8.6 eq., 2.4 x 10^{-4}, 105 mg) were stirred in DCM/DMF mixture (1:1, 1 mL). *C*-3-aminopropyl-pyrogallol[4]arene **35** (1.0 eq., 2.8 x 10^{-5} mol, 22 mg) and PS-DIEA (25 eq., 7 x 10^{-4}, 200 mg) were added with DCM/DMF (1:1, 1 mL) to the mixture. It was then subjected to microwave irradiation (25 W, PowerMax) for 10 min at 75 ºC. After filtration under vacuum, the resin was washed with DMF (2 mL). The solution was evaporated to dryness and triturated with methanol/diethyl ether (1:1, 2 mL) to obtain 66 mg of the crude product that was used for NMR analysis showing trace of the tetra substituted compound.

^{1}H NMR (400 MHz, d_6-DMSO) δ = 7.87 (m, 4 H), 6.75 (s, 4 H, ArH), 4.16 (m, 4 H, CH),), 3.56 (s, 8 H), 3.42 (dd, 16 4.2, 32 H), 3.36 (q, J=5.2 Hz, 20 H), 3.05 (q, *J*=6.40 Hz, 8 H), 2.94 (q, *J*=6.40 Hz, 8 H), 2.83 (m, 8 H), 2.38 (d, *J*=6.87 Hz, 4 H), 2.29 (m, 4 H), 2.32 (m, 8 H), 1.58 (q, *J*=6.30 Hz, 16 H, CH$_2$+CH$_2$), 1.36 (s, 36 H, CH$_3$) ppm.

^{13}C NMR (101 MHz ,DMSO-d$_6$) δ = 174.1, 170.9, 155.6, 139.7, 133.0, 128.2, 123.9, 113.8, 113.7, 77.4, 69.8, 69.6, 68.1, 51.3, 40.4, 37.3, 35.8, 34.0, 30.2, 29.8, 29.7, 29.4, 28.9, 28.3, 26.1 ppm.

39)   General method for peptide synthesis

In a SPPS reaction vessel, Fmoc protected Wang resin (0.1 mmol) was swelled in a DMF/DCM mixture (1:1, 5 mL) for 30 min and was then drained and rinsed with DMF (5 mL). Resin deprotection was done by addition of piperazine (0.58 M, 7 mL) and reacted for 30 sec at 75 ℃ (Δ5 ℃, 50 W), drained and piperazine was added (0.58 M, 7 mL) and reacted for further 3 min at 75 ℃ (Δ5 ℃, 50 W). The deprotected was drained under vaccum and rinsed with DMF (5 mL x 3). Fmoc protected amino acid (2.5 eq., 0.25 mmol) dissolved in DMF (2.5 mL) was added to the deprotected resin with HBTU (0.474 M, 1 mL,) and DIEA in NMP (2.58 M, 500 µL). The reaction was performed under microwave irradiation using different temperature and coupling time depending on the amino acid used. Generally, all amino acids expect from arginine, histidine and cysteine, were reacted for 5 min at 75 ℃ (Δ5 ℃, 25 W). Arginine was reacted for 30 min at 25 ℃ (Δ5 ℃, 0 W). Histidine and cysteine were reacted for 10 min at 50 ℃ (Δ5 ℃, 25 W), drained and more amino acid (2.5 eq., 0.25 mmol) was added and reacted for further 10 min at 25 ℃ (Δ5 ℃, 0 W).

Final deprotection was done by addition of piperazine (7 mL x 2). The reaction mixture was drained, washed with DMF (3 x 5 mL) and rinsed with DCM (3 x 5 mL) and left to dry under air for 15 min. The resin was then transferred into a cleavage mix solution containing H_2O (0.25 mL), TIS (0.1 mL), DODT (500 µL) and TFA (9.4 mL) and stirred at room temperature for 3 hours. The peptide was filtered into a chilled solution of diethyl ether (100 mL) and the resin washed with DCM (2 x 2 mL). The ether solution was placed in the freezer for at least 1 hour, until the formation of a white precipitate. The mixture was centrifuged (10 min, 3000 rpm, <10 ℃), the supernatant removed and clean chilled diethyl ether (30 mL) was added. The process was repeated two more times. The recovered white waxy solid was left to dry overnight or dry-freeze. Peptide purity was analysed using HPLC using the gradient 95% H_2O / 5% CH_3CN / 0.1% TFA to 5% H_2O / 95% CH_3CN / 0.1% TFA, over 60 min at a flow rate of 500 µL.min^{-1}, the UV detector was set at 215 nm.

C-3-Ala-Ala-Ala-Asp-propyl-resorcin[4]arene 50
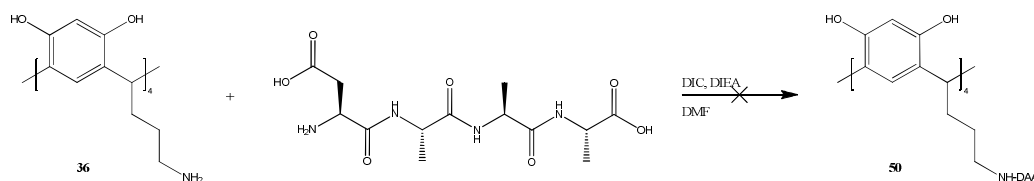
Asp-Ala-Ala-Ala (2 eq., 9.4 x 10^{-5} mol, 34 mg), DIC (2.7 eq., 1.27 x 10^{-4} mol, 20 µL), DIEA (2 eq., 9.2 x 10^{-5} mol, 16 µL) and *C*-3-aminopropyl-resorcin[4]arene **36** (1 eq., 2.1 x10^{-5} mol 42 mg), were stirred in DCM/DMF mixture (1:1, 1 mL) for 24 hours. After filtration, the solvent was evaporated and the oil sonicated in water (1 mL), forming a white solid (5mg) that was used for analysis. The HPLC analysis revealed 3 main peaks at 2.59 min (34%), 3.26 min (11%) and 3.61 min (12%). The MALDI-TOF MS *m/z* for $C_{92}H_{132}N_{20}O_{36}$ calcd. 2094.14, found: 2889, 1713 and 714 $[RsC_3NH_2]^+$ respectively, did not allow the characterisation of the compound.

41)   **AAA-p53(108-122)-A 51**
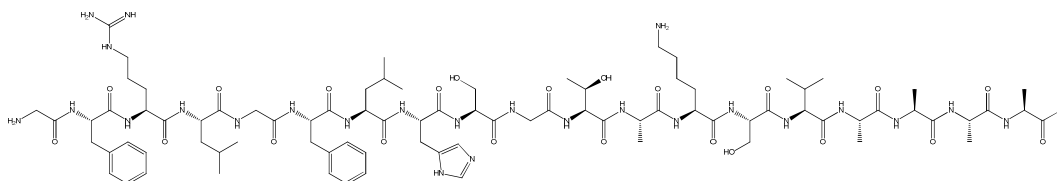
The following sequence AAAGFRLGFLHSGTAKSVA was synthesised using the general method for peptide synthesis resulting in a nearly quantitative yield. However the MS results indicated that 50% were still Fmoc protected. Cleaved AAA-p53(108-122)-A unprotected peptide (2 eq., MW= 1873.01g.mol^{-1}, 2.6 x 10^{-5}, 50 mg) was dissolved in DMF/DCM mixture (1:1, 2 mL) with aminopropyl-pyrogallol[4]arene **35** (1 eq., 5.2 x 10^{-5}, 4.2 mg), PS-DCC (8 eq., 4.1 x 10^{-5}, 31.5 mg) and PS-DIEA (6 eq., 3.12 x 10^{-5}, 8.5 mg). After pre-stirring (15 s), the mixture was heated (75ºC) by microwaves (25 W, PowerMax) for 10 min. The resin was then drained and washed with DMF (3 x 2 mL), the combined filtrate were evaporated under vacuum and triturated with cold diethyl ether (10 mL) resulting in a white solid that was used for analysis showing only possible trace of the compound.

^{1}H NMR (400 MHz , d_6 DMSO) δ = 8.62 (br. s., 2 H), 8.27 - 8.10 (m, 3 H), 8.06 - 7.88 (m, 4 H), 7.88 - 7.61 (m, 5 H), 7.38 - 7.11 (m, 4 H), 6.83 (br. s., 1 H), 5.16 - 4.96 (m, 2 H), 4.96 - 4.83 (m, 1 H), 4.40 - 4.13 (m, 6 H), 3.97 (br. s., 1 H), 3.91 - 3.74 (m, 2 H), 3.67 - 3.50 (m, 4 H), 3.39 (dt, *J* = 0.9, 7.0 Hz, 6 H), 3.15 - 2.97 (m, 2 H), 2.66 -

2.43 (m, 7 H), 2.39 - 2.13 (m, 3 H), 2.06 - 1.91 (m, 2 H), 1.89 - 1.72 (m, 2 H), 1.70 - 1.64 (m, 1 H), 1.49 (quin, J = 6.1 Hz, 4 H), 1.36 - 1.16 (m, 6 H), 1.03 (d, J = 5.6 Hz, 2 H), 0.84 (dd, J = 6.9, 15.7 Hz, 10 H) ppm. ^{13}C NMR (101 MHz , d_6-DMSO) δ = 226.3, 217.3, 188.3, 153.7, 139.7, 129.0, 128.9, 120.2, 114.3, 82.6, 72.4, 64.9, 15.2. MALDI-TOF *m/z* for $C_{84}H_{133}N_{25}O_{23}$ calcd. 1861.11, found: 1874.01 [M]$^+$ and 1897.91 [M+Na]$^+$.

42) HOOC-(CH$_2$)$_3$COO-p53 (108-122)-A 52
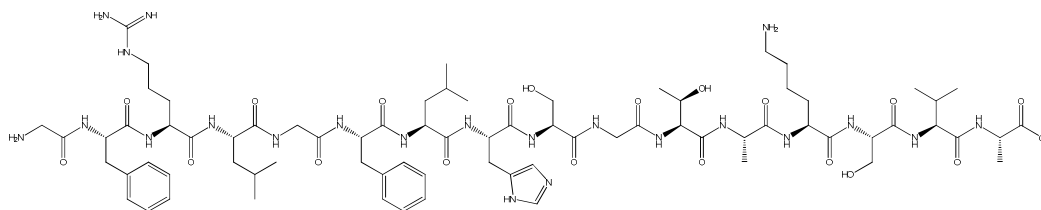
The following sequence GFRLGFLHSGTAKSVA was synthesised using the method previously described (1 x 10^{-4} mol). To the Fmoc deprotected peptide was added glutaric anhydride (2.2 eq., 2.2 x 10^{-4} mol, 25 mg) with HBTU (0.474 M, 1 mL) and DIEA in NMP (2.58 M, 500 µL). The reaction mixture was heated to 75 ºC for 10 min under microwave irradiations (25 W). The resin was drained and washed with DMF (2 x 5 mL) and a solution of aminopropyl pyrogallol[4]arene (1.4 x 10^{-5} mol, 11mg) was added with HBTU (0.474 M, 1 mL,) and DIEA in NMP (2.58 M, 500 µL). The reaction mixture was heated to 75 ºC for 10 min under microwave irradiations (25 W). The resin was drained, washed and cleaved using the general procedure. The white product collected after centrifugation (83 mg, 4.65 x 10^{-5} mol, 46%) was 74 % pure by HPLC. The MALDI-TOF *m/z* for $C_{80}H_{124}N_{22}O_{23}$ calcd. 1761.97, found 1785.68 [HOOC-(CH$_2$)$_3$COO-p53 (108-122)-A +Na]$^+$

43)   PS-PgC₃OH 53

53
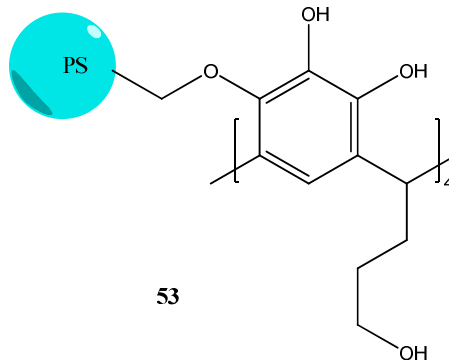
Method 1: (**53**) Merrifield polymer Hertz resin 200 – 400 mesh (1 eq., 0.2 mmol, subst. 1.0 -1.5 mmol.g⁻¹, 0.25 g) was swelled in a mixture a DMF / DCM mixture (1:1, 5 mL) for 30 min and was then drained. A solution of *C*-3-hydroxypropyl-pyrogallol[4]arene **25** (1.28 eq., 0.32 mmol, 0.25 g) in DMF (2 mL) and K_2CO_3 (12 eq., 3.6 mmol, 0.50 g) was then added. The reaction mixture was subjected to microwave irradiation for 10 min at 100 ºC (100 W). The reaction mixture was drained, washed with DMF (3 x 5 mL) and rinsed with H_2O (3 x 5 mL), MeOH (3 x 5 mL) resulting in a pink resin. (**53**)

IR (ν): 3432.15, 3132.66, 2938.50, 1646.93, 1478.96, 1383.54, 1352.25, 1239.26, 1265.84, 1235.27, 1094.14, 1057.24, 1005.04, 978.42, 778.67, 694.92, 663.23 cm⁻¹.

The resin was transferred to a cleavage mix solution containing H_2O (500 μL) and TFA (9.5 mL) and stirred at room temperature for 3 hours. The mix was then transferred into H_2O (50 mL), the solid that crashed out was then filtered and use for NMR analysis revealing the starting pyrogallol[4]arene **25**.

¹H NMR (400 MHz, d_6-DMSO) δ = 6.88 (s, 4 H, ArC$_l$H), 4.15 (t, *J* = 7.8 Hz, 4 H, C$_7$H), 2.17 (q, *J* = 7.3 Hz, 8 H, C$_{11}$H$_2$), 1.35 (m, 8 H, C$_{10}$H$_2$), 1.24 (m, 8 H, C$_9$H$_2$) ppm.

Method 2: Merrifield polymer Hertz resin 200 – 400 mesh (1 eq., 0.2 mmol, subst 1.0 -1.5 mmol.g⁻¹, 0.25g) was swelled in a mixture a DMF / DCM mixture (1:1, 5 mL) for 30 min and was then drained. A solution of *C*-3-hydroxypropyl-pyrogallol[4]arene **25** (0.25 g, 0.32 mmol, 1.28 eq.) in DMF (2 mL) and pyridine (32 eq., 6.4 mmol, 500 μL) was then added. The reaction mixture was subjected to microwave irradiation for 30 min at 75 ºC (Δ5 ºC, 50 W). The reaction mixture was

drained, washed with DMF (3 x 5 mL) and rinsed with MeOH (3 x 5 mL) resulting in a pink resin that was used as such. (**54**)

IR (ν): 3311.15, 3024.66, 2923.50, 2829.56, 1601.93, 1492.96, 1451.54, 1420.92, 1316.08, 1265.84, 1213.27, 1110.14, 1024.24.13 910.04, 824.42, 761.67, 699.92, 674.23, 543.48 cm^{-1}.

The resin was transferred to a cleavage mix solution containing H_2O (500 µL) and TFA (9.5 mL) and stirred at room temperature for 3 hours. The mix was then transferred into H_2O (50 mL), the solid that crashed out was then filtered and use for NMR analysis.

^{1}H NMR (400 MHz, d_6-DMSO) δ = 6.88 (s, 4 H, ArC$_l$H), 4.15 (t, J = 7.8 Hz, 4 H, C$_7$H), 2.17 (q, J = 7.3 Hz, 8 H, C$_{11}$H$_2$), 1.35 (m, 8 H, C$_{10}$H$_2$), 1.24 (m, 8 H, C$_9$H$_2$) ppm.
IR cleaved resin (ν): 3026.24, 2917.25, 1731.33, 1685.00, 1600.96, 1492.09, 1451.60, 1199.11, 1120.68, 1026.91, 799.12, 756.90, 696.97, 537.14, 412.71, 395.91 cm^{-1}.

44) PS-PgC$_3$O-SO$_2$CH$_3$ 55

55
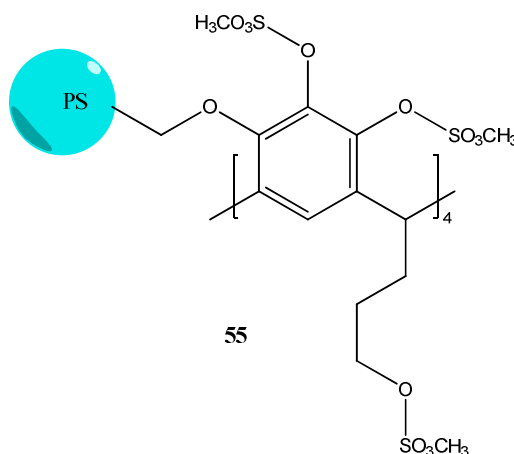
The resin was functionalised as previously described with *C*-hydroxypropyl-pyrogallol[4]arene **25** (0.100 g, 0.4 mmol) and swelled in DMF (1 mL) for 15 min. After being washed and dried, methane sulfonyl chloride (17 eq., 1.7 mmol, 131 µL) and pyridine (17 eq., 1.7 mmol, 136 µL,) was added and the mixture subjected to microwave irradiation for 10 min at 150 ºC (100 W). The resin was then drained and washed with DMF (2 x 5 mL) and MeOH (2 x 5 mL). The resin was used for SEM analysis, revealing the presence of sulphur.

IR (ν ATR): 3023.60, 2919.88, 2157.34, 1600.59, 1178.50, 1027.82, 756.68, 697.03, 534.08 cm^{-1}

45)   UV titration

To the substituted resin (5 to 10 mg) was added piperazine (1 mL, 0.58M) and shaked for 15 min. After 10 min of centrifugation, a 100 µL of the mixture was added to 10 mL of DMF. Using the UV spectrometer, the absorption was then measured at 301 nm and corrected with the blank. The substitution was then assessed using the following equation : subst. (in meq.) = (A x dilution)/weigh.

46)   PS-PgC$_3$NH-Fmoc 56
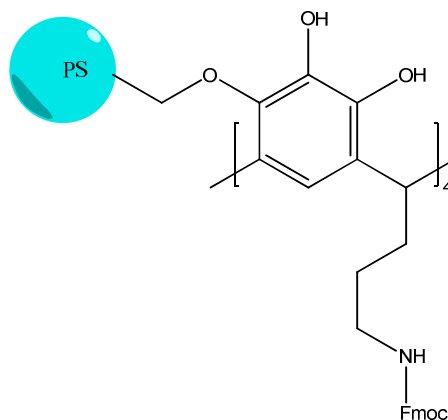
Merrifield polymer Hertz resin (0.25 g, 0.8 mmol, 100- 200 mesh, subst. 1.0 - 1.5 mmol.g^{-1}) was swelled in a mixture a DMF/DCM mixture (1:1, 5 mL) for 30 min and was then drained. A solution of Fmoc-aminopropyl pyrogallol[4]arene (1 eq., 6.5 x 10^{-5} mol, 0.11 g) in DMF (3 mL) and pyridine (10 eq., 6.4 mmol, 500 µL) was then added. The reaction mixture was subjected to microwave irradiation for 1 hour at 75 ºC (Δ5 ºC, 50 W). The reaction mixture was drained, washed with DMF (3 x 5 mL), rinsed with MeOH (3 x 5 mL) and dried. The substitution was assessed by UV to be 1.06 meq. /g.

47)   PS-PgC₃OCys(Ac) 57
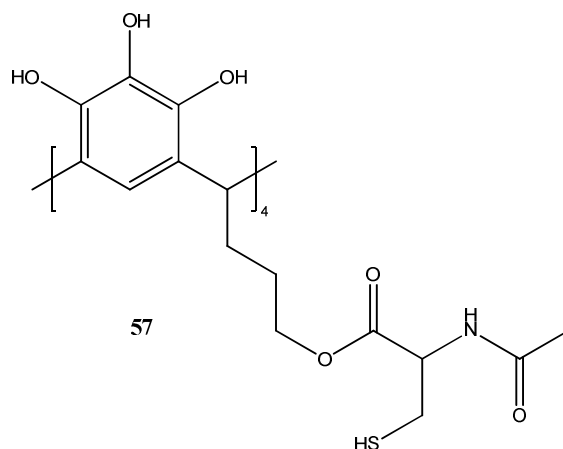
The resin was functionalised as previously described (0.500 g, 1.52 mmol). To the washed resin, was added a solution of *N*-acetyl-*L*-cysteine (6.1 mmol, 1 g,) in DMF (2.5 mL), DIC (6.07 µmol, 941 µL,) and a catalytic amount of DMAP. The resin was transferred to a cleavage mix solution containing H_2O (500 µL) and TFA (9.5 mL) and stirred at room temperature for 3 hours. The mix was then transferred into H_2O (50 mL), the solid that precipitated was then filtered and used for IRanalysis.

IR resin (ν): 3311.15, 3024.83, 2923.50, 2829.56, 2158.22, 1601.93, 1420.92, 1316.08, 1265.84, 1110.14, 1024.13, 824.42, 761.67 cm^{-1}.

48)   Butyl 2-(-2-(-2-aminopropanamido)-propanamido)propanoate pyrogallol[4]arene 58
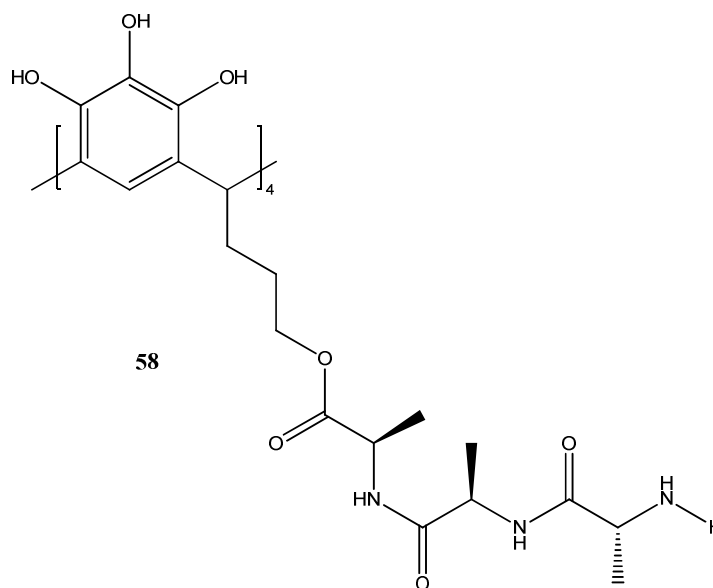
Merrifield polymer Hertz resin (0.49 mmol, 100-200 mesh, subst. 1.0 -1.5 mmol.g^{-1}, 0.499 g,) was swelled in a mixture a DMF/DCM mixture (1:1, 5 mL) for 30 min and was then drained. A solution of *C*-hydroxypropyl pyrogallol[4]arene (1 eq., 1 mmol, 0.781g) in DMF (3 mL) and pyridine (6.4 eq., 6.4 mmol, 500 µL,) was then added. The reaction mixture was subjected to microwave irradiation for 30 min at 75 ºC (Δ5 ºC, 50 W). The resin was drained, washed with DMF (3 x 5 mL) and rinsed with MeOH (3 x 5 mL). The AAA sequence was synthesised on the resin as previously described (general method). After the final deprotection, the resin was drained, washed with DMF (3 x 5 mL) and DCM (3 x 5 mL), left to dry under air for 15 min. The resin was then transferred into a cleavage mix solution containing H_2O (250 µL), TIS (100 µL), DODT (500 µL) and TFA (9.4 mL) and stirred at room temperature for 3 hours. The peptide was filtrated into a chilled solution of diethyl ether (100 mL) and the resin washed with MeOH (2 x 2 mL). The ether solution was placed in the freezer for 24 hours resulting in the formation of a white precipitate. NMR indicates trace of the expected compound but could not be purified.

MALDI-TOF *m/z* for starting material found: 807.45, 913.507, 1015.758, 1073.778, 1512.124.MALDI-TOF *m/z* for $C_{76}H_{108}N_{12}O_{28}$ calcd.: 1636.74, found: 945.16, 1015.57, 1792.88 (indicate 11 alanine, which could be 3 x AAA and 1 x AA).

E. CHAPTER V:

49)   Haemolysis assay[391]

Freshly drawn human blood (30 mL) were centrifuged in a polypropylene vial with physiological serum (NaCl 0.9%, 30 mL) for 5 min at 1200 *g*. The supernatant was removed and this operation was repeated twice. The volume of the washed erythrocytes was adjusted with PBS (72 mL). To the 10% DMSO / PBS buffered solution of calixarene derivatives(500 µL), was added the suspension of erythrocytes (500 µL). After moderate manual stirring, the mixture was incubated (30 min.) in a thermostated bath (37 ºC) and centrifuged (1200 × *g* for 5 min). An aliquot of the supernatant (20 µL) was added to the Drabkin reagent (2 mL). The quantity of haemoglobin was assayed spectrophotometrically at 540 nm. To ensure result reproducibility all assays were repeated three times. Positive and negative controls have been realised by replacing the sample with water (total haemolysis due to hypotonic stress), 10% DMSO / PBS and PBS. The percentage of haemolysis is expressed as the ratio between the absorbance of the sample (corrected using the value obtained for PBS) and the absorbance of the positive control.

50)   Culturing of Murine Bone Marrow Dendritic Cells

BMDC were generated as described by Inaba and co-workers with modification.[395] The hind limbs from immunologically naive mice were taken and all of the muscle and fat removed using forceps and scissors. After cutting the ends of the bones, bone marrow was flushed with BM-DC media (RPMI 1640 + 5% FCS + 10 mM HEPES Buffer + 50 µM 2-mercaptoethanol + 50 U/mL Penicillin/Streptomycin + 0.25 µg/mL fungizone). The flushed cells and media were collected, centrifuged (1500 rpm, for 3 min at 4°C), resuspended in 4 mL of BM-DC media and then counted in acetic acid and trypan blue using a haemocytometer. The dendritic cells were plated at $1x10^6$ cells per mL/well with GM-CSF (1 ng/mL) and incubated (37°C, 5% CO_2). On days 2 and 4, non-adherent cells were washed gently by removing the media (700 µL) and replacing it by fresh BM-DC media (750 µL) of containing GM-CSF (100 ng/mL).

51) Maturing Bone Marrow Dendritic cells

On day 7, BMDC were harvested, counted and supplemented with of LipoPolySaccharide (LPS, 1µg/mL) to induce maturation and then incubated at 37°C, 5% CO_2 overnight. On day 8, the cells were washed with fresh media supplemented with polyIC (12.5 µL) and incubated for 2 hour at 37°C, 5 % CO_2.

52) Fluorescent Activated Cell Sorting (FACS)

The two colonies of DCs cultured either with the standard method (method A)[395] or the alternative one (method B)[397] were collected. The DCs were fixed with paraformaldehyde and CD16/CD32 Fc blocker to minimise the non-specific binding and lower the background. The cells were then treated with the appropriate surface marker antibodies in order to characterise the various populations, *i.e.* MHC class II (HLA-DR-FITC, abcam), CD11c-RPE (Hamster antimouse, Serotec) and CD86-RPE (Rat antimouse, Serotec). All of these markers were tested using the monoclonal antibodies as well as their isotype controls in order to confirm the purity of the DCs population. In this experiment the dendritic cells have not been fixed with paraformaldehyde, but a CD16/CD32 Fc blocker as been used to minimise the non specific binding, which lowers the background. The results are presented by percentage of cells gated.

53) Vialight® HS Assay

The assay was performed according to the manufacturer instructions. BMDC were generated as previously described, on day 7 the cells were replated at 1 x 10^5 cells/well/100 µL of media containing various concentrations of calixarene. After 24 hours, the lysing reagent was added for 10 min, followed by the ATP monitoring reagent of the Vialight® HS Kit (Lonza). The plate was placed in the luminometer and the intensity of the light measured. The percentage of bioluminescence is expressed as the ratio between the reading of the sample and the reading of the untreated cells as the positive control.

54)   Toxilight® BioAssay

The assay was performed according to the manufacturer instructions. BMDC were generated as previously described, on day 7 the cells were replated at 2.5 x 10^5 cells/well/mL of media containing various concentration of calixarene. After 24 hours, the ATP monitoring reagent from the Toxilight® BioAssay Kit (Lonza), was added. Finally, the plate was placed in the luminometer and the intensity of the light measured. The percentage of bioluminescence is expressed as the ratio between the reading of the sample and the reading of the untreated cells as the positive control. On day 4, non-adherent cells were washed gently by removing the media (700 µL) and replacing it by fresh BM-DC media (750 µL) containing GM-CSF (100 ng/mL) of and various concentrations of calixarene. On day 7, the Toxilight assay was repeated.

55)   Propidium Iodide Assay

BMDC were generated as previously described. On day 7 the cells were replated at 5000 cells/well/100µL of media containing various concentrations of calixarene. After 24 hours, the media was removed and the cells were washed three times with PBS. Ice cold ethanol (70 %) was added as a positive control and cells were incubated on ice for 15 min. After removal of the ethanol, propidium iodide solution (P484-10 mL, 1 mg/L, Aldrich, 5 µL) was added to each well and incubated at 37 ºC for 30 min. The wells were then washed three times with PBS and dried. The cell count was performed using the ELISPOT, using the ImmunoSPot UV program. The scanning mode used was Fluorocell Configuration, using a red filter. The QC analysis was performed using an inverted method, large diffused spot, with gating set between 0.00001 nm^2 0.0153 nm^2. The percentage of PI positive cells is expressed as the ratio between the cell count of (corrected by percentage of the well area covered) the sample of the sample and ethanol permeabilised cells.

REFERENCES

1. D. N. Reinhoudt and M. Crego-Calama, *Science*, 2002, **295**, 2403-2407.
2. J. W. Steed and J. L. Atwood, *Supramolecular Chemistry* 2edn., John Wiley & Sons, Ltd, Chischester, UK, 2009.
3. J.-M. Lehn, *Chem. Soc. Rev.*, 2007, **36**, 151-160.
4. S. J. Dalgarno, *Ann. Rep. Prog. Chem., Sect. B:Org.*, 2010, **106**, 197-215.
5. F. M. Menger, *Proc. Natl. Acad. Sci. U. S. A.*, 2002, **99**, 4818-4822.
6. T. Steiner, *Angew. Chem. Int. Ed.*, 2002, **41**, 48-76.
7. N. T. Southall, K. A. Dill and A. D. J. Haymet, *J. Phys. Chem. B*, 2001, **106**, 521-533.
8. J. W. Steed, D. R. Turner and K. Wallace, *Core Concepts in Supramolecular Chemistry and Nanochemistry*, John Wiley & Sons, Ltd, Chichester, UK, 2007, 307 pp.
9. P. J. Cragg, *A Practical Guide to Supramolecular Chemistry*, John Wiley & Sons, Ltd, Chichester, 2005, 203 pp.
10. G. McMahon, S. O'Malley and K. Nolan, *ARKIVOC*, 2003, **vii**, 23-31.
11. C. D. Gutsche, *Acc. Chem. Res.*, 1983, **16**, 161-170.
12. J. W. Cornforth, P. D. Hart, G. A. Nicholls, R. J. W. Rees and J. A. Stock, *Br. J. Pharmacol. Chemother.*, 1955, **10**, 73-86.
13. C. D. Gutsche, in *Calixarenes for Separations*, ACS symposium series, 2000, vol. 757, 2-9.
14. M. Takagaki, A. Hosoda, H. Mori, Y. Miyake, K. Kimura, H. Taniguchi and E. Nomura, *Green Chem.*, 2008, **10**, 978-981.
15. A. W. Coleman, A. N. Lazar and E. Da Silva, *Encyclopedia of Supramolecular Chemistry*, 2004, 137 - 144.
16. A. D. Hamilton and Q. Lin, *C. R. Chimie*, 2002, **5**, 441-450.
17. A. Casnati, M. Fabbi, N. Pelizzi, A. Pochini, F. Sansone, R. Unguro, E. Di Modugno and G. Tarzia, *Bioorg. Med. Chem. Lett.*, 1996, **6**, 2699-2704.
18. A. W. Coleman, F. Perret, A. Moussa, M. Dupin, Y. Gu and H. Perron, *Creative Chemical Sensor Systems*, 2007, vol. 277, 31-88.
19. E. Da Silva, A. N. Lazar and A. W. Coleman, *J. Drug Deliv. Sci. Technol.*, 2004, **14**, 3-20.
20. K. Subodh, P. Dharam and S. Harjit, *ARKIVOC*, 2006, **ix**, 17-25.
21. L. M. Tunstad, J. A. Tucker, E. Dalcanale, J. Weiser, J. A. Bryant, J. C. Sherman, R. C. Helgeson, C. B. Knobler and D. J. Cram, *J. Org. Chem.*, 1989, **54**, 1305-1312.
22. K. Paek, H. Ihm, S. Yun, H. C. Lee and K. T. No, *J. Org. Chem.*, 2001, **66**, 5736-5743.
23. B. W. Purse and J. Rebek, *Proc. Natl. Acad. Sci. U. S. A.*, 2005, **102**, 10777-10782.
24. W. Śliwa and M. Deska, *Chem. Heterocycl. Compd.*, 2002, **38**, 646-667.
25. J. L. Atwood, L. J. Barbour and A. Jerga, *Chem. Commun.*, 2001, 2376-2377.
26. S. J. Dalgarno, N. P. Power and J. L. Atwood, *Coord. Chem. Rev.*, 2008, **252**, 825-841.
27. S. Kunsagi-Mate, L. Nagy, G. Nagy, I. Bitter and L. Kollar, *J. Phys. Chem. B*, 2003, **107**, 4727-4731.
28. A. Lutzen, O. Hass and T. Bruhn, *Tetrahedron Lett.*, 2002, **43**, 1807-1811.

29. D. P. Nikolelis, D. A. Drivelos, M. G. Simantiraki and S. Koinis, *Anal. Chem.*, 2004, **76**, 2174-2180.

30. P. Vitovic, D. P. Nikolelis and T. Hianik, *BBA - Biomembranes*, 2006, **1758**, 1852-1861.

31. E. H. Kazakova, A. U. Ziganshina, L. A. Muslinkina, J. E. Morozova, N. A. Makarova, A. R. Mustafina and W. D. Habicher, *J. Inclusion Phenom. Macro.*, 2002, **43**, 65-69.

32. A. R. Mustafina, S. V. Fedorenko, N. A. Makarova, E. K. Kazakova, Z. G. Bazhanova, V. E. Kataev and A. I. Konovalov, *J. Inclusion Phenom. Macro.*, 2001, **40**, 73-76.

33. C. L. D. Gibb and B. C. Gibb, *J. Am. Chem. Soc.*, 2006, **128**, 16498-16499.

34. P. Sakhaii, I. Neda, M. Freytag, H. Thonnessen, P. G. Jones and R. Schmutzler, *Z. Anorg. Allg. Chem.*, 2000, **626**, 1246-1254.

35. A. V. Leontiev, A. W. Saleh and D. M. Rudkevich, *Org. Lett.*, 2007, **9**, 1753-1755.

36. A. Ruderisch, W. Iwanek, J. Pfeiffer, G. Fischer, K. Albert and V. Schurig, *J. Chromatogr. A*, 2005, **1095**, 40-49.

37. A. Ruderisch, J. Pfeiffer and V. Schurig, *J. Chromatogr. A*, 2003, **994**, 127-135.

38. T. Sokoließ, U. Menyes, U. Roth and T. Jira, *J. Chromatogr. A*, 2002, **948**, 309-319.

39. D. Moore, G. W. Watson, T. Gunnlaugsson and S. E. Matthews, *New J. Chem.*, 2008, **32**, 994-1002.

40. A. G. S. Hoegberg, *J. Org. Chem.*, 1980, **45**, 4498-4500.

41. E. Dueno, A. Hunter, M. Zeller, T. Ray, R. Salvatore and C. Zambrano, *J. Chem. Crystallogr.*, 2008, **38**, 181-187.

42. G. Bazylak, L. J. Nagels and H. J. Geise, *Com. Chem. High T. Scr.*, 2004, **7**, 345-359.

43. T. Sokoließ, J. Schonherr, U. Menyes, U. Roth and T. Jira, *J. Chromatogr. A*, 2003, **1021**, 71-82.

44. P. Timmerman, W. Verboom and D. N. Reinhoudt, *Tetrahedron*, 1996, **52**, 2663-2704.

45. G. Cometti, E. Dalcanale, A. Du Vosel and A.-M. Levelut, *J. Chem. Soc., Chem. Com.*, 1990, 163-165.

46. F. Weinelt and H. J. Schneider, *J. Org. Chem.*, 1991, **56**, 5527-5535.

47. H. Konishi, T. Nakamura, K. Ohata, K. Kobayashi and O. Morikawa, *Tetrahedron Lett.*, 1996, **37**, 7383-7386.

48. G. Rumboldt, V. Bohmer, B. Botta and E. F. Paulus, *J. Org. Chem.*, 1998, **63**, 9618-9619.

49. J. Štursa, H. Dvoráková, J. Smidrkal, H. Petricková and J. Moravcová, *Tetrahedron Lett.*, 2004, **45**, 2043-2046.

50. B. Botta, M. C. Digiovanni, G. Delle Monache, M. C. Derosa, E. Gacsbaitz, M. Botta, F. Corelli, A. Tafi, A. Santini, E. Benedetti, C. Pedone and D. Misiti, *J. Org. Chem.*, 1994, **59**, 1532-1541.

51. W. Iwanek, *Tetrahedron*, 1998, **54**, 14089-14094.

52. W. Iwanek, M. Urbaniak and M. Bochenska, *Tetrahedron*, 2002, **58**, 2239-2243.

53. N. K. Beyeh and K. Rissanen, *Tetrahedron Lett.*, 2009, **50**, 7369-7373.

54. B. A. Roberts, G. W. V. Cave, C. L. Raston and J. L. Scott, *Green Chem.*, 2001, **3**, 280-284.

55. J. Antesberger, G. W. V. Cave, M. C. Ferrarelli, M. W. Heaven, C. L. Raston and J. L. Atwood, *Chem. Commun.*, 2005, 892-894.

56.   M. Hedidi, S. M. Hamdi, T. Mazari, B. Boutemeur, C. Rabia, F. Chemat and M. Hamdi, *Tetrahedron*, 2006, **62**, 5652-5655.

57.   C. Yan, W. Chen, J. Chen, T. Jiang and Y. Yao, *Tetrahedron*, 2007, **63**, 9614-9620.

58.   J. Chen, W. Chen and C. Yan, *Chin. J. Chem.*, 2009, **27**, 1703-1706.

59.   D. J. Cram, R. C. Helgeson, C. B. Knobler and E. F. Maverick, *Tetrahedron Lett.*, 2000, **41**, 9465-9470.

60.   B. M. O'Leary, T. Szabo, N. Svenstrup, C. A. Schalley, A. Lutzen, M. Schafer and J. Rebek, *J. Am. Chem. Soc.*, 2001, **123**, 11519-11533.

61.   L. R. MacGillivray and J. L. Atwood, *Angew. Chem. Int. Ed.*, 1999, **38**, 1018-1033.

62.   R. M. McKinlay, P. K. Thallapally and J. L. Atwood, *Chem. Commun.*, 2006, 2956-2958.

63.   L. Avram and Y. Cohen, *J. Am. Chem. Soc.*, 2002, **124**, 15148-15149.

64.   F. Davis, M. Gerber, N. Cowlam and C. J. M. Stirling, *Thin Solid Films*, 1996, **284-285**, 678-682.

65.   A. T. Gubaidullin, I. L. Nikolaeva, A. R. Burilov, I. A. Litvinov, M. A. Pudovik, W. D. Habicher and A. I. Konovalov, *Russ. J. Gen. Chem.*, 2001, **71**, 396-402.

66.   G. W. V. Cave, M. C. Ferrarelli and J. L. Atwood, *Chem. Commun.*, 2005, 2787-2789.

67.   Y. Tanaka, M. Miyachi and Y. Kobuke, *Angew. Chem. Int. Ed.*, 1999, **38**, 504-506.

68.   O. V. Kulikov, M. M. Daschbach, C. R. Yamnitz, N. Rath and G. W. Gokel, *Chem. Commun.*, 2009, 7497-7499.

69.   S. J. Dalgarno, G. W. V. Cave and J. L. Atwood, *Angew. Chem. Int. Ed.*, 2006, **45**, 570-574.

70.   Y. Sun, C. G. Yan, Y. Yao, Y. Han and M. Shen, *Adv. Funct. Mater.*, 2008, **18**, 3981-3990.

71.   Y. Sun, Y. Yao, C. G. Yan, Y. Han and M. Shen, *ACS Nano*, 2010, **4**, 2129-2141.

72.   L. R. MacGillivray and J. L. Atwood, *Nature*, 1997, **389**, 469-472.

73.   T. Gerkensmeier, W. Iwanek, C. Agena, R. Fröhlich, S. Kotila, C. Näther and J. Mattay, *Eur. J. Org. Chem.*, 1999, **1999**, 2257-2262.

74.   J. L. Atwood, L. J. Barbour and A. Jerga, *Supramol. Chem.*, 2001, **1**, 131-134.

75.   Q.-F. Zhang, R. D. Adams and D. Fenske, *J. Inclusion Phenom. Macro.*, 2005, **53**, 275-279.

76.   Y. Cohen, L. Avram and L. Frish, *Angew. Chem. Int. Ed.*, 2005, **44**, 520-554.

77.   N. K. Beyeh, M. Kogej, A. Åhman, K. Rissanen and C. A. Schalley, *Angew. Chem. Int. Ed.*, 2006, **45**, 5214-5218.

78.   K. S. Iyer, M. Norret, S. J. Dalgarno, J. L. Atwood and C. L. Raston, *Angew. Chem. Int. Ed.*, 2008, **47**, 6362-6366.

79.   Y. Cohen, T. Evan-Salem and L. Avram, *Supramol. Chem.*, 2008, **20**, 71-79.

80.   L. Avram and Y. Cohen, *Org. Lett.*, 2003, **5**, 3329-3332.

81.   S. J. Dalgarno, J. Antesberger, R. M. McKinlay and J. L. Atwood, *Chem. Eur. J.*, 2007, **13**, 8248-8255.

82.   G. W. V. Cave, S. J. Dalgarno, J. Antesberger, M. C. Ferrarelli, R. M. McKinlay and J. L. Atwood, *Supramol. Chem.*, 2008, **20**, 157-159.

83.   G. W. V. Cave, A. Jochen, L. J. Barbour, R. M. McKinlay and J. L. Atwood, *Angew. Chem. Int. Ed.*, 2004, **43**, 5263-5266.

84. O. V. Kulikov, N. P. Rath, D. Zhou, I. A. Carasel and G. W. Gokel, *New J. Chem.*, 2009, **33**, 1563-1569.

85. M. W. Heaven, G. W. V. Cave, R. M. McKinlay, J. Antesberger, S. J. Dalgarno, P. K. Thallapally and J. L. Atwood, *Angew. Chem. Int. Ed.*, 2006, **45**, 6221-6224.

86. L. Avram and Y. Cohen, *Org. Lett.*, 2008, **10**, 1505-1508.

A. Shivanyuk and J. Rebek, *Chem. Commun.*, 2001, 2374-2375.

88. A. Shivanyuk and J. Rebek, *Chem. Commun.*, 2001, 2424-2425.

89. T. Evan-Salem, I. Baruch, L. Avram, Y. Cohen, L. C. Palmer and J. Rebek, *Proc. Natl. Acad. Sci. U. S. A.*, 2006, **103**, 12296-12300.

90. L. Avram and Y. Cohen, *J. Am. Chem. Soc.*, 2003, **125**, 16180-16181.

91. L. C. Palmer and J. Rebek, *Org. Lett.*, 2005, **7**, 787-789.

92. L. Avram and Y. Cohen, *Org. Lett.*, 2006, **8**, 219-222.

93. J. L. Atwood, L. J. Barbour and A. Jerga, *Proc. Natl. Acad. Sci. U. S. A.*, 2002, **99**, 4837-4841.

94. L. Avram and Y. Cohen, *J. Am. Chem. Soc.*, 2004, **126**, 11556-11563.

95. N. P. Power, S. J. Dalgarno and J. L. Atwood, *New J. Chem.*, 2007, **31**, 17-20.

96. P. Jin, S. J. Dalgarno, C. Barnes, S. J. Teat and J. L. Atwood, *J. Am. Chem. Soc.*, 2008, **130**, 17262-17263.

97. R. M. McKinlay, P. K. Thallapally, G. W. V. Cave and J. L. Atwood, *Angew. Chem. Int. Ed.*, 2005, **44**, 5733-5736.

98. P. Jin, S. J. Dalgarno and J. L. Atwood, *Coord. Chem. Rev.*, 2010, **254**, 1760-1768.

99. S. J. Dalgarno, N. P. Power, J. E. Warren and J. L. Atwood, *Chem. Commun.*, 2008, 1539-1541.

100. R. M. McKinlay, G. W. V. Cave and J. L. Atwood, *Proc. Natl. Acad. Sci. U. S. A.*, 2005, **102**, 5944-5948.

101. O. V. Kulikov, R. Q. Li and G. W. Gokel, *Angew. Chem. Int. Ed.*, 2009, **48**, 375-377.

102. P. Jin, S. J. Dalgarno, J. E. Warren, S. J. Teat and J. L. Atwood, *Chemical Communications*, 2009, 3348-3350.

103. A. K. Maerz, H. M. Thomas, N. P. Power, C. A. Deakyne and J. L. Atwood, *Chem. Commun.*, 2010, **46**, 1235-1237.

104. S. J. Dalgarno, N. P. Power and J. L. Atwood, *Chem. Commun.*, 2007, 3447-3449.

105. N. P. Power, S. J. Dalgarno and J. L. Atwood, *Angew. Chem. Int. Ed.*, 2007, **46**, 8601-8604.

106. J. L. Atwood, E. K. Brechin, S. J. Dalgarno, R. Inglis, L. F. Jones, A. Mossine, M. J. Paterson, N. P. Power and S. J. Teat, *Chem. Commun.*, 2010, **46**, 3484-3486.

107. R. Li, O. V. Kulikov and G. W. Gokel, *Chemical Commun.,* 2009, 6092-6094.

108. M. Nakazono, Y. Ohba and K. Zaitsu, *Chem. Pharm. Bull.*, 1999, **47**, 569-570.

109. P. T. Lewis, C. J. Davis, M. C. Saraiva, W. D. Treleaven, T. D. McCarley and R. M. Strongin, *J. Org. Chem.*, 1997, **62**, 6110-6111.

110. C. J. Davis, P. T. Lewis, M. E. McCarroll, M. W. Read, R. Cueto and R. M. Strongin, *Org. Lett.*, 1999, **1**, 331-334.

111. M. He, R. J. Johnson, J. O. Escobedo, P. A. Beck, K. K. Kim, N. N. St. Luce, C. J. Davis, P. T. Lewis, F. R. Fronczek, B. J. Melancon, A. A. Mrse, W. D. Treleaven and R. M. Strongin, *J. Am. Chem. Soc.*, 2002, **124**, 5000-5009.

112. G. I. Richard, H. M. Marwani, S. Jiang, S. O. Fakayode, M. Lowry, R. M. Strongin and I. M. Warner, *Appl. Spectrosc.* 2008, **62**, 476-480.
113. E. S. Barrett, T. J. Dale and J. Rebek, *Chem. Commun.*, 2007, 4224-4226.
114. S. J. Dalgarno, S. A. Tucker, D. B. Bassil and J. L. Atwood, *Science*, 2005, **309**, 2037-2039.
115. E. S. Barrett, T. J. Dale and J. Rebek, *J. Am. Chem. Soc.*, 2008, **130**, 2344-2350.
116. E. S. Barrett, T. J. Dale and J. Rebek Jr., *J. Am. Chem. Soc.*, 2007, **129**, 3818-3819.
117. J. L. Whetstine, K. K. Kline, D. A. Fowler, C. M. Ragan, C. L. Barnes, J. L. Atwood and S. A. Tucker, *New J. Chem.*, 2010, 34, 2587-2591.
118. S. J. Dalgarno, T. Szabo, A. Siavosh-Haghighi, C. A. Deakyne, J. E. Adams and J. L. Atwood, *Chem. Commun.*, 2009, 1339-1341.
119. S. J. Dalgarno, D. B. Bassil, S. A. Tucker and J. L. Atwood, *Angew. Chem. Int. Ed.*, 2006, **45**, 7019-7022.
120. D. B. Bassil, S. J. Dalgarno, G. W. V. Cave, J. L. Atwood and S. A. Tucker, *J. Phys. Chem. B*, 2007, **111**, 9088-9092.
121. J. R. Moran, S. Karbach and D. J. Cram, *J. Am. Chem. Soc.*, 1982, **104**, 5826-5828.
122. C. L. D. Gibb and B. C. Gibb, *J. Am. Chem. Soc.*, 2004, **126**, 11408-11409.
123. K. Srinivasan and B. C. Gibb, *Org. Lett.*, 2007, **9**, 745-748.
124. V. A. Azov, P. J. Skinner, Y. Yamakoshi, P. Seiler, V. Gramlich and F. Diederich, *Helv. Chim. Acta*, 2003, **86**, 3648-3670.
125. B. C. Gibb, R. G. Chapman and J. C. Sherman, *J. Org. Chem.*, 1996, **61**, 1505-1509.
126. B. C. Gibb, A. R. Mezo, A. S. Causton, J. R. Fraser, F. C. S. Tsai and J. C. Sherman, *Tetrahedron*, 1995, **51**, 8719-8732.
127. C. Berghaus and M. Feigel, *Eur. J. Org. Chem.*, 2003, 3200-3208.
128. A. R. Mezo and J. C. Sherman, *J. Org. Chem.*, 1998, **63**, 6824-6829.
129. X. Liu and R. Warmuth, *Nat. Protoc.*, 2007, **2**, 1288-1296.
130. N. K. Beyeh, J. Aumanen, A. Åhman, M. Luostarinen, H. Mansikkamaki, M. Nissinen, J. Korppi-Tommola and K. Rissanen, *New J. Chem.*, 2007, **31**, 370-376.
131. K. J. Smith, J. D. Wilcox, G. E. Mirick, L. S. Wacker, N. S. Ryan, D. A. Vensel, R. Readling, H. L. Domush, E. P. Amonoo, S. S. Shariff and T. J. Wenzel, *Chirality*, 2003, **15**, S150-S158.
132. A. Szumna, M. Gorski and O. Lukin, *Tetrahedron Lett.*, 2005, **46**, 7423-7426.
133. S. Shimizu, N. Shimada and Y. Sasaki, *Green Chem.*, 2006, **8**, 608-614.
134. S. Nummelin, D. Falabu, A. Shivanyuk and K. Rissanen, *Organic Lett.*, 2004, **6**, 2869-2872.
135. A. I. Vovk, A. M. Shivanyuk, R. V. Bugas, O. V. Muzychka and A. K. Melnyk, *Bioorg. Med. Chem. Lett.*, 2009, **19**, 1314-1317.
136. C. M. O'Farrell, K. A. Hagan and T. J. Wenzel, *Chirality*, 2009, **21**, 911-921.
137. M. Pietraszkiewicz, P. Prus and O. Pietraszkiewicz, *Tetrahedron*, 2004, **60**, 10747-10752.
138. C. M. O'Farrell, J. M. Chudomel, J. M. Collins, C. F. Dignam and T. J. Wenzel, *J. Org. Chem.*, 2008, **73**, 2843-2851.
139. I. Stoll, A. Mix, A. B. Rozhenko, B. Neumann, H.-G. Stammler and J. Mattay, *Tetrahedron*, 2008, **64**, 3813-3825.

140. S. N. Pod'yachev, V. Syakaev, S. Sudakova, R. Shagidullin, D. Osyanina, L. Avvakumova, B. I. Buzykin, S. Latypov, I. Bauer, W. Habicher and A. I. Konovalov, *J. Inclusion Phenom. Macro.*, 2007, **58**, 55-61.
141. C. Zambrano, J. Kass, E. Dueno, Y. Ke and H.-C. Zhou, *J. Chem. Crystallogr.*, 2006, **36**, 67-70.
142. C. Zambrano, R. E. Thomas, M. Zeller, R. N. Salvatore and E. Dueno, *Acta Crystallogr. E*, 2007, **63**, o3452-o3453.
143. Y. J. Jeon, H. Kim, K. Kim, M. Lee, C. Han and K. J. Kim, *Bull. Kor. Chem. Soc.,* 2008, **29**, 2284-2286.
144. S. F. Alshahateet, F. Kooli, M. Messali, Z. M. A. Judeh and A. S. ElDouhaibi, *Mol. Cryst. Liq. Cryst.*, 2007, **474**, 89-110.
145. J. Han, X. Song, L. Liu and C. Yan, *J. Inclusion Phenom. Macro. Chem.*, 2007, **59**, 257-263.
146. P. Britz-Mckibbin and D. D. Y. Chen, *Anal. Chem.*, 1998, **70**, 907-912.
147. S. J. Dalgarno, N. P. Power, J. Antesberger, R. M. McKinlay and J. L. Atwood, *Chem. Commun.*, 2006, 3803-3805.
148. A. Burilov, A. Gazizov, M. Pudovik and A. I. Konovalov, *Russ. J. Gen. Chem.*, 2007, **77**, 98-102.
149. T. Haino, D. M. Rudkevich, A. Shivanyuk, K. Rissanen and J. Rebek, *Chem. Soc. Rev.*, 2000, **6**, 3797-3805.
150. B. Botta, F. D'Acquarica, L. Nevola, F. Sacco, Z. V. Lopez, G. Zappia, C. Fraschetti, M. Speranza, A. Tafi, F. Caporuscio, M. C. Letzel and J. Mattay, *Eur. J. Org. Chem.*, 2007, **2007**, 5995-6002.
151. B. Botta, G. Delle Monache, P. Ricciardi, G. Zappia, C. Seri, E. Gacs-Baitz, P. Csokasi and D. Misiti, *Eur. J. Org. Chem.*, 2000, **2000**, 841-847.
152. B. Botta, G. Delle Monache, G. Zappia, D. Misiti, M. C. Baratto, R. Pogni, E. Gacs-Baitz, M. Botta, F. Corelli, F. Manetti and A. Tafi, *J. Org. Chem.*, 2002, **67**, 1178-1183.
153. B. Botta, I. D'Acquarica, G. Delle Monache, L. Nevola, D. Tullo, F. Ugozzoli and M. Pierini, *J. Am. Chem. Soc.*, 2007, **129**, 11202-11212.
154. J. D. Faull and V. K. Gupta, *Langmuir*, 2001, **17**, 1470-1476.
155. S. Bozkurt, M. Durmaz, M. Yilmaz and A. Sirit, *Tetrahedron Asymmetry*, 2008, **19**, 618-623.
156. K. Kobayashi, Y. Asakawa, Y. Kato and Y. Aoyama, *J. Am. Chem. Soc.*, 1992, **114**, 10307-10313.
157. R. Yanagihara, M. Tominaga and Y. Aoyama, *J. Org. Chem.*, 1994, **59**, 6865-6867.
158. S. Saito, D. M. Rudkevich and J. Rebek, *Org. Lett.,* 1999, **1**, 1241.
159. F. Hauke, A. J. Myles and J. Rebek Jr., *Chem. Commun.*, 2005, 4164-4166.
160. L. Pirondini, D. Bonifazi, E. Menozzi, E. Wegelius, K. Rissanen, C. Massera and E. Dalcanale, *Eur. J. Org. Chem.*, 2001, 2311-2320.
161. S. M. Butterfield and J. Rebek Jr., *J. Am. Chem. Soc.*, 2006, **128**, 15366-15367.
162. B. W. Purse, S. M. Butterfield, P. Ballester, A. Shivanyuk and J. Rebek, *J. Org. Chem.*, 2008, **73**, 6480-6488.
163. A. Rafai Far, Y. Lag Cho, A. Rang, D. M. Rudkevich and J. Rebek Jr., *Tetrahedron*, 2002, **58**, 741-755.
164. S. Memon, M. Tabakci, D. M. Roundhill and M. Yilmaz, *React. Funct. Polym.*, 2006, **66**, 1342-1349.
165. A. Burilov, A. Gazizov, N. Kharitonova, M. Pudovik, W. Habicher, I. Baier and A. I. Konovalov, *Russ. Chem. Bull.*, 2007, **56**, 330-335.

166. B.-H. Huisman, E. U. T. van Velzen, F. C. J. M. van Veggel, J. F. J. Engbersen and D. N. Reinhoudt, *Tetrahedron Lett.*, 1995, **36**, 3273-3276.
167. E. U. T. Vanvelzen, J. F. J. Engbersen, P. J. Delange, J. W. G. Mahy and D. N. Reinhoudt, *J. Am. Chem. Soc.*, 1995, **117**, 6853-6862.
168. H. X. Chen, M. Lee, S. W. Choi, J. H. Kim, H. J. Choi, S. H. Kim, J. B. Lee and K. N. Koh, *Sensors*, 2007, **7**, 1091-1107.
169. K. Fairfull-Smith, P. M. J. Redon, J. W. Haycock and N. H. Williams, *Tetrahedron Lett.*, 2007, **48**, 1317-1319.
170. R. E. Brewster, K. L. Caran, J. S. Sasine and S. B. Shuker, *Curr. Org. Chem.*, 2004, **8**, 867-881.
171. F. Sansone, S. Barboso, A. Casnati, M. Fabbi, A. Pochini, F. Ugozzoli and R. Ungaro, *Eur. J. Org. Chem.*, 1998, **1998**, 897-905.
172. F. Sansone, S. Barboso, A. Casnati, D. Sciotto and R. Ungaro, *Tetrahedron Lett.*, 1999, **40**, 4741-4744.
173. R. E. Brewster and S. B. Shuker, *J. Am. Chem. Soc.*, 2002, **124**, 7902-7903.
174. A. Casnati, F. Sansone and R. Ungaro, *Acc. Chem. Res.*, 2003, **36**, 246-254.
175. F. Sansone, L. Baldini, A. Casnati, M. Lazzarotto, F. Ugozzoli and R. Ungaro, *Proc. Natl. Acad. Sci. U. S. A.*, 2002, **99**, 4842-4847.
176. L. Baldini, F. Sansone, G. Faimani, C. Massera, A. Casnati and R. Ungaro, *Eur. J. Org. Chem.*, 2008, **2008**, 869-886.
177. L. Baldini, F. Sansone, F. Scaravelli, C. Massera, A. Casnati and R. Ungaro, *Tetrahedron Lett.*, 2009, **50**, 3450-3453.
178. B. Botta, P. Iacomacci, C. Digiovanni, G. Dellemonache, E. Gacsbaitz, M. Botta, A. Tafi, F. Corelli and D. Misiti, *J. Org. Chem.*, 1992, **57**, 3259-3261.
179. B. Botta, G. Delle Monache, M. C. De Rosa, C. Seri, E. Benedetti, R. Iacovino, M. Botta, F. Corelli, V. Masignani, A. Tafi, E. Gacs-Baitz, A. Santini and D. Misiti, *J. Org. Chem.*, 1997, **62**, 1788-1794.
180. B. Botta, G. Delle Monache, P. Salvatore, F. Gasparrini, C. Villani, M. Botta, F. Corelli, A. Tafi, E. GacsBaitz, A. Santini, C. F. Carvalho and D. Misiti, *J. Org. Chem.*, 1997, **62**, 932-938.
181. B. Botta, M. Botta, A. Filippi, A. Tafi, G. Delle Monache and M. Speranza, *J. Am. Chem. Soc.*, 2002, **124**, 7658-7659.
182. A. Tafi, B. Botta, M. Botta, G. Delle Monache, A. Filippi and M. Speranza, *Chem. Eur. J.*, 2004, **10**, 4126-4135.
183. B. Botta, D. Subissati, A. Tafi, G. Delle Monache, A. Filippi and M. Speranza, *Angew. Chem. Int. Ed.*, 2004, **43**, 4871-4874.
184. B. Botta, F. Caporuscio, D. Subissati, A. Tafi, M. Botta, A. Filippi and M. Speranza, *Angew. Chem. Int. Ed.*, 2006, **45**, 2717-2720.
185. B. Botta, F. Caporuscio, I. D'Acquarica, G. Delle Monache, D. Subissati, A. Tafi, M. Botta, A. Filippi and M. Speranza, *Chem. Eur. J.*, 2006, **12**, 8096-8105.
186. B. Botta, G. Delle Monache, C. Fraschetti, L. Nevola, D. Subissati and M. Speranza, *Int. J. Mass Spectrom.*, 2007, **267**, 24-29.
187. B. Botta, A. Tafi, F. Caporuscio, M. Botta, L. Nevola, I. D'Acquarica, C. Fraschetti and M. Speranza, *Chem. Eur. J.*, 2008, **14**, 3585-3595.
188. B. Botta, C. Fraschetti, F. R. Novara, A. Tafi, F. Sacco, L. Mannina, A. P. Sobolev, J. Mattay, M. C. Letzel and M. Speranza, *Org. Biomol. Chem.*, 2009, **7**, 1798-1806.
189. B. Botta, I. D'Acquarica, G. Delle Monache, D. Subissati, G. Uccello-Barretta, M. Mastrini, S. Nazzi and M. Speranza, *J. Org. Chem.*, 2007, **72**, 9283-9290.

190.   B. Botta, C. Fraschetti, I. D'Acquarica, M. Speranza, F. R. Novara, J. Mattay and M. C. Letzel, *J. Phys. Chem. A*, 2009, **113**, 14625-14629.

191.   M. Speranza, F. Gasparrini, B. Botta, C. Villani, D. Subissati, C. Fraschetti and F. Subrizi, *Chirality*, 2009, **21**, 69-86.

192.   M. Speranza, I. D'Acquarica, C. Fraschetti, B. Botta, A. Tafi, L. Bellucci and G. Zappia, *Int. J. Mass Spectrom.*, 2010, **291**, 84-89.

193.   M. Charnley, K. Fairfull-Smith, S. Haldar, R. Elliott, S. L. McArthur, N. H. Williams and J. W. Haycock, *Adv. Mat.*, 2009, **21**, 2909-2915.

194.   S. Loeve, *Hyle*, 2010, **16**, 3-18.

195.   ObservatoryNano, *Public funding of Nanotechnology*, 2010.

196.   J. Chen, N. Jonoska and G. Rozenberg, *Nanotechology: Science and Computation*, Springer, Verlag Berlin Heidelberg, 2006.

197.   R. Kelsall, I. W. Hamley and M. Geoghegan, *Nanoscale Science and Technology*, John Wiley & Sons, Chischester, 2005.

198.   T. Shelley, *Nanotechnology: new promises, new dangers*, Zed Books, London, 2006.

199.   J. R. A. Freitas, *Nanomedicine: Nanotechnology, Biology and Medicine*, 2005, **1**, 2-9.

200.   P. Couvreur and C. Vauthier, *Pharm. Res.*, 2006, **23**, 1417-1450.

201.   V. Vogel, *Nanotechnology, Volume 5: Nanomedicine*, Wiley, Weinheim, 2009, 445 pp.

202.   R. A. Petros and J. M. DeSimone, *Nat. Rev. Drug Discov.*, 2010, **9**, 615-627.

203.   D. A. LaVan, D. M. Lynn and R. Langer, *Nat. Rev. Drug Discov.*, 2002, **1**, 77-84.

204.   P. Ruenraroengsak, J. M. Cook and A. T. Florence, *J. Control. Release*, 2010, **141**, 265-276.

205.   W. R. Sanhai, J. H. Sakamoto, R. Canady and M. Ferrari, *Nat. Nanotechnol.*, 2008, **3**, 242-244.

206.   G. Sahay, D. Y. Alakhova and A. V. Kabanov, *J. Control. Release*, 2010, **145**, 182-195.

207.   I. Brigger, C. Dubernet and P. Couvreur, *Adv. Drug Delivery. Rev.*, 2002, **54**, 631-651.

208.   M. Wang and M. Thanou, *Pharmacol. Res.*, 2010, **62**, 90-99.

209.   J. Kreuter, *Int. J. Pharm.*, 2007, **331**, 1-10.

210.   Hits to the search "nanoparticle and cancer" on www.clinicaltrials.gov

211.   K. Y. Kim, *Nanomedicine: Nanotechnology, Biology and Medicine*, 2007, **3**, 103-110.

212.   M. Ferrari, *Trends Biotechnol.*, 2010, **28**, 181-188.

213.   D. A. Scheinberg, C. H. Villa, F. E. Escorcia and M. R. McDevitt, *Nat. Rev. Clin. Oncol.*, 2010, **7**, 266-276.

214.   J. F. Kukowska-Latallo, K. A. Candido, Z. Cao, S. S. Nigavekar, I. J. Majoros, T. P. Thomas, L. P. Balogh, M. K. Khan and J. R. Baker, Jr., *Cancer Res.*, 2005, **65**, 5317-5324.

215.   C. Loo, A. Lowery, N. Halas, J. West and R. Drezek, *Nano Lett.*, 2005, **5**, 709-711.

216.   D. Peer, J. M. Karp, S. Hong, O. C. Farokhzad, R. Margalit and R. Langer, *Nat. Nanotechnol.*, 2007, **2**, 751-760.

217.   A. Jemal, T. Murray, E. Ward, A. Samuels, R. C. Tiwari, A. Ghafoor, E. J. Feuer and M. J. Thun, *CA Cancer J Clin*, 2005, **55**, 10-30.

218.   C. Sonnenschein and A. M. Soto, *Semin. Cancer Biol.*, 2008, **18**, 372-377.

219. G. Pratesi, *Surgical Oncology*, 2007, **16**, 143.
220. M. F. Ullah and M. Aatif, *Cancer Treat. Rev.*, 2009, **35**, 193-200.
221. D. Hanahan and R. A. Weinberg, *Cell*, 2000, **100**, 57.
222. G. P. Dunn, L. J. Old and R. D. Schreiber, *Immunity*, 2004, **21**, 137-148.
223. S. Mocellin and D. Nitti, *Med. Res. Rev.*, 2008, **28**, 413-444.
224. C. D. Marcus, V. Ladam-Marcus, C. Cucu, O. Bouché, L. Lucas and C. Hoeffel, *Crit. Rev. Oncol./Hematol.*, 2009, **72**, 217-238.
225. L. Fass, *Mol. Oncol.*, 2008, **2**, 115-152.
226. C. N. Baxevanis and M. Papamichail, *Cancer Immunol. Immunother.*, 2004, **53**, 893-903.
227. L. Zitvogel, L. Apetoh, F. Ghiringhelli and G. Kroemer, *Nat. Rev. Immunol.*, 2008, **8**, 59-73.
228. J. M. M. Terwogt, J. H. M. Schellens, W. W. t. B. Huinink and J. H. Beijnen, *Cancer Treat. Rev.*, 1999, **25**, 83-101.
229. M. Rescigno, F. Avogadri and G. Curigliano, *BBA-Rev. Cancer*, 2007, **1776**, 108-123.
230. R. A. Goldsby, *Kuby immunology*, 4th ed. edn., New York : W. H. Freeman, , 2000.
231. J. B. Gibbs, *Science*, 2000, **287**, 1969-1973.
232. M. A. Neller, J. A. López and C. W. Schmidt, *Semin. Immunol.*, 2008, **20**, 286.
233. B. Goldman and L. DeFrancesco, *Nat. Biotechnol.*, 2009, **27**, 129-139.
234. T. A. Waldmann, *Nat Med*, 2003, **9**, 269-277.
235. R. Yaneva, C. Schneeweiss, M. Zacharias and S. Springer, *Mol. Immunol.*, 2010, **47**, 649-657.
236. M. Schott and J. Seissler, *Trends Endocrin. Met.*, 2003, **14**, 156-162.
237. A. Ballestrero, D. Boy, E. Moran, G. Cirmena, P. Brossart and A. Nencioni, *Adv. Drug Deliver. Rev.*, 2008, **60**, 173-183.
238. M. E. D. Chamuleau, G. J. Ossenkoppele and A. A. van de Loosdrecht, *Immunobiology*, 2006, **211**, 619-625.
239. S. K. Mallapragada and B. Narasimhan, *Int. J. Pharm.*, 2008, **364**, 265.
240. G. Schuler, *Eur. J. Immunol.*, 2010, **40**, 2123-2130.
241. C. A. Nicolette, D. Healey, I. Tcherepanova, P. Whelton, T. Monesmith, L. Coombs, L. H. Finke, T. Whiteside and F. Miesowicz, *Vaccine*, 2007, **25**, B47-B60.
242. J. M. Rojas, S. E. B. McArdle, R. B. V. Horton, M. Bell, S. Mian, G. Li, S. A. Ali and R. C. Rees, *Cancer Immunol. Immunother.*, 2005, **54**, 243-253.
243. E. Celis, *J. Clin. Investig.*, 2002, **110**, 1765.
244. J. J. Bosch, J. A. Thompson, M. K. Srivastava, U. K. Iheagwara, T. G. Murray, M. Lotem, B. R. Ksander and S. Ostrand-Rosenberg, *Cancer Res.*, 2007, **67**, 4499-4506.
245. R. P. M. Sutmuller, L. R. H. M. Schurmans, L. M. van Duivenvoorde, J. A. Tine, E. I. H. van der Voort, R. E. M. Toes, C. J. M. Melief, M. J. Jager and R. Offringa, *J. Immunol.*, 2000, **165**, 7308-7315.
246. I. Nakase, T. Takeuchi, G. Tanaka and S. Futaki, *Adv. Drug Delivery. Rev.*, 2008, **60**, 598-607.
247. L. J. Peek, C. R. Middaugh and C. Berkland, *Adv. Drug Delivery. Rev.*, 2008, **60**, 915-928.
248. S. T. Reddy, M. A. Swartz and J. A. Hubbell, *Trends Immunol.*, 2006, **27**, 573-579.

249. Y. Krishnamachari, S. Geary, C. Lemke and A. Salem, *Pharm. Res.*, 2011, **28**, 215-236.
250. D. T. O'Hagan and N. M. Valiante, *Nat. Rev. Drug Discov.*, 2003, **2**, 727-735.
251. M. Funck, D. P. Guest and G. W. V. Cave, *Tetrahedron Lett.*, 2010, **51**, 6399-6402.
252. W. Śliwa and C. Kozlowski, *Calixarenes and Resorcinarenes*, Wiley-VCH, Weinheim, 2009, 316 pp.
253. P. Lidström, J. Tierney, B. Wathey and J. Westman, *Tetrahedron*, 2001, **57**, 9225-9283.
254. O. C. Kappe, D. Dallinger and S. S. Murphee, *Practical Microwave synthesis for Organic Chemist*, Wiley-VCH, Weinheim, 2009, 299 pp.
255. O. C. Kappe and D. Dallinger, *Mol. Divers.*, 2009, **13**, 71-193.
256. A. G. S. Hoegberg, *J. Am. Chem. Soc.*, 1980, **102**, 6046-6050.
257. L. Nicod, F. Chitry, E. Gaubert, M. Lemaire and H. Barnier, *J. Inclusion Phenom. Macro. Chem.*, 1999, **34**, 143-154.
258. Jumina, R. E. Sarjono, B. Paramitha, I. Hendaryani, D. Siswanta, S. J. Santosa, C. Anwar, H. Sastrohamidjojo, K. Ohto and T. Oshima, *J. Chin. Chem. Soc.*, 2007, **54**, 1167-1178.
259. S. N. Pod'yachev, A. R. Mustafina, A. H. Koppehele, M. Grüner, W. D. Habicher, B. I. Buzykin and A. I. Konovalov, *Russ. Chem. Bull.*, 2004, **53**, 1181-1188.
260. K. Deleersnyder, H. Mehdi, I. T. Horvath, K. Binnemans and T. N. Parac-Vogt, *Tetrahedron*, 2007, **63**, 9063-9070.
261. A. Mustafina, I. Zagidullina, V. Maslennikova, O. Serkova, T. Guzeeva and A. Konovalov, *Russ. Chem. Bull.*, 2007, **56**, 313-319.
262. H. Singh and R. Kaur, *J. Inclusion Phenom.*, 1997, **28**, 105-116.
263. G. N. Al'tshuler, O. N. Fedyaeva and E. V. Ostapova, *Russ. Chem. Bull.*, 2001, **50**, 1379-1381.
264. G. N. Al'tshuler, O. N. Fedyaeva and E. V. Ostapova, *Russ. Chem. Bull.*, 2000, **49**, 1468-1470.
265. H. N. Al'tshuler, L. Sapozhnikova, E. Ostapova, O. Fedyaeva and O. Altshuler, *Solvent Extr. Ion Exch.*, 2002, **20**, 263 - 271.
266. H. Ito, T. Nakayama, M. Sherwood, D. Miller and M. Ueda, *Chem. Mater.*, 2007, **20**, 341-356.
267. T. Krause, M. Gruner, D. Kuckling and W. D. Habicher, *Tetrahedron Lett.*, 2004, **45**, 9635-9639.
268. B. Mendrek and B. Trzebicka, *Eur. Polym. J.*, 2009, **45**, 1979-1993.
269. S. Seyhan, Ö. Özbayrak, N. Demirel, M. Merdivan and N. Pirinççioglu, *Tetrahedron: Asymmetry*, 2005, **16**, 3735-3738.
270. S. R. Foster, A. Pearce, A. J. Blake, M. J. Welham and J. Dowden, *Chem. Commun.*, 2007, 2512-2514.
271. N. M. Felix, A. De Silva and C. K. Ober, *Adv. Mater.*, 2008, **20**, 1303-1309.
272. M. J. McIldowie, M. Mocerino, B. W. Skelton and A. H. White, *Org. Lett.*, 2000, **2**, 3869-3871.
273. H. Dvoráková, J. Štursa, M. Čajan and J. Moravcová, *Eur. J. Org. Chem.*, 2006, **2006**, 4519-4527.
274. O. Middel, W. Verboom, R. Hulst, H. Kooijman, A. L. Spek and D. N. Reinhoudt, *J. Org. Chem.*, 1998, **63**, 8259-8265.
275. D. Volkmer, M. Fricke, C. Agena and J. Mattay, *Cryst. Eng. Comm.*, 2002, 288-295.

276. P. van der Sluis and A. L. Spek, *Acta Crystallogr., Sect. A: Found. Crystallogr.*, 1990, **46**, 194-201.
277. V. Gomez-Benitez, R. A. Toscano and D. Morales-Morales, *J. Inclusion Phenom. Macro. Chem.*, 2004, **50**, 199-202.
278. S. Grabowski, *Hydrogen Bonding - New Insights*, Springer, Dordrecht, The Netherland, 2006.
279. L. R. MacGillivray and J. L. Atwood, *Supramol. Chem.*, 2000, **11**, 293 - 299.
280. H. Frost and R. Q. Snurr, *J. Phys. Chem. C*, 2007, **111**, 18794-18803.
281. P. O. Brown, G. D. Enright and J. A. Ripmeester, *Cryst. Growth Des.*, 2006, **6**, 719-725.
282. A. K. Jain, V. K. Gupta, L. P. Singh, P. Srivastava and J. R. Raisoni, *Talanta*, 2005, **65**, 716-721.
283. X. Gui and J. C. Sherman, *Chem. Commun.*, 2001, 2680-2681.
284. P. Amrhein, A. Shivanyuk, D. W. Johnson and J. Rebek, *J. Am. Chem. Soc.*, 2002, **124**, 10349-10358.
285. O. Middel, W. Verboom and D. N. Reinhoudt, *Eur. J. Org. Chem.*, 2002, **2002**, 2587-2597.
286. M. D. Giles, S. Liu, R. L. Emanuel, B. C. Gibb and S. M. Grayson, *J. Am. Chem. Soc.*, 2008, **130**, 14430-14431.
287. S. M. Grayson and B. C. Gibb, *Soft Matter*, 2010, **6**, 1377-1382.
288. S. Busi, H. Saxell, R. Fröhlich and K. Rissanen, *Cryst. Eng. Comm.*, 2008, **10**, 1803-1809.
289. H. Mansikkamaki, M. Nissinen and K. Rissanen, *Cryst. Eng. Comm.*, 2005, **7**, 519-526.
290. L. J. Barbour, Columbia, 2003, p. Program for calculating the molecular volume of closed capsules.
291. A. Gavezzotti, *Acc. Chem. Res.*, 1994, **27**, 309-314.
292. A. Gavezzotti and G. Filippini, *J. Phys. Chem.*, 1994, **98**, 4831-4837.
293. A. A. Momose and E. Bosch, *Cryst. Growth Des.*, 2010, **10**, 4043-4049.
294. A. T. Gubaidullin, Y. E. Morozova, A. R. Mustafina, E. K. Kazakova, I. A. Litvinov and A. I. Konovalov, *Mendeleev Commun.*, 1999, **9**, 9-10.
295. O. D. Fox, M. G. B. Drew and P. D. Beer, *Angew. Chem. Int. Ed.*, 2000, **39**, 135-140.
296. O. D. Fox, M. G. B. Drew, E. J. S. Wilkinson and P. D. Beer, *Chem. Commun.*, 2000, 391-392.
297. N. P. Power, S. J. Dalgarno and J. L. Atwood, *New J. Chem.*, 2007, **31**, 17-20.
298. J. J. N. Veerman, J. Klein, R. W. M. Aben, H. W. Scheeren, C. G. Kruse, J. H. van Maarseveen, F. Rutjes and H. Hiemstra, *Eur. J. Org. Chem.*, 2002, 3133-3139.
299. M. Mäkinen, P. Vainiotalo, M. Nissinen and K. Rissanen, *J. Am. Soc. Mass Spectrom.*, 2003, **14**, 143-151.
300. H. Mansikkamaki, M. Nissinen, C. A. Schalley and K. Rissanen, *New J. Chem.*, 2003, **27**, 88-97.
301. H. Mansikkamaki, C. A. Schalley, M. Nissinen and K. Rissanen, *New J. Chem.*, 2005, **29**, 116-127.
302. A. Åhman, M. Luostarinen, K. Rissanen and M. Nissinen, *New J. Chem.*, 2007, **31**, 169-177.
303. K. Bowman-James, *Acc. Chem. Res.*, 2005, **38**, 671-678.
304. K. Murayama and K. Aoki, *Chem. Commun.*, 1997, 119-120.
305. M. Nahmany and A. Melman, *Org. Biomol. Chem.*, 2004, **2**, 1563-1572.

306. G. Appendino, A. Minassi, N. Daddario, F. Bianchi and G. C. Tron, *Org. Lett.*, 2002, **4**, 3839-3841.
307. A. Åhman, M. Luostarinen, C. A. Schalley, M. Nissinen and K. Rissanen, *Eur. J. Org. Chem.*, 2005, **2005**, 2793-2801.
308. H. Takahashi, M. Kosaka, Y. Watanabe, K. Nakade and Y. Fukuyama, *Bioorg. Med. Chem.*, 2003, **11**, 1781-1788.
309. S. Bhattacharyya, *Mol. Divers.*, 2005, **9**, 253-257.
310. C. M. Mooy and P. T. V. M. De Jong, *Surv. Ophthalmol.*, 1996, **41**, 215-228.
311. S. Mojsov and G. Barany, *J. Peptide Sci.*, 2008, **90**, 162-174.
312. G. B. Fields, in *Molecular Biomethods Handbook*, eds. R. Rapley and J. M. Walker, Humana Press, 1998, 527-545.
313. M. L. Becker, J. Liu and K. L. Wooley, *Biomacromol.*, 2004, **6**, 220-228.
314. P. D. Barata, A. I. Costa, P. Granja and J. V. Prata, *React. Funct. Polym.*, 2004, **61**, 147-151.
315. E. Rezaei-Seresht and F. Hokmabadi, *Tetrahedron Lett.*, 2010, **51**, 2473-2476.
316. S. Memon, M. Tabakci, D. Max Roundhill and M. Yilmaz, *Polymer*, 2005, **46**, 1553-1560.
317. V. K. Jain, R. A. Pandya, S. G. Pillai, P. S. Shrivastav and Y. K. Agrawal, *Sep. Sci. Technol.*, 2006, **41**, 123 - 147.
318. O. Gungor, S. Memon, M. Yilmaz and D. M. Roundhill, *React. Funct. Polym.*, 2005, **63**, 1-9.
319. N. Tadatomi, K. Atsushi and K. Hiroto, *Polym. J.*, 2003, **35**, 213-229.
320. G. N. Altshuler and L. A. Sapozhnikova, *J. Struct. Chem.*, 2004, **45**, S174-S176.
321. G. Granata, G. M. L. Consoli, S. Sciuto and C. Geraci, *Tetrahedron Lett.*, 2010, **51**, 6139-6142.
322. R. Santini, M. C. Griffith and M. Qi, *Tetrahedron Lett.*, 1998, **39**, 8951-8954.
323. S. Kobayashi and Y. Aoki, *Tetrahedron Lett.*, 1998, **39**, 7345-7348.
324. A. Vidal-Ferran, N. Bampos, A. Moyano, M. A. Pericas, A. Riera and J. K. M. Sanders, *J. Org. Chem.*, 1998, **63**, 6309-6318.
325. D. Stones, D. J. Miller, M. W. Beaton, T. J. Rutherford and D. Gani, *Tetrahedron Lett.*, 1998, **39**, 4875-4878.
326. M. R. Tremblay and D. Poirier, *J. Com. Chem.*, 1999, **2**, 48-65.
327. M. Guino and K. K. Hii, *Org. Biomol. Chem.*, 2005, **3**, 3188-3193.
328. I. Deben, J. Goorden, E. van Doornum, H. Ovaa and E. Kellenbach, *Eur. J. Org. Chem.*, 1998, **1998**, 697-700.
329. B. Yan, H.-U. Gremlich, S. Moss, G. M. Coppola, Q. Sun and L. Liu, *J. Com. Chem.*, 1998, **1**, 46-54.
330. C. E. Le, N. Lewis, C. Ribas and A. Wells, *Org. Process Res. Dev.*, 2000, **4**, 606-610.
331. M. Siu, V. A. Yaylayan, J. M. R. Bélanger and J. R. J. Paré, *Tetrahedron Lett.*, 2005, **46**, 3737-3739.
332. F. Guillier, D. Orain and M. Bradley, *Chem. Rev.*, 2000, **100**, 2091-2158.
333. B. Yan, J. B. Fell and G. Kumaravel, *J. Org. Chem.*, 1996, **61**, 7467-7472.
334. C. Braunshier, C. Hametner, J. Fröhlich, J. Schnöller and H. Hutter, *Tetrahedron Lett.*, 2008, **49**, 7103-7105.
335. G. C. Look, C. P. Holmes, J. P. Chinn and M. A. Gallop, *J. Org. Chem.*, 1994, **59**, 7588-7590.
336. F. Lorgé, A. Wagner and C. Mioskowski, *J. Com. Chem.*, 1998, **1**, 25-27.
337. Z. Zhu and B. McKittrick, *Tetrahedron Lett.*, 1998, **39**, 7479-7482.

338.   M. M. Meloni, R. C. D. Brown, P. D. White and D. Armour, *Tetrahedron Lett.*, 2002, **43**, 6023-6026.

339.   J. I. Borrell, J. Teixidó, E. Schuler and E. Michelotti, *Tetrahedron Lett.*, 2001, **42**, 5331-5334.

340.   A. Stadler and C. O. Kappe, *Eur. J. Org. Chem.*, 2001, **2001**, 919-925.

341.   A. Kluczyk, M. Rudowska, P. Stefanowicz and Z. Szewczuk, *J. Pept. Sci.*, 2010, **16**, 31-39.

342.   P. Shahgaldian, E. Da Silva and A. W. Coleman, *J. Inclusion Phenom. Macro. Chem.*, 2003, **46**, 175-177.

343.   F. Perret, Bonnard, Vanessa, Danylyuk, Oksana, Suwinska, Kinga, Coleman, Anthony W., *New J. Chem*, 2006, **30**, 987-990.

344.   F. Perret, A. N. Lazar and A. W. Coleman, *Chem. Commun.*, 2006, **23**, 2425-2438.

345.   M.-H. Paclet, C. Rousseau, C. Yannick, F. Morel and A. W. Coleman, *J. Inclusion Phenom. Macro. Chem.*, 2006, **55**, 353-357.

346.   A. W. Coleman, S. Jebors, S. Cecillon, P. Perret, D. Garin, D. Marti-Battle and M. Moulin, *New J. Chem.*, 2008, **32**, 780-782.

347.   N. Douteau-Guevel, F. Perret, A. W. Coleman, J.-P. Morel and N. Morel-Desrosiers, *J. Chem. Soc., Perkin Trans. 2*, 2002, 524-532.

348.   A. W. Coleman, L. G. Baggetto, A. N. Lazar, M. H. Michaud and S. Magnard, *Derivatives of calixarenes as anticancer agent*, 2007, Centre National de la Recherche Scientifique, France, 41 pp.

349.   V. Paquet, A. Zumbuehl and E. M. Carreira, *Bioconjug. Chem.*, 2006, **17**, 1460-1463.

350.   F. Sansone, M. Dudic, G. Donofrio, C. Rivetti, L. Baldini, A. Casnati, S. Cellai and R. Ungaro, *J. Am. Chem. Soc.*, 2006, **128**, 14528-14536.

351.   M. Dudic, A. Colombo, F. Sansone, A. Casnati, G. Donofrio and R. Ungaro, *Tetrahedron*, 2004, **60**, 11613-11618.

352.   M. Grare, M. Mourer, S. Fontanay, J.-B. Regnouf-de-Vains, C. Finance and R. E. Duval, *J. Antimicrob. Chemother.*, 2007, **60**, 575-581.

353.   M. Grare, M. Mourer, J. B. Regnouf de Vains, C. Finance and R. E. Duval, *Pathol. Biol.*, 2006, **54**, 470-476.

354.   M. Mourer, H. M. Dibama, S. Fontanay, M. Grare, R. E. Duval, C. Finance and J.-B. Regnouf-de-Vains, *Bioorg. Med. Chem.*, 2009, **17**, 5496-5509.

355.   M. Grare, H. M. Dibama, S. Lafosse, A. Ribon, M. Mourer, J. B. Regnouf-de-Vains, C. Finance and R. E. Duval, *Clin. Microbiol. Infect.*, 2010, **16**, 432-438.

356.   S. Viola, S. Merlo, G. M. L. Consoli, F. Drago, C. Geraci and M. A. Sortino, *Pharmacology*, 2010, **86**, 182-188.

357.   M. J. Colston, H. C. Hailes, E. Stavropoulos, A. C. Herve, G. Herve, K. J. Goodworth, A. M. Hill, P. Jenner, P. D. Hart and R. E. Tascon, *Infect. Immun.*, 2004, **72**, 6318-6323.

358.   K. Krenek, M. Kuldova, K. Hulikova, I. Stibor, P. Lhotak, M. Dudic, J. Budka, H. Pelantova, K. Bezouska, A. Fiserova and V. Kren, *Carbohyd. Res.*, 2007, **342**, 1781-1792.

359.   C. Geraci, G. M. L. Consoli, E. Galante, E. Bousquet, M. Pappalardo and A. Spadaro, *Bioconjug. Chem.*, 2008, **19**, 751-758.

360.   S. M. Sebti and A. D. Hamilton, *Oncogene*, 2000, **19**, 6566-6573.

361.   S. M. Sebti, A. D. Hamilton and R. Jain, *Growth factor binding coumpounds*

having a plurlity of acyclic isophthalic acid groups attached to a non-peptide organic scaffold, and method of use, 2005, University of South Florida, U. S. A., 51 pp.

362. K. H. Mayo, T. R. Hoye and X-Chen, *Preparation of calixarene-based peptides conformation mimetics and their biological activity,* 2006, University of Minessota, U. S. A., 115 pp.

363. K. H. Mayo, T. R. Hoye and X-Chen, *Calixarene-based peptide conformation mimetics, method od use and method of making,* 2008, University of Minessota, U. S. A., 155 pp.

364. J. Z. Sun, M. A. Blaskovich, R. K. Jain, F. Delarue, D. Paris, S. Brem, M. Wotoczek-Obadia, Q. Lin, D. Coppola, K. H. Choi, M. Mullan, A. D. Hamilton and S. M. Sebti, *Cancer Res.*, 2004, **64**, 3586-3592.

365. M. H. B. Grote Gansey, A. S. de Haan, E. S. Bos, W. Verboom and D. N. Reinhoudt, *Bioconjug. Chem.,* 1999, **10**, 613-623.

366. G. M. L. Consoli, G. Granata, E. Galante, I. Di Silvestro, L. Salafia and C. Geraci, *Tetrahedron*, 2007, **63**, 10758-10763.

367. R. Lalor, J. L. DiGesso, A. Mueller and S. E. Matthews, *Chem. Commun.*, 2007, 4907-4909.

368. R. B. Durairaj, *Resorcinol: Chemistry, Technology and Applications*, Springer Verlag, Berlin, Heildelberg, 2005, 748 pp

369. S. R. Baerson, J. Schröder, D. Cook, A. M. Rimando, Z. Pan, F. E. Dayan, B. P. Noonan and S. O. Duke, *Plant Signal. Behav.*, 2010, **5**, 1286-1289.

370. A. Kozubek, R. Zarnowski, M. Stasiuk and J. Gubernator, *Cell. Mol. Biol. Lett.*, 2001, **6**, 351-355.

371. E. Klarmann, *J. Am. Chem. Soc.*, 1926, **48**, 2358-2367.

372. A.C. Lagrange and H. Borowiak, *Topical process for lightening the skin or treating pigmental blemishes using a composition containing 4-thioresorcin derivatives,* 1995, L'Oreal (Paris, FR): U. S. A., 6 pp.

373. G.A. Symons and D.R. Hampton, *Coated implantable medical devices such as catheters, vascular grafts, sutures, cardiac leads and valves, pumps and drug-eluting stents, with repellent coating such as calixarenes and resorcarenes.* 2008, Camstent Ltd Mbe, UK . 13 pp.

374. S. Ehrler, U. Pieles, A. Wirth-Heller and P. Shahgaldian, *Chem. Commun.*, 2007, 2605-2607.

375. H. Wolf and J. M. Dormann, *Calixarenes for use as excipient for an active substance*, 2006, USA, 8 pp.

376. O. Hayashida, N. Ogawa and M. Uchiyama, *J. Am. Chem. Soc.*, 2007, **129**, 13698-13705.

377. O. Hayashida and M. Uchiyama, *Tetrahedron Lett.*, 2006, **47**, 4091-4094.

378. O. Hayashida and M. Uchiyama, *J. Org. Chem.*, 2006, **72**, 610-616.

379. O. Hayashida and M. Uchiyama, *Org. Biomol. Chem.*, 2008, **6**, 3166-3170.

380. P. Niederhafner, J. Sebestik and J. Jezek, *J. Pept. Sci.*, 2008, **14**, 2-43.

381. O. Hayashida, K. Mizuki, K. Akagi, A. Matsuo, T. Kanamori, T. Nakai, S. Sando and Y. Aoyama, *J. Am. Chem. Soc.*, 2003, **125**, 594-601.

382. Y. Aoyama, T. Kanamori, T. Nakai, T. Sasaki, S. Horiuchi, S. Sando and T. Niidome, *J. Am. Chem. Soc.*, 2003, **125**, 3455-3457.

383. T. Nakai, T. Kanamori, S. Sando and Y. Aoyama, *J. Am. Chem. Soc.*, 2003, **125**, 8465-8475.

384. S. Horiuchi and Y. Aoyama, *J. Controlled Release*, 2006, **116**, 107-114.

385.   D. Anselmetti, F. W. Bartels, A. Becker, B. Decker, R. Eckel, M. McIntosh, J. Mattay, P. Plattner, R. Ros, C. Schafer and N. Sewald, *Langmuir*, 2008, **24**, 1365-1370.
386.   A. Messerschmidt, H. Niessen, D. Abt, O. Einsle, B. Schink and P. M. H. Kroneck, *Proc. Natl. Acad. Sci. U. S. A.*, 2004, **101**, 11571-11576.
387.   W. H. Park, Y. H. Han, S. H. Kim and S. Z. Kim, *Toxicology*, 2007, **235**, 130-139.
388.   G. Upadhyay, A. Kumar and M. P. Singh, *Eur. J. Pharmacol.*, 2007, **565**, 190-201.
389.   J. L. Mazzei, D. N. da Silva, V. Oliveira, R. Z. Hosomi, R. R. do Val, C. B. Pestana and I. Felzenszwalb, *Food Chem. Toxicol.*, 2007, **45**, 643-648.
390.   S.J Harris, *Preparation of calixarene-based compounds having antibacterial, antifungal, anticancer, and anti-HIV activity*. 1995, Ireland. . p. 148 pp
391.   E. Da Silva, P. Shahgaldian and A. W. Coleman, *Int. J. Pharm.*, 2004, **273**, 57-62.
392.   H. C. Ansel and G. E. Cabre, *J. Pharm. Sci.*, 1970, **59**, 478-481.
393.   M. Samoszuk, M. E. Reid and P. T. C. Y. Toy, *Transfusion*, 1983, **23**, 405-405.
394.   N. C. Santos, J. Figueira-Coelho, J. Martins-Silva and C. Saldanha, *Biochem. Pharmacol.*, 2003, **65**, 1035-1041.
395.   K. Inaba, M. Inaba, N. Romani, H. Aya, M. Deguchi, S. Ikehara, S. Muramatsu and R. M. Steinman, *J. Exp. Med.*, 1992, **176**, 1693-1702.
396.   M. B. Lutz, N. Kukutsch, A. L. J. Ogilvie, S. Rößner, F. Koch, N. Romani and G. Schuler, *J. Immunol. Methods*, 1999, **223**, 77-92.
397.   H. Tsujimoto, P. A. Efron, T. Matsumoto, R. F. Ungaro, A. Abouhamze, S. Ono, H. Mochizuki and L. L. Moldawer, *Immunology Lett.*, 2006, **107**, 155-162.
398.   L. Bruno, *Methods Mol Biol.*, 2007, **380**, 47-57.
399.   L. E. Tze, K. Horikawa, H. Domaschenz, D. R. Howard, C. M. Roots, R. J. Rigby, D. A. Way, M. Ohmura-Hoshino, S. Ishido, C. E. Andoniou, M. A. Degli-Esposti and C. C. Goodnow, *J. Exp. Med.*, 2011, **208**, 149-165.
400.   J. Weyermann, D. Lochmann and A. Zimmer, *Int. J. Pharm.*, 2005, **288**, 369-376.
401.   S. Schaffer, W. E. Müller and G. P. Eckert, *Pharmacol. Res.*, 2010, **62**, 322-327.
402.   S. Miret, E. M. De Groene and W. Klaffke, *J. Biomol. Screen.*, 2006, **11**, 184-193.
403.   G. M. Sheldrick, *SHELXS-97*, (1997), University of Gottinghen, Germany.
404.   G. M. Sheldrick, *SHELXL-97*, (1997), University of Gottinghen, Germany.
405.   L. J. Barbour, *J. Supramol. Chem.*, **1**, 189-191.
406.   *PovRay*, (1994-2007) Hallam Oaks Pty. Ltd, www.povray.org.